UNIVERSITY OF LONDON THESIS

PhD Year 2007 Name of Author LIAM SEAN LLOYD MCCARTHY

Extracellular matrix biology in normal and abnormal bladder development

by Liam Sean Lloyd McCarthy

A thesis submitted to the University of London
in fulfilment of the requirement for the degree of
Doctor of Philosophy

2006

Nephro-Urology Unit, Institute of Child Health,
University College London

ProQuest LLC
789 East Eisenhower Parkway
P.O. Box 1346
Ann Arbor, MI 48106-1346

To my children Abigail, Max and Rosie,

but most of all to my wife Kate

who looked after the children

and gave me the support,

and time to finish this thesis

Abstract

Previous work demonstrated that fibronectin is expressed in embryonic mouse detrusor smooth muscle cells (DSMC). Integrins are cell surface receptors for extracellular matrix (ECM) molecules, including fibronectin. The general hypothesis explored here is that ECM/integrin interactions are important in normal and pathological DSMC differentiation.

The first specific hypotheses tested were that the candidate fibronectin receptor integrin $\alpha5\beta1$ and the laminin 1/2 candidate receptor integrin $\alpha7\beta1$ are expressed by developing DSMC, Using immunohistochemistry, Western blots, and flow cytometry, these proteins were found to be expressed during murine bladder differentiation.

This led to the second specific hypothesis, namely that embryonic nascent DSMC adhere to fibronectin, a process mediated by integrin $\alpha5\beta1$. Fibronectin substrate was shown to enhance the adhesion of disaggregated embryonic mouse bladder cells. Blocking integrin receptors using RGD oligopeptides modestly but significantly decreased adherent cells expressing desmin, and reduced cell spreading.

To explore roles for fibronectin in whole bladders, rather than isolated cells, embryonic mouse organ cultures were established which recapitulated some in vivo differentiation features. However, no specific effects on growth or differentiation could be demonstrated using presumed 'fibronectin-blocking' antibodies. Time did not allow testing of RGD oligopeptides.

Last, the following hypotheses were explored: that fibronectin is expressed during normal human fetal DSMC differentiation, and that this pattern is

altered in bladders from fetuses with presumed bladder outflow obstruction. Fibronectin was indeed found to be expressed during normal human detrusor differentiation and its expression was sometimes reduced in malformed human fetal bladders.

These studies provide further descriptive, and hence circumstantial, evidence that ECM/integrin interactions may be important in normal DSMC development. Further studies are warranted to resolve the apparently conflicting/ambiguous organ and cell culture data regarding possible roles for fibronectin and its receptors. The studies also provide preliminary evidence of abnormal fibronectin expression in human congenital bladder anomalies.

Acknowledgements

I would like to thank those organizations that funded this work: Kidney Research Aid Fund, and Great Ormond Street Hospital and Institute of Child Health. I would like to thank my supervisors Mr DT Wilcox and Professor AS Woolf, for their guidance, support and encouragement of this project. I would also like to thank the following collaborators: Dr K Hodivala-Dilke, Dr P Winyard and Dr R Scott. I would also like to thank Prof M Goligorsky for his technical advice.

Many of the techniques I have used were taught to me by my colleagues in the Nephro-Urology Unit at the Institute of Child Health. I would like to thank particularly Miss N Smeulders, Mr N Thiruchelvam, Dr S Welham, Dr J Pitera, Dr K Price, Dr D Long, Dr HT Huang, Dr P Winyard, Dr D Gonzalez, Dr L Romio and Mrs V Shah.

Abbreviations

αSMA	α smooth muscle actin
µg	microgram
µl	microlitre
µM	micromolar
6Wks	6 weeks of postnatal age
ANOVA	analysis of variance
ARK	animal research kit
ATP	adenosine triphosphate
BCA	bicinchoninic acid
BOO	bladder outflow obstruction
bp	base pairs (DNA)
BrdU	5-bromo-2-deoxyuridine
BSA	bovine serum albumin
CD31	platelet endothelial cell adhesion molecule (PECAM)
CDD	collagen, dispase, DNase
CO_2	carbon dioxide
CT	connective tissue
D1	post natal day 1
DAB	diaminobenzidene
DMEM	Dulbecco's modified Eagle's medium
DNA	deoxyribosenucleic acid
DNase	deoxyribosenuclease
DPX	distyrene (polystyrene), a plasticizer (dibutylphthalate), and xylene
DSM	detrusor smooth muscle
DSMC	detrusor smooth muscle cell
E12	embryonic day 12
E14	embryonic day 14
E16	embryonic day 16
E18	embryonic day 18
ECM	extracellular matrix

ELISA	enzyme linked immunosorbent assay
Fab	the part of an antibody containing the antigen binding site
FACS	fluorescence activated cell sorter
FCS	fetal calf serum
FITC	fluorescein isothyocyanate
H_2O_2	hydrogen peroxide
HRP	horseradish peroxidase
IgG	immunoglobulin G
IHC	immunohistochemistry
ILK	integrin linked kinase
ITS	insulin transferrin and selenium
kDa	kilodalton
LDH	lactate dehydrogenase
mg	milligram
ml	millilitre
mM	millimolar
mm^2	square millimetre
mm^3	cubic millimetre
NaCl	sodium chloride
ng	nanogram
nm	nanometres
NP40	nonidet P40
°C	degrees centigrade
OCT	optimum cutting temperature
PAGE	polyacrylamide gels
PBS	phosphate buffered saline
PBS	Prune Belly syndrome
PBSABC	PBS with magnesium and calcium chloride to 1mM
PCD	programmed cell death
PCNA	proliferating cell nuclear antigen
PMSF	phenoxymethyl sulfoxide
POD	peroxidase
PS1	Drosophila laminin receptor integrin α subunit

PS2	Drosophila RGD receptor integrin α subunit
PUV	posterior urethral valves
RAD	arginine-alanine-aspartate
RBC	red blood cell
RGD	arginine-glycine-aspartate
rTDT	terminal deoxynucleotidyl transferase
SDS	sodiumdodecylsulphate
SEM	standard error of the mean
SMC	smooth muscle cells
TEMED	tetramethylethylenediamine
TNF	tumour necrosis factor
TRITC	tetramethylrhodamine isothiocyanate
TUNEL	terminal rTDT-mediated UTP nick end labelling
UGS	urogenital sinus
UK	United Kingdom
VSMC	vascular smooth muscle cell
WB	Western blot

Contents

ABSTRACT **3**

ACKNOWLEDGEMENTS **5**

ABBREVIATIONS **6**

CONTENTS **9**

LIST OF FIGURES **22**

LIST OF TABLES **29**

PREFACE. HYPOTHESIS, AIMS AND OVERVIEW **31**

OVERALL HYPOTHESIS 31

OVERVIEW 31

LONG-TERM SIGNIFICANCE 33

CHAPTER 1. INTRODUCTION **34**

EMBRYOLOGY OF BLADDER DEVELOPMENT 37

Time-table for embryogenesis of the mouse bladder *42*

Changes in cell phenotype during detrusor development *43*

Urothelial development *44*

THE HIERARCHICAL STRUCTURE OF CONNECTIVE TISSUE 47

Interstitial matrix *47*

Components of basal lamina *48*

LAMININS 52

Structure of laminins *52*

Classification of laminin sub-types *54*

Laminin production and polymerization *56*

Laminin receptors *61*

Laminin expression in the mammalian urinary tract *64*

Candidate laminin integrin receptor in detrusor *66*

FIBRONECTIN 67

Fibronectin structure *68*

Fibronectin receptors *72*

Fibronectin polymerization *75*

Fibronectin matrix assembly *76*

Fibronectin Function *79*

Fibronectin expression in the bladder *80*

Candidate fibronectin integrin receptor *81*

INTEGRINS 82

Integrin structure *83*

Integrin subunit cytoplasmic binding sites *89*

Cytoplasmic binding sites of integrin α subunits *89*

Cytoplasmic binding sites of integrin β subunits *89*

Actin binding proteins *90*

Signalling molecules that bind β-integrin cytoplasmic tails *94*

β4 integrins are a component of hemidesmosomes *96*

Integrin activation *99*

Clustering of integrins and focal complex formation *99*

Focal adhesions form from focal complexes *100*

Fibrillar adhesions *101*

Three-dimensional focal adhesions *101*

Phylogeny of integrins *101*

Integrins expressed in the bladder *105*

DSMC integrins *105*

Urothelial integrins *105*

CELL SHAPE AND FATE 106

MECHANICAL STRETCH AND NORMAL DEVELOPMENT OF THE BLADDER 107

Integrins as mechanoreceptors *107*

Mechanical stretch in vivo *107*

Is it stretch, or pressure, or both? *108*

ORIGINS OF CONNECTIVE TISSUE 110

Connective tissue and the cells that produce it *110*

SOLUBLE GROWTH FACTORS INVOLVED IN BLADDER DEVELOPMENT 112

Normal patterning *112*

Response to stretch *113*

CONGENITAL BLADDER OUTFLOW OBSTRUCTION 115

Causes of fetal bladder outflow obstruction *115*

Posterior urethral valves *115*

Prune belly syndrome (Triad syndrome, Eagle-Barrett syndrome) *116*

Female pseudo-prune belly *117*

Urethral atresia *117*

Patent urachus *118*

Accuracy of radiological diagnosis of antenatal bladder outflow obstruction *119*

Uncertainty of diagnosis of BOO in post mortem specimens *120*

Consequences of fetal bladder outflow obstruction *121*

Renal dysplasia and obstructive uropathy *122*

Response of the bladder to obstruction *124*

Extracellular matrix in BOO *128*

CONCLUSION 132

ECM MOLECULES STUDIED IN THIS THESIS 133

Fibronectin *133*

Laminin *134*

CANDIDATE INTEGRIN RECEPTORS STUDIED IN THIS THESIS 136

Candidate fibronectin integrin receptor *136*

Candidate laminin integrin receptor in detrusor *136*

CHAPTER 2. HYPOTHESES AND EXPERIMENTAL STRATEGY 137

OVERALL HYPOTHESIS 137

SPECIFIC HYPOTHESES 137

Study 1 (Chapter 5): Analysis of expression of adhesion molecules fibronectin and laminin-1/2 and their candidate receptors during fetal mouse bladder development *137*

Study 2 (Chapter 6): Functional interaction between DSMC and fibronectin matrix in cell culture. *138*

Study 3 (Chapter 7): Mouse fetal bladder explant fibronectin blocking experiment. *140*

Study 4 (Chapter 8): Fibronectin expression in normal and pathological development of human fetal bladders *141*

CHAPTER 3. MATERIALS 143

MOUSE TISSUE 143

HUMAN FETAL TISSUE 143

REAGENTS 150

CHAPTER 4. METHODS 154

STUDY 1I: IMMUNOHISTOCHEMISTRY 154

Frozen sections 154

Controls 155

Mouse primary antibodies on mouse tissue – immunostaining using Dako animal research kit (ARK) 156

Antibody specificity 156

STUDY 1II : WESTERN BLOTTING 159

STUDY 1III: FLOW CYTOMETRY 168

Generating a cell suspension. 172

Quantification of cell counts. 172

Cell viability 173

Coating of slides with fibronectin 173

Adhesion experiment 174

Analysis 176

Quantification of proliferation 177

Quantification of Apoptosis 178

TUNEL test 178

Chromagenic TUNEL test in immunocytochemistry *180*

Measurement of cell death using LDH assay *181*

STUDY 3: ORGAN CULTURE EXPERIMENT 183

Generating the model *183*

Embryonic bladder explant experiments using anti-fibronectin antibody *184*

STUDY 4: HUMAN FETAL IMMUNOHISTOCHEMISTRY, MORPHOMETRIC ANALYSES 187

Paraffin Sections *187*

Masson's trichrome *187*

Van Gieson stain *191*

Immunohistochemistry *194*

Desmin-fibronectin colocalization *197*

Muscle morphology ('Muscle dysmorphology' score) *197*

Renal dysplasia *199*

Pulmonary hypoplasia *201*

Immunofluorescent TUNEL assay *201*

STATISTICAL ANALYSES 202

CHAPTER 5. ANALYSIS OF EXPRESSION OF ADHESION MOLECULES FIBRONECTIN AND LAMININ-1/2 AND THEIR

CANDIDATE RECEPTORS DURING FETAL MOUSE BLADDER DEVELOPMENT 204

HYPOTHESIS 204

BACKGROUND 204

AIMS 204

RESULTS 205

Fibronectin and candidate fibronectin receptor expression 205

Laminin and laminin binding integrins 214

DISCUSSION 220

Fibronectin and integrin α5β1 (a candidate DSMC fibronectin receptor) 220

Laminin and integrin α7β1 (laminin receptor) 225

CONCLUSION 230

CHAPTER 6. MOUSE BLADDER CELL CULTURE AND ADHESION BLOCKING EXPERIMENTS 231

HYPOTHESIS 231

BACKGROUND 231

AIMS 232

RESULTS 233

Cell adhesion to fibronectin substrate *233*

Characterisation of adherent cells *238*

Effect of fibronectin on proliferation *240*

Adhesion blocking experiments *242*

Adhesion in presence of anti-fibronectin antibody *242*

Blocking adhesion using anti-fibronectin receptor oligopeptides *242*

RGD/RAD oligopeptide apoptosis activation and toxicity *246*

DISCUSSION 246

CHAPTER 7. MOUSE FETAL BLADDER EXPLANT CULTURE 256

HYPOTHESIS 256

BACKGROUND 256

AIMS 257

RESULTS 257

Generating the explant model. *257*

Explant growth in presence of fibronectin blocking antibody. *261*

Explant growth *264*

Explant proliferation *266*

Differentiation *269*

DISCUSSION 271

AN EX-VIVO MODEL OF FETAL BLADDER MATURATION 271

CONCLUSION 278

HYPOTHESES 279

BACKGROUND 279

AIMS 280

RESULTS 280

NORMAL DEVELOPMENT: 280

Muscle *280*

Collagen *284*

Wall thickness *286*

Fibronectin *288*

Cell turnover in normal bladder development *291*

Comparison of normal male and female fetal bladders *291*

BLADDERS FROM FETUSES WITH PRESUMED BLADDER OUTFLOW OBSTRUCTION 293

Muscle *293*

Muscle morphology *293*

Collagen *294*

Fibronectin *298*

Renal dysplasia, muscle dysmorphology and fibronectin expression... 303

Proliferation and apoptosis in presumed obstructed fetal bladders..... 307

COMPARISONS BETWEEN NORMAL FETAL BLADDERS AND PRESUMED OBSTRUCTED FETAL BLADDERS 309

DISCUSSION 313

Normal development of the human fetal bladder..... 313

Fetal bladder outlet obstruction..... 316

Reliability of methods of quantification..... 318

Is renal dysplasia a marker for severity of bladder outlet obstruction?. 323

Study groups: presumed fetal bladder outlet obstruction and normal fetuses 323

Implications..... 325

Hypothetical models of response of human fetal bladders to obstruction 327

CONCLUSION 330

CHAPTER 9. FINAL DISCUSSION AND FUTURE WORK..... 331

A HYPOTHETICAL CELL BIOLOGY MODEL FOR BLADDER DEVELOPMENT 331

Role of Fibronectin..... 333

NORMAL AND PATHOLOGICAL HUMAN FETAL BLADDER DEVELOPMENT 335

FUTURE WORK 336

CONCLUSION 337

REFERENCES 339

APPENDIX 1 384

Integrin α5 positive control 384

Data from fibronectin, integrin α5 and β1 Western Blots 387

Integrin α6 subunit immunohistochemistry 389

Integrin α7 subunit immunohistochemistry 392

Integrin α7 subunit FACS analysis 395

APPENDIX 2: DATA FOR CELL ADHESION EXPERIMENTS 398

BACKGROUND DATA FOR CELL ADHESION EXPERIMENTS 398

1) Fibronectin plating concentration. 398

2) Immunocytochemistry 402

CD31 402

Cytokeratin 18 406

αSMA 409

3) Fibronectin proliferation experiment 412

4) RGD oligopeptides concentration 413

APPENDIX 3 417

Generating fetal mouse bladder explant model 417

APPENDIX 4 420

Assessment of cell turn-over in human fetal bladders 426

Ki67 426

Apoptosis 429

Muscle area, muscle percentage of surface area (%), Collagen and collagen percentage of surface area (%) and Muscle Collagen ratio ... 434

List of figures

Figure 1.1: Embryology of the bladder – Gastrulation and body folding 39

Figure 1.2: Embryology of the bladder - Cloacal separation 41

Figure 1.3: Reciprocal induction gives rise to the layers of the bladder 46

Figure 1.4: Hierarchical structure of connective tissue 51

Figure 1.5: Structure of laminin α1, β1 and γ1 subunits, laminin 1 trimer 53

Figure 1.6: Laminin polymerization 58

Figure 1.7: Laminin proteolytic fragments 59

Figure 1.8: Laminin-1 receptors 60

Figure 1.9: Structure of fibronectin 71

Figure 1.10: Integrin α and β subunit structure 85

Figure 1.11: Integrins may undergo a conformational change during activation 88

Figure 1.12: Activation of integrins 97

Figure 1.13: Integrin signalling pathways 98

Figure 1.14: Phylogenetic relationship of human integrin α subunits. 103

Figure 1.15: Phylogenetic relationship of human integrin β subunits. 104

Figure 1.16: Connective tissue cells make matrix, which in turn modifies cell behaviour 111

Figure 1.17: Partial bladder outflow obstruction in a rabbit model 127

Figure 4.1: Linearity/Saturation controls in Western blots 166

Figure 4.2: Demonstration of linear response from 25%-200% protein loading 167

Figure 4.3: Generating fetal murine bladder explant model..... 185

Figure 4.4: Setting up explant blocking experiment using immunoglobulins 186

Figure 4.5: Muscle area measurement using ImageJ..... 189

Figure 4.6: Morphometric analysis of bladder wall thickness 190

Figure 4.7: Measurement of Collagen proportion of surface area of sections of bladder using ImageJ 192

Figure 4.8: High power view of collagen fibres..... 193

Figure 4.9: Semi–quantification of fibronectin expression in fetal bladders. 196

Figure 4.10: Muscle dysmorphology score..... 198

Figure 4.11: Renal dysplasia associated with congenital bladder outflow obstruction..... 200

Figure 5.1: Fibronectin expression E14 to 6 wks postnatal 207

Figure 5.2: Integrin α5 expression E14 to 6 wks postnatal..... 208

Figure 5.3: Rabbit isotype control antibody E14 to 6wks postnatal 209

Figure 5.4: Quantification of fibronectin and fibronectin receptor by Western blot 210

Figure 5.5: Integrin β1 expression E14 to 6wks post natal murine bladders 213

Figure 5.6: Laminin α1 expression E14 to 6wks post natal murine bladders215

Figure 5.7: Laminin α2 expression E14 to 6wks postnatal murine bladders 216

Figure 5.8: Integrin α7 expression E14 to 6wks postnatal..... 219

Figure 5.9: Relative trends in fibronectin and fibronectin receptor expression 224

Figure 5.10: Western blot expression laminins versus integrin α7 flow cytometry 227

Figure 6.1: Adherence of whole bladder cell suspensions to fibronectin 235

Figure 6.2: Adhesion of E14 to adult bladder cell suspensions to fibronectin 237

Figure 6.3: Immunocytochemistry of adherent cells 239

Figure 6.4: BrdU incorporation by adherent E18 Cells 241

Figure 6.5: Non-specific effect of immunoglobulin on E18 whole bladder cell suspensions 244

Figure 6.6: Effect of RGD oligopeptides on adhesion and cell morphology. 245

Figure 6.7 Apoptosis and death associated with RGD oligopeptides 250

Figure 6.8: Hypothetical model of cell adhesion and spreading on fibronectin 252

Figure 7.1: Generating an explant model of fetal bladder development 259

Figure 7.2: Inhibitory effect of fetal calf serum on explant growth 260

Figure 7.3: Filtration and dialysis of IgG, explant experimental layout..... 262

Figure 7.4: Bladder variation at the start of the explant experiments..... 263

Figure 7.5: Outcome of explant fibronectin blocking experiment..... 265

Figure 7.6: PCNA expression in explants..... 268

Figure 7.7 Desmin expression in explants..... 270

Figure 7.8: Explant growth in cell numbers versus in vivo bladders 274

Figure 7.9: Smooth muscle maturation of explants versus in vivo bladders 275

Figure 8.1: Masson's trichrome staining of normal human fetal bladders from 14 weeks of gestational age to 31 weeks..... 282

Figure 8.2: Desmin immunostaining of normal human fetal bladders from 14 weeks of gestational age to 31 weeks..... 283

Figure 8.3: Van Gieson staining of normal human fetal bladders from 14 weeks of gestational age to 31 weeks..... 285

Figure 8.4: Morphometry of normal human fetal bladders..... 287

Figure 8.5: Fibronectin immunostaining of normal human fetal bladders from 14 weeks of gestational age to 31 weeks..... 289

Figure 8.6: Desmin and fibronectin double immunostaining in normal bladders (18 weeks gestational age) 290

Figure 8.7: Proliferation and apoptosis in normal fetal bladders..... 292

Figure 8.8: Fetal bladder outflow obstruction Masson's trichrome and Van Gieson stains 295

Figure 8.9: Morphometry of fetal bladder outflow obstruction..... 296

Figure 8.10: Muscle morphology in fetal bladder outflow obstruction..... 297

Figure 8.11: Fibronectin expression compared to muscle morphology in fetal bladder outflow obstruction. 299

Figure 8.12: Fibronectin and desmin double immunostaining in thick–walled obstructed bladder. 300

Figure 8.13: Fibronectin and desmin double immunostaining in disrupted, thin-walled obstructed bladder. 301

Figure 8.14: Fibronectin and desmin double immunostaining in the detrusor of normal, and fetal bladder outflow obstruction. 302

Figure 8.15: Detrusor muscle morphology and renal dysplasia 305

Figure 8.16: Detrusor fibronectin immunostaining and renal dysplasia 306

Figure 8.17: Proliferation and apoptosis in congenital bladder outflow obstruction 308

Figure 8.18: Comparison of total wall, detrusor and lamina propria thickness in congenital bladder outflow obstruction and normal bladders 311

Figure 8.19: Comparisons of fetal bladder outflow obstruction and normals 312

Figure 8.20: Comparison of linear, area, volume/mass measurements and concentration measurements 321

Figure 8.21: Hypothetical models of bladder dysgenesis resulting from fetal bladder outlet obstruction 329

Appendix 1: figure 1.1: Positive control for integrin α5 385

Appendix 1: figure 1.2: Positive control integrin β1 386

Appendix 1: figure 1.3: Laminin α1 (laminin-1) positive control 388b

Appendix 1: figure 1.4: Integrin α6 subunit positive control 390

Appendix 1: figure 1.5: Integrin α6 subunit immunohistochemistry 391

Appendix 1: figure 1.6: Optimisation of fixation for integrin α7 393

Appendix 1: figure 1.7: Myoblast positive control for integrin α7 immunostaining 394

Appendix 1: Figure 1.8: Dot-plots of integrin α7 flow cytometry 396

Appendix 2: Figure 2.1: Preliminary fibronectin adhesion experiment..... 401

Appendix 2: figure 2.2: CD31 positive control umbilical artery E14 403

Appendix 2: figure 2.3: CD31 expression in the developing bladder, in comparison with photography of microdissections 404

Appendix 2: figure 2.4: CD31 immunocytochemistry..... 405

Appendix 2: figure 2.5: Cytokeratin 18 immunostaining during mouse bladder development..... 407

Appendix 2: figure 2.6: Cytokeratin immunocytochemistry E18 bladder cell suspension on fibronectin-coated slides 408

Appendix 2: figure 2.7: αSMA immunostaining during mouse bladder development..... 410

Appendix 2: figure 2.8: αSMA immunocytochemistry E18 bladder cell suspension on fibronectin-coated slides 411

Appendix 2: figure 2.9: Fibronectin vs. RGD/RAD oligopeptide vs. blockade (%) 415

Appendix 2: figure 2.10: TUNEL test negative control (rTdT) not included, DNA nicks not labelled. 416

Appendix 3: Figure 3.1: Comparison in explant growth over 3 days: Antibiotics and FCS vs FCS vs ITS 418

Appendix 3: Figure 3.2: PCNA positive control 419

Appendix 4: figure 4.1: Positive control anti-human fibronectin antibody, Fetal Kidney 421

Appendix 4: figure 4.2: Positive control anti-human desmin antibody, muscle of fetal GIT 422

Appendix 4: figure 4.3: Ki67 immunostaining, positive control 427

Appendix 4: figure 4.4: Technique for assessing Ki67 positive cells 428

Appendix 4: figure 4.5: Confocal immunofluoresce TUNEL and PI in human fetal bladder urothelium 430

Appendix 4: figure 4.6: Confocal immunofluoresce TUNEL and PI in human fetal bladder lamina propria 431

Appendix 4: figure 4.7: Confocal immunofluoresce TUNEL and PI in human fetal bladder detrusor 432

Appendix 4: figure 4.8: Technique for counting apoptotic nuclei 433

List of tables

Table 1.1: Laminin subtype classification by subunit composition..... 55

Table 3.1: Morphologically 'Normal' human fetuses..... 145

Table 3.2: Human fetuses with presumed bladder outflow obstruction 148

Table 4.1: Primary antibodies..... 158

Appendix 1: Table 1.1: Fibronectin WB data..... 387

Appendix 1: Table 1.2: Integrin α5 WB data..... 387

Appendix 1: Table 1.3: Integrin β1 WB data..... 387

Appendix 1: Table 1.4: β-actin expression was unchanged throughout murine bladder development..... 387

Appendix 2: Table 2.1: Initial phase contrast adhesion experiment. 399

Appendix 2: Table 2.2: Fibronectin adhesion proliferation data..... 412

Appendix 2: Table 2.3: Preliminary RGD/RAD oligopeptides concentrations vs Fibronectin concentration. Percentage blockade is calculated from total cell numbers adherent for a cell suspension in presence of RAD (control peptide) minus total cell numbers adherent in presence of RGD (active blocking peptide), divided by RAD total and expressed as a percentage. 413

Appendix 3: Table 3.1: Comparison media additives and explant growth after three days 417

Appendix 4: Table 4.1: Tabulated results for human bladders 423

Appendix 4: Table 4.2: Tabulated results for human bladders – cell turnover 424

Appendix 4: Table 4.3: Area of fibronectin immunostaining vs. area of detrusor muscle..... 425

Preface. Hypothesis, aims and overview

Overall hypothesis

Extracellular matrix (ECM)/integrin interactions may be important in the early steps of normal bladder muscle growth and differentiation. Specifically, fibronectin acting through a candidate integrin receptor (integrin α5β1) may be important during bladder smooth muscle development in that it may maintain fetal smooth muscle cells (SMC) in a proliferative phenotype. Laminins acting through a candidate muscle laminin receptor integrin α7β1, may induce a maturation response, and might help maintain adult SMC in the differentiated form. These ECM/integrin interactions may also be important in pathological bladder morphogenesis as occurs in human fetal obstructive uropathy.

Overview

The results section of this thesis is arranged into four chapters as follows:

Study 1 (Chapter 5): Analysis of expression of adhesion molecules fibronectin and laminin-1/2 and their candidate receptors during fetal mouse bladder development

Hypothesis: During murine bladder development, the candidate fibronectin receptor integrin α5β1 may be expressed by detrusor smooth muscle cells (DSMC), and that laminin 1/2 candidate receptor integrin α7 may be expressed by DSMC.

Aims: 1) To examine if expression of candidate fibronectin receptor integrin $\alpha5\beta1$ and laminin 1/2 receptor integrin $\alpha7\beta1$ occurs in mouse bladders during fetal development and postnatal maturation by immunohistochemistry; 2) to further quantify this protein expression by using Western blots, or flow cytometry.

Study 2 (Chapter 6): Functional interaction between DSMC and fibronectin matrix in cell culture.

Hypothesis: In Vitro DSMC may adhere to fibronectin, possibly modifying cell behaviour, and that this adherence may be mediated by the candidate fibronectin receptor integrin $\alpha5\beta1$.

Aims: 1) to examine adhesion of disaggregated bladder cells from fetal and mature murine bladders to a fibronectin substrate; 2) characterise these adherent cells; 3) Examine any proliferative effect that fibronectin adhesion may have on fetal bladder cells; 4) Examine any effect blockade of fibronectin/integrin interaction may have on adhesion of cells from whole bladder suspensions.

Study 3 (Chapter 7): Mouse fetal bladder explant fibronectin blocking experiment.

Hypothesis: Fibronectin-integrin interactions in ex vivo bladders may be important in modulating DSMC development.

Aims: 1) Generate a fetal bladder explant model; 2) use this model to investigate the effect of disrupting fibronectin-integrin interactions on fetal bladder DSMC development.

Study 4 (Chapter 8): Fibronectin expression in normal and pathological development of human fetal bladders

Hypothesis: Fibronectin may be expressed in the basal lamina during normal human fetal DSMC development, furthermore altered fibronectin expression might be implicated in detrusor smooth muscle pathology in human bladder outflow obstruction (BOO).

Aims: 1) Demonstrate the normal pattern of fibronectin expression in human fetal bladders, and to correlate this with gestational age, and measures of cell turnover. 2) Describe the abnormal pattern of muscle, and fibronectin expression in presumed fetal BOO and to compare this with normal development.

Long-term Significance

An understanding of the role on matrix-integrin interactions in normal and pathological bladder development may contribute to a better understanding of the processes involved in normal development and in congenital uropathy. This may in the future provide an idea as to how the disease process may be modified and ultimately could lead to information useful in constructing a tissue-engineered neobladder.

Chapter 1. Introduction

The urinary bladder is a unique organ. It is the most distensible organ in the body, able, under normal circumstances in an adult human, to store 400-500mls of urine at low pressure, and then to expel this completely, several times a day (Chang et al 1998). This compliance is determined in part by the structural properties of the extracellular matrix (ECM) and cells that make up the bladder wall (Ewalt et al 1992). In congenital uropathies, such as posterior urethral valves (PUV), fetal urinary obstruction may be associated with a derangement of normal development, leading to a fibrotic, poorly compliant, high pressure reservoir and renal impairment. In man, posterior urethral valves are the commonest single cause of end-stage renal failure in childhood (Woolf and Thiruchelvam 2001) and PUV-associated bladder dysfunction may further damage the kidneys postnatally (Parkhouse et al 1988). Renal functional and structural outcome is therefore intimately linked to bladder function and hence bladder development.

An understanding of the molecular processes that influence bladder growth during development, and the role that ECM plays in this, is beginning to emerge. That fibronectin is an instructive molecule in fetal development can be seen by the severe mesodermal defects, and peri-implantation lethality of homozygous fibronectin null mutant mice. Two further lines of evidence demonstrate a role for ECM in normal bladder organogenesis: first, expression of the ECM components fibronectin and laminin are

developmentally regulated in the developing murine bladder (Smeulders et al 2002, 2003); second, smooth muscle cells grown on fibronectin are synthetic and proliferative (Morla and Mogford 2000), whereas these cells grown on laminins are more contractile (Thyberg and Hultgardh-Nilsson 1994). An important class of cell surface receptors for ECM are integrins. These heterodimers are formed from α and β subunits. So far more than 20 subtypes of integrin have been described in man, with different, but overlapping ligand affinities. These integrins have a structural role connecting ECM to the cell cytoskeleton, but also have important signalling roles in determining cell fate. Integrin sub-types have been reviewed by (Hynes 2002).

This thesis focuses on detrusor smooth muscle (DSM) cell development and on the accompanying changes in extracellular matrix, as described in the preface. The hypothesis for this thesis is that specific ECM proteins (fibronectin and laminins) interact with their integrin receptors (integrin $\alpha5\beta1$ as a candidate fibronectin receptor, integrin $\alpha7\beta1$ as a candidate laminin receptor) and that this may be important not only in the early steps of detrusor smooth muscle cell differentiation, but also in the pathological response to bladder outflow obstruction.

Described below are normal bladder embryology, and the changes in cell phenotype during organogenesis. The components of ECM are described, as is the hierarchical structure of connective tissue. Specifically the reasons for choosing the candidate matrix molecules are highlighted. Integrin structure, classification and function are reviewed, and the choice of integrin subtype to be examined in this thesis is justified.

The role of mechanical factors are in normal bladder development will be discussed both at the level of the whole organ, and at a cellular level. The role that integrins play in mechanotransduction – communicating physical forces from outside cells to the cytoskeleton - will be highlighted.

Finally, pathological bladder outflow obstruction (BOO) will be discussed.

Embryology of bladder development

Embryology of the mammalian urinary bladder involves the patterning of the tissues by gastrulation, then three dimensional body folding to create the cloaca. In placental mammals the cloaca is then divided, the anterior part becoming the urogenital sinus (UGS). The bladder forms from the cranial part of the UGS, and its surrounding mesenchyme, but also by incorporation of the distal mesonephric ducts to form the trigone (Larsen 2001).

Tissues formed by gastrulation. By day 14 post conception the human embryo consists of 2 layers: the epiblast and hypoblast. (These were previously termed ectoderm and endoderm.(Larsen 2001)) On day 15 the primitive streak appears on the dorsum. It is at this point that the fundamental axes of the body are established: cranial/caudal, left/right, ventral/dorsal. The definitive endoderm and intra-embryonic mesoderm form by gastrulation through the primitive streak (figure 1.1). Thus the epiblast gives rise to the ectoderm, mesoderm and endoderm. During the third week 2 depressions appear in the ectoderm, which fuse tightly with the endoderm, preventing ingrowth of the mesoderm: these are the buccopharyngeal membrane and the cloacal membrane. The allantois is a diverticulum of the endoderm that extends into the body stalk (Larsen 2001).

Cloaca created by 3D body folding. Embryonic folding occurs during the fourth week of human development converting the flat trilaminar germ disc into a three dimensional structure. This occurs because of rapid growth of the embryonic disc compared to the yolk sac. The endoderm at the lateral edge of

the embryonic disc is attached to the yolk sac, so the expanding disc bulges into a convex shape. As a result of this folding the cephalic, lateral and caudal folds meet in the mid-line. The endoderm now forms cranial and caudal blind-ending tubes (foregut and hindgut respectively), with the future midgut between them, widely connected to the yolk sac. The foregut ends in the buccopharyngeal membrane and the hind-gut at the cloaca, which abuts the cloacal membrane. The buccopharyngeal and the cloacal membranes have moved onto the ventral surface of the embryo, as has the body stalk (figure 1.1). The ectoderm that was immediately caudal to the cloacal membrane in the bilaminar disc has now been rotated to lie adjacent to the body stalk, *cranial* to the cloacal membrane. The cloaca has a ventral diverticulum which is formed by the allantois, which in turn passes through the umbilical ring, into the body stalk (Larsen 2001).

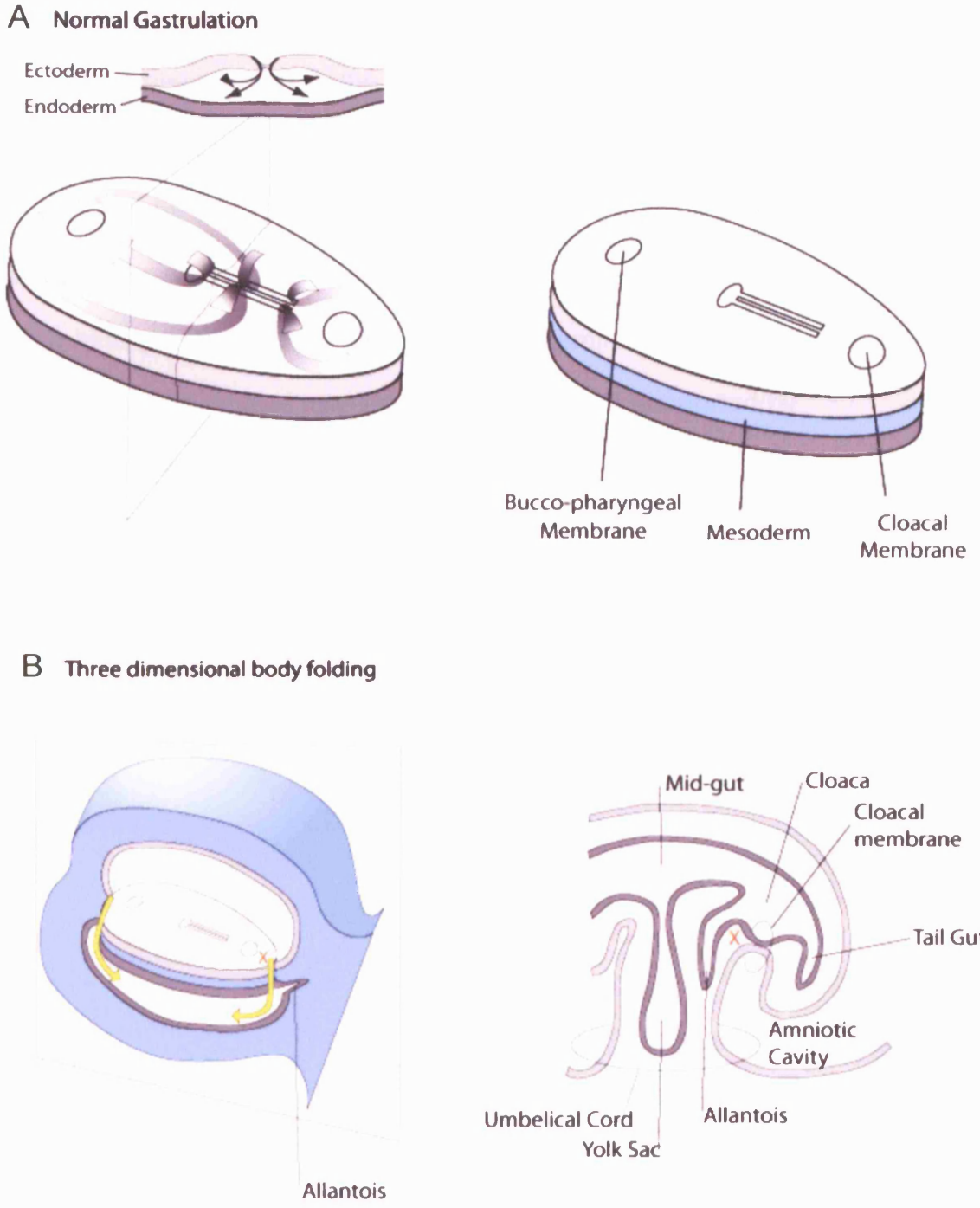

Figure 1.1:Embryology of the bladder – Gastrulation and body folding (A) Gastrulation is the process by which patterning of the embryonic tissues occurs, and cell and determined. (B) The tissues are then arranged in their correct anatomical relationship by the process of three dimensional body folding. Modified from Larsen 2001.

Division of cloaca into anterior urogenital sinus and posterior rectum. The wedge of mesoderm between the allantois and the yolk sac elongates and forms the Tourneux fold. Rathke's folds in the lateral wall of the cloaca fuse with the Tourneux fold growing down from cranially to produce the urorectal septum that separates the cloaca into an anterior urogenital sinus and a posterior hind-gut (figure 1.2). Eventually the bilaminar buccopharyngeal membrane and the cloacal membrane, which are not supported by mesoderm, break-down. This anterior urogenital sinus has a cranial component which will form the bladder, a pelvic component which will form the urethra in the female and posterior urethra in the male, and an external part which forms the introitus in the female and the urethra in the male (Larsen 2001; Thomas et al 2002).

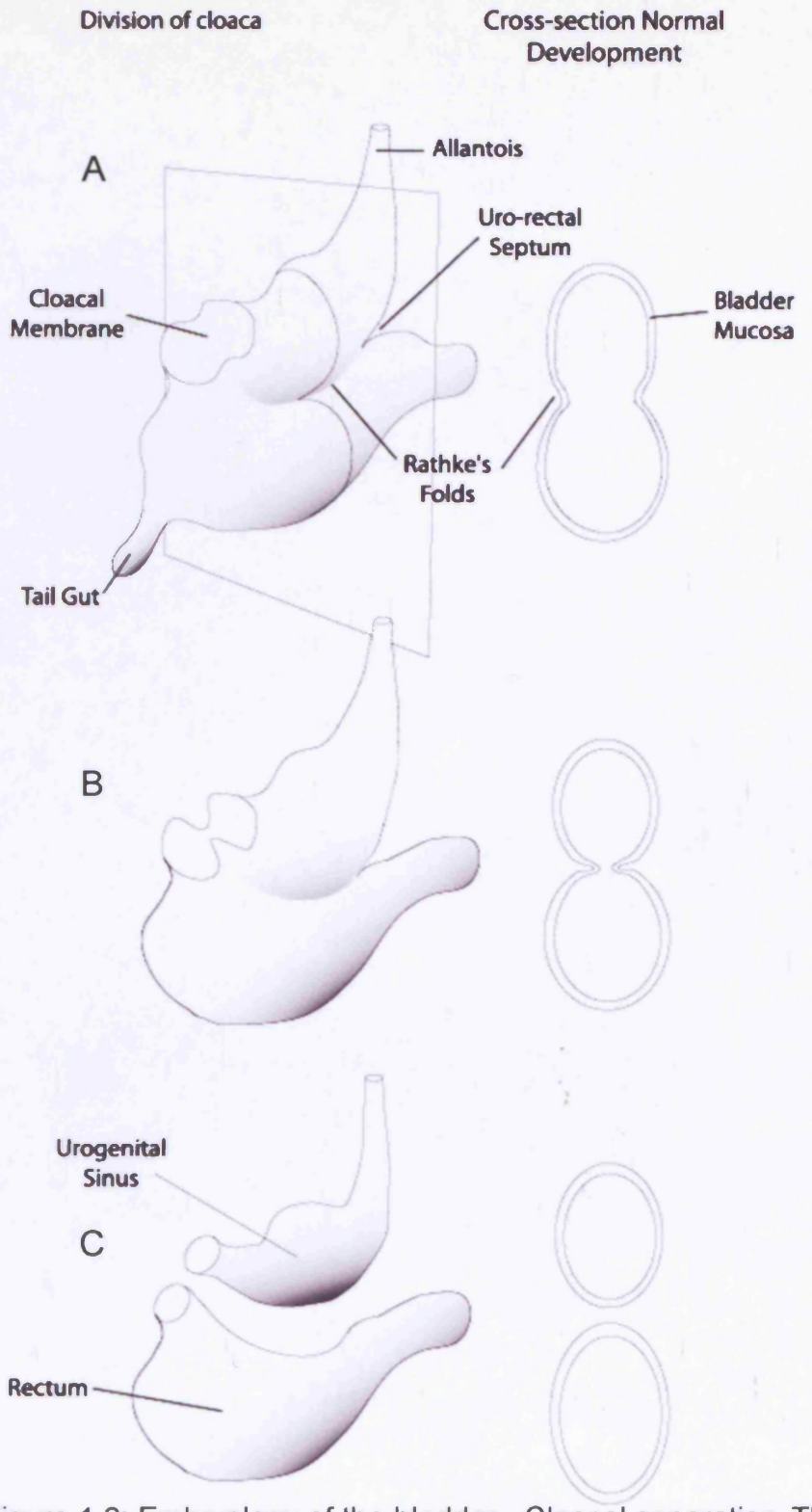

Figure 1.2: Embryology of the bladder - Cloacal separation The embryo is pictured supine, with the head posteriorly to the right, and tail anterior to the left. Only the endoderm is drawn for clarity. (A-C) the cloaca is progressively divided by the Tourneux fold (urorectal septum) from cranially and the Rathke's folds from laterally. Modified from Thomas 2002.

Formation of the bladder. The human urinary bladder develops from the cranial part of the urogenital sinus: the inner, endoderm gives rise to the bladder epithelium and its surrounding mesenchyme to the middle lamina propria and the outer smooth muscle layer. The exception is the base of the bladder, the trigone, where the caudal ends of the mesonephric ducts (the common excretory ducts) and their ureteric buds were thought to be gradually incorporated into the bladder wall, explaining the ureteric position in duplex renal anomalies (Mackie and Stephens 1975). More recently, it has been shown that in the mouse the common excretory duct undergoes apoptosis (Batourina et al 2005). By seven weeks the human bladder has a primitive urothelium, surrounded by undifferentiated mesenchyme. The mature bladder therefore has an inner urothelium, subjacent to this is the lamina propria, rich in interstitial collagens and blood vessels, surrounded by the detrusor layer of smooth muscle, covered by serosa (figures 1.3 and 1.4B).

Time-table for embryogenesis of the mouse bladder

The mouse provides an easily accessible, accurately timed source of embryonic bladder tissue, so this is the model studied. The cranial part of the urogenital sinus can be detected in the mouse at embryonic day 12 (E12). Incorporation of the distal mesonephric ducts occurs over days 12 and 13, so the bladder is a recognizable entity by embryonic day 14 (E14). This is equivalent to Carnegie stage 20 in the human (Kaufman 2003), or seven weeks gestational age (Hunter et al 2003). Bladder development has

therefore been studied in this thesis from embryonic day 14 onwards. Subsequent time-points include E16, E18 and neonatal day1 mouse bladders. Mice reach maturity by 6 weeks of postnatal age, so this was the final developmental time-point examined.

Changes in cell phenotype during detrusor development

In the mouse, the mesenchymal cells of the primitive bladder are initially highly proliferative (Smeulders et al 2002). Differentiation of these mesenchymal cells into smooth muscle cells requires mesenchymal-epithelial interaction (Baskin et al 1996b) (figure 1.3). Paradoxically, this smooth muscle differentiation first occurs at the periphery of the bladder, with the expression of smooth muscle markers such as α-smooth muscle actin (α-SMA), desmin, and smooth muscle myosin, expressed by fetal smooth muscle cells (Baskin et al 1996c;Wu et al 1999a). This is associated with a peak in expression of fibronectin in the ECM neonatally (Smeulders et al 2003). As bladder development progresses these fetal smooth muscle cells (SMC) become increasingly differentiated and decreasingly proliferative culminating in the mature adult SMC which in normal circumstances is non-proliferative (figure1.4A) (Smeulders et al 2002). Simultaneously, in the basal lamina surrounding these cells, fibronectin is replaced by laminin (Smeulders et al 2003). Ultrastructural examination, allows the synthetic fetal cells to be differentiated from the purely contractile adult cells (Wu et al 1999a): Fetal smooth muscle cells have prominent Golgi apparatus, a prominent 'fibronexus' (fibronectin fibrils in association with focal adhesions – please see

section on integrins), and prominent caveolae, yet still have a contractile apparatus; adult smooth muscle cells no longer have the synthetic apparatus, or the 'fibronexus', but do have more contractile machinery (Wu et al 1999a).

Urothelial development

In human bladders at 7 weeks, there is an initial primitive epithelium that is bilayered, with cuboidal glycogen rich epithelium. By 13-17 weeks of gestation this has developed a third layer and by 17-21 weeks, has become a 3-4 cell thick epithelium with the ultrastructural characteristics of urothelium (Newman and Antonakopoulos 1989). These 3 layers have been called basal, intermediate and superficial or umbrella cell layer, and are capable of sliding movement one over the other (De La et al 2002).

Epithelia can be classified according to their expression of cytokeratin intermediate fibres. There are approximately 20 sub-types described. In columnar epithelium simple cytokeratins are expressed – which include 8, 18, 19 and 20. Squamous epithelia elaborate instead cytokeratins 4 and 13 in non-keratinizing epithelia and 4 and 13 in keratinizing epithelia. Transitional epithelium (urothelium) contains both simple cytokeratins 8 and 18, but also squamous cytokeratins 4 and 13 (De La et al 2002).

Baskin et al have demonstrated that in rat bladders the urothelium initially expresses cytokeratins 7,8,18 and 19 at 15 days gestation (equivalent to embryonic day 14 in the fetal mouse), with the addition of cytokeratin 5 at 17 days gestation, and upregulation of cytokeratin 14 in the newborn bladder

(Baskin et al 1996c). De La Rosette et al have further shown that these cytokeratins are expressed in human epithelium also, but that there are specific layers of epithelium that particularly express some of these cytokeratins: cytokeratin 18 is predominantly expressed in the superficial, umbrella cell layer antenatally, whereas it is more generally expressed in all layers apart from the basal layer in postnatal bladders; cytokeratin 20 is expressed in intermediate and umbrella cell layers antenatally, but only in umbrella cells post natally; finally cytokeratin 5 is a marker of basal cells (De La et al 2002). This stratified expression of cytokeratins has been used by (Scriven et al 1997) to demonstrate reconstitution of transitional epithelium from monolayer culture.

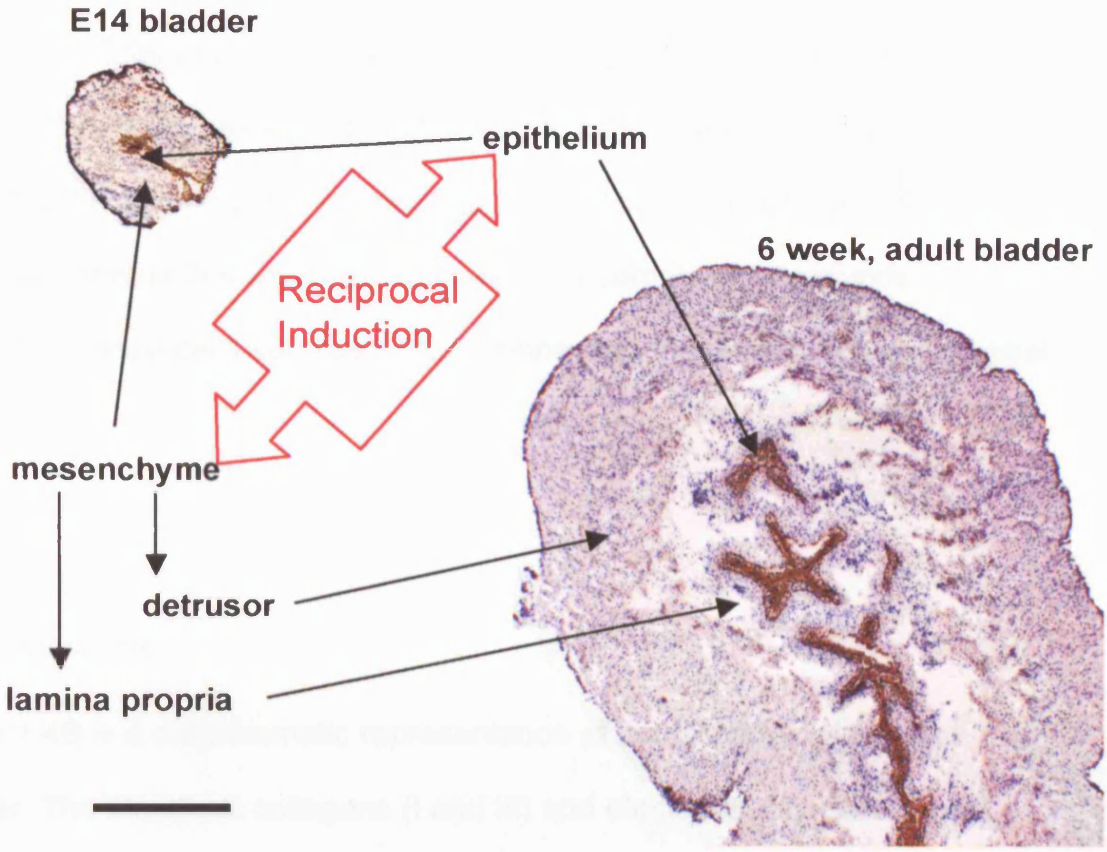

Figure 1.3. Reciprocal induction gives rise to the layers of the bladder. Embryonic day 14 (E14) mouse urinary bladder and 6 week, adult bladder, showing immunostaining for cytokeratin 18 (epithelial marker). These bladders are shown to the same scale (bar 1mm). The bladder at E14 is composed of only 2 layers: mesenchyme and epithelium. Reciprocal induction (red lines) between epithelium and mesenchyme is necessary for differentiation of smooth muscle cells, and for maturation of the epithelium to urothelium. The mature bladder has three layers to its wall: detrusor, lamina propria, and urothelium.

The hierarchical structure of connective tissue

That extracellular matrix is composed of two regions, the basal lamina (basement membrane) and interstitial matrix, can be seen on electron microscopy (Bosman and Stamenkovic 2003). The basal lamina is a condensed matrix that underlies epithelia, and completely surrounds connective tissue cells such as SMCs, connecting these cells to the interstitial matrix.

Interstitial matrix

Figure 1.4B is a diagrammatic representation of the histology of the mature bladder. The structural collagens (I and III) and elastin largely determine the mechanical properties of the bladder wall (Ewalt et al 1992). Most of the work that has been done on the changes in ECM during bladder development has therefore concentrated on these. The structural collagens are present predominantly in the lamina propria, underlying the urothelium, subserosally, and between the muscle fibres in the detrusor (Smeulders et al 2003). These collagens connect to the basal lamina which in turn adheres to the cells, via cell surface receptors, the most important of which are integrins, forming a hierarchical structure (figure 1.4C).

Components of basal lamina

The basal lamina is a specialised subset of the ECM that underlies epithelia and endothelia, and surrounds 'connective tissue cells' such as fibroblasts and smooth muscle cells. It is highly conserved, with the same four basic components being present in worms, fruit flies and man (Hynes and Zhao 2000) and reviewed by (Hutter et al 2000). These are laminins, collagen IV, nidogen (also known as entactin) and perlecan. The laminins are adhesive and bind cell surface receptors including integrins. These then bind to collagen IV, the cross-links being stabilised by nidogen and perlecan. Collagen IV is linked to the structural collagens (I and III) by adhesive collagens such as collagen VII and IX. Fibronectin in contrast is a later evolutionary innovation only present in the basal lamina of vertebrates (Hynes and Zhao 2000), not being present in *Caenorhabditis elegans* (Hutter et al 2000).

Collagen IV is secreted by connective tissue cells, including fetal SMCs (Baskin et al 1993b). Purified collagen IV will spontaneously polymerize forming a branching network (Yurchenco and Furthmayr 1984), similar to that seen in vivo (Yurchenco and Ruben 1987). This collagen network will bind to cell surface receptors (e.g. integrins $\alpha 1\beta 1$, and $\alpha 2\beta 1$) and to nidogen. Collagen IV null mutant mice survive until late gestation, coincident with the onset of muscle contractions, suggestive that there may be a role for collagen IV in resisting mechanical stress (Guo et al 1991).

Nidogen exists as two sub-types, nidogen-1 and nidogen-2, with similar structures. It is widely expressed in basal laminae. Nidogen-1 (entactin-1) is

150 kDa sulphated glycoprotein that consists of three globular domains connected by rod domains (Fox et al 1991). Nidogen-1 binds laminin, collagen IV perlecan and fibulins, forming a ternary structure. Blocking antibodies to integrin $\alpha 3\beta 1$ and $\alpha 6\beta 1$ have been shown to inhibit cell adhesion to nidogen-2 in cell culture, including A431 human epidermal cell line and HBL-100 human cell line (Salmivirta et al 2002). Cell culture studies demonstrated that antibodies to nidogen-G3 domain (laminin binding site) inhibited basement membrane formation (Aumailley et al 1993), but nidogen null mutant *C Elegans* (Kang and Kramer 2000) and nidogen-1 null mutant mice were able to from basal lamina, although the phenotypes were not normal (Murshed et al 2000). 'Compensation' appears to take place when nidogen-1 or -2 are knocked out.

Perlecan is a proteoglcan, consisting of a core protein of 400 kDa, with heparan sulphate or chondroitin sulfate attached. It is capable of binding nidogen, dystroglycan, and to immobilize fibroblastic growth factor (FGF) amongst other growth factors (Hopf et al 1999;Hopf et al 2001;Mongiat et al 2001). It is also widely expressed in basal lamina and cartilage (Handler et al 1997). Integrins have been shown to bind to perlecan, through an RGD independent mechanism (Hayashi et al 1992). Dystroglycan has recently been shown to be important for binding of perlecan to laminin (Kanagawa et al 2005). In homozygous perlecan null mice basal lamina failure occurred in myocardial basement membranes and also in basal lamina separating developing neuroectoderm from underlying mesenchyme (Costell et al 1999). These results suggest that there is a role for perlecan in basement membrane assembly and also in cell adhesion, making these membranes more resistant

to mechanical stress. In human disease mutant perlecans have been found in chondrodysplasia associated with myotonia (Stum et al 2005).

Taken together these observations have lead to Yurchenco et al (2004a) to suggest a hypothetical model of basal lamina formation in which cell surface receptors (integrins, dystroglycans and syndecans) bind to laminin G regions, leading to polymerization of laminin. This initial basal lamina subsequently has incorporation of nidogen and perlecan, which allow linkage with collagen IV to form a stable basement membrane (Yurchenco et al 2004a).

Other components of basal lamina include SPARC, fibulins, tenascins and fibronectin. Fibronectin is discussed below.

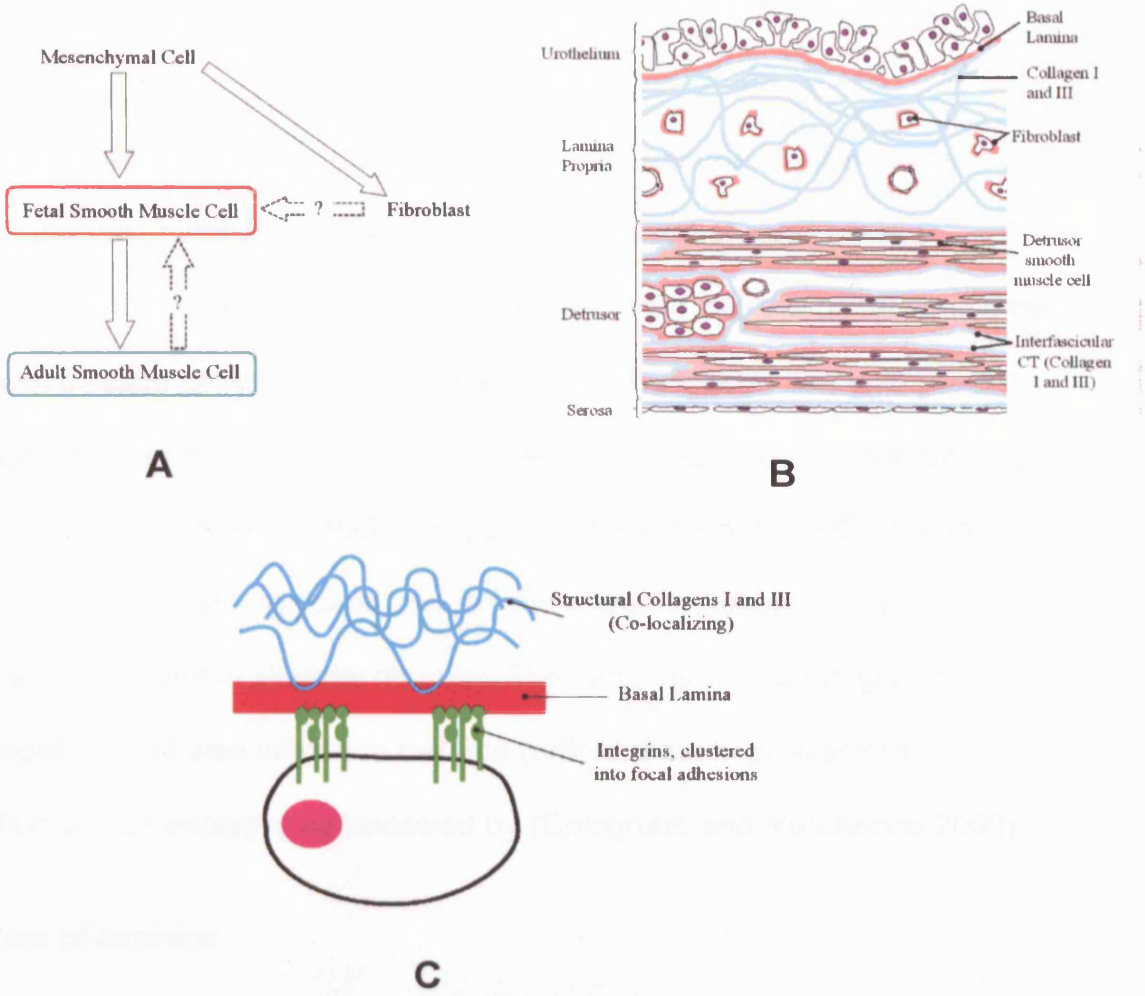

Figure 1.4 Hierarchical structure of connective tissue. (A) Mesenchymal cell differentiation pathways. Mesenchymal cells can differentiate into a fetal SMC phenotype stabilised by fibronectin (red box), which can in turn mature into an adult SMC phenotype maintained by laminins (green box), or can become fibroblasts. Dotted arrows with question marks show possible dedifferentiation/transdifferentiation pathways. Figure 1.4B: Histology of bladder wall: Collagen I and III, blue, predominates in lamina propria, inter-fascicular spaces of the detrusor, and sub-serosally. Lamina propria, pink, underlies urothelium, but completely surrounds SMCs in smooth muscle fibres. Figure 1.4C: Hierarchical structure of extracellular matrix. The structural collagens I and III, blue lines, link to basal lamina, pink. Cells adhere and interact with basal lamina through integrins, shown in green. Modified from McCarthy et al 2003.

Laminins

Twelve different sub-types of laminin have been described in the human (Colognato and Yurchenco 2000). Laminins are cross shaped trimers consisting of α, β and γ subunits. These are secreted into the basal lamina by connective tissue cells, where spontaneous polymerization can take place, although at physiological concentrations receptor mediated polymerization is important (Colognato et al 1999;Colognato and Yurchenco 2000). These receptors include dystroglycans and laminin integrins (integrin α7β1 is especially important in skeletal muscle). The laminins provide a 'glue' to link cells together, but also influence cell fate (differentiation, proliferation, migration and phenotype) as reviewed by (Colognato and Yurchenco 2000).

Structure of laminins

Laminins are eccentric cross-shaped trimers consisting of α, β and γ subunits. Heterotrimers are large proteins with a molecular mass ranging from 500 kDa to 1000 kDa. Each laminin subunit (α,β or γ chain) consists of: first an N terminal short arm of the laminin subunit laminin domain VI, and a globular laminin domain IV connected by multiple repeats of EGF domains; second, a coiled-coil-forming domain which forms the long arm. Ionic interactions between repeated heptad motifs on the coiled coil domain allow formation of the triple helix of the long arm (Beck et al 1993). It is the short arm domains that are involved in calcium dependent, spontaneous, reversible polymerization (Paulsson et al 1988;Cheng et al 1997).

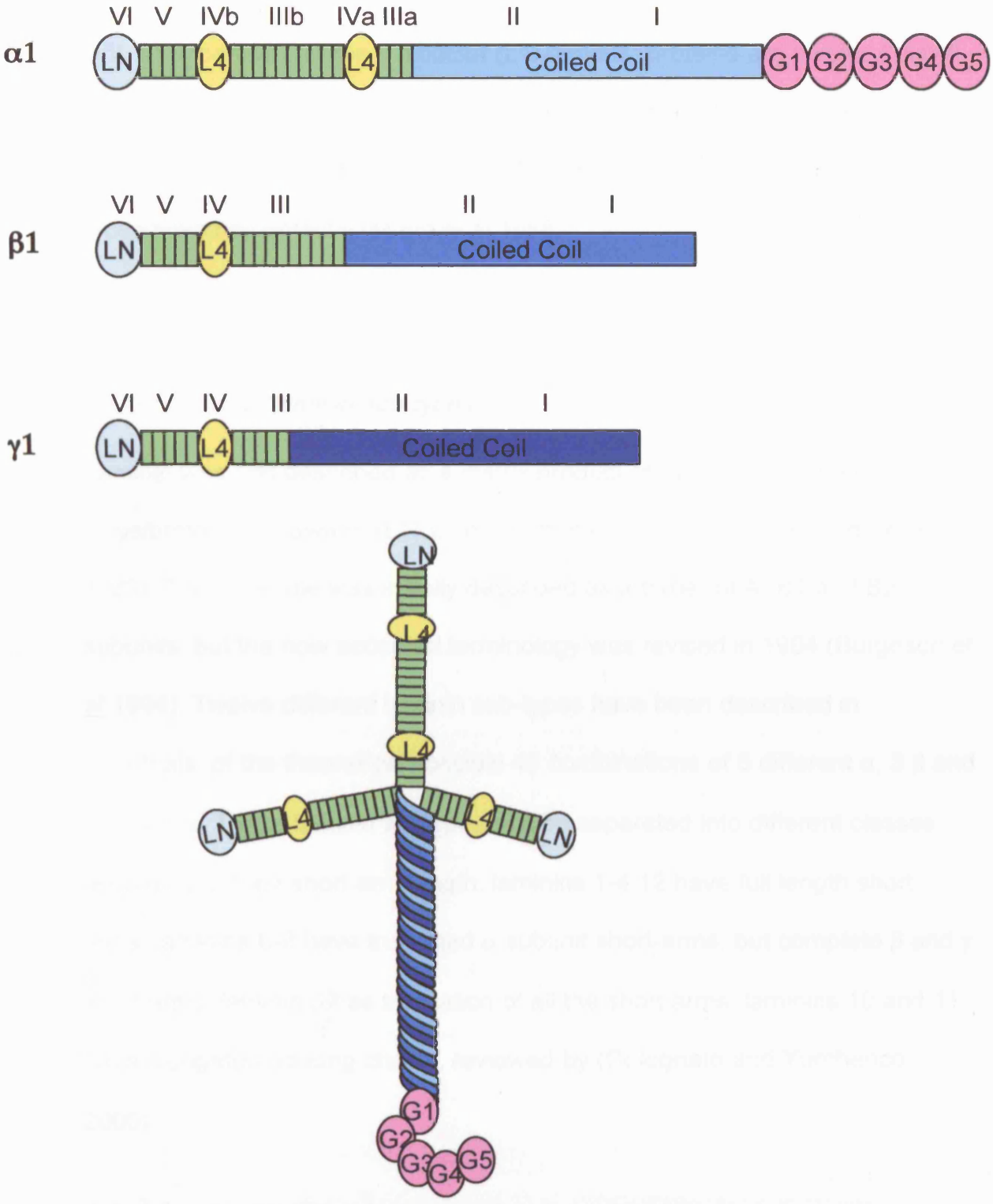

Figure 1.5: Laminin α,β,γ subunits form a laminin hetero trimer. Schemata for laminin α1,β1 and γ1 subunits. Together these form the laminin-1 heterotrimer. Modified from Colognato et al 1999

Laminin α subunits have 5 additional globular carboxy terminal domains, (G1-G5). The carboxy terminal globular (LG regions) proteins are involved in cell receptor binding (integrin α7β1 and α-dystroglycan-dystrophin in skeletal muscle cells) (Colognato et al 1999). Collagen IV binds to laminins and is also cross-linked by entactin (Mann et al 1988).

Classification of laminin sub-types

Laminin was first described as a matrix product of murine sarcoma cells, Engelbroth-Holm-Swarm (EHS) cells (Chung et al 1979; Brauer and Keller 1989). The molecule was initially described as a trimer of A, B1 and B2 subunits, but the now accepted terminology was revised in 1994 (Burgeson et al 1994). Twelve different laminin sub-types have been described in mammals, of the theoretical possible 45 combinations of 5 different α, 3 β and 3 γ chains. These laminin subtypes can be separated into different classes according to their short arm length: laminins 1-4,12 have full length short arms; laminins 6-9 have truncated α subunit short-arms, but complete β and γ short arms; laminin 5 has truncation of all the short arms; laminins 10 and 11 have elongated α5 long chains, reviewed by (Colognato and Yurchenco 2000).

Table 1.1: Laminin subtype classification by subunit composition

Laminin	Subunits
Laminin-1	α1β1γ1
Laminin-2	α2β1γ2
Laminin-3	α1β2γ2
Laminin-4	α2β2γ1
Laminin-5	α3β3γ2
Laminin-6	α3β1γ1
Laminin-7	α3β2γ1
Laminin-8	α4β1γ1
Laminin-9	α4β2γ1
Laminin-10	α5β1γ1
Laminin-11	α5β2γ1
Laminin-12	α2β1γ3

The distribution of different subunits (and hence different laminins) has been described. For example Laminin α1 is expressed in the developing embryo as part of the initial basal lamina in the developing embryo (Smyth et al 1999;Li et al 2002). Laminin α2 is expressed in skeletal and cardiac muscle, and in peripheral nerves and brain (Sunada et al 1995a;Sunada et al 1995b). Laminin α3 however is predominantly present in laminins in the basal lamina of skin and other epithelia – as demonstrated by the abnormalities of the

homozygous LAMA3 knockout mouse (Ryan et al 1999). Similarly whilst β1 subunit expression is widespread (Sasaki et al 1987), β2 expression is limited to the kidney (Noakes et al 1995) and neuromuscular junction (Hunter et al 1989) and β3 expression is present in epithelia (Pulkkinen et al 1995). Laminin γ1 is widely expressed, but γ2 is predominantly expressed in epithelia (Pulkkinen et al 1994), whereas γ3 is expressed in skin, heart, lung and reproductive tracts (Koch et al 1999).

Laminin production and polymerization

Laminins are produced by connective tissue cells, and epithelial cells. Specifically fetal SMCs have been shown to be produce laminin in culture (Baskin et al 1993b). The laminin α1, β1 and γ1 subunits are synthesized and secreted as laminin trimers. These laminin monomers then interact with cell surface receptors (integrins, dystroglycan and syndecan) through their G modules, allowing these trimers to become anchored. Polymerization spontaneously through their short arms then follows. This receptor-mediated polymerization has been specifically described in skeletal muscle myotubes by Colognato et al (1999), and in murine embryoid bodies (a model of gastrulation) by Li et al (2002). Once receptor mediated polymerization has occurred on skeletal cell myotube, a further reorganization of the cell surface receptors (dystroglycans, and integrins) occurs together with a conformational change in the attached cytoskeleton, producing a polygonal network of laminin extracellularly, and receptors and actin cytoskeleton intracellularly (Colognato et al 1999). There may well be signalling activated by this two-

stage process of receptor mediated laminin self-assembly, followed by cortical cytoskeleton rearrangement.

The amount of laminin expressed in basal lamina represents a balance between synthesis and breakdown. Matrix metalloproteinases are most probably important in the breakdown of ECM, and ultimately maintaining this balance.

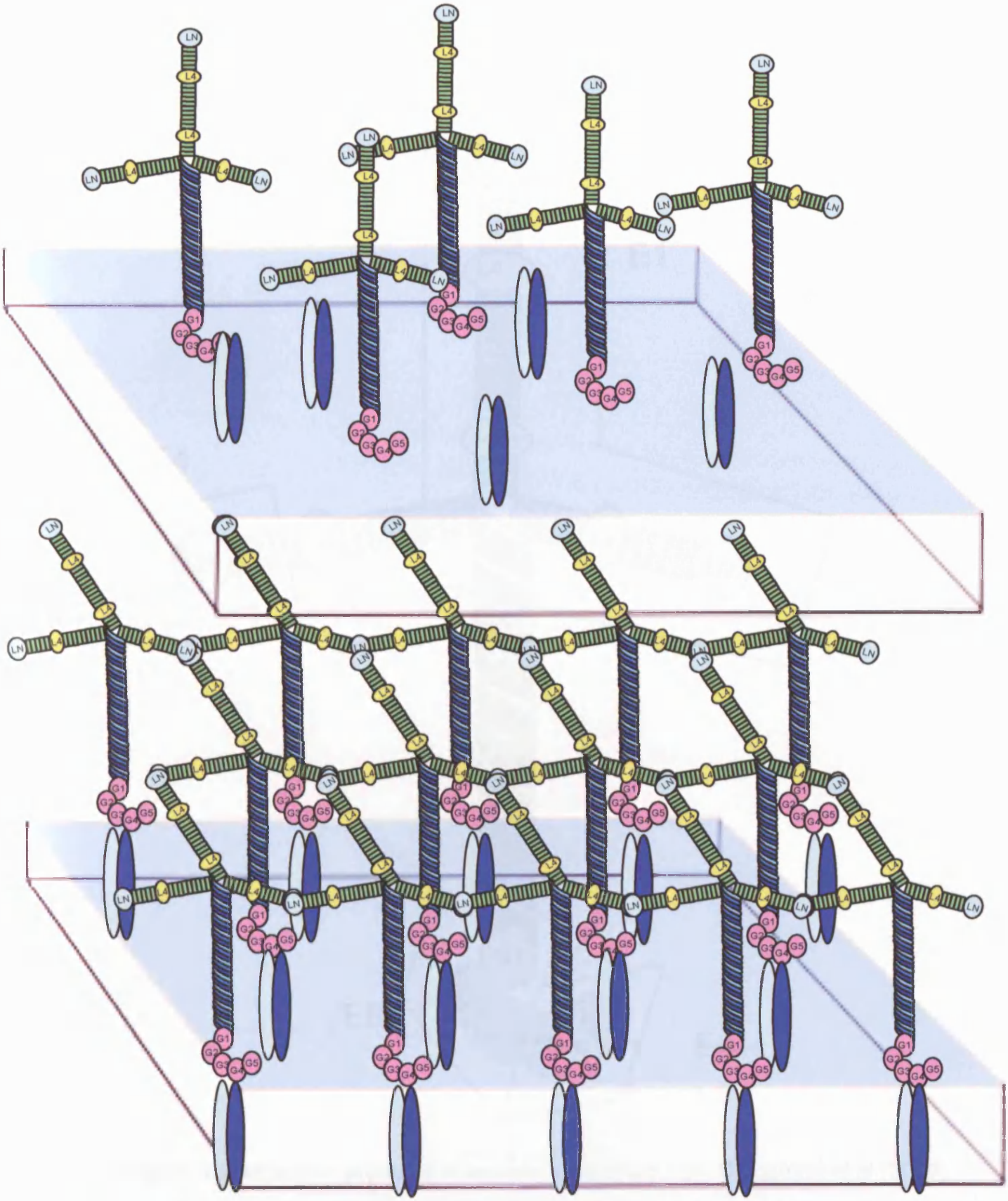

Figure 1.6: Receptor mediated laminin polymerization. Laminin-1 heterotrimers bind membrane bound receptors (e.g. integrins), and amino terminal short arms polymerize. The cell surface receptors become organized in turn, leading to cytoskeleton rearrangement. Modified from Colognato et al 1999.

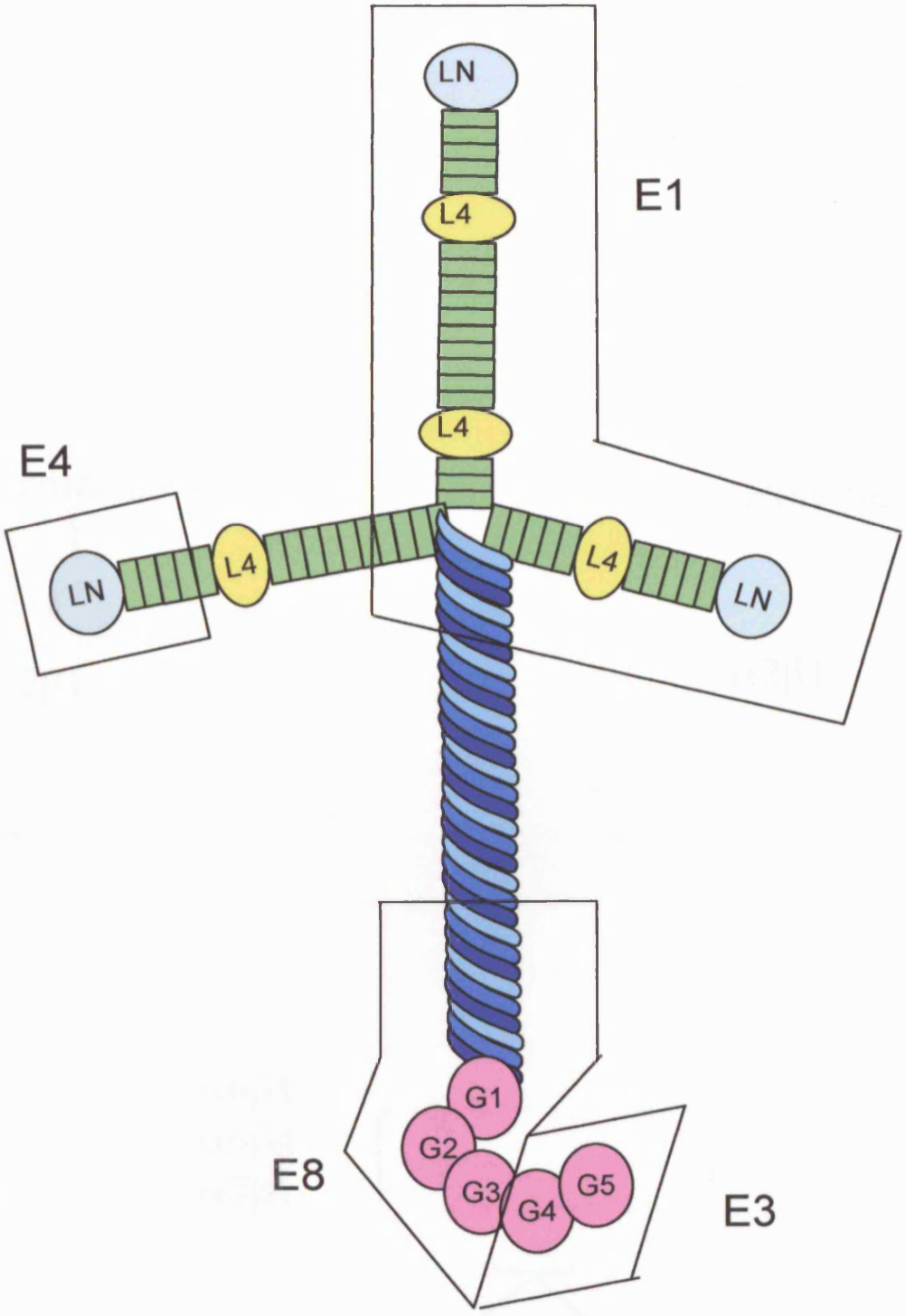

Figure 1.7: digestion products of laminin-1. Modified from Colognato et al (2000).

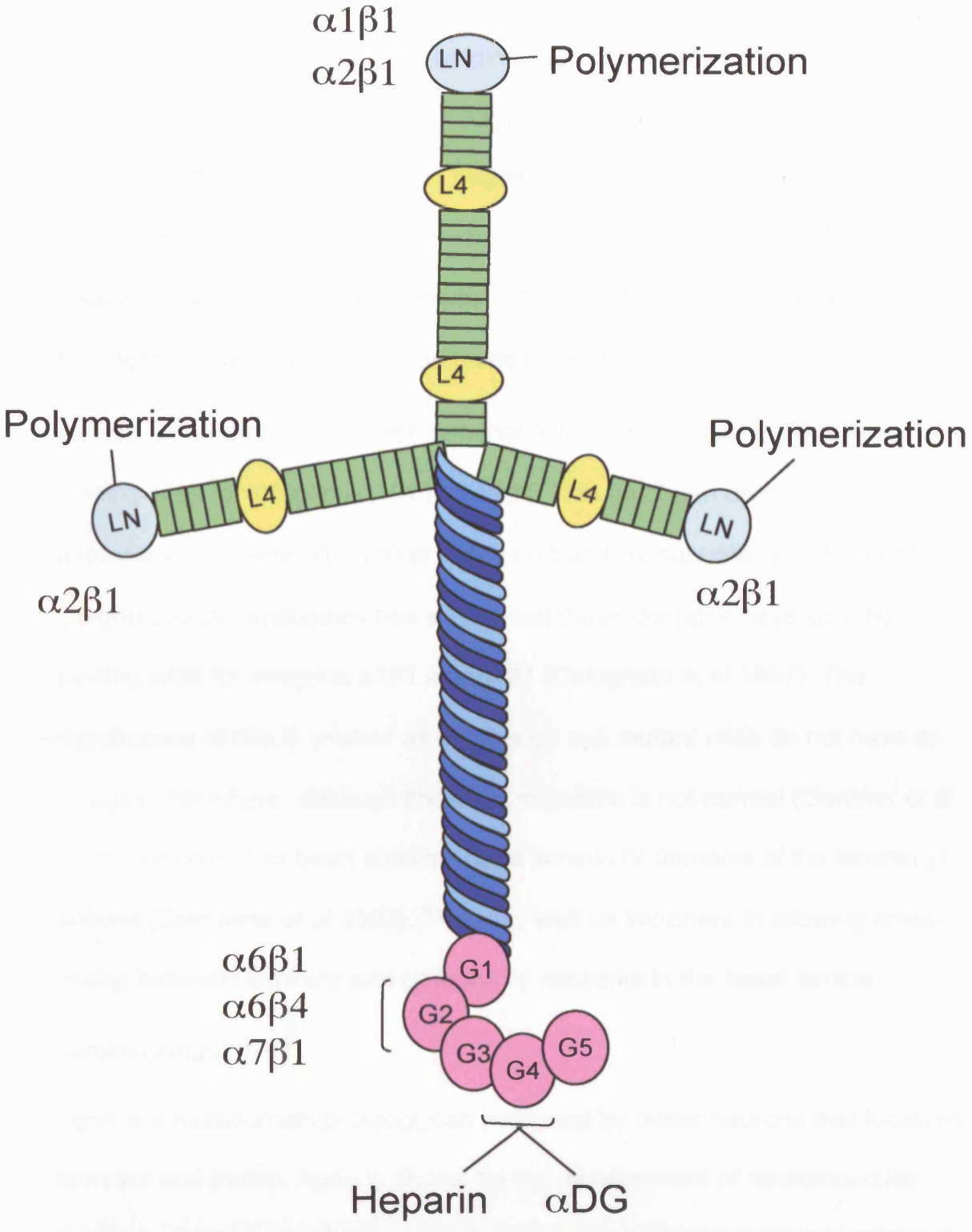

Figure 1.8: binding sites of laminin-1. α1β1, α2β1, α6β1, α6β4, α7β1 are integrin receptors. αDG is a-dystroglycan. Modified from Colognato et al (2000).

Laminin receptors

Receptors for laminin can ligate binding sites on the short arms, long arm, or G domain of laminin. Proteolysis fragments of laminins have been used to investigate these interactions: E1 fragment containing short arms of laminin α and γ chains, E8 containing the carboxy terminal of the long arms of α, β, and γ subunits, as well as the G domains G1 to G3 of the laminin α chain. The E3 fragment includes laminin α G domains G4 and G5.

Laminin short arms: The amino terminal of laminin α subunits have specific binding sites for integrins $\alpha1\beta1$ and $\alpha2\beta1$. This has been demonstrated by expressing domains IVb to VI of laminin $\alpha1$ and $\alpha2$ subunits. Blocking with integrin specific antibodies has shown that these domains have specific binding sites for integrins $\alpha1\beta1$ and $\alpha2\beta1$ (Colognato et al 1997). The significance of this is unclear as integrin $\alpha1$ null mutant mice do not have an obvious phenotype, although fibroblast migration is not normal (Gardner et al 1996). Nidogen has been shown to bind laminin IV domains of the laminin $\gamma1$ subunit (Salmivirta et al 2002). This may well be important in allowing cross-linking between laminins and collagen IV networks in the basal lamina.

Laminin long arms:

Agrin is a multidomain proteoglycan produced by motor neurons that localizes to motor end plates. Agrin is crucial for the development of neuromuscular junctions. It has been shown to bind to a region on the long arm of laminins 1, 2 and 4 (specifically to a 20 AA section of laminin $\gamma1$) (Kammerer et al 1999).

Laminin G domains:

E8 fragment (domains G1-G3): Integrin α6β1 and α6β4 bind specific regions of the G1-3 domains (fragment E8) (Aumailley et al 1990). Knockout mouse mutants of integrin α6 and β4 are neonatally lethal due to severe skin blistering as occurs in human junctional epidermolysis bullosa (Georges-Labouesse et al 1996).

Similarly integrin α7β1 binds the E8 fragment of laminins – which contains the G1-3 domains (Kramer et al 1991). This integrin binds laminin-2 and 4 more strongly than laminin 5 (Yao et al 1996b). Integrin α7 is reported to be expressed in skeletal muscle, cardiac muscle and smooth muscle (Yao et al 1996a;Yao et al 1997).

Integrin α3β1 also binds the E8 fragment of laminins, (G1-G3 domains). Recombinant soluble α3β1 has been shown to adhere to laminin 5, 10 and 11, but not laminin 1 or 2 (Eble et al 1998).

E3 fragment (domains G4, G5): The G4 domain contains a binding site for α-moiety of α-dystroglycan (Andac et al 1999; Hohenester and Engel 2002). Homozygous α-dystroglycan mouse mutants are lethal at peri-implantation at embryonic day 6.5 (Williamson et al 1997). Chaemeric mice for α-dystriglycan knockouts survive longer and develop a muscular dystrophy-like phenotype (Cote et al 1999).

The E3 fragment (domains G4 and G5) are also capable of binding heparin, heparan sulphates and sulfatides (Roberts et al 1985; Sung et al 1997). There is also a heparan binding site on the L4 domain of the short arm of the laminin α chain (Colognato-Pyke et al 1995).

Laminin function

Laminins are functionally important in two main ways.

1) Structurally, laminins are important in maintaining the mechanical properties of basal lamina acting. The interaction with nidogen, perlecan and collagen IV allows a 'ternary' structure to develop from the laminin and collagen IV networks. They are therefore important in maintaining the hierarchical structure of connective tissue.

2) Laminins are capable of acting as signals. A number of different examples exist including cell culture experiments, murine models of organogenesis and human diseases.

Determining cell differentiation in cell culture: Vascular SMC grown on fibronectin become synthetic and proliferative, whereas when similar cells are grown on laminins, they become differentiated, non-proliferative and contractile (Morla and Mogford 2000).

An intriguing possible role for laminin signalling has been described by Schuger et al (1997) in myogenesis in the lung bud: in this system mesenchymal-epithelial interaction results in laminin-1 expression only at the interface between the primitive epithelium and the lung-bud mesenchyme. The effect of this expression is to cause elongation of the mesenchymal cells and subsequent differentiation to a smooth muscle phenotype. Associated with this is upregulation of laminin-2 expression which further promotes smooth muscle differentiation (Schuger et al 1997;Relan et al 1999).

Basal lamina of skeletal muscle is rich in laminins, especially laminin 2 and 4. Defects in these laminins (especially laminin $\alpha 2$ subunit) and in their integrin (integrin $\alpha 7\beta 1$) and dystroglycan receptors result in congenital muscular dystrophy, (Mayer et al 1997; Burkin et al 2001; Yurchenco et al 2004b).

The signalling function of laminins may occur in two ways. Firstly, the receptor facilitated laminin self-assembly can induce laminin cortical rearrangement mediated through the cell surface receptors (integrins and dystroglycans) in skeletal muscle (Colognato et al 1999). Cell shape can influence differentiation and survival, as will be discussed below in the section on geometric control of cell fate (Relan et al 1999). Secondly, once the ternary structure of basal lamina (collagen IV and laminin networks stabilise by nidogen and perlecan), then the cell surface receptors for laminin, particularly integrins) can transmit signals either by mechanotransduction or by activating signalling pathways. This will be discussed further below.

Laminin expression in the mammalian urinary tract

Urinary bladder detrusor expression: Generic laminin expression progressively, as assessed by immunohistochemistry and Western blot, increases during murine detrusor smooth muscle (DSM) development (Smeulders et al 2003), and is strongly expressed, as assessed by immunohistochemistry, in the basal lamina of DSMC in adult human bladders (Wilson et al 1996). No published sub-typing of laminins has been described in the DSMC basal lamina. Fetal DSMC have been shown to produce laminin in culture (Baskin et al 1993b), but no sub-typing of laminins is described.

Urothelial basement membrane expression: The literature on urothelial basement membrane laminin production is more extensive. In murine bladders laminin is expressed in the urothelial basement membrane during development, however these laminins were not sub-typed (Baskin et al 1996a; Smeulders et al 2003). Wilson et al show that laminin is strongly expressed in the urothelium of human adult bladders, but again is not sub-typed (Wilson et al 1996). The prognostic significance of loss of decreased laminin 5 (as assessed by laminin $\gamma 2$ subunit immunostaining) from the basement membrane and increased stromal and intracellular immunostaining has been described with progression of urothelial carcinoma (Hindermann et al 2003; Kiyoshima et al 2005).

Expression in ureters: Hattori et al (2003) have demonstrated the pattern of expression of laminin subunits by real time polymerase chain reaction (RT PCR) of mRNA from cultured cells from adult human ureters (These were obtained from three radical nephrectomies performed for renal cell carcinoma. Adjacent ureteral tissue was examined histologically to confirm that cultured tissue was benign). Urothelial cells and stroma were cultured separately. Immunofluorescence of frozen sections of whole ureter probed with anti-laminin α chain antibodies was performed. This demonstrated that urothelial cells synthesized laminin $\alpha 1$, $\alpha 3$ (strongest signal on western blotting), and $\alpha 5$ chains, and that laminin 5 ($\alpha 3\beta 3\gamma 1$) was only present in the urothelial basement membrane, not elsewhere within the ureter. Stromal cells synthesized laminin $\alpha 1$, $\alpha 2$, $\alpha 4$ (most strongly staining on Western blot), $\beta 1$, $\beta 2$ and $\gamma 1$ subunits. The predominant laminins present in the stroma were

laminins 8 and 9 – although laminin α2 subunit was also present in this compartment (constituent of laminin 2, 4 and 12) (Hattori et al 2003).

Candidate laminin integrin receptor in detrusor

From preliminary results reported in Chapter 5 and the review of laminin subunits described above, receptors for laminin 1 (α1β1γ1) G domains (ie integrins α6β1 and α7β1) and laminin 2 and 4 (α2β1γ1 and α2β2γ1) G domains (i.e. integrin α3β1, α6β1 and α7β1) would be appropriate choices as candidate laminin receptors. In the Appendix preliminary immunohistochemistry results for integrin α6 immunostaining are described. No immunostaining was found in the developing murine detrusor layer. Integrin α7β1 was therefore chosen as the candidate integrin laminin receptor for this thesis.

Fibronectin

Fibronectin was first described by Hynes in 1973. It was identified by surface iodination as a 250 kDa protein present on the surface of normal tissue cultured cells, and easily removed by proteolytic digestion. Viral transformation inhibited its expression. Initially termed large external transformation sensitive (LETS) protein (Hynes 1973), LETS had a major effect on cell adhesion and morphology (Ali et al 1977), and was found on immunostaining to have a fibrillar pattern (Vaheri et al 1976). Mosher and Vaheri together with Ruoislahti coined the name 'fibronectin' for LETS. It was found to exist in two forms: as an ECM protein, and as a plasma protein. This plasma form binds fibrinogen and precipitates at 4°C which had lead Edsall in 1947 to name it 'cold insoluble globulin' (Edsall et al 1947). Fibronectin was subsequently found to not just adhere to fibrinogen, but also to denatured collagen (gelatin) allowing gelatin affinity chromatography to be used to purify it (Engvall and Ruoslahti 1977). Using an adhesion blocking antibody, and digestion fragments of the molecule, a 108 amino acid sequence was identified that promoted cell adhesion (Pierschbacher et al 1982). Subsequently the site of cell adhesion was isolated to a 4 amino acid moiety RGDS (Pierschbacher and Ruoslahti 1984). Using the RGD peptide coupled to sepharose allowed the identification of an RGD receptor that bound vitronectin, not fibronectin (and was subsequently found to be integrin $\alpha v\beta 3$) (Pytela et al 1985a). Using the active cell-binding domain of fibronectin as the

ligand instead allowed isolation of the fibronectin receptor (Pytela et al 1985b).

Fibronectin fibrils extracellularly parallel the actin cytoskeleton intracellularly, and connect to them (Heggeness et al 1978). These transmembrane connecting proteins were initially identified as 'fibronectin' receptors and named integrins (Tamkun et al 1986).

Fibronectin structure

Fibronectin normally exists as a dimer composed of 230-270 kDa subunits. Cellular fibronectin is produced by many cell types and is a component of basal lamina, whereas plasma fibronectin is a soluble molecule present at 300 μg/ml. Plasma fibronectin may be involved in wound healing and haemostasis.

Kornblihtt et al described the primary structure in 1985. Each monomer is composed of a mosaic of three fibronectin sub-types (termed fibronectin modules or repeats type I, II and III, 40, 60 and 90 residues long respectively). These are arranged as follows: amino- terminal of molecule 20 residues long; five type I repeats; a connecting strand; type I repeat; two type II repeats; three type I repeats; one type III repeat (in more recent literature this is termed fibronectin III-1); a connecting strand; 14 units of type III repeats (fibronectin III-2 to15); one connecting strand IIICS (also termed the variable region); one type III repeat; one connecting strand; three type I repeats; terminal carboxy- segment (Kornblihtt et al 1985).

Fibronectin monomers are covalently linked to form dimers by 2 disulphide bonds in the COOH terminal.

Alternative splicing can occur at three sites: EIIIA (Extradomain (ED)-A), EIIIB (ED-B), and the variable region V (IIICS) (Schwarzbauer et al 1989). This alternative splicing of the mRNA transcript has been reviewed by Ffrench-Constant (1995). The EIIIA domain is an extra type III repeat between the 11^{th} and 12^{th} type III repeats that can be included or excluded by exon skipping (Kornblihtt et al 1985). Similarly the EIIIB repeat, between fibronectin type III 7 and 8 repeats, can be included or excluded (Schwarzbauer et al 1987). The V-region can be alternatively spliced, with 5 different transcripts described in the human (V0 – no connecting AA residues in the variable region, V64 – 64 amino acid residues, V89, V95 and V120); three are described in the rat (V0, V95, V120); two are described in the chicken (V76 and V120) as reviewed by (ffrench-Constant 1995). Overall twenty different fibronectin isoforms have been described in the human, with 12 murine variants as reviewed by (ffrench-Constant 1995).

Plasma fibronectin produced by liver hepatocytes almost completely lacks EDA and EDB (Schwarzbauer et al 1987). Conversely, cellular fibronectin is detected by immunostaining with antibodies for EDA and EDB (Paul et al 1986). The expression of these EDA and EDB regions is developmentally regulated. EDA and EDB being present in fetal fibronectin, but is variably downregulated in post natal fibronectin in different tissues in frogs (DeSimone et al 1992) and chickens (Ffrench-Constant and Hynes 1989).

In skin wound healing in adult rats in situ hybridization data shows up-regulation of EDA and EDB in fibronectin mRNA (Ffrench-Constant et al 1989). Similarly RT-PCR has shown an upregulation of EDA in regenerating rat liver (Caputi et al 1995). This suggests a role in developmental regulation and wound healing for these splice variants of fibronectin. However, Muro et al have generated mouse mutants that constitutively expressed fibronectin containing EDA, or were homozygous for EDA absent fibronectin. These mice were all viable, and developed normally. Both mutants had shortened lifespans, but the EDA absent mice also had poor wound healing of their skin (Muro et al 2003). Similarly, the in vivo role of the EDB exon in mice has been investigated by producing EDB negative mice. These mice were normal and fertile, although fibroblasts from these mice did produce less fibronectin in vitro (Fukuda et al 2002).

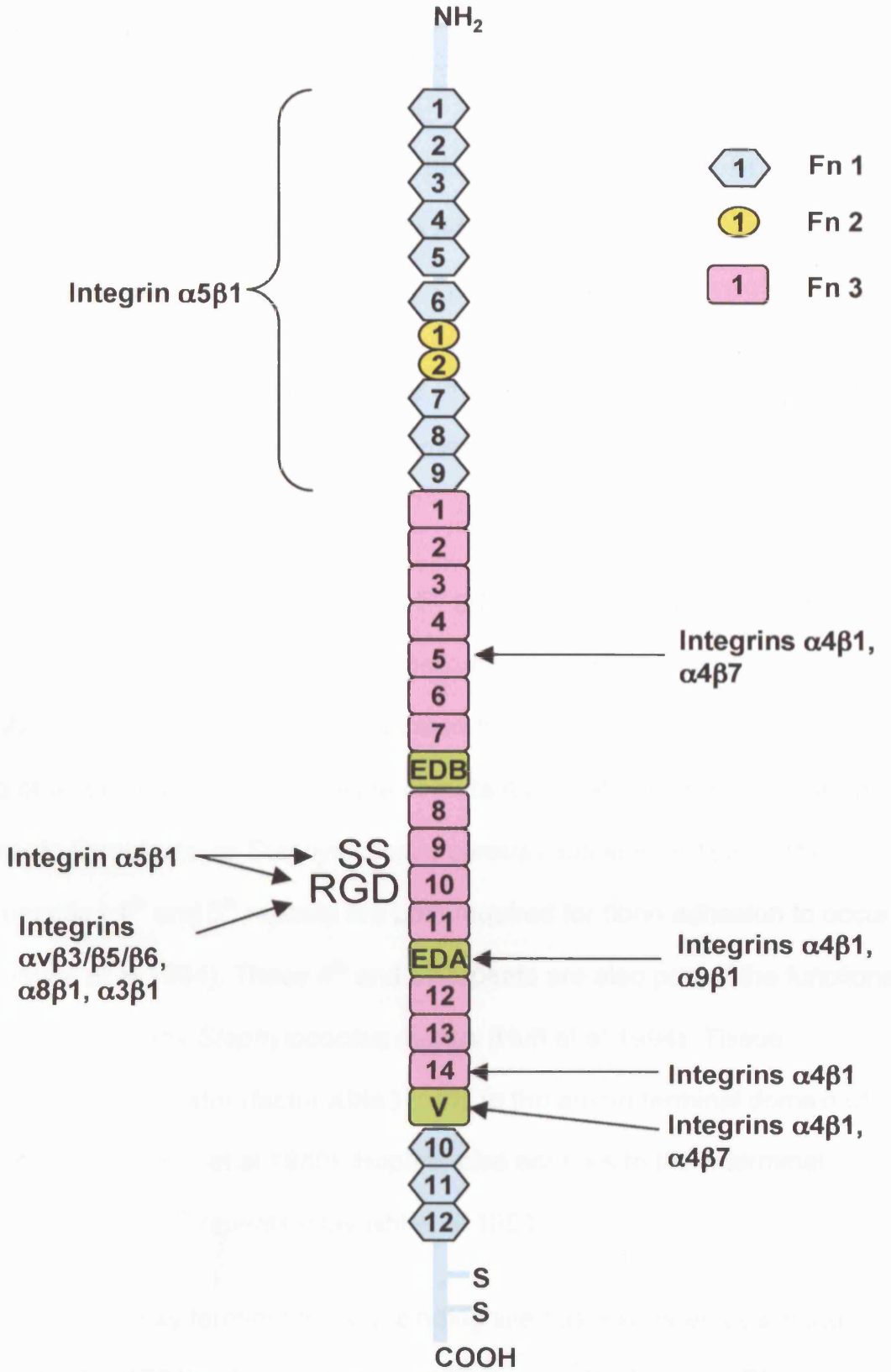

Figure1. 9: Structure of fibronectin, with integrin binding sites. Fn 1, fibronectin type 1 repeat , Fn 2 , fibronectin type 2 repeat; Fn 3, fibronectin type 3 repeat. RGD – arginine-glycine-aspartate recognition site. SS, synergy sequence. Modified from Pankov et al (2002).

Fibronectin receptors

Fibronectin molecules are capable of binding multiple ligands. ECM ligand sites, sites of fibronectin to fibronectin adhesion and integrin binding sites are discussed below.

1) ECM ligands: By using the strategy of protease digestion, and selective absorption onto ligands bound to agarose beads, several functional domains of fibronectin were identified.

The amino-terminal fibronectin I 1^{st} - 5^{th} (FNI 1-5) repeats are important for cellular fibronectin binding and polymerization as demonstrated by mutation analysis of fibronectin, in which truncated fibronectin was produced lacking one or all of these units, and failure of mutant truncated fibronectin to adhere either to fibroblasts, or *Staphylococcus aureus* (Sottile et al 1991). The fibronectin I 4^{th} and 5^{th} repeats are both required for fibrin adhesion to occur (Matsuka et al 1994). These 4^{th} and 5^{th} repeats are also part of the functional domain also binds *Staphylococcus aureus* (Huff et al 1994). Tissue plasminogen activator (factor XIIIa) binds to the amino terminal domain of fibronectin (Mosher et al 1980). Heparin also adheres to the n-terminal fibronectin I 1^{st} -5^{th} repeats (Hayashi et al 1980).

A second carboxy terminal heparin binding site has also been described (Richter et al 1981), which resides on 13^{th} fibronectin III repeat (FNIII 13). The binding site is formed from a 'cationic cradle' of 4 arginine residues and with interaction from a 2 further arginine and a lysine residue (Busby et al 1995).

Another glycosaminoglycan binding site has been described in the V region of fibronectin (Mostafavi-Pour et al 2001).

The collagen-binding domain of fibronectin was found by protease digestion of the intact molecule using trypsin (Ruoslahti et al 1979). This has been shown to be a functional domain containing FNI 6, FNII 1-2, FNI 7-9 (Skorstengaard et al 1994). It is a separate domain to the 'cell-binding' domain of fibronectin.

The 'cell-binding' domain of fibronectin was found to be an arginine-glycine aspartate (RGD) moiety on the 10^{th} fibronectin type III repeat (FNIII-10) (Pytela et al 1985b), that acts as an integrin binding site. Analysis of the crystal structure shows that the RGD moiety is on a 'stalk' projecting away from a molecule (approximately 10 angstroms (Å)), composed form FNIII 7-10 (Leahy et al 1996). Adhesion to this site is greatly increased by the presence of the 'synergistic' binding sites on FNIII 8 and 9 (Aota et al 1991). These domains are found to be 'facing' the RGD moiety on FNIII 10 on analysis of the crystal structure (Leahy et al 1996).

2) Fibronectin binding sites: Five fibronectin-fibronectin binding sites have been identified. These are: 1) the assembly domain, FNI 1-5 (Sottile et al 1991), 2) two binding partners for the assembly domain, FNIII 1-2 (Aguirre et al 1994) and FNIII 12-14 (Bultmann et al 1998); 3) FNIII 2-3 binding FNIII 12-14 (Johnson et al 1999) and FNIII 1 binds FNIII 7 (Ingham et al 1997). The assembly site (FNI 1-5) and the assembly partners are important in the polymerization of fibronectin dimmers to form fibrils (discussed below). The intramolecular interactions are important in maintaining plasma fibronectin in its compact form, preventing fibril formation (Cheng et al 1997).

3) Integrin binding sites on fibronectin:

EDA and V region: Integrin α4β1 has been shown to recognize the Heparin II binding region of fibronectin, FNIII12-14, and the 'V' region (Wayner et al 1989), allowing cell adhesion and migration of cultured melanoma cells (This integrin can also recognize vascular cell adhesion molecule-1 (VCAM-1). A specific amino acid sequence IDAPS is recognized in the heparin II binding region, on FNIII14 (Mould and Humphries 1991). Similarly the EDA region is a ligand for integrin α9β1, which is widely expressed in murine smooth muscle (Palmer et al 1993;Liao et al 2002). This integrin is upregulated transiently in cutaneous wound healing (Singh et al 2004).

FNIII 5: A similar short amino acid sequence on fibronectin type III repeat to that on FNIII 14 is recognized by integrin α4β1 and α4β7 (Moyano et al 1997). The functional significance of this is unclear.

N-Terminal FNI 1-9, FNII 1-2: The amino-terminal region when digested from intact fibronectin yields a 70 kDa fragment that contains the fibronectin assembly region and is recognised by a complex formed from the cell binding region of fibronectin and integrin α5β1 (Dzamba et al 1994).

FNIII10 RGD moiety: Integrin α5β1, αvβ3 (αvβ1,avβ5,avβ6), α8β1 and αIIbβ3 recognize this binding site. The 'vitronectin receptor' integrin αvβ3 was the original integrin identified using RGD in an affinity column (Pytela et al 1985a), with integrin α5β1 requiring the synergy site in FNIII 8-9 to also be included in the affinity column in order to adhere (Pytela et al 1985b). Integrin α8β1 has been shown to be a fibronectin, vitronectin and tenascin mediated by the RGD

moiety (Schnapp et al 1995a). This integrin is expressed in murine smooth muscle cells (Schnapp et al 1995b). The RGD sequence is also recognized by integrin αIIbβ3 expressed by platelets, but inclusion of the synergy binding site present in the central cell binding domain improves adhesion (Ginsberg et al 1985).

The evidence for integrin α3β1being an RGD receptor is conflicting. Integrin α3β1 (originally described as extra-cellular matrix receptor I (ECMR1) and VLA3) was described as being a receptor for collagen, laminin and fibronectin (Wayner and Carter 1987;Takada et al 1988). However at physiological salt concentrations human integrin α3β1 does not bind to fibronectin affinity columns (Hynes et al 1989). In contrast Elices et al have shown that integrin α3β1 may act as an RGD receptor (Elices et al 1991).

Fibronectin polymerization

Fibronectin matrix can be deposited by two mechanisms: firstly, deposition of a cellular fibronectin matrix which requires active cellular intervention; secondly, tissue injury results in the extravasation of plasma proteins and the formation of an 'injury associated' matrix in which fibronectin becomes bound.

Fibronectin matrix assembly

The process of fibronectin fibril assembly requires fibronectin-integrin interaction, fibronectin conformational change, and then polymerization.

Fibronectin-integrin adhesion: 1) Initially integrin-bound fibronectin is diffusely localized at the cell surface. 2) Receptor clustering associated with this dimeric FN cause the formation of complexes of integrin $\alpha 5\beta 1$, the cytoplasmic tails of which become associated with intracellular adapter proteins and actin cytoskeleton, forming fibrillar adhesions (Ohashi et al 2002). These fibrillar adhesions are composed of integrin $\alpha 5\beta 1$, focal adhesion kinase (FAK), vinculin and paxillin (Sechler and Schwarzbauer 1997), and are enriched with tensin in comparison to focal adhesions. Focal adhesions are fixed and contain integrin $\alpha v\beta 3$, paxillin and vinculin. It is from these fixed points that fibrils grow (in a centripetal direction towards the cell nucleus), 'pulled' by the fibrillar adhesions containing integrin $\alpha 5b1$, along actin stress fibres (Ohashi et al 2002). Cytochalasin B inhibits actin cytoskeleton and prevents further fibronectin fibrillogenesis, with some fibrils contracting (Ohashi et al 2002); similarly division of a growing fibronectin fibril using a laser causes the fibril to retract (Ohashi et al 1999). 3) The stretching of fibronectin fibrils may expose cryptogenic binding sites, and promote further polymerization.

Other cell-surface receptors can bind fibronectin and participate in fibrillogenesis. These include syndecan-4 (a transmembrane heparan sulphate proteoglycan) can bind FN. This stimulates RHO GTPases and FAK, enhancing fibrillogenesis (Saoncella et al 1999). The urokinase plasminogen

activator receptor (uPAR) has been shown on binding its P-25 ligand to promote integrin $\alpha5\beta1$ mediated fibronectin fibrillogenesis (Monaghan et al 2004).

Fibronectin conformation changes during fibrillogenesis: Soluble, plasma fibronectin has a compact conformation (Johnson et al 1999), held in this form by intramolecular interactions between FNIII2-3 and FNIII12-14. Recombinant fibronectin lacking FNIII1-7 rapidly assembles on the cell surface into detergent insoluble fibronectin aggregates (Sechler et al 1996). Fluorescence resonance energy transfer (FRET) has also been used to examine changes in fibronectin folding during fibrillogenesis. Random labelling using donor and acceptor fluorophores allows changes in FRET to identify alternative fibronectin conformations (Baneyx et al 2001). Fibronectin is compact in solution and on initial cell adhesion, but during initial clustering becomes more extended, with fibronectin dimmers in fibronectin fibrils being highly extended (Baneyx et al 2001, 2002). The highly extended conformation could allow further exposure of cryptic fibronectin binding sites (Baneyx et al 2002). Different alignments are possible because of the multiple fibronectin binding sites available on each molecule.

Fibronectin polymerization: Initially fibronectin is incorporated into short fibrils at the cell periphery. Subsequently the fibrils become thicker and longer (Ohashi et al 1999, 2002). Fibronectin dimers are incorporated into the growing fibrils by two processes: firstly by integrin binding (Fogerty et al 1990), secondly by fibronectin-fibronectin interactions independent of the RGD binding site (Sechler et al 1996). Initially these fibrils are deoxycholate

(DOC) soluble, but over a period of 2-3 hours become irreversibly insoluble (McKeown-Longo and Mosher 1983). This mechanism could be by covalent disulphide bridge formation between dimers, however biochemical analysis fails to support this. DOC insolubility may be due to the formation of stable non-covalent intermolecular interactions (Chen and Mosher 1996).

Initial fibronectin fibrillogenesis requires an activated integrin fibronectin receptor (often integrin $\alpha5\beta1$ (Pankov et al 2000)), fibronectin adhesion, and an intact cytoskeleton to generate tension (Wu et al 1995). Tensin dependent movement of the integrin $\alpha5\beta1$ complexes, along actin cytoskeleton, relative to fixed focal adhesions (containing integrin $\alpha v\beta3$) could be important in inducing conformational change in bound fibronectin dimers, exposing further binding sites (Pankov et al 2000).

Fibronectin fibril matrix maintenance is dynamic: In fibroblast culture, fibronectin matrix turnover is slow (McKeown-Longo and Mosher 1983), but continual, mediated by a caveolin-1 dependent endocytosis (Sottile and Chandler 2005). Continual fibronectin polymerization is necessary for maintenance of the fibronectin fibril network, which is in turn necessary for collagen I and thrombospondin deposition (Sottile and Hocking 2002).

Provisional matrix in wound healing: Tissue injury results in the extravasation of plasma proteins and the formation of an 'injury associated' matrix, the principle components of which are fibrin, which by the action of activated factor XIII, is cross-linked by plasma-derived fibronectin (Okada et al 1985). This fibronectin in concert with growth factors such as platelet derived growth factor and transforming growth factor β result in migration of fibroblasts, and

their transformation into myofibroblasts (Lariviere et al 2003). This results in wound contraction, ECM synthesis, including locally produced cellular fibronectin, and wound healing (Gabbiani 2003).

Fibronectin Function

Evidence for a functional relevance of fibronectin expression comes from several lines of research including cell culture work, and knockout mouse mutants. Smooth muscle function can depend on ECM, as vascular smooth muscle cells can be switched from a contractile phenotype when cultured on laminin, to a synthetic type on fibronectin (Thyberg and Hultgardh-Nilsson 1994). Similarly on fibronectin VSMC are more proliferative than when cultured on laminin (Morla and Mogford 2000). It has been shown that a fibronectin matrix is necessary for the polymerization of collagen I and III (Velling et al 2002).

Homozygous fibronectin null mouse mutants are lethal, suffering severe mesodermal defects including impaired angiogenesis (George et al 1993). These homozygous mutants implant, gastrulation starts, but have no notochord, or somites, with variable degrees of deformity of the heart, intra and extra-embryonic vasculature and amnion. This reinforces the general requirement for this ECM protein during development, but unfortunately these mouse mutants die at embryonic day 8, before bladder development has started. These mutants are therefore uninformative with regards bladder development (George et al 1993).

The composition of the ECM surrounding a connective tissue cell is a balance between synthesis of the ECM components and their breakdown (for example by matrix metalloproteinases). The ECM in turn influences the behaviour of the cells. This has been demonstrated by (Hedin et al 1997) who found that VSMCs cultured on laminin whilst initially non-proliferative, became so after a number of hours with the production of their own fibronectin matrix. This required the expression of the fibronectin receptor integrin α5β1 (see below).

Fibronectin expression in the bladder

The descriptive murine urinary bladder studies of Smeulders et al have demonstrated that detrusor fibronectin expression rises form embryonic day 14 (E14) to a peak at the end of gestation, neonatal day 1(D1), by western blot, with a fall in levels postnatally with maturation at 6weeks, in parallel to the expression of the fetal smooth muscle cell phenotype (Smeulders et al 2002, 2003). E14 is the first day in the fetal mouse that the bladder can be easily isolated as a discrete organ. Smeulders et al used Chemicon AB2033, as used in this thesis. In a study of adult human bladders fibronectin is shown to be expressed in the detrusor SMC basal lamina (Wilson et al 1996). In ultrastructural studies of the developing rat bladder (from E14, E18 newborn and adults), fetal SMCs are shown to have a fibronexus (Wu et al 1999a). This fibronexus has previously been shown to consist in part of fibronectin fibrils, actin cytoskeleton and connecting proteins in both SV40 transformed, cultured hamster fibroblasts, and cultured human fibroblasts (Singer 1979).

Candidate fibronectin integrin receptor

Possible candidates include integrins $\alpha 4\beta 1$, $\alpha 5\beta 1$, $\alpha v\beta 3$, $\alpha 8\beta 1$. Integrin $\alpha IIb\beta 3$ is predominantly a platelet expressed integrin although ectopic expression has been described in tumours. Integrin $\alpha 5\beta 1$ is the archetypal fibronectin receptor and important not just in ligation of fibronectin, but also in fibrillogenesis; for these reasons it was the candidate fibronectin receptor studied in this thesis.

Integrins

As described above in the introductory section to fibronectin, the first 'integrin' identified was the vitronectin receptor, followed by the fibronectin receptor. It rapidly became apparent that there was a family of heterodimeric receptors that had similar structure and function. These receptors connected ECM and the intracellular cytoskeleton – 'integrating' the inside and outside of the cell, influencing cell migration and adhesion. (Hynes 1987) coined the term integrin in a review article, and labelled the subunits as α or β.

Eighteen α subunits, and eight β subunits have been described, forming by noncovalent interaction 24 different integrin subtypes, as reviewed by (Hynes 2002). Further complexity is achieved by post-translational modification, modulation of integrin ligand affinity and interactions with ECM, cell surface and intracellular molecules. Integrins can adopt a low affinity state for their ECM ligands, which on activation (which may be an 'outside-in' or 'inside-out' signal), clump together to form focal adhesions, reinforcing ECM cell cytoskeleton interactions and recruiting many other cell surface molecules that can act as receptors, as well as proteins many with dual structural and signalling function.

Integrin receptors are 'polygamous', capable of recognizing many different ECM ligands, often via common minimal recognition sequences. Ligand binding is, however, greatly modified by the context of these sequences: firstly ligand conformation regulates availability of the recognition site, e.g. RGD binding site of fibronectin is more readily available than the cryptic RGD site on collagen which only becomes available on damaging the collagen molecule; secondly, neighbouring sequences on the ligand modify integrin

receptor binding, e.g. the fibronectin synergy binding site composed of FNIII repeats 8-9 modifies integrin $\alpha 5\beta 1$ ligation of fibronectin (Aota et al 1991). Integrin-ligand binding has been reviewed by (Plow et al 2000). Loss of one subtype of integrin receptor can be compensated by another integrin subtype as reviewed by (De Arcangelis and Georges-Labouesse 2000).
Below will be reviewed integrin structure, classification, integrin 'binding sites', activation, focal adhesion formation and function, interaction between cell shape and integrin function, and mechanotransduction.

Integrin structure

Integrins are heterodimers of one α subunit, and one β subunit, noncovalently associated. Each subunit is composed of a large extracellular component formed from multiple structural domains composed of several hundred amino acid residues, a transmembrane domain, and a small cytoplasmic domain of between 20 and 70 residues.
α-subunit basic structure. Extracellular domain 1) The amino terminal has a 7-fold β propeller head (which complexes with the β subunit I-like domain), 2) connects to a thigh domain (1^{st} β sheet domain), a linker domain which can act as a 'genu' or knee and connects to 3) calf-1 domain (2^{nd} β sheet domain), and 4) calf-2 domain (3^{rd} β sheet domain). This connects to a transmembrane domain, which in turn connects to the cytoplasmic domain. The membrane proximal cytoplasmic domain has a highly conserved GFFKR amino acid sequence involved in binding the cytoplasmic tail of the β subunit, and control of integrin activation (O'Toole et al 1991;O'Toole et al 1994).

I/A Domain: α subunits can be classified by the presence or absence of an extra I/A domain. α subunits lacking the I/A domain include α3, α6, α7, α5, αv and α8. α subunits including the I/A domain include α1 ,α2, α10, α11, α4 and α9.

β-subunit basic structure. The head of the β subunit is formed from a loop formed by the disulphide bonding of the N-terminal PSI-like domain to the distal end of the β subunit leg. The most distal end of the loop is therefore formed from the β I/A domain. The 'leg' of the β subunit is formed from 4 I-EGF domains (numbered 1-4) connected to the β tail domain that connects to the transmembrane domain, and then the cytoplasmic domain. This cytoplasmic domain varies between the β subunits, but all have a proximal cytoplasmic domain that is highly conserved and interacts with the membrane proximal domain of the α subunit forming a 'clasp' (O'Toole et al 1991; O'Toole et al 1994).

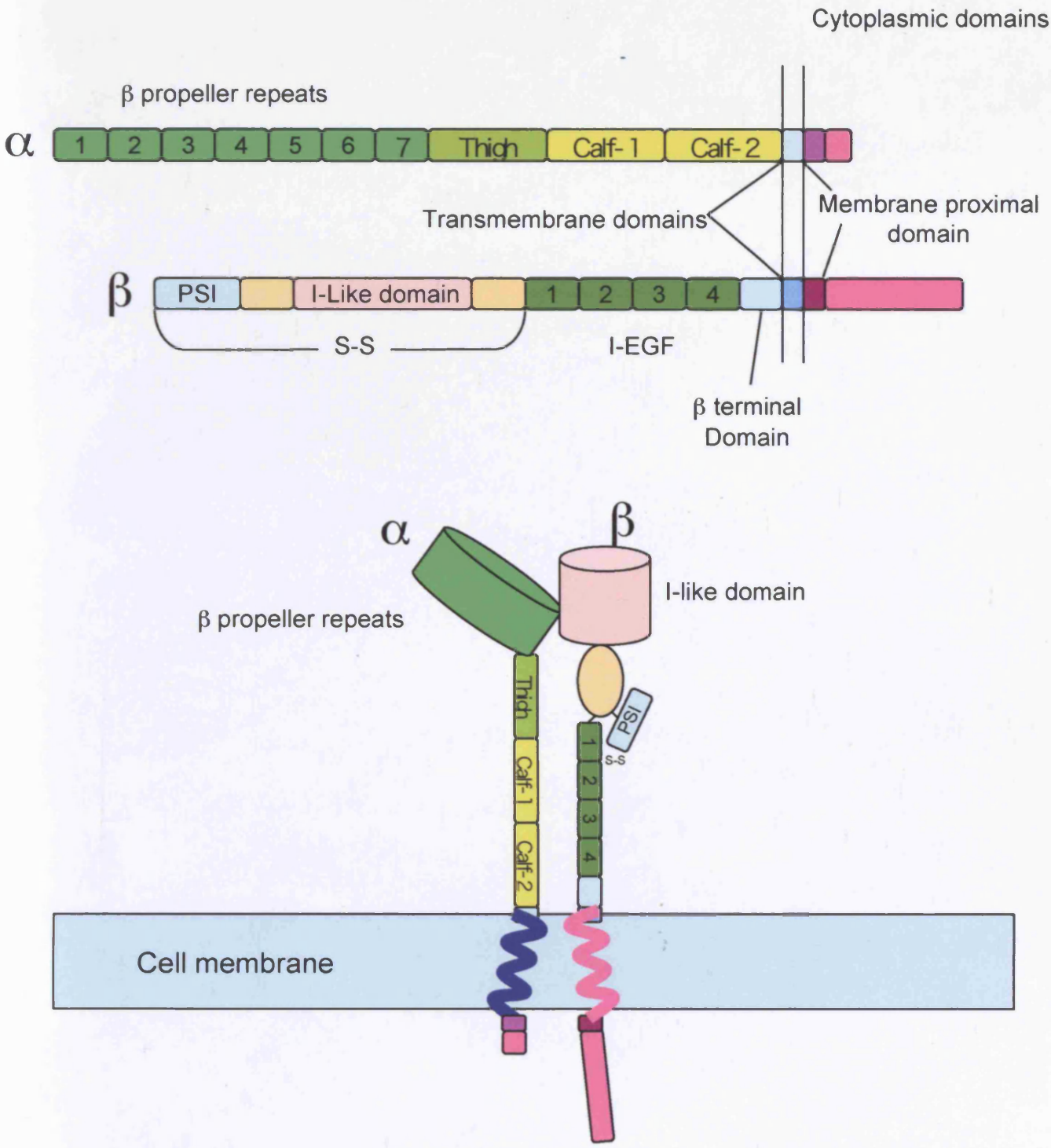

Figure 1.10: Integrin subunit structure. Modified from Hynes 2002.

Inactivated integrin structure. The crystal structure of the integrin αvβ3 has been described which reveals that this integrin is bent over at 135°, with a 'genu' or knee between the thigh and calf of the α subunit and a similar bend between I-EGF 2 and 3 of the β subunit. The I/A domain of the β domain is in close proximity to the β propeller of the α subunit (Xiong et al 2001), forming the ligand binding head of the integrin. This is thought to represent the low affinity or inactivated conformation of the integrin heterodimer. When RGD oligopeptides are added, there is no change in conformation (Xiong et al 2002), but the RGD oligopeptides bind at the α and β subunit interface.
In the inactive state there is a salt bridge between the α and β proximal cytoplasmic domains that maintains the integrin in an inactive state. Deletion of either of these regions results in a constitutively active integrin receptor (O'Toole et al 1991;O'Toole et al 1994).

Activated integrin structure. By using molecular electron microscopy, unligated integrin α5β1 head-piece has been shown to adopt a 'closed' conformation similar to the 'closed' conformation of integrin αvβ3 when unligated, but when fibronectin fragments are allowed to ligate, this integrin straightens-out (Takagi et al 2003). This 'opening-out' does not appear to happen when a similar experiment is repeated with fibronectin fragments and integrin αvβ3 (Adair et al 2005). The evidence is therefore conflicting about the straightening and 'opening-out' of the whole integrin receptor on activation, but other studies support at least the opening of the interface between the α subunit β propeller and the β subunit I/A domain: Mould et al (1997) has shown using monoclonal antibodies to the binding sites of integrin α5 and β1 and competitive inhibition of binding using RGD or fibronectin

central cell binding region peptide, that the RGD sequence of fibronectin binds β-I/A domain, whereas it is the synergy site which interacts with the propeller (Mould et al 1997); similarly both the synergy site and the RGD site of fibronectin are necessary for maximum activation of integrin α5β1 (Garcia et al 2002); also in the 'closed model' of integrin αvβ3 described by Xiong (Xiong et al 2002), several residues on the α subunit propeller are covered by the β I/A domain which are the binding sites of function blocking antibodies for several integrins, as reviewed by (Humphries 2002).

Activated integrins do have a loss of association between α and β subunits (Luo et al 2004). This is capable of putting the integrin into its activated form as demonstrated on NMR studies of the cytoplasmic domains of αIIb and β3 subunits (Vinogradova et al 2002; Vinogradova et al 2004). Talin has been shown to also inactivate the 'clasp' between these subunits (Vinogradova et al 2002). Activated, ligated integrins may then further cluster due to interaction of their transmembrane domains (Li et al 2003).

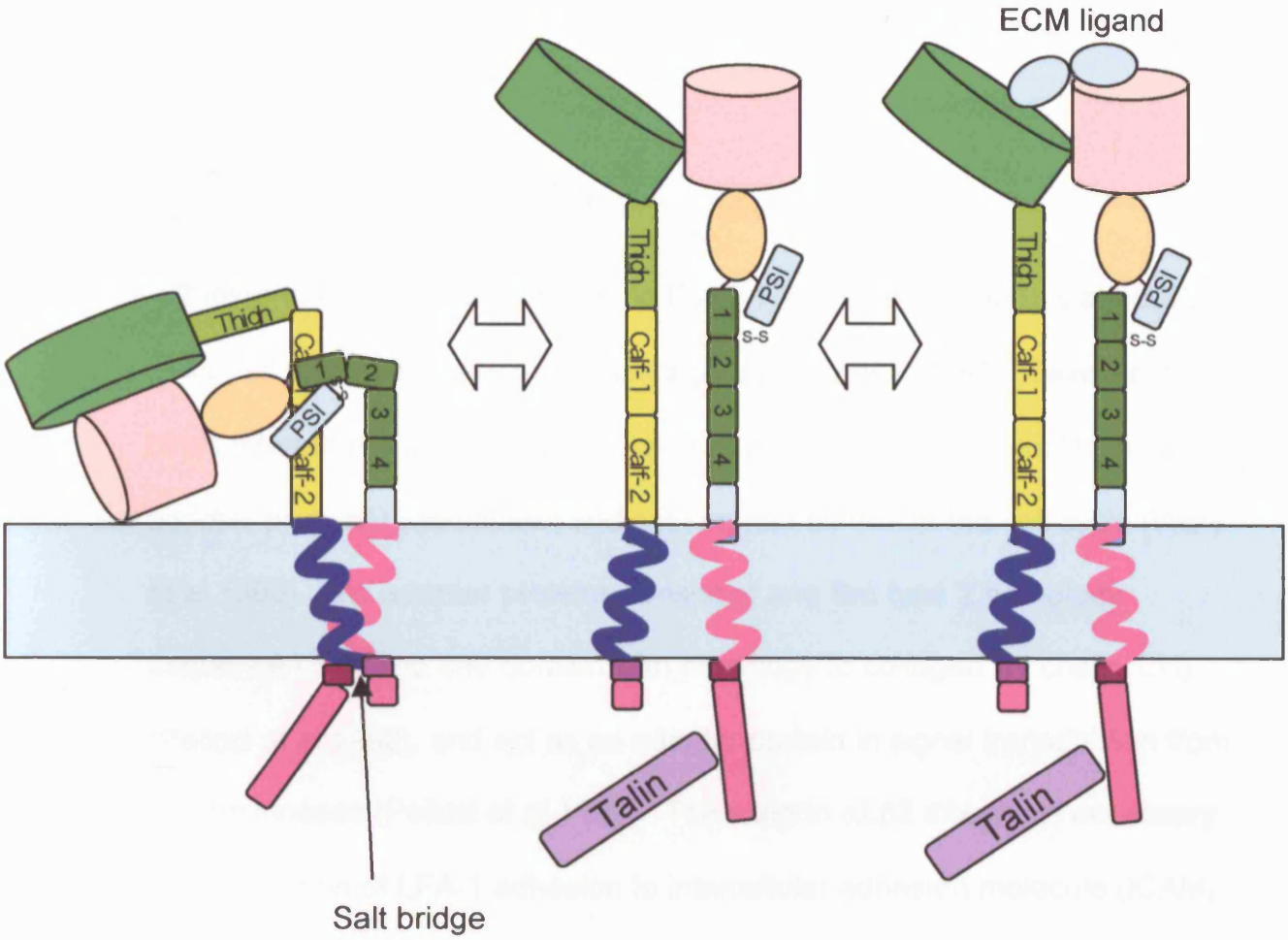

Figure 1.11: Integrin activation. Talin binding to the cytoplasmic tail of β subunit results in 'unclasping' of the membrane proximal salt bridge between the integrin α and β subunits - leading to a conformational change that exposes the ligand binding site, and may or may not be associated with straightening of the whole integrin dimer. Modified from Hynes 2002.

Integrin subunit cytoplasmic binding sites

The cytoplasmic tails of both the α and β subunits have both been shown to possess ligand-binding sites, although the β subunits have a much larger range of potential ligands and are perhaps most functionally important.

Cytoplasmic binding sites of integrin α subunits

α2 integrin has been shown to bind F-actin (Kieffer et al 1995). Calreticulin has been shown to ligate α2 subunits (Coppolino et al 1995). Caveolin-1 binds integrin α subunits and mediates adapter protein shc (Src Homology adapter proteins) recruitment and subsequent control of the cell cycle (Wary et al 1998). Shc adapter proteins consist of one Src type 2 homology sequence (Sh), and one domain with homology to collagen α1 chain (CH) (Pelicci et al 1992), and act as an adapter protein in signal transduction from protein kinases (Pelicci et al 1992). The integrin αLβ2 integrin is necessary for modulation of LFA-1 adhesion to intercellular adhesion molecule (ICAM), and this is mediated through the cytoplasmic domain of the αL subunit (Tohyama et al 2003).

Cytoplasmic binding sites of integrin β subunits

Integrin β cytoplasmic tails are central to many integrin functions. Loss of the cytoplasmic domains in β1, β2 and β3 integrins causes failure to localize to focal adhesions (Solowska et al 1989), reduced ligand binding (Hayashi et al 1990), and decreased activation of downstream signalling activity (O'Toole et

al 1994). Many different proteins bind the β-integrin cytoplasmic tails including actin binding proteins and signalling proteins.

Actin binding proteins

In order for cells to change shape and migrate and assemble fibronectin matrix, connection to the actin cytoskeleton is necessary. Adapter proteins include talin, paxillin, α-actinin, and filamin.

Talin is an antiparallel homodimer of 270 kDa units, each consisting of a 50kDa head (which binds β integrin subunits) and a 220 kDa tail. It binds β1A, β1D, β2, β3 and β5, with weak β7 adhesion (Pfaff et al 1998; Sampath et al 1998; Calderwood et al 1999). The head region contains a FERM domain (four-point-one, ezrin, radixin, moesin), which are known to bind the cytoplasmic tails of transmembrane proteins (Calderwood et al 2002). Talin binding of integrin β cytoplasmic tails can cause integrin activation, e.g. platelet integrin αIIbβ3 (Calderwood et al 2002). Inhibition of talin using small interfering RNA (RNAi) prevents conformational change of integrins, preventing activation on the cell surface, and cannot be overcome by over-expressing other putative integrin binding proteins (Tadokoro et al 2003).

Talin is necessary for the normal development of mice, flies and worms: talin null mutant mice die at E8.5 having failed to undergo gastrulation (Monkley et al 2000); *D. melanogaster* talin null mutants show failure to form focal adhesions on the cell surface, and failure of integrin-cytoskeleton interaction) (Brown et al 2002); in *C. elegans* talin deficiency resulted in loss of normal cytoskeletal organization and adhesion in contractile cells as well as deficient

migration) (Cram et al 2003). Integrin activation due to talin binding occurs as a result of disruption of the 'clasp' formed by a salt bridge between the membrane proximal regions of the integrin α and β subunits (Patil et al 1999; Vinogradova et al 2002; Garcia-Alvarez et al 2003; Ulmer et al 2003). Integrin dimers assume an activated conformation as described above. Once bound to the β integrin subunit, talin provides an initial link between integrin clusters and the cytoskeleton (as described on initial integrin αvβ3 clustering in the presence of fibronectin) (Jiang et al 2003). Application of mechanical force to these clusters results in further cytoskeleton recruitment mediated by talin (Giannone et al 2003). Talin is also necessary for subsequent paxillin and filamin binding into these focal complexes (Giannone et al 2003). Inhibition of talin binding can occur as a result of phosphorylation of the NPXY motif of β subunit cytoplasmic tails by Src (Garcia-Alvarez et al 2003).

Paxillin is an adapter protein that binds β1 integrin cytoplasmic tails. It was first described by (Glenney and Zokas 1989), and described as a focal adhesion and vinculin binding protein by (Turner et al 1990). It consists of 4 carboxy terminal LIM domains that bind to focal adhesions (Dawid et al 1998), 5 leucine rich 'LD' domains that bind proteins such as FAK and vinculin through conserved paxillin-binding sub-domains (Brown et al 1998). Several proline-rich SH3 binding motifs are present in the amino terminus (Weng et al 1993) as are several serine/threonine and tyrosine phosphorylation sites. Paxillin can bind syndecans, integrins, serpentine receptors, growth factor receptors, and link these to integrin-linked kinase (ILK), FAK, vinculin, actopaxin amongst others. An important function of paxillin is to integrate signals from integrins and growth factors, as reviewed by (Brown and Turner

2004). Paxillin is one of the first proteins to be localised to focal complexes in areas of cell protrusion (Laukaitis et al 2001). Homozygous paxillin knockout mice are embryonically lethal (Hagel et al 2002), with a phenotype similar to fibronectin knockout mice (Hagel et al 2002). Paxillin expression is regulated during development, expression of paxillin occurring after mid-gastrulation, with strong expression in the dorsal aorta, endocardium and notochord (Hagel et al 2002). Paxillin is expressed in the dense plaques of smooth muscle (Turner et al 1991).

Filamins: Three filamin isoforms have been described. They are actin filament cross-linking proteins formed from 2 parallel 250 kDa subunits (Turner et al 1990). Each subunit has an actin binding amino terminal, with a repeated 100-residue rod domain containing repeated 6-9 amino acid sequences, alternating with 3-4 amino-acid sequences (Gorlin et al 1990). Filamins cross-link actin filaments and bind transmembrane proteins including integrins β1A, β1D, β2, β3, and β7 (Sharma et al 1995; Loo et al 1998). The type of actin network that filamin cross-linking produces in part depends on the ratio of filamin to actin present: a high molar ratio of 1:10-50 produces parallel actin 'stress fibres', whilst a lower ration 1: 150-740 produces a loose, orthogonal network (Brotschi et al 1978; Dabrowska et al 1985). Filamin can also act as a scaffold for the binding of signalling proteins such as GTPases, including Rho, Rac and Ras, which can then lead on to filopodia formation (see below) (Ohta et al 1999). Filamin c is expressed in the dense plaques and dense bodies of mature smooth muscle (Tachikawa et al 1997).

α-actinin is a member of the spectrin family and consists of anti-parallel homodimers of 100kDa. The amino terminal contains two calponin homology

domains that bind actin, the central part of the molecule is formed from 4 spectrin-like repeats, and the carboxy terminal contains two EF hands which can bind divalent cations such as calcium (Baron et al 1987). α-actinin can bind the cytoplasmic tails of β integrins to actin stress fibres (Pavalko et al 1998), and is recruited to focal adhesions (Cattelino et al 1999). α-actinin also serves as a scaffold binding signalling molecules at focal adhesions, for example MEKK1 which is an activator of other kinases including p38 and ERK (Christerson et al 1999). Activity of α-actinin has been shown to be modulated by four mechanisms: firstly by calpain, which promotes focal adhesion disassembly by inhibiting α-actinin recruitment to focal adhesions (Bhatt et al 2002); secondly, binding of phophatidyl inositol products (of phosphatidyl inositol 3-kinase activity) reduces α-actinin binding of β-integrin cytoplasmic tails and actin and promotes dissipation of focal adhesions (Greenwood et al 2000); thirdly, phosphorylation of α-actinin can modify its activity, with increased phosphorylation in activated platelets (Izaguirre et al 1999), but when phosphorylated by FAK, reduced binding to actin fibres (Izaguirre et al 2001); fourthly, for the non-muscle isoforms of α-actinin, increased Ca^{2+} binding reduces actin ligation (Burridge and Feramisco 1981).

Skelemin has been shown to bind the membrane proximal region of the cytoplasmic tails of β1 and β3 integrins, and is a member of a superfamily that modulate the binding of myosin to actin (Reddy et al 1998).

Signalling molecules that bind β-integrin cytoplasmic tails

Two kinases have been reported to bind integrin cytoplasmic tails, focal adhesion kinase (FAK) and integrin-linked kinase (ILK). These are implicated in inside-out and outside-in signalling.

Focal adhesion kinase is a 119kDa protease that is rapidly phosphorylated and associated with focal adhesions when cells are plated onto ECM such as fibronectin (Hanks et al 1992). It consists of an amino-terminal FERM domain, (four-point-one, ezrin, radixin, moesin domain), which binds β-integrin cytoplasmic tails (Schaller et al 1995), a central catalytic domain, and a carboxy-terminal 'focal adhesion targeting' domain (FAT), which leads to binding at focal adhesions (Martin et al 2002). Clustering of integrins leads to rapid phosphorylation of FAK at tyrosine 397 (tyr397), amongst others, maximising activation of FAK signalling pathways (Calalb et al 1995). This creates a high affinity binding site for the SH2 domain of Src kinases (Schaller et al 1994), which in turn causes further phosphorylation of FAK (Owen et al 1999). This stimulates the recruitment of phosphoinositol 3-kinase (PI3 kinase) (Akagi et al 2002), phospholipase c (PLC) and the adapter protein Grb7 (Han and Guan 1999). The c-terminal domain FAT contains a binding site for paxillin, and 2 SH3 proline rich binding sites that can ligate Cas (Harte et al 1996) and regulators of small GTPases (GRAF and GAP which modulate Rho, and ASAP which modulates Arf1 and Arf6) (Liu et al 2002). These small GTPases are important in cytoskeletal reorganization (see bellow). FAK, via Cas binding to Crk stimulates cell migration (Cary et al 1998;Klemke et al 1998), which in turn may involve DOCK180 activating Rac (Kiyokawa et al 1998;Brugnera et al 2002). Cell adhesion mediated via integrins is synergistic

for the proliferation that growth factors cause via MAP kinase pathway. ECM adhesion stimulates MAP kinase activity in the absence of growth factors (Moro et al 1998), conversely growth factors cannot efficiently activate the Raf-MEK-Erk pathway when cells are in suspension and the integrin signal blocked (Renshaw et al 1997). This integrin signal is mediated by FAK activation (Renshaw et al 1999). Integrins via FAK modulate small GTPase activity (Rac and Rho) which determine cell shape, and motility, and via FAK modulate MAPK/MEK/ERK pathway and influence cell proliferation.

Integrin linked kinase (ILK) is a 59kDa protein originally identified by its interaction with β1 integrin cytoplasmic tail (Hannigan et al 1996). It consists of monomers containing four ankyrin-like repeats at the amino terminal, a pleckstrin homology domain, and a kinase at the carboxy terminal (Hannigan et al 1996). It has binding sites for a number of other proteins including integrin β1, PINCH (Tu et al 1999) and the adapter protein families α and β parvin, which are actin binding proteins (Olski et al 2001;Tu et al 2001). ILK localises to focal adhesions (Hannigan et al 1996), and to fibrillar adhesions, associated with fibronectin fibrillogenesis in diabetic nephropathy (Guo et al 2001). Homozygous ILK null mutant *D. melanogaster* are embryonically lethal, with loss of actin binding at muscle attachment sites (Zervas et al 2001). ILK can phosphorylate PKB/AKT, suppressing caspase-3 and inhibiting apoptosis and anoikosis (Persad et al 2000;Persad et al 2001). It is also capable of upregulating cyclin D1 in murine mammary cells – promoting cell cycle progression (D'Amico et al 2000). ILK can also increase AP1 activity resulting in increased matrix metalloproteinase 9 expression, and the potential for increased ECM remodelling or invasiveness (Troussard et al 2000).

β4 integrins are a component of hemidesmosomes

Integrin α6β4 is an integrin with a specificity for laminins that is associated with formation of hemidesmosomes in epithelia. Specifically the β4 cytoplasmic tails contains fibronectin type III repeats that are involved with attachment to hemidesmosomes (Spinardi et al 1993). Loss of this integrin can result in epidermolysis bullosa and neonatal lethality (Georges-Labouesse et al 1996).

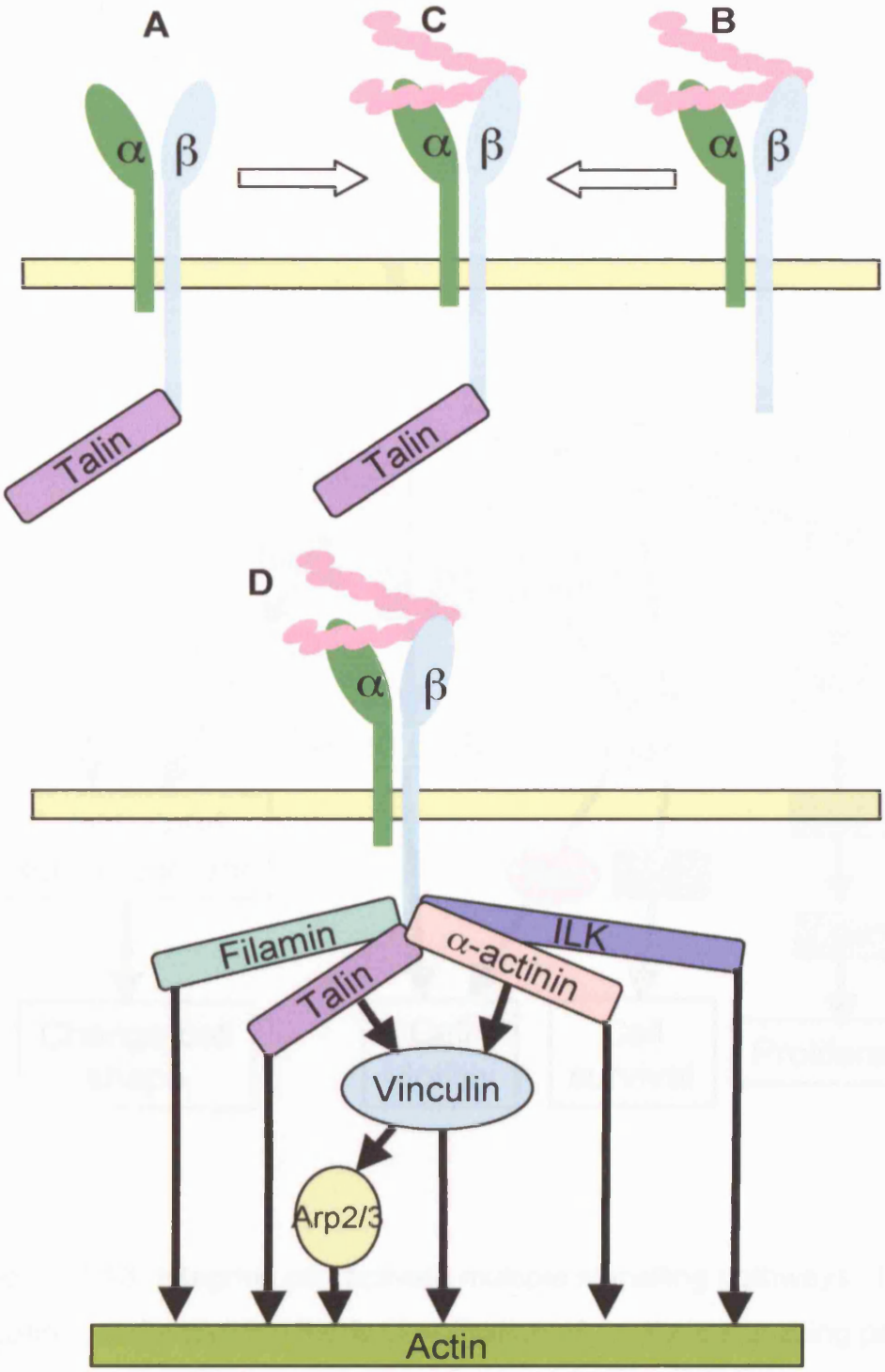

Figure 1.12: Integrin activation and actin binding: (A) 'inside-out' signalling: talin binding to the β-integrin cytoplasmic tail activates the integrin dimer allowing ligation of ECM protein e.g. fibronectin. (B) 'outside-in' fibronectin ligation by integrin dimer leads to (C) adapter protein binding eg talin. These adapter proteins then link to actin. Talin (and α-actinin) can in turn bind vinculin which can bind actin filaments, with Arp 2/3 acting as a nucleation site for further actin polymerization (D). ILK, integrin linked kinase, which acts as an adapter protein, but also as a kinase. Modified from Brakebusch et al (2003)

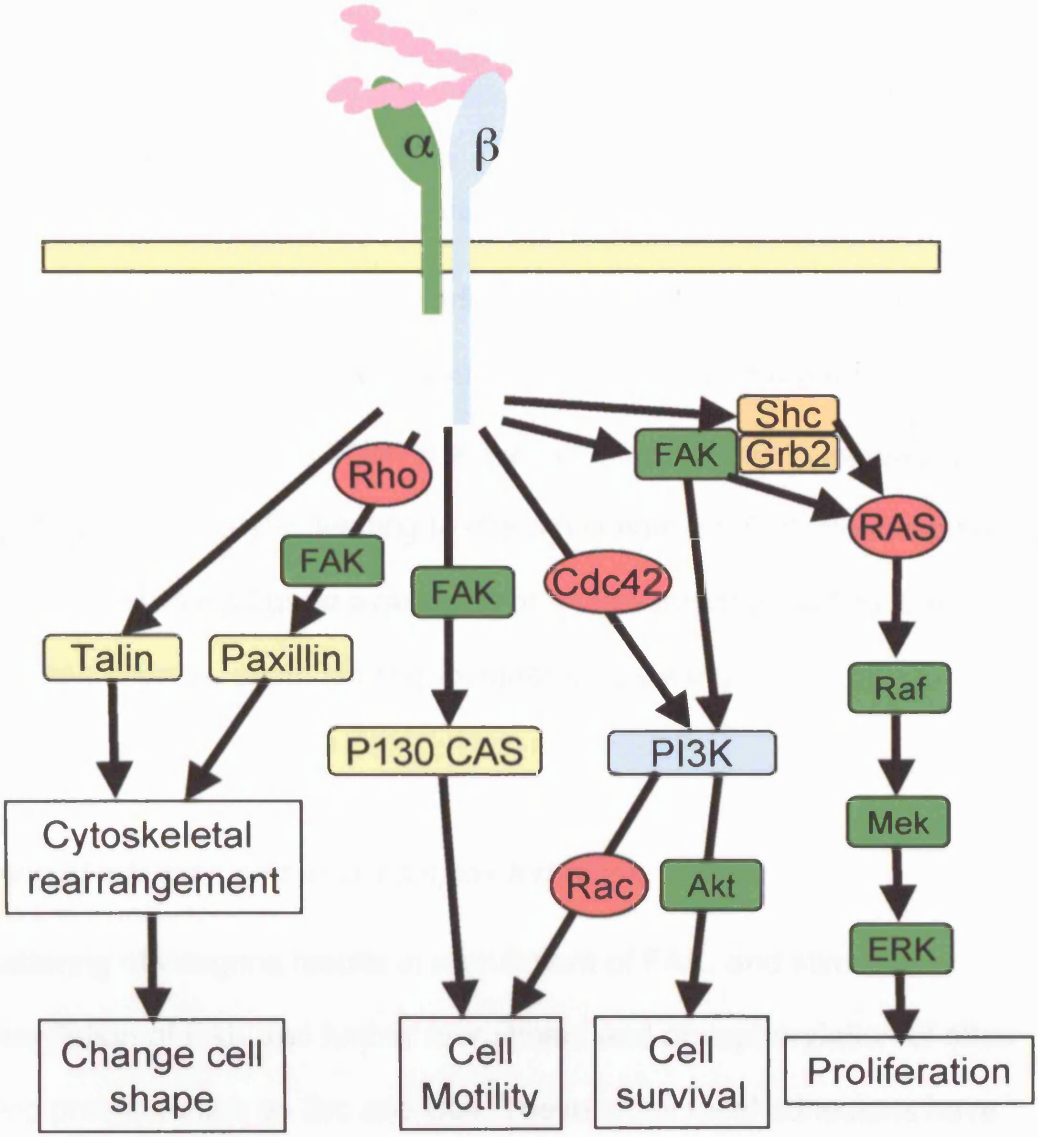

Figure 1.13: Integrins can activate multiple signalling pathways. Integrin ligation and activation leads to activation of multiple signalling pathways, including small GTPases (red) e.g. Rac, Rho, Ras, Cdc42; protein kinases (green) including FAK, Akt, Raf, Mek, ERK, in turn leading to alterations in cell shape, cell motility, survival and proliferation. FAK, focal-adhesion kinase; PI3K, phosphoinositide 3-kinase. Modified from Hynes 1999.

Integrin activation

Integrin activation can proceed from outside-in, or inside-out.

Inside-out signalling involves talin binding to the β-cytoplasmic tail, and 'unclasping' of the salt bridge between the α and β subunit membrane proximal domains. A conformation change can occur, allowing increased binding of ligand externally, leading to integrin clustering. Outside-in signalling occurs when increased ligand availability promotes integrin binding and conformation change, again leading to integrin clustering.

Clustering of integrins and focal complex formation

The clustering of integrins results in recruitment of FAK, and stimulates phosphorylation of FAK and further recruitment and phosphorylation of other signalling proteins such as Src and Cas. These small focal adhesions have been called focal complexes and are present at the periphery of cells. These focal complexes are regulated by Rac and CDC42 (small GTPases) (Nobes and Hall 1995). CDC42 promotes filopodia formation, whereas Rac promotes lamellopodia formation, stabilised by these initial focal complexes into which paxillin and α-actinin are recruited (Laukaitis et al 2001). Src recruitment can lead to phosphorylation of the integrin β-subunits, which can lead to focal complex disassembly, or the focal complexes can persist. The formation of these focal complexes involves further recruitment of ligated integrins (initially these are integrin αvβ3 in the model used by Zaidel-Barr et al (2003)), and

has been shown to be hierarchical with talin and paxillin incorporated next, followed by vinculin and FAK (Zaidel-Bar et al 2003).

Focal adhesions form from focal complexes

Remodelling occurs with an increase in FAK and vinculin, with zyxin and tensin recruited for the first time, associated with an increase in β1 integrins - leading to formation of focal adhesions (Zaidel-Bar et al 2003). The formation of these focal adhesions is under the control of the small GTPase Rho (Ridley and Hall 1992;Chrzanowska-Wodnicka and Burridge 1996), and is associated with force generation and actin stress fibre formation.

Force acting on cells modifies the type of focal adhesion formed. The force may have an extracellular origin, or may be intracellularly generated.

'Intracellular force' is generated by actin-myosin contraction driven by myosin ATPase activity. This activity is modulated by myosin light chain phosphorylation, which occurs as a result of the action of the Rho effector, Rho Kinase (ROCK) (Amano et al 1996;Kimura et al 1996;Kureishi et al 1997).

'External force' when applied to adherent cells has been shown to result in cell stiffening and new focal adhesion formation, mediated by integrins (Wang and Ingber 1995). Similarly, using optical tweezers to increasingly 'pull' on a fibronectin coated bead has been shown to increase strength and rigidity of the cytoskeleton (Choquet et al 1997). Mechanical force can increase focal adhesion formation (Balaban et al 2001), and can cause maturation of focal adhesions (Galbraith et al 2002).

Fibrillar adhesions

Fibrillar adhesions are formed from focal adhesions, and contain integrin $\alpha5\beta1$ and tensin. These adhesions are associated with fibronectin fibrillogenesis, as described above (Pankov et al 2000).

Three-dimensional focal adhesions

Fibroblasts seeded into floating collagen gel become quiescent and assume a three-dimensional 'dendritic' shape typical of fibroblasts in resting connective tissue (Grinnell et al 2003). Mammary epithelial cells seeded onto EHS derived matrix form three dimensional structures after 8 days in culture, becoming differentiated, assuming an acinar conformation, and producing milk (Barcellos-Hoff et al 1989). 'Three-dimensional' focal adhesions formed in vivo or in three-dimensional culture are different to those formed by cells on a two-dimensional substrate (Cukierman et al 2001). Specifically fibroblasts produced three-dimensional focal adhesions that had no $\beta3$ integrin, instead contained $\alpha5\beta1$ integrin unlike focal adhesions; and included FAK, paxillin and vinculin unlike fibrillar adhesions. Three-dimensional matrices also had enhanced biological activity (adhesion, movement, cell morphology, and proliferation), blocked by a function blocking antibody to integrin $\alpha5\beta1$ (Cukierman et al 2001).

Phylogeny of integrins

The single sponge integrin has homology with both the *C. elegans* α-integrin subunits and the RGD, and laminin integrins expressed in *D. melanogaster.* RGD and laminin binding receptors are present in all vertebrates and invertebrates studied so far. These RGD integrins are *C. elegans* α1, *D.*

melanogaster PS2, and human integrins α5, α8 and αV. The laminin binding integrins include *C. elegans* α2, Drosophila PS1 and human α3, α6 and α7. *D. melanogaster* include a group of receptors not present in vertebrates (PS3 group), and vertebrates include 2 further groups not present in *C. elegans*, or *D. melanogaster*. These are the I/A domain integrins (so-called because of an extra domain in the α subunit that is thought to be associated with collagen binding), and a second group comprised of two members, integrin α4 and α9 (Hughes 2001).

Hughes (2001) reported a possible mechanism for the growth in numbers of the members of the integrin families. The original laminin and RGD integrins present in Drosophila and vertebrates may have undergone a series of linked duplications: One ancestral pair of laminin (PS1) and RGD (PS2) integrins could have both been duplicated onto another chromosome (chromosome 17 in the human) – giving rise to integrins α3 and αIIb. The original pair could then have been duplicated once more giving rise to chromosome 2 integrins α6 and αV, and to chromosome 12 integrins α7 and α5 (Hughes 2001).

The family trees of the integrin α and β subunits has been described (Hughes 2001). A simplified version showing only the human α integrins (figure 1.14), and β integrins (figure 1.15) is shown here.

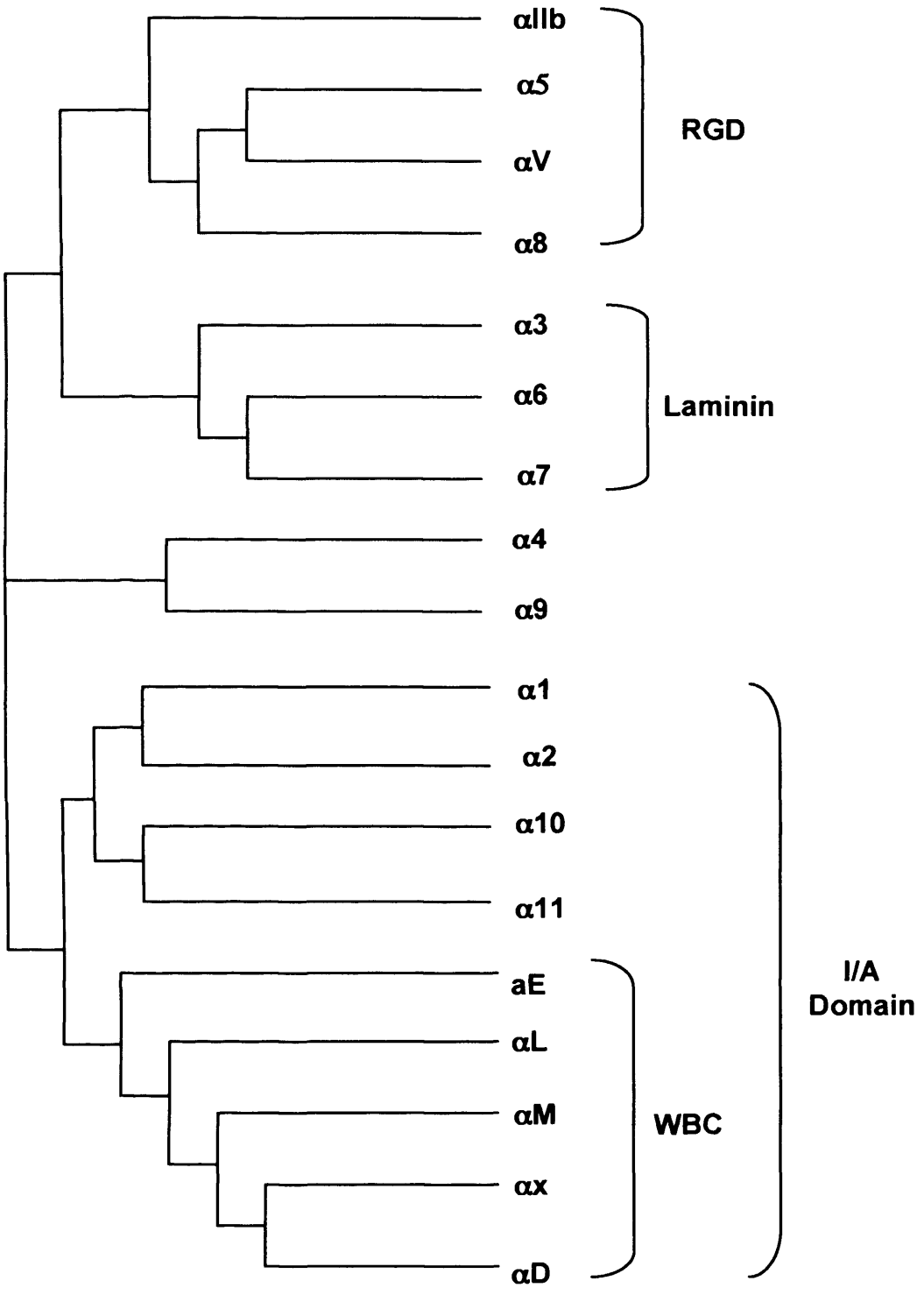

Figure1.14: Phylogenetic relationship of human integrin α subunits is. Adapted from Hughes et al 2001. WBC, white blood cell.

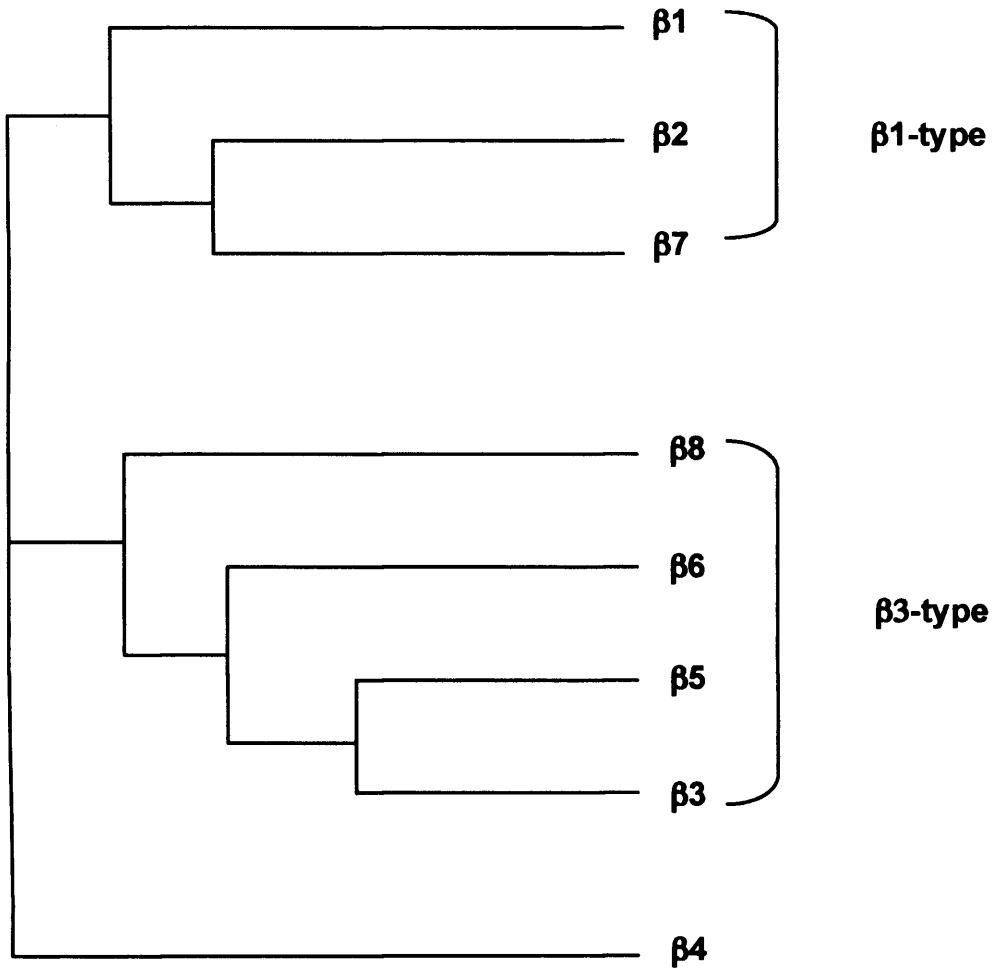

Figure 1.15 : Phylogenetic relationship of human integrin β subunits. Adapted from Hughes et al 2001.

Integrins expressed in the bladder

DSMC integrins

Integrins expression in the human bladder detrusor has been described by (Wilson et al 1996). This was a descriptive study only using immunohistochemistry (IHC), using samples of tissue obtained from an adult human cystectomy, and a normal post-mortem bladder. These specimens were probed using antibodies to integrin α3, α5, αv, αvβ3, β1, β3 and β4.

Fibronectin was expressed in the basal lamina of DSMC, with immunostaining of the DSMC strongly for α5, and integrin β1, with and weak to moderate staining for αv and αvβ3 antibodies. Similarly, there was strong immunostaining of the DSMC basal lamina for a generic laminin antibody, and weak to moderate immunostaining for integrin α3. α6β4, although only the β4 component was examined, is the integrin that forms hemidesmosomes in epithelia and endothelia, and this was the pattern described by the authors in this paper. There was no β4 immunostaining of the detrusor muscle, only epithelial basement membrane.

Integrin β3 has been shown by analysis of mRNA to be expressed in the fetal murine bladder (Le Gat et al 2003).

Urothelial integrins

The bladder urothelium was shown to express integrin α3, some integrin αv, integrin β1 and β4 strongly in immunohistochemistry performed on adult

human bladder (Wilson et al 1996). There was no staining of the urothelium with an antibody to integrin α5. Southgate et al (1995) report that in urothelium, integrin α2β1, α3β1 are expressed in all layers of the urothelium, whereas α6β4 and αvβ4 are expressed in the basal lamina. In cell culture, these urothelial cells expressed integrin α5β1 (Southgate et al 1995). Similarly it has been shown that adhesion of cultured urothelial cell lines including HCV29 (a non malignant urothelial cell line held by the Polish Academy of Sciences) to laminin is blocked by antibodies to integrin subunits α3 and β1; to fibronectin by antibodies to α5 and α3; but that anti-α3 antibody increased adhesion to collagen IV (Litynska et al 2002). Normal integrin α6β4 expression in urothelial bladder cancer has been correlated with improved long-term patient survival (Grossman et al 2000). Conversely, loss of integrin β4 expression in specimens of human bladder carcinoma significantly correlated with tumour grade (Mialhe et al 1997).

Cell shape and fate

Physical factors such as the space a cell occupies (cell shape), and degree of mechanical stretch can alter cell fate. It has been demonstrated that the degree of spread of a cell can influence cell survival, independently of the area of contact between ligand (fibronectin) and receptor (β1 integrin) (Chen et al 1997). The degree to which cells can spread has also been shown to influence differentiation: mesenchymal cells limited in their ability to spread do not differentiate, but if allowed adequate space will differentiate into smooth muscle cells (Yang et al 1999).

Mechanical stretch and normal development of the bladder

Integrins as mechanoreceptors

How is mechanical stretch detected by cells? It has been demonstrated that integrins can act as mechanotransducers (Chicurel et al 1998; Alenghat and Ingber 2002). The degree of stretch of human detrusor cells in culture (obtained from a 2 year old boy undergoing ureteric reimplantation) has been shown to influence whether cells undergo hypertrophy or proliferation (Orsola et al 2002). That integrins are important in this response has been shown by the inhibition of the proliferative response to stretch when RGD oligopeptides are added to stretched, cultured adult rat detrusor cells (Upadhyay et al 2003). Stretch-injured rat bladders also demonstrated an upregulation of collagen genes I and III, and of integrin sub-units including β1, β3 and αv (Upadhyay et al 2003).

Mechanical stretch in vivo

That a degree of normal 'physiological stretch' is necessary for normal bladder growth has been demonstrated in explant and animal in vivo models. In an explant model of fetal rat bladder growth, sealing the urethra and ureters of rats' bladders caused more normal collagen alignment, on histological examination of these explants (Beauboeuf et al 1998). Similarly if a fetal sheep bladder is bypassed by performing ureterostomies bilaterally at day 90

of gestation, and ligating distal ureters then bladder growth is affected: defunctioned bladders weighed less; on histological examination there was a decrease in the surface area of the muscle bundles with increased amounts of connective tissue through out all layers and a loss of the normal muscle morphology as compared to controls, as assessed by histology (Matsumoto et al 2003).

Is it stretch, or pressure, or both?

Intravesical pressure is easily measured in the clinical setting with a urethral catheter. The measurement of intravesical pressure, and use of a rectal line to allow subtraction of intra-abdominal pressure, allows a calculation of detrusor pressure to be made. The pressure and volume of a bladder (radius) will determine the wall tension (LaPlace's law for spheres, wall tension=(pressure x radius)/wall thickness), so stretch has been used in cell culture to mimic this effect (Baskin et al 1993a; Upadhyay et al 2003).

However, Haberstroh et al have reported that hydrostatic pressure itself (in the absence of stretch) can modulate DSMC behaviour in culture (Haberstroh et al 1999). These DSMC were harvested from neonatal lambs, and passaged between 3 and 5 times. DSMC grown under even moderate hydrostatic pressures of 4 to 8 cm of water induced a proliferative response, at least in part mediated by a soluble mitogenic factor (Haberstroh et al 1999). Furthermore, exposure to hydrostatic pressures of 20 cm or 40 cm of water for 24 hrs has been shown to result in cultured human DSMC upregulating matrix metalloproteinase -1 (MMP-1) and over 7 days down regulation of MMP-2 and

MMP-9. Simultaneously there was an upregulation of tissue inhibitor of matrix metalloproteinase (TIMP), an inhibitor of MMPs. Taken together this could mean a decrease in the breakdown of extracellular matrix components, and a possible mechanism for increased connective tissue deposition (Backhaus et al 2002). When cultured ovine DSMC are simultaneously stretched (25% strain) and exposed to pressures of 40cm water then HB EGF and collagen III transcripts were both significantly upregulated (Haberstroh et al 2002). None of these pressure studies, however, used fetal DSMC. Indeed, the only study to examine stretch in cultured fetal DSMC has been Baskin et al (1993), which used fetal bovine DSMC.

Origins of connective tissue

Connective tissue and the cells that produce it

The basal lamina and interstitial collagens are produced by the cells embedded in them (Alberts et al 1994). Myofibroblasts are capable of producing collagens (e.g. collagen I, III, IV) as well as laminins and fibronectin (Gabbiani 2003). In a similar manner, bovine fetal detrusor smooth muscle cells in culture have been shown to produce collagens I, III and IV, and fibronectin (Baskin et al 1993b).

A hypothetical feedback loop is possible (figure 1.16A): the local basal lamina is secreted by the developing fetal smooth muscle cells, which in turn influences the behaviour and fate of the cells which produced it. Fibronectin as discussed above has been associated with a synthetic and proliferative phenotype in vascular smooth muscle cells. It can be speculated that further production of fibronectin might reinforce this proliferative, synthetic phenotype. However laminins have been associated with a contractile smooth muscle phenotype that no longer produces any ECM. What is the signal for this change? When do cells stop reinforcing their synthetic phenotype by down regulating fibronectin? Other factors such as growth factors and cytokines, physiological stretch, and the geometric shape, may play a role in modifying the genetic programme that the cells are following (figure 1.16B).

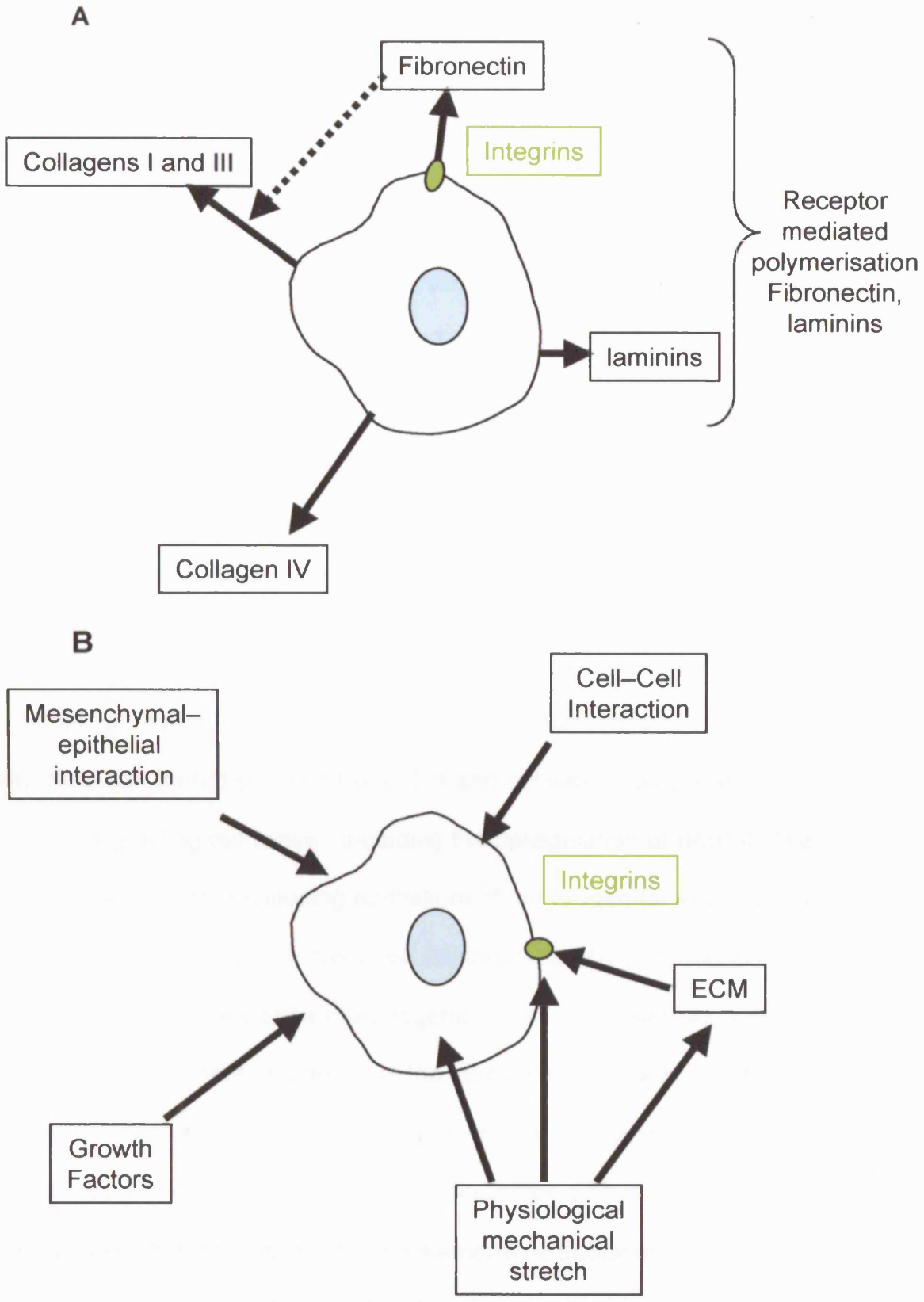

Figure1.16: Connective tissue cells make matrix, which in turn modifies cell behaviour (A) Connective tissue cells make matrix. (B) the matrix substrate and the space into which cells can expand are important factors in determining cell behaviour, and ultimately differentiation and fate.

Soluble growth factors involved in bladder development

Normal patterning

Cell-cell interactions are vital in determining patterning during embryonic development. Many of these interactions are controlled by signalling proteins such as the hedgehog group of peptides. There are three members of this group Desert, Indian and Sonic hedgehog (Dhh, Ihh, and Shh). Shh can act as a morphogen in a dose dependent manner – inducing differentiation in target cells, but is also capable of acting as a mitogen – inducing a proliferative response (Bitgood and McMahon 1995).

Shh binds to the cell surface receptor patched (Ptch) which in turn stops Ptch from inhibiting/binding to smoothened (Smo) – another transmembrane protein. Smo can then dissociate from Ptch and activate downstream intracellular signalling pathways - including the upregulation of BMP-4. The presence of Shh in the developing epithelium of the urogenital sinus in fetal mice from embryonic day 11.5 has been demonstrated by (Bitgood and McMahon 1995). Similarly bone morphogenic protein – 4 (BMP-4), a down-stream signalling element, is present in the surrounding mesenchyme (Bitgood and McMahon 1995). Homozygous knockout mice express anorectal malformations (Mo et al 2001). Similarly in the ureter, Shh is expressed in the urothelium, with Ptch expressed in the mesenchyme subjacent to this, with BMP-4 induced as a result (Yu et al 2002).

Yu et al have gone on to suggest a model for ureteral smooth muscle maturation whereby Shh has a morphogenic and mitogenic effect: 1)

expressed by the ureteral urothelium acts through Ptch to induce Bmp-4 expression which causes smooth muscle differentiation in the smooth muscle, but 2) that this differentiation is inhibited by the local effect of Shh, whilst 3) Shh acts locally as a mitogen to cause proliferation of the mesenchymal cells that are the smooth muscle progenitor cells (Yu et al 2002).

Vascular endothelial growth factor (VEGF) is present as are its receptors VEGF receptors 1 and 2 (VEGFR1, VEGFR2) in murine fetal bladders at E14 and E18 (Burgu et al 2006). Exogenous VEGF increases endothelial cell growth, but also increase DSMC growth, and decreases DSMC apoptosis in fetal murine bladder explant culture (Burgu et al 2006), an effect inhibited by adding VEGFR1/Fc, a blocker of VEGF. This work was done using the fetal bladder explant model established in this thesis.

Response to stretch

Soluble factors have been implicated in the response of DSMC to stretch in cell culture. Angiotensin II has been implicated in the response of cultured DSMC to stretch – acting in a paracrine fashion, through angiotensin II receptors, to cause release of heparin-binding epidermal growth factor-like growth factor (HB-EGF) (Park et al 1998). Mice deficient in angiotensinogen converting enzyme, angiotensin II and angiotensin II receptor I deficient mice have hydronephrosis with poor muscle development in the renal pelvis and ureter (Yosypiv et al 2006). Angiotensin II receptor 1 null mutant mice develop renal failure, massive hydronephrosis with deficient smooth muscle of the renal pelvis and ureter. In organ culture, these mutants are resistant to

angiotensin II (Yosypiv et al 2006).

Congenital bladder outflow obstruction

Causes of fetal bladder outflow obstruction

Bladder outflow obstruction in the fetus can be mechanical or functional in origin. Mechanical causes include conditions that may occur in the male posterior urethral valves (PUV), conditions which may occur in either sex such as urethral atresia, BOO due to an ectopic ureterocele, and female pseudo-prune belly syndrome (associated with urethral atresia). Functional obstruction may occur when the bladder fails to empty either because of smooth muscle myopathy as in megacystis microcolon syndrome, or neuropathy – although this predominantly presents postnatally. Prune belly syndrome may be the end-point of mechanical obstruction, or could be due to a primary mesodermal defect, and therefore overlaps both the mechanical obstruction group and the functional obstruction group (Workman and Kogan 1990; Shimada et al 2000).

Posterior urethral valves

Posterior urethral valves are the single commonest cause of fetal BOO, occurring in approximately 1/4000 live male births. Furthermore, PUV are the single commonest urological cause of end stage renal failure in children (Woolf and Thiruchelvam 2001). Originally classified as type I, II or III by Young in 1919 – type II valves are not now thought to be obstructive (Young et al 1919). Posterior urethral valves arise from the inferior edge of the verumontanum, and pass distally to the membranous urethra, attaching to the

proximal part of the membranous urethra (in Young's classification Type I valves), or form a ring-like membrane just distal to the verumontanum (Young's type III valves) (Gonzales et al 2004). Type I valves are thought to arise as remnants of the distal mesonephric duct with an ectopic anterior insertion (Gonzales et al 2004), whereas type III membranes may represent a persistence of the cloacal membrane (Gonzales et al 2004). Anterior urethral valves occur but are rare, and often associated with an anterior urethral diverticulum as a result of a ruptured Cowper's gland (McLellan et al 2004). Transient obstruction of the anterior urethra may occur fetally as a result of a syringocele arising in Cowper's glands.

Prune belly syndrome (Triad syndrome, Eagle-Barrett syndrome)

This is a triad of absence or hypoplasia of the anterior abdominal wall muscles, a large, hypotonic bladder with tortuous ureters, and bilateral cryptorchidism (Smith et al 2004). By definition this complete form of the condition has to affect male fetuses only, with an incidence of 1 in 35,000 to 1 in 50,000 live births.

There are two hypotheses for the pathogenesis of this condition: either it is due to over distension of the bladder (perhaps with transient fetal ascites that is subsequently reabsorbed), resulting in stretching and attenuation of the musculature, and a blockage to normal descent of the testes; alternatively it may be due to a primary defect of the mesoderm during embryogenesis (Shimada et al 2000). Gestation may proceed without complication, but oligohydramnios is common. The urethra may be hypoplastic, but megalourethra may also occur (Smith et al 2004). Weber et al (2005) describe

a consanguinous family in which four boys were born with PUV, one of the boys also having Prune belly syndrome. There was a normal daughter in this family.

Female pseudo-prune belly

Although prune belly syndrome strictly is a male syndrome, the term pseudo-prune has been applied to females with laxity of the anterior abdominal wall musculature, although they often do not have severe urological abnormalities these may coexist (Smith et al 2004). Of nine prune belly syndrome fetuses (Shimada et al 2000) found that five were male, two female and two were of indeterminate sex. Reinberg et al (1991) described seven female patients with the female equivalent of Prune belly syndrome. Urethral atresia was common in these cases and may have been central to the pathogenesis of the condition.

Urethral atresia

Urethral atresia occurs either when there is a complete obstruction of the urethra by a membrane, or when the urethra has failed to form. The urethra distal to the obstruction is hypoplastic as it has never been dilated by the passage of urine. In males this membrane is distal to the prostatic urethra (Gonzalez et al 2001). Survival is only possible if there is some communication from the bladder to the amniotic cavity by a vesicocutaneous fistula, or a patent urachus, or vesicoamniotic shunt placement (Gonzalez et

al 2001). Very often this condition coexists with Prune belly syndrome, affecting both males and females (Reinberg et al 1993).

Patent urachus

The urachus, which arises from the allantois, forms a blind ending diverticulum of the yolk sac, and comprises part of the body stalk. During 3D body folding the urachus becomes incorporated into the base of the umbilical cord. It is associated with formation of the umbilical vessels. In the chicken egg amnion, and allantois remain separate (Piechotta et al 1998).

In clinically normal neonatal calves there is no urachal remnant in the umbilicus (Watson et al 1994), whereas there is a patent urachus passing into the umbilicus in newborn foals (Reef and Collatos 1988). In fetal sheep the urachus is patent and opens into the amniotic cavity (Nyirady et al 2002). There is a spectrum of urachal patency amongst different species of mammals at birth.

In human fetuses the urachus has previously been reported to close by 12 week (Begg 1930). Antenatal diagnosis of patent urachus involves detection of a cyst of the umbilical cord – suggestive that even when persistence of this diverticulum occurs, there is no communication with the amniotic cavity unless a pathological rupture occurs (Tolaymat et al 1997; Schiesser et al 2003; Shima et al 2003; Kilicdag et al 2004). At birth, the patent urachus passing into the umbilical cord could be divided with cutting of the umbilical cord – leaving a patent route connecting bladder to skin. In reviews of postnatally presenting urachal abnormalities, no BOO was associated (Mesrobian et al

1997; Cilento et al 1998), although it has been described as a rare association with PUV (Kaefer et al 1995).

Accuracy of radiological diagnosis of antenatal bladder outflow obstruction

In currently-established clinical practice, antenatal radiological diagnosis of congenital BOO, which is most commonly due to PUV, depends on the identification of the structural features that go with this congenital obstruction. These include bilateral hydronephrosis, a thick-walled bladder, a dilated posterior urethra, and oligohydramnios. These appearances can also occur in urethral atresia and prune belly syndrome. It has been reported that only 35% of antenatally-diagnosed 'obstructive uropathy' actually had PUV (14 of 40 patients), on postnatal imaging, cystoscopy and postmortem (Holmes et al 2001). Similarly Abbott et al report that after an antenatal diagnosis of PUV was made on the basis of megacystis and hydronephrosis (10/22 had oligohydramnios), only 8 of 19 followed up had confirmation of posterior urethral valves, and 1 had urethral atresia (47% congenital BOO) post natally. (Abbott et al 1998). Aspiration of fetal urine and measurement of electrolytes has been advocated to detect the renal impairment that may be associated with abnormalities of the lower urinary tract, however this is invasive and carries with it a risk of miscarriage and fetal death, and may also occur in a non-obstructed fetal urinary tract. In a recent report elevated fetal urinary sodium was only 44% sensitive, but 100% specific for predicting abnormally elevated infant creatinine and renal impairment (Miguelez et al 2006). Similarly fetal cystoscopy has been advocated, but this has only been

reported to be diagnostic, in one report, in five of 13 suspected cases of obstructive uropathy, with fetal loss in two cases soon after the intervention, and 2 further late deaths (Welsh et al 2003). In another report of antenatally diagnosed obstructive uropathy (bilateral hydroureteronephrosis, megacystis, dilated posterior urethra, and oligohydramnios), in whom fetal cystoscopy was performed, 14 of 36 had PUV, 1 of 36 had urethral atresia (42% congenital BOO), whereas the others did not have obstructive uropathy (Holmes et al 2001). There was a fetal mortality rate of 43% in this series (Holmes et al 2001).

Uncertainty of diagnosis of BOO in post mortem specimens

Fetuses could be identified from antenatal diagnosis and from postnatal examination and investigation. The available antenatal modalities include anatomical description (fetal ultrasound), fetal urine electrolyte estimation, and fetal cystourethroscopy. All these modalities have limitations as described above.

Postnatal anatomical description can be suggestive of BOO, but without examination of the posterior urethra histologically or by imaging either directly or radiologically, must be considered to be a 'presumed' diagnosis. The histological examination of the urethra is not done as part of the routine postmortem examination of the urethra at UCH as the yield in identifying any obstructive lesion is poor. Similarly post natal cystourethrograms have not been performed as part of the routine post mortem examination at UCH, so retrospective use of the specimens from this embryo bank do not have this information. The reliability of this investigation in the post mortem fetus has

not been quantified. Postmortem examination of the urethra by cystourethroscopy has not been described.

Postnatal BOO is again suggested by an antenatal and postnatal history. Postnatal imaging by ultrasound examination of the urinary tract may be suggestive of BOO, however confirmation by radiology (micturating cystourethrography (MCUG)) and direct examination (cystourethroscopy) is necessary. MCUG can be diagnostic in many cases, but are not always predictive. In a recent study, abnormal MCUG predicted an infravesical obstruction that was only confirmed by cystourethroscopy in 76%, but 24% of abnormal MCUGs as assessed by a panel of radiologists and urologists were subsequently shown to have no infravesical urethral obstruction (de Kort et al 2004). The 'gold-standard' in children has been taken to be cystourethroscopy, but this still includes a value judgement by the surgeon on whether a urethral 'ring' visualised is in fact obstructive. Urodynamic investigation (urine flow rate measurement) to diagnose BOO is widely and reliably used in adults, as reviewed by (Belal and Abrams 2006).

In discussing fetuses who have had a post mortem examination to determine the presence of BOO, if no other imaging modality is used, the term presumed bladder outflow obstruction (presumed BOO) will be used in this thesis.

Consequences of fetal bladder outflow obstruction

Severe BOO is associated with renal hypoplasia (Potter IV abnormality-see below) and dysplasia (Potter II abnormality-see below), oligohydramnios-

pulmonary hypoplasia sequence (Potters sequence) and consequent neonatal death from respiratory failure, or termination of pregnancy following antenatal detection (Scott and Goodburn 1995; Clark et al 2003). Obstructive uropathy is also a leading cause of neonatal ascites (Gonzales et al 2004).

Renal dysplasia and obstructive uropathy

By 28 days of gestation in the human, the ureteric bud has branched from the mesonephric duct (Woolf et al 2004). Over the next few days renal mesenchyme condenses from the intermediate mesenchyme around the tip of the ureteric bud, or ampulla. Urothelium of the renal pelvis and ureter is derived from the ureteric bud, whereas the epithelial lining of the urogenital sinus gives rise to the bladder urothelium. Some of the renal mesenchyme undergoes epithelial conversion to form nephrons. The ureteric bud undergoes repeated branching: the first 6-10 branches become the calyces and renal pelvis, the last 6-9 divisions form the collecting ducts. Early ureteric branching is not associated with nephrogenesis in the human. From 8 to 15 weeks, with each generation of branching one branch of the ampulla is associated with the already formed nephrons, whilst the other branch is associated with new nephron induction. Nephrogenesis continues up to 32-36 weeks of gestational age, resulting in 'arcades of nephrons in the cortical 'nephrogenic zone' (Woolf et al 2004).

Potter described four types of congenital cystic kidneys (reviewed by (Woolf et al 2004)): Type I (autosomal recessive polycystic kidney disease (PKD)); type II severely dysplastic kidneys (MCDK); type III (mostly autosomal dominant

PKD); and type IV. Type II kidneys lack of normal tissues (nephrogenic zone, glomeruli and collecting ducts) and instead have primitive tubules embedded in fibro-muscular stroma, with cartilage, and abnormal nerves and blood vessels. In type IV malformations, the first layers of nephrons form normally, but the outermost nascent glomeruli become cystic, the nephrogenic zone disrupted and collecting ducts are dilated. It is thought that back-pressure due to BOO most affects the 'newest' nephrons, ie those still attached to the ampullae, resulting in subcortical cysts. Early branching is unaffected, as are the first nephrons formed, so urine production is possible. In contrast, Potter originally described type II cystic kidneys as non-functional, but more recent studies have suggested that there are some functioning nephrons present, in which case this type may represent the most extreme end of the spectrum (Woolf et al 2004).

In both animal and human models early obstruction can result in severe renal malformations, as well as bladder distension and hydronephrosis, but later in gestation only bladder distension and hydronephrosis, with milder nephron deficits occur, as reviewed by (Aslan and Kogan 2003). In a late model of ureteric obstruction in second and third trimester rhesus monkeys it has been shown that changes of renal dysplasia occur including development of sub-cortical cysts (Tarantal et al 2001). Ultrasonographically demonstrated cortical cysts correlated with renal dysplasia (Crombleholme et al 1990), as did oligohydramnios, whereas maintenance of liquor volume predicted better renal function (Glick et al 1985).

Response of the bladder to obstruction

In congenital uropathies, such as PUV, fetal urinary obstruction is associated with derangement of normal development, leading postnatally to a fibrotic, poorly compliant, high-pressure reservoir (the 'valve bladder') and renal impairment. In man, posterior urethral valves are the commonest single cause of end-stage renal failure in childhood (Woolf and Thiruchelvam 2001) and PUV-associated bladder dysfunction is associated with progressive damage of the kidneys postnatally (Parkhouse et al 1988). Postnatal renal functional and structural outcome is therefore apparently linked to bladder function and hence bladder development.

Levin et al (1997) have described a rabbit model of partial bladder outflow obstruction in adult rabbits, and compared these changes with those in the human bladder as a result of benign prostatic hyperplasia (Levin et al 2000): first, there is an initial hypertrophic response of the DSMC which lasts 1–14 days; second the rabbit bladder reaches a compensated phase, during which bladder mass and contractility remain approximately constant, and the patient asymptomatic; third, there is a decompensation with deterioration in contractility and function. In the rabbit model the initial phase is associated with smooth muscle hypertrophy, increased collagen synthesis, urothelial and interstitial fibroblast hyperplasia. The specific triggers for decompensation are unknown: further increase in bladder mass may result in loss of response to stimulation, and progressive loss of bladder contractility. Ischaemia could be one of these triggers for decompensation (Ghafar et al 2002). (Levin et al

2000) have suggested five markers associated with this decompensation: 1) increasing muscle mass, 2) denervation, 3) progressive decrease in compliance, 4) decreased sarcoplasmic reticulum calcium ATPase and 5) mitochondrial dysfunction. In the rabbit, end–stage decompensation may take two forms, a large thin walled, fibrous bladder, with large capacity, or a small, thick walled, poorly compliant fibrous bladder. Contractility is poor or absent in either case, with loss of smooth muscle cells. A change in smooth muscle phenotype has been described in animal models with a shift towards synthetic phenotype. Histological evidence for this in humans has been seen by connective tissue infiltration around smooth muscle cells within smooth muscle bundles in adult human bladders (Levin et al 2000). A similar histological pattern was described by Nyirady et al in an ovine model of fetal bladder outflow obstruction (Nyirady et al 2002;Thiruchelvam et al 2003). If partial BOO is created at 75 days of gestation in fetal sheep, by urachal ligation with partial urethral obstruction using a ring, and the fetuses are examined at 30 days then the bladders are grossly distended, and thin walled compared to sham operated controls (Nyirady et al 2002;Thiruchelvam et al 2003), consistent with decompensation as described in adult human bladders. If however the same model, created at around 75 days is allowed to run for only 9 days, then a thick-walled, hyperplastic bladder is generated (Farrugia et al 2006a). Similar increase in detrusor muscle mass (marked hypertophy, some hyperplasia), has been described in a fetal ovine model as a result of BOO created at 60 days (Peters et al 1992b). The fetal BOO pattern described by Nyirady et al and subsequently by Farrugia would be consistent with the changes described in the post natal rabbit model: first, an initial

hypertrophic, hyperplastic response as (Buttyan et al 1997;Farrugia et al 2006a, b); ultimately, if obstruction persists then 'decompensation' occurs (Buttyan et al 1997;Nyirady et al 2002;Thiruchelvam et al 2003).

Partial fetal BOO in a rabbit model results in an increase in bladder weight, urodynamic changes of 'denervation hypersensitivity' (loss of field sensitivity, but increased contraction when stimulated with potassium chloride or bethanecol), with histological changes of smooth muscle hypertrophy and increased connective tissue within the detrusor layer (Rohrmann et al 1997). This differed from the response of adult rabbit bladders to obstruction, in which there was increased connective tissue subserosally. However, in fetal bladder outflow obstruction there was a similar time-course in the response with compensatory hypertrophy, followed by decompensation at a variable time later.

In cultured human DSMC (2 year old), stretch initially resulted in increased protein synthesis, a 'hypertrophic' response, but prolonged stretch induced increased DNA synthesis, a 'hyperplastic' response (Orsola et al 2002).

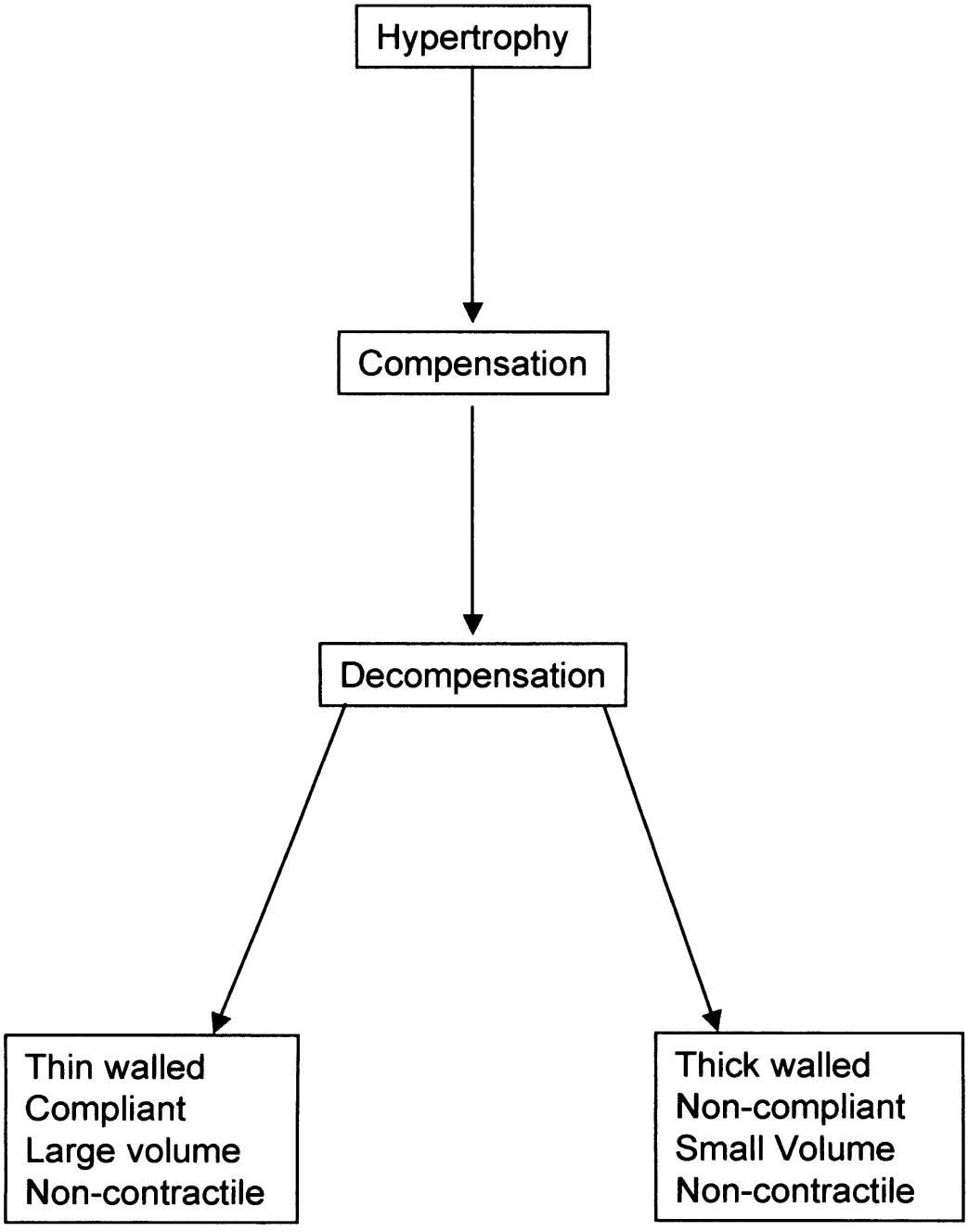

Figure1.17 : Partial bladder outflow obstruction in a rabbit model (Levin et al 2000).

Extracellular matrix in BOO

The change in the pattern of collagen expression has been described during fetal bladder development in normal and obstructed human fetal bladders by (Kim et al 1991a, b). In comparison between 15 normal bladders from fetuses between 20 and 35 weeks gestational age (GA), and ten BOO fetuses (Kim et al 1991b), the muscle thickness was markedly increased, with an increase in thick collagen fibres compared to thin fibres, as assessed by histological examination. Thick collagen fibres have a larger proportion of collagen I than collagen III, compared to thin fibres (Romanic et al 1991). There was a relative increase in muscle compared to collagen in the obstructed bladders (Kim et al 1991b). Freedman et al (1997) compared 9 fetuses with BOO (6 PUV, 3 urethral atresias) with 10 urologically normal fetuses (GA 9-40 weeks) and found the bladder wall was markedly increased, but that the muscle/connective tissue ratio was unchanged (Freedman et al 1997). In a study comparing normal fetal bladders to those diagnosed with PUV and PBS, muscle thickness was found to be increased in the PUV group, and in a subset of the PBS group, compared to the rest of the PBS group and normals (Workman and Kogan 1990). In this series the proportion of connective tissue was unchanged (Workman and Kogan 1990).

In postnatal human bladders that have been obstructed either mechanically, or by neurogenically an increase in the interstitial connective tissue of the lamina propria has been described, with an increase, or infiltration of connective tissue between the muscle bundles, and within the muscle

bundles, with disruption of the normal architecture in extreme cases. In a comparison of 9 men suffering form benign prostatic hyperplasia causing chronic BOO, with 8 non-obstructed controls (aged 46-73 years) no smooth muscle hypertrophy was described, but dense connective tissue was seen in the detrusor layer separating the muscle fibres, and separating the muscle cells in the muscle bundles (Gosling and Dixon 1980). Whereas Gilpin et al (1985) described 14 BOO (66-76 years) compared to 37 controls (20-72 years), in which smooth muscle hypertrophy was histologically present in BOO, in comparison to the controls (Gilpin et al 1985). There was similar infiltration of connective tissue into the muscle bundles in BOO as described in the previous series (Gilpin et al 1985). In a comparison between 9 non-compliant neurogenic bladders (1-21 years) and 14 controls (6weeks-8years), there was increased expression in the detrusor of in BOO, with marked upregulation of collagen III, as assessed by immunohistochemistry, between and within the muscle bundles (Ewalt et al 1992).

Fetal DSMC are contractile, but also synthetic. Baskin et al have demonstrated that cultured (primary culture passaged once) fetal bovine (mid to late gestation) and human (3, 6 and 8 yrs of age) DSMC can produce fibronectin and collagens I and III in culture (Baskin et al 1993b). At an ultrastructural level, fetal rat DSMCs are surrounded by fibronectin fibrils (Wu et al 1999a), which are intimately associated with focal adhesions forming the 'fibronexus' (Wu et al 1999a;Eyden 2001). Fibronectin expression peaks neonatally in the mouse model, as assessed by immunohistochemistry and Western blot (Smeulders et al 2003), and is then down–regulated with postnatal maturation. Murine detrusor laminin expression and is then

upregulated, as assessed by immunohistochemistry and western blot (Smeulders et al 2003). Fibronectin has been implicated as a factor in normal collagen synthesis (Velling et al 2002), so could be expected to also be expressed in the interstitial spaces between muscle bundles and in the lamina propria. The pattern of fibronectin expression has not been described however in the human fetal bladder.

Cyclical stretch of cultured mid to late gestation fetal bovine DSMC results in upregulation of collagen I, down regulation of collagen III and upregulation of fibronectin, whereas cyclical stretch of cultured urothelial cells results in downregulation of collagen III and upregulation of collagen I and fibronectin, as assessed by enzyme linked immunosorbent assays (ELISA) of protein levels (Baskin et al 1993a). Similarly in an adult rat model in which bladders were transurethrally over-distended, collagen I mRNA transcription was 3 fold decreased, whereas collagen III was upregulated 2.5 fold (Capolicchio et al 2001). Whereas (Upadhyay et al 2003) have described in vivo distension of rat bladders resulting in upregulation of both collagen I and collagen III mRNA (Upadhyay et al 2003).

Fibronectin is a signal for cardiac smooth muscle cell hypertrophy (Chen et al 2004). It can be postulated in fetal partial bladder outflow obstruction that fibronectin would initially be increased as bladder hypertrophy and hyperplasia occurred. In decompensation there might be infiltration of the muscle bundles and loss of DSMC, with a loss of their basal lamina fibronectin.

Another mechanism altering fibronectin expression might involve over-stretch of the lamina propria causing tissue damage. This could be associated with expression of a primary injury matrix with deposition of fibronectin and fibrin, which in turn could be associated with activation of fibroblasts to myofibroblasts and a wound healing response. In the lamina propria, and between the muscle bundles increased collagen synthesis could be expected to occur, as in other models of fibrosis, such as in pulmonary fibrosis and liver fibrosis (Gabbiani 2003).

The consequences of human fetal BOO include three types of urodynamic abnormality: myogenic failure, hyperreflexia, poorly compliant (Peters et al 1990). Particularly in the final group, the so-called 'valve bladder', the bladder becomes thick walled and fibrotic. The abnormal bladder in turn goes on to further compromise renal function, and can also produce incontinence. Abnormal matrix deposition is part of the pathological process in the development of this 'valve bladder'.

It would therefore seem likely that integrin ECM interactions would be important in normal and pathological bladder development. It can be hypothesized that specifically: 1) during normal human bladder development DSMC would proliferate and hypertrophy in close association with fibronectin. 2) In human fetal bladder outlet obstruction, there is a spectrum of bladder responses from compensation to decompensation. The degree of decompensation would in turn be related to the severity of obstruction. Decompensated bladders would be associated with severe obstruction. 3) Detrusor hyperplasia and hypertrophy would be associated with increased

fibronectin expression in the basal lamina. Loss of smooth muscle cells in the decompensated bladders would be associated with loss of the basal lamina fibronectin. 4) Tissue damage and activation of fibroblasts in the lamina propria would be predicted to be associated with increased fibronectin and collagen synthesis.

Conclusion

ECM is an evolutionarily ancient and preserved structure. The basal lamina components can influence cell fate and differentiation: it can be hypothesised that fibronectin reinforces the proliferative synthetic fetal smooth muscle cell phenotype, and laminin provides a differentiation signal favouring mature DSMCs. The cell surface receptors for ECM include integrins, which are also ancient and highly preserved molecules. There is a structural hierarchy that extends from the interstitial collagens to the basal lamina, through cell surface receptors – predominantly integrins – to the cytoskeleton of the cell. Integrin receptors are not just structural but also mediate instructive signals from fibronectin and laminins respectively. Integrins can also act as mechanotransducers allowing normal physiological stretch to contribute to normal detrusor morphology and development. In pathological obstruction, integrin/ECM interactions may be important in determining the pathological response.

ECM molecules studied in this thesis

Fibronectin

Three main lines of evidence suggest that fibronectin might play a functional role in bladder organogenesis: firstly, abnormalities of fibronectin null knockout mutants show that fibronectin may have a (non-bladder) role in organogenesis; secondly, the descriptive work demonstrating presence and developmental regulation of fibronectin in murine bladder development; thirdly, VSMC culture experiments using different substrates, such as fibronectin and laminin modulate the phenotype of these cultured cells.

1) Fibronectin null knockout mouse mutants

That fibronectin is essential for normal embryogenesis can be seen by the lethal nature of homozygous fibronectin null knockout mice. These mutants have mesodermal abnormalities that cause lethality at around the time of implantation (embryonic day 8.5). This is before the bladder is recognizable as a distinct structure so these mutants are not specifically informative for bladder development (George et al 1993).

2) Descriptive studies of fibronectin expression in developing murine bladder

Work by Smeulders et al (2003) has demonstrated that fibronectin is present in the detrusor of fetal murine bladders, and that this ECM protein is upregulated antenatally then downregulated postnatally.

3) Cell culture experiments

Fibronectin can modify the behaviour of vascular smooth muscle cells (VSMC) grown in culture. These VSMC become proliferative and synthetic (Thyberg and Hultgardh-Nilsson 1994;Morla and Mogford 2000) in the presence of fibronectin.

Laminin

That laminin might play a functional role in maturation of DSMC is suggested by several lines of evidence: 1) cell culture work; 2) descriptive studies of murine bladder development; 3) differentiation of mesenchymal cells in murine lung bud; 4) role of laminins in skeletal muscular dystrophy.

1) Cell culture experiments

VSMC in culture become less proliferative, and more contractile when cultured on laminin (Thyberg and Hultgardh-Nilsson 1994; Morla and Mogford 2000).

2) Descriptive studies of mouse bladders

Work by Smeulders et al (2002, 2003) has shown that maturation of DSMC during development is associated with generic laminin upregulation.

3) Laminin-1 and laminin-2 in the developing lung bud

Based on Schuger and colleague's work (1997) laminin-1 is initially expressed at the interface between the primitive epithelium and mesenchyme in the lung-bud (Schuger et al 1997), and influences subsequent differentiation of the

mesenchyme into smooth muscle, with expression of laminin-2 and reinforcement of the smooth muscle phenotype (Relan et al 1999).

4) Muscular dystrophy

Colognato et al (1999) have shown that laminin polymerization is a key step in the development of basal lamina, that this is receptor mediated, and that COOH terminal domains, and the receptors that bind them are crucial in this. Human and mouse muscular dystrophy is associated with mutations in laminin genes (Yurchenco et al 2004b).

Candidate integrin receptors studied in this thesis

Candidate fibronectin integrin receptor

Possible candidates include integrins α4β1, α5β1, αvβ3, α8β1. Integrin αIIbβ3 is predominantly a platelet expressed integrin although ectopic expression has been described in tumours. Integrin α5β1 is the archetypal fibronectin receptor and important not just in ligation of fibronectin, but also in fibrillogenesis. For these reasons it was the candidate fibronectin receptor studied in this thesis.

Candidate laminin integrin receptor in detrusor

From preliminary results reported in Chapter 5 and the review of laminin subunits described above, receptors for laminin 1 (α1β1γ1) G domains (i.e. integrins α6β1 and α7β1) and laminin 2 and 4 (α2β1γ1 and α2β2γ1) G domains (i.e. integrin α3β1, α6β1 and α7β1) would be appropriate choices. In the Appendix preliminary immunohistochemistry results for integrin α6 immunostaining are described. No immunostaining was found in the developing murine detrusor layer. Integrin α7β1 was therefore chosen as the candidate integrin laminin receptor for this thesis.

Chapter 2. Hypotheses and Experimental strategy

Overall Hypothesis

Fibronectin acting through a candidate integrin receptor (integrin α5β1) may be important during bladder smooth muscle development in that it may maintain fetal smooth muscle cells in a proliferative phenotype. Laminins acting through a candidate muscle laminin receptor integrin α7β1, may induce a maturation response, and might help maintain adult smooth muscle cells in the differentiated form.

Specific hypotheses

Study 1 (Chapter 5): Analysis of expression of adhesion molecules fibronectin and laminin-1/2 and their candidate receptors during fetal mouse bladder development

Hypothesis: During murine bladder development, the candidate fibronectin receptor integrin α5β1 may be expressed by detrusor smooth muscle cells (DSMC), and that laminin 1/2 candidate receptor integrin α7 may be expressed by DSMC.

Background: In order for a ligand and receptor to interact, their expression should temporally and spatially overlap, i.e. they need to be in the same place at the same time to allow a response to occur. If these putative ligands (fibronectin and laminin-1 or lamini-2) are not expressed in the basal lamina of

the DSMC, and these DSMC do not express the putative receptors (integrin $\alpha5\beta1$ and $\alpha7\beta1$) then the hypothesis is disproved.

Aims: 1) To examine if expression of candidate fibronectin receptor integrin $\alpha5\beta1$ occurs in mouse bladders during fetal development and postnatal maturation by immunohistochemistry; and to further quantify this protein expression by using Western blots, or flow cytometry. 2) Determine if laminin 1/2 are expressed in the basal lamina of DSMC, and if this coordinates with the candidate receptor integrin $\alpha7\beta1$.

Study 2 (Chapter 6): Functional interaction between DSMC and fibronectin matrix in cell culture.

Hypothesis: In Vitro DSMC may adhere to fibronectin, possibly modifying cell behaviour, and that this adherence may be mediated by the candidate fibronectin receptor integrin $\alpha5\beta1$.

Background: That fibronectin is present in ECM of fetal DSMC during murine bladder development has been shown by (Smeulders et al 2003). Furthermore bovine DSMC are capable of secreting fibronectin in cell culture (Baskin et al 1993b). In cell culture vascular SMC adhere to fibronectin and become proliferative and synthetic on this substrate (Morla and Mogford 2000; Thyberg and Hultgardh-Nilsson 1994). Bourdoulous et al (1998) has shown that for endothelial cells and fibroblasts, fibronectin is necessary for cell cycle progression and proliferation. Hornberger et al (2000) has shown that adhesion dependent EGF stimulated growth of human fetal myocytes is enhanced by stimulation of integrin $\alpha5\beta1$. Nguyen et al (2005) have shown

that β1 integrins including integrin α5β1 are important in airway smooth muscle growth on collagen I, or fibronectin substrate. Could there be a functional interaction between the fibronectin and fibronectin receptor integrin α5β1, and modulation of proliferation of these murine DSMC?

The strategy of this chapter was to use whole bladders disaggregated into a bladder cell suspension. The cells in suspension would therefore closely resemble those from the in vivo bladder. Using this heterogenous suspension of detrusor, connective tissue, vascular and urothelial cells the following aspects could be examined: 1) did bladder cells stick to fibronectin; 2) what is the nature of these cells, this would be examined by immunocytochemistry: are DSMC cells adhering, as demonstrated by smooth muscle markers such as αSMA and desmin; and do these cells express the candidate integrin receptor α5β1; 3) what is the nature of the effect of fibronectin adhesion on these cells with regards proliferation; 4) can adhesion of these cells be inhibited either by antibody blocking the fibronectin, or by use of RGD oligopeptides to block the integrin binding site for fibronectin.

Aims: 1) to examine adhesion of disaggregated bladder cells from fetal and mature murine bladders to a fibronectin substrate, 2) characterise these adherent cells. 3) Examine any proliferative effect that fibronectin adhesion may have on fetal bladder cells. 4) Examine any effect blockade of fibronectin/integrin interaction may have on adhesion of cells from whole bladder suspensions.

Study 3 (Chapter 7): Mouse fetal bladder explant fibronectin blocking experiment.

Hypothesis: Fibronectin-integrin interactions in ex vivo bladders may be important in modulating DSMC development.

Background: Two strategies are possible for the examination of the role of ECM and integrin interactions in-situ in whole bladder development: first examination of the phenotype of null mutant mice lacking these genes in vivo; second, using ex-vivo organ culture. Unfortunately null mutant mice for fibronectin, integrin α5 and β1 are embryonically lethal before bladder development occurs, and are therefore not informative. Embryonic bladder organ culture has not, however, been used to specifically examine fibronectin/integrin interactions, although a comparable, metanephric, model has been used to study the role of matrix using blocking antisera (Zent et al 2001). The functional role of fibronectin and integrin receptors in branching morphogenesis have also been studied in mouse salivary gland explants (Sakai et al 2003). Cell culture has been extensively used to examine the effects of different ECM substrates on cell behaviour, but recreating the mesenchymal-epithelial interactions that occur during bladder development and the 3D ECM is difficult. Using an explant model of mouse bladder development is a novel strategy to explore the functional relationship between matrix, integrins and DSM development. This would allow mesenchymal-epithelial reciprocal induction to occur, and would have the correct progenitor cells embedded in their native 3D matrix. Generating these 3D arrangements and interactions in cell culture would be challenging.

Aims: 1) Generate a fetal bladder explant model; 2) use this model to investigate the effect of disrupting fibronectin-integrin interactions on fetal bladder DSMC development.

Study 4 (Chapter 8): Fibronectin expression in normal and pathological development of human fetal bladders

Hypothesis: Fibronectin may be expressed in the basal lamina during normal human fetal DSMC development; furthermore altered fibronectin expression might be implicated in detrusor smooth muscle pathology in human bladder outflow obstruction (presumed BOO), and correlate with dysmorphogenesis of the whole urinary tract.

Background: Fibronectin is upregulated in the ECM of fetal murine DSMC (Smeulders et al 2003), which are proliferative (Smeulders et al 2002). This leads to questions about the expression of fibronectin in human bladders; 1) is fibronectin expressed in the basal lamina of fetal human bladders? 2) What the pattern of expression of fibronectin and the morphology of these bladders in obstruction? 3) How does normal development and development of the urinary tract (kidneys and bladder) in obstruction differ? In order to be able to compare the normal and obstructed kidneys and bladders a measure of renal dysplasia (renal dysplasia score) needs to be generated, as does a scoring scheme for muscle abnormality in the bladder (muscle dysmorphology score).

Ethical committee approval to identify normal and abnormal human fetuses (diagnosed as having congenital bladder outflow obstruction on post mortem)

from the human embryo bank held at UCH by Dr R Scott, was sought from University College, London. Information from the post mortem certificates, and from IHC examination of the urinary tracts (bladders and kidneys) could be used to answer these questions.

Aims: 1) Demonstrate if fibronectin is expressed in human fetal bladders, and to correlate this with gestational age, and measures of cell turnover. 2) Describe the abnormal pattern of muscle, and possible fibronectin expression in fetal presumed BOO and to compare this with normal development.

Chapter 3. Materials

Mouse tissue

The mouse strain used in this study was the CD1 mouse from Charles River. This is a wild-type mouse strain. Bladders were harvested from timed mated CD1 mice, where the time of finding the plug was taken as the start of gestation (E0). Embryonic bladders from day 14, 16 and 18 of gestation, postnatal day 1 (D1) and 6 weeks of age (6Wks) were harvested, and the specimens separated into male and female sex. For fetuses the male and female gonads are distinctly different at E14: the testis is ovoid and 'striped', whereas the ovary has greater longitudinal length and is not 'striped'. Postnatal animals can be differentiated by examination of the perineum: in males the urethral meatus and the anus are widely separated, whereas the urethral meatus and anus are close together in the females. All animals were sacrificed by cervical dislocation, under Schedule 1 of the Animals Act (1987), this was initially covered by Prof AS Woolf's informal license, then by my own personal license.

Human fetal tissue

Human fetal material came from the archive held by Dr R. Scott (Consultant Fetal Pathologist) at University College Hospital, London. This work was

covered by local ethical committee approval (UCH/UCLH joint research ethical committee 03/0080). Fetuses with presumed bladder outflow obstruction (BOO), and morphologically normal controls, were identified from the database held by Dr Scott. Cases which had appropriate consent for scientific examination were used in this study. Annonymised post mortem reports were obtained for each case, kidney slides were examined, and sections of formalin fixed, paraffin embedded bladder were obtained for each case.

Normal unmacerated fetuses were identified from the database. Twelve normals were initially identified, with gestational ages from 16-30 weeks. Four were spontaneous abortions, five had been still births and 3 were terminations of pregnancy for intra-uterine death. All these fetuses were morphologically normal. Data from the post-mortem forms is detailed in table 3.1.

Table 3.1: Morphologically 'Normal' human fetuses

Number	Sex	GA	Cause of Delivery	Associated Anomalies
1	M	16	SA	Nil
2	F	16	TOP - IUD, Chorioamnionitis	Nil
3	M	18	SA	Nil
4	M	20	SA - Chorioamnionitis	Nil
5	F	20	SA	Nil
6	M	21	TOP - IUD	Nil
7	M	24	SB	Nil
8	M	26	SB - Chorioamnionitis	Nil
9	F	27	SB	IUGR
10	F	28	SB	Nil
11	M	30	TOP - IUD	IUGR
12	F	31	SB	Nil

SA – Spontaneous abortion, SB – Still Birth, TOP – Termination of pregnancy, IUD – Intra-uterine death,

IUGR – intra-uterine growth retardation

Fetuses which had evidence of prune belly syndrome were excluded, as were isolated urethral atresias. No specific attempt had been made either to demonstrate the obstructing valve histologically, or to demonstrate obstruction on a post-mortem cystogram. Instead macroscopic examination, looking particularly for a wide-open bladder neck, and dilated posterior urethra (an equivalent of the antenatal ultrasound 'keyhole' sign, as used in some series to define infravesical bladder outflow obstruction (Welsh et al 2003)), was used to diagnose these fetuses. These specimens were analysed retrospectively, so this clinical description was all that was available for analysis. The diagnosis of bladder outflow obstruction is therefore presumed, and so the term presumed BOO is used in this thesis.

Fetuses with a diagnosis of bladder outflow obstruction were identified from the database. Three 'prune belly' fetuses were also identified (2 male, 1 female), and two urethral atresias were found (1 male, 1 female). These were not included in the obstructed group, and have not been analysed further.

The indications, as detailed in the post mortem forms, for the decision leading to termination of pregnancy have been listed in table 3.3. These included: possible bladder rupture; oligohydramnios and bilateral hydroureteronephrosis; bilateral hydroureteronephrosis and megacystis; megacystis with hydrops; hydroureteronephrosis with increased renal echogenicity (suggests renal dysplasia) with a thick-walled bladder; oligohydramnios, ascites, hydronephrosis and megacystis; bilateral hydronephrosis, oligohydramnios and trisomy 21; and megacystis with

megaureters. The post mortem findings for these fetuses are described in table 3.2, and reflect the pathologists' interpretation of the gross appearances of the specimens, and any postmortem imaging performed.

Table 3.2: Human fetuses with presumed bladder outflow obstruction

Number	Sex	GA	Cause of Death	BOO	Bladder	Ureters	Kidneys/Ureters	Associated anomalies
1	M	18	TOP	Sub-total PBOO	distended, thick wall	dilated, left VUR	normal kidneys, no hydronephrosis	single umbilical artery
2	M	18	TOP	PBOO	thickened wall, PUV	gross distension	gross hydrourteronephrosis	Pulmonary hypoplasia
3	M	18	TOP	PBOO	thickened wall, distended	No comment	hydronephrotic, dysplastic	hypospadias, imperforate anus, micrognathia. Low set ears
4	M	19	TOP	PBOO	distended, thin walled	mild distension	mild hydronephrosis, renal dysplasia	hydrops
5	M	20	TOP	PBOO	thick walled, distended	distended	hydroureteronephrosis, dysplastic kidneys	
6	M	21	TOP	PBOO	distended	bilaterally dilated	hydronephrotic,dysplastic kidneys	bilateral talipes
7	M	22	TOP	PBOO	distended, thick walled	bilaterally dilated and tortuous	hydronephrotic, dysplastic kidneys	Trisomy 21
8	M	24	TOP - IUD	PBOO	thick walled	mega-ureters	cystic dysplasia, left kidney, hydronephrosis right kidney	dilated urachus

PBOO –presumed bladder outflow obstruction; TOP – termination of pregnancy; VUR – vesico-ureteric reflux; GA – gestational age; IUD – in utero death

Table 3.3: Clinical indications leading to termination of pregnancy.

Fetus	GA	Reason for TOP / Delivery
1	18	?ruptured bladder. (Not ruptured at PM), left VUR, right megaureter,
2	18	probable PUV, Oligohydramnios and right hydro-ureteronephrosis 16/40, left hydro-ureteronephrosis 18/40
3	18	bilateral hydronephrosis, hydro-ureter and distended bladder
4	19	distended bladder in utero with hydrops
5	20	dilated ureters, increased renal echogenicity, thick-walled bladder
6	21	severe oligohydramnios, ascites, enlarged bladder and hydronephrosis
7	22	bilateral hydronephrosis, oligohydramnios and Trisomy 21.
8	24	IUD megacystis and mega ureters

Reagents

2-mercaptoethanol (M6250, Sigma)

5-bromo-2-deoxyuridine (BrdU) kit (1444611, Roche Diagnostics GMBH, Mannheim, Germany)

ABC horse-radish peroxidase detection kit (K0355, DAKO)

Acetone (15296, BDH)

Acrylamide (A3699, Sigma)

Alcohol (Ethanol, UN1170, Hayman)

Ammonium persulphate (A-7460, Sigma)

Animal research kit (ARK) (K3954, DAKO)

Anti-mouse IgG, FITC conjugated (11-4011-85, eBioscience)

Aprotonin (Protease inhibitor bovine lung) (A-6279, Sigma)

Bicinchoninic acid (BCA) protein assay (23227, Pierce, Perdio Science UK Ltd, Cheshire, UK)

Bovine serum albumin (fraction V) (A-2153, Sigma)

Bromophenol blue

Butanol (100616J, BDH)

Calcium Chloride (C5080, Sigma)

Citifluor (Glycerol/PBS) (AF1, Citifluor, London, UK)

Citric Acid (C0759, Sigma)

Collagenase A (103 578 Roche Diagnostics GMBH, Mannheim, Germany)

Cytotoxicity detection kit (1 644 793 Roche Diagnostics GMBH, Mannheim, Germany)

Diaminobenzidene (DAB) (K3466, DAKO)

Dispase (17105, GIBCO)

DMEM/F12 (31330-038, Gibco/Invitrogen)

DNase I (1 284 932 Roche Diagnostics GMBH, Mannheim, Germany)

DPX (360294H, BDH)

Enhanced chemiluminescence reagent (ECL) for Western Blotting (RPN 2106, Amersham Bioscience, Buckinghamshire, UK)

Envision kits (anti mouse IgG labelled polymer K4006, anti-rabbit IgG labelled polymer K4011, DAKO)

Fat-free milk powder (Marvel) (Premier foods Ltd, Spalding, Lincs, UK)

Fetal calf serum (01020-160, Gibco BRL)

Fluorescent TUNEL detection kit (1 684 795 Roche)

Glycerol (G5516, Sigma)

Glycine (G8898, Sigma)

Goat anti-rabbit IgG (P0448, DAKO)

Goat anti-rabbit IgG FITC conjugated (65/6111 Zymed)

Goat ant-mouse IgG conjugated with TRITC (SC2092, Santa Cruz)

Goat ant-rabbit HRP conjugated (P0448 Dako)

Haematoxylin (Mayers) (MHS-32, Sigma)

Haemocytometer (962-9 Sigma Brightline Z35)

Hanks' balanced salt solution (HBSS; 14170-088; Gibco BRL)

Histoclear (HS-200, RA Lamb)

Hydrogen Peroxide (H1009, Sigma)

Hybond C nitrocellulose membrane (RPN 303C, Amersham)

Insulin, selenium and transferrin supplements (ITS) (I3146, Sigma)

L15 Leibowitz medium (11415-049, Gibco/Invitrogen)

Lab-tek 4 chamber slides (177399), 8 chamber slides (177402, Nunc Nalge International, Naperville, Illinois, USA)

Magnesium Chloride (M8266, Sigma)

Methanol (65548, Fluka Chemikon)

Methylene blue (180-8, Sigma)

Milli-Q water

Monoclonal mouse ant-human PGP 9.5 (13C4, Ultraclone, Isle of Wight, UK)

Monoclonal mouse anti-human Ki67 MEB-1 (M7240, DAKO)

Monoclonal mouse anti-human β-actin (A5441, Sigma)

Mouse anti-integrin α7 monoclonal antibody (3C12, MBL, Japan)

N,N,N-N-tetramethylethylenediamine (TEMED) (T9281-Sigma)

Nonidet P40 (NP40) (NP-40 alternative, 492016, Calbiochem)

O.C.T Tissue Tech (4583, RA Lamb, Eastbourne, Sussex, UK)

Phenylmethanesulfonyl fluoride (PMSF) (P7626, Sigma)

Phosphate buffered saline (PBS) (BR0014G, Oxoid, Basingstoke, UK)

Ponceau S (P7170, Sigma)

Proliferative cell nuclear antigen (PCNA), biotinylated mouse anti-human IgG (555567, Pharmingen)

Propidium iodide (P4170, Sigma)

Rabbit anti-human fibronectin IgG (A0245, DAKO)

Rabbit anti-mouse fibronectin (AB2033, Chemicon)

Rabbit anti-mouse HRP conjugated (P0260 Dako)

Rabbit anti-mouse integrin α5 – gift Dr K. Hodivala Dilke

Rabbit anti-mouse integrin β1 – gift Dr K. Hodivala Dilke

Rabbit anti-mouse integrin β3 – gift Dr K. Hodivala Dilke

Rabbit immunoglobulin G (Chemicon)

Rabbit immunoglobulin G (IgG) (I5006 Sigma)

RAD - cyclo-arginine-glycine-aspartate-D-Phenylalanine-Valine (H4088, Bachem)

Rainbow marker (RPN 800, Amersham life Science)

Rat immunoglobulin G (IgG) (I4131, Sigma)

Rat plasma fibronectin (F0635 Sigma)

RGD - cyclo-arginine-glycine-aspartate-D-Phenylalanine-Valine (H2574 Bachem)

Sodium azide (S8032, Sigma)

Sodium chloride (S7653, Sigma)

Sodium deoxycholate (D6750, Sigma)

Sodium dodecylsulphate (SDS) (15525-017, Invitrogen)

Sodium orthovanadate (S6508, Sigma)

Tonsillar tissue – GOSH histology department.

TRIS (T1503, Sigma)

Triton X-100 (X100, Sigma)

Trypan blue (T-8154, Sigma)

TUNEL test - Promega deadend colorimetric system (G7360, Promega)

Tween-20 (P9416, Sigma)

Van Gieson stain

Whatman 3mm paper Chromatography (3030917, Whatman)

Chapter 4. Methods

Study 1i: Immunohistochemistry

Frozen sections

Bladders were frozen in an optimum cutting temperature (OCT) formulation of water-soluble glycols and resins (Tissue-Tek) at -20°C, along with positive control tissue - normally a paw (see section below on positive controls), and subsequently cut into 8-10 µm sections using a cryostat. The sections were then air dried and stored at -80°C until used. Prior to staining, the slides were warmed and dried, then either (1) re-hydrated using phosphate buffered saline (PBS) for 5 minutes and fixed using 4% paraformaldehyde solution (diluted using PBS with magnesium and calcium chloride to 1mM – PBSABC) for 10 minutes as described by (Hertle et al 1991); or (2) fixed using acetone at -20°C for 10 minutes. Following this, the slides were rinsed in PBSABC and wax rings were drawn around the individual sections. These were then permeabilised using 0.5% NP40 in PBSABC, at room temperature for 10 minutes. Endogenous peroxidase activity was quenched with 10% H_2O_2 in PBSABC. The sections were then blocked with 0.1%-1% bovine serum albumin (fraction V) with 0.2% Triton X-100 in PBSABC.

Most of the immunostaining was performed using rabbit anti-mouse antibodies, in which case the staining is described below. However for antibodies raised in mice the DAKO animal research kit (ARK) was used, as described below.

Test-runs were performed to find optimal dilutions of rat and rabbit primary antibodies (using a range 1/50 to 1/500). Primary antibody (1/100-1/200 dilutions of 1mg/ml), depending on type, were added to each section and incubated for 1 hour at 37°C, or overnight at 4°C. The antibody was tipped off, and the slide rinsed in PBSABC three times. The horse-radish peroxidase (HRP) secondary antibody (DAKO anti-rabbit P0448) was allowed to incubate for 30 minutes at room temperature, tipped off and the slides rinsed three times with PBS. Finally diaminobenzidene (DAB) was added. The reaction was allowed to proceed until a brown stain was visible. The slides were then washed in running water for 2 minutes, counter-stained with haematoxylin for 1 minute, dehydrated by being placed in serial alcohols of ascending concentration, and then Histoclear for 2 minutes. Coverslips were mounted using DPX.

Controls

A negative control was included on each slide by substituting the primary antibody for a non-immune antibody of the same isotype i.e. non-immune rabbit immunoglobulin G for primary rabbit antibody. This was added in the same concentration as the optimised primary antibody.

A positive control tissue was present on each slide in the form of a paw from a fetus from the same time-point as the bladders had been harvested from (fetal and neonatal timepoints), or skin from an adult mouse. This provided skin and skeletal muscle positive controls for integrin expression.

Mouse primary antibodies on mouse tissue – immunostaining using Dako animal research kit (ARK)

Detecting exogenous mouse IgG in the presence of endogenous mouse IgG in the tissue section, may require a modified technique. If the primary antibody is conjugated with biotin or horse-radish peroxidase (HRP) then detection of the primary antibody is not confounded by the endogenous IgG. Unfortunately, the only commercially available anti-integrin α7 antibody is raised in mice. The Dako ARK system obviates this technical problem: the primary antibody is mixed with a solution containing an excess of anti-mouse Fab fragments of a secondary antibody (these are biotinylated). The primary and secondary antibodies bind, leaving an excess of the secondary. This is then bound by an excess of non-immune mouse IgG. No secondary antibody is left to bind with endogenous mouse IgG in the histological sections when this solution is added to the slide. The secondary antibody is detected using streptavidin-conjugated HRP, and DAB as described above.

Antibody specificity

Rabbit anti-mouse integrin α5 – gift Dr K. Hodivala Dilke, St. Bartholomew's Hospital Medical School and The London Queen Mary's School Of Medicine and Dentistry, UK. This antibody was raised against a synthetic peptide equivalent to the terminal 23 amino acids of human integrin α5 subunit, (Hynes et al 1989). This sequence (KRSLPYGTAMEKAQLKPPATDSA) is from the cytoplasmic tail of this integrin sub-unit.

Rabbit anti-mouse integrin β1 was a gift Dr K. Hodivala Dilke. This antibody was prepared against an antigen from the carboxy terminus of the integrin β1

subunit (amino acid sequence CREFAKFEKEKMNAKWDTGENPIYKSAVTTVVNPKYEGK) (Marcantonio and Hynes 1988).

Mouse anti-integrin α7 monoclonal antibody (3C12, MBL, Japan). This commercially available monoclonal antibody was originally prepared by immunization of integrin α7 knockout mice with mouse myoblasts. Subsequently, hybridomas were produced by fusion of mouse myeloma cells with spenocytes from the immunized mice. The antibody was purified using protein-A sepharose from the hybridoma supernatant (Mayer et al 1997).

Rabbit anti-human fibronectin IgG (A0245, DAKO). This polyclonal antibody is commercially available, prepared by immunising rabbits using pooled citrated human plasma fibronectin. Cross reacting antibodies were removed by solid phase absorption with other human plasma proteins (A0245 DakoCytomation data sheet).

Rabbit anti-mouse fibronectin (AB2033, Chemicon). Rabbits were immunised with fibronectin purified from mouse plasma. Radioimmunoassay shows less than 0.1% reactivity with mouse laminin, and collagen types I, III, and IV, as described in the Chemicon datasheet.

Table 4.1: Primary antibodies

Primary antibody (Source)	Isoform control	Secondary antibody	Reference
Rabbit anti-mouse integrin α5 (Gift K Hodivala-Dilke)	Pre-immune rabbit IgG	DAKO anti-rabbit P0448	(Hynes et al 1989)
Rabbit anti-mouse integrin β1 (Gift K Hodivala-Dilke)	Pre-immune rabbit IgG	DAKO anti-rabbit P0448	(Marcantonio and Hynes 1988)
Mouse anti-integrin α7 (3C12, MBL, Japan)	Pre-immune mouse IgG	DAKO ARK kit K3954	(Mayer et al 1997)
Rabbit anti-mouse fibronectin (AB2033, Chemicon).	Pre-immune rabbit IgG	DAKO anti-rabbit P0448	AB2033, Chemicon datasheet
HRP-labelled mouse anti-human Desmin (U7023, DAKO)	-	-	
HRP labelled mouse anti-human α-SMA (U7033, DAKO)	-	-	(Skalli et al 1986)
Rat anti-mouse CD31 (550274; Pharmingen)	Pre-immune rat IgG	Vector Biotinylated anti-rat, DAKO HRP-stretavidin	(Piali et al 1995)
Mouse monoclonal anti-cytokeratin 18 (MAB3234 Chemicon)	Pre-immune mouse IgG	DAKO ARK kit K3954	(Smedts et al 1992)
Rabbit anti-human fibronectin IgG (A0245, DAKO).	Pre-immune rabbit IgG	DAKO Envision kit K4011	(Kirkpatrick and d'Ardenne 1984)
Biotinylated mouse anti-human PCNA IgG (555567, Pharmingen)	-	DAKO HRP-stretavidin	(Smeulders et al 2002) (Mathews et al 1984)
Monoclonal mouse anti-human Ki67 MEB-1 (M7240, Dako)	Pre-immune mouse IgG	Dako Envision kit K4006	(Huuhtanen et al 1999)

Study 1ii : Western blotting

Proteins were extracted from tissue samples, denatured and separated on sodium dodecyl sulphate polyacrylamide gels (SDS-PAGE). These were then transferred to a nitrocellulose membrane; the primary antibody was applied to bind the protein of interest. This was detected as a band on the membrane by using conjugated secondary antibodies, and a chemiluminescent technique, as described by Sambrook et al (1989).

Protein extraction. This was performed by collecting the tissues from timed mated animals as discussed above, and homogenising them in 4°C RIPA buffer (150 mM NaCl, 50 mM TRIS pH 8.0, 1% Nonidet P40, 0.5% sodium deoxycholate, 0.1% SDS) to which were added fresh proteinase inhibitors (30 µg/ml aprotonin, 100 mM sodium orthovanadate, 100 mM phenoxymethyl sulfoxide (PMSF)). Homogenisation was performed by mincing the tissues, and then triturating the sample through increasing fine calibre pipette tips. The suspension was then sonicated for 10-15 seconds twice. This was then spun at 20,000g on a desk top centrifuge for 30 minutes, at 4°C. At the end of this the supernatant containing the protein was aspirated and saved. This was either used immediately or stored at -80°C.

Protein quantification. The protein concentration was measured in duplicate for each sample using the bicinchoninic acid (BCA) protein assay (Smith et al 1985). This involves the reduction of copper II to copper I ion, by protein in an alkaline medium. Two molecules of BCA chelate with one cuprous ion to produce a purple coloured product. This has a strong absorbance at 562 nm,

with a linear response to protein concentrations from 20 – 2,000 µg/ml. Standard protein concentrations of bovine serum albumin (BSA) were made by serial dilution in the range from 2 mg/ml (stock solution) to 62.5 ng/ml. These were measured in duplicate each time the BCA protein assay was performed.

Each protein specimen was diluted to the same concentration as the most dilute protein specimen used. Fifteen µl of sample were then mixed an equal volume of electrophoresis sample buffer (1 ml glycerol, 0.5ml β-mercaptoethanol, 3 ml 10 % SDS, 1.25 ml of 1M Tris pH 6.8 and 1 mg of bromophenol blue). These mixed samples were heated to 98°C for 5 minutes to denature the protein and allow SDS to bind. By heating the sample of protein with an excess of thiol and SDS, any disulphide links are cleaved and the proteins are dissociated into component polypeptides. SDS is an ionic detergent, which, under these conditions, binds to the polypeptide backbone in a constant ratio of 1.4g SDS: 1g polypeptide. This imparts a negative charge to the polypeptides according to size (Weber and Osborn 1969). These were then placed on ice prior to loading into lanes on a SDS-PAGE gel.

Gels. The gels were divided into an upper 'stacking' low percentage (5%) low pH (6.8) and resolving higher percentage (8%) higher pH (8.8) resolving gel. The stacking gel has larger pores, allowing the SDS bound negatively charged protein to move through it more easily than through the resolving gel with its smaller pores. Glycine exists as a zwitterion (no charge, favoured by low pH) in equilibrium with glycinate (negatively charged, favoured by high

pH). When the electric field is applied, the glycinate moves towards the anode, but when it enters the lower pH stacking gel, the equilibrium shifts towards glycine zwitterions, which are immobile. This generates a high local localized voltage gradient between a leading edge of Cl^- ions and a trailing edge of glycinate. Anionic SDS-protein migrate rapidly, but if they migrate in front of the Cl^- ions, the high local voltage difference is lost and so they slow down. This concentrates the protein in a disc between the Cl^- front and the glycinate. As the proteins encounter the running gel, with its small pore size, their migration slows. Once the glycine reaches the higher pH running gel, the glycinate ion is favoured, and there is no longer an ion deficiency, and the local voltage gradient is lost. There is a uniform voltage gradient across the gel. The protein samples enter the resolving gel as a tight band, and resolution of the gel is improved (Davis 1964;Ornstein 1964). 8% SDS-PAGE resolving gels have been used for all the western blots. The resolving gel was made in 20 ml aliquots, enough for 2 gels. Each aliquot contained 9.3 ml milli-q water, 5.3 ml of 30 % acrylamide, 5 mls of 1.5M Tris (ph 8.8), 200 µl 10% SDS, 200µl of freshly made, and 12µl N,N,N,N-tetramethylethylenediamine (TEMED). Polymerisation of the acrylamide was caused by the action of ammonium persulphate and TEMED. The 5% stacking gel was made in 10 ml aliquots using 6.8 mls milli-q water, 1.7 ml 30% acrylamide, 1.25 ml of 1.0M Tris pH 6.8, 100µl 10% SDS, 100µl of ammonium persulphate and 10 µl of TEMED.

Setting up the apparatus. The Mini-Protean gel apparatus was used with two glass plates, separated by 1.5 mm spacers. The resolving gel (8%) was poured between the glass plates, up to a level a third from the top, and the

remaining space topped up with water saturated butan-1-ol.This 'flattens' the top of the gel and prevents oxygen diffusing in and inhibiting polymerisation. Once the gel had set (normally 45 minutes at room temperature), the butanol was washed off, and the space above the resolving gel was washed twice with milli-q water, and dried using Whatman 3mm paper. The stacking gel was then poured on top. A 10 lane comb was then placed into the top of the gel frame, and the stacking gel allowed to set.

A Laemmli discontinuous buffer system was used, with the upper part of the gels bathed in one bath of buffer (of which the gel plates formed 2 walls) connected to the anode, and the base of the gels was bathed by another – acting as the cathode(Laemmli 1970). Tris-glycine buffer was used (diluted from a 10x stock solution containing 25 mM trizma-base, 250 mM glycine, 0.1% SDS).

Loading and running the gel: A molecular weight marker (15µl) was loaded into lane 1 on each gel. All lanes were loaded with protein specimens to ensure even running. Electrophoresis was performed at 80 V, with the cathode at the top of the gel, the proteins running towards the anode at the base. This was continued until the correct size of molecular weight marker had reached the bottom of he gel.

Electroblotting. Proteins were transferred from the gel onto a nitrocellulose membrane using a semi-dry electroblotter. The glass plates were removed form the running tank, and the resolving part of the gel placed in transfer buffer (0.02 M Tris base, 0.15M glycine, 20% methanol, 0.00275% SDS). On the lower plate (anode) were placed 3 sheets of Whatman 3MM paper

(soaked in transfer buffer). Bubbles and excess buffer were removed by rolling a glass pipette over each layer after it was applied. The nitrocellulose membrane was then placed on this followed by the resolving gel. Saran wrap was placed around the gels, to prevent a short circuit by-passing the gels. This was then covered with 3 more layers of 3MM paper. The cathode was then placed on top of the stack, and electroblotting performed at 12V for 45-55 minutes.

Ponceau S staining. To confirm that protein transfer had occurred, the membranes were washed in Ponceau S for 2 minutes, and then rinsed in de-ionised water for 2 minutes. The Ponceau S reversibly binds to protein, especially immunoglobulins. Pink protein bands were visible where protein had been transferred.

Blocking, primary and secondary antibodies: Once the proteins had been transferred onto the nitrocellulose membrane, blocking of non-specific binding was performed. The membrane was then probed with a primary antibody, washed and blocked again, then this was detected with a secondary antibody, conjugated with horse-radish peroxidase. This was then detected using chemiluminescence.

The membranes were immersed in blocking solution (5% wt/vol fat-free milk powder (Marvel), 0.1% BSA, 0.1% Tween-20 in PBS) for a period of 1 hour at 37°C, or overnight at 4°C.

Probing of the membrane was performed using primary antibodies: rabbit anti-mouse integrin α5 1/2,000 overnight at 4°C; rabbit anti-mouse integrin β1

1/1,000 overnight at 4°C; rabbit anti-mouse integrin β3 1/1,000 overnight at 4°C; Rabbit anti-mouse fibronectin (Chemicon AB2033) 1/2,000 overnight at 4°C. The house keeping gene β-actin was detected using monoclonal mouse anti-human β-actin (Sigma A5441) at 1/10,000 dilution for 30 minutes at room temperature. The membranes were then washed twice using PBS / 0.1% Tween-20 for 10 minutes, and once using the blocking solution. Secondary antibody was applied (Dako goat ant-rabbit HRP conjugated (P0448), 1/1,000 dilution, or Dako rabbit anti-mouse HRP conjugated (P0260), 1/2,000), as appropriate for the primary antibody. This was allowed to incubate for 30 minutes at room temperature. The membranes were then washed three times in PBS/Tween-20 for 5 minutes, then PBS twice for 5 minutes. Excess PBS was then allowed to drain off the membranes.

Chemiluminescence. The secondary antibodies used were all HRP conjugated. Enhanced chemiluminescence reagent (ECL), was applied to each membrane for exactly 1 minute. The excess was drained off and the membranes wrapped in saran wrap and placed in an X-ray cassette. X-ray films were then exposed, the timing depending on the intensity of the signal. Comparison with the molecular weight markers allowed the size of the protein band to be detected.

Loading controls. Two controls were used: Firstly, Ponceau S staining was performed to show equal loading of the original gels and transfer onto the nitrocellulose membrane; and secondly, the house keeping gene β-actin was measured.

Densitometry of the bands was measured using scanned images of the x-ray films, and the ImageJ analysis software produced by the National Institute of Health, USA. All protein loading was standardized by factoring each result against the β-actin band density for that sample on that blot. The time-points E14, E16, E18, D1 and 6wks were compared by ANOVA, with a $p<0.05$ defined as significant.

Probing the blots with antibody against integrin α5 produced a band at the expected size (140 kD), similarly probing blots with rabbit anti-mouse β1 produced a band at the expected size. I therefore re-used blots to measure both these integrins. Mouse anti-human β-actin antibody produced a very strong band at 40 kD, the expected size.

Determination of linearity of densitometry data. A particular problem associated with the use of western blots is the possibility of saturating the densitometry data. This would produce a non-linear result for quantitation. In order to 1) ensure equivalent antibody exposure for all samples, 2) determine a linear response all samples were run on 4 blots at the same time (figure 4.1). These samples were run with 3 control proteins from a day1 sample – each blot used the same day1 sample. These control proteins were loaded at 200%, 100% and 25% of the normal protein loading per well. The absorbance of these control bands therefore allowed a plot of concentration against densitometry to be made. Blots were exposed 'instantly', 1min, 3 mins 5 mins and then 10 mins etc. The exposure that produced the most linear response for the loading controls was then analysed (figure 4.2).

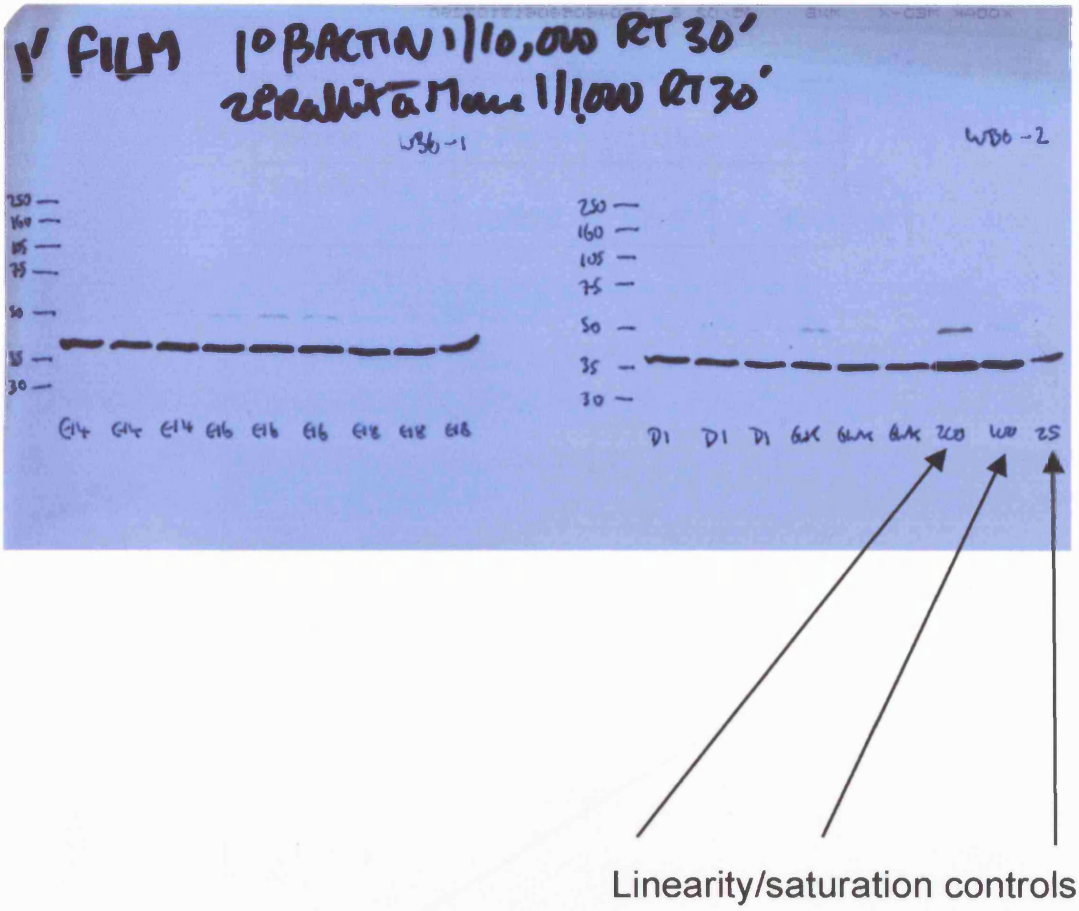

Figure 4.1: Linearity/Saturation controls in Western blots. Variation was reduced by running 4 blots simultaneously, and exposing all blots to the same antibody at the same time. 2 of 4 blots shown here.

A

Protein loading	200%	100%	25%
Densitometry	25552	10644	413

B

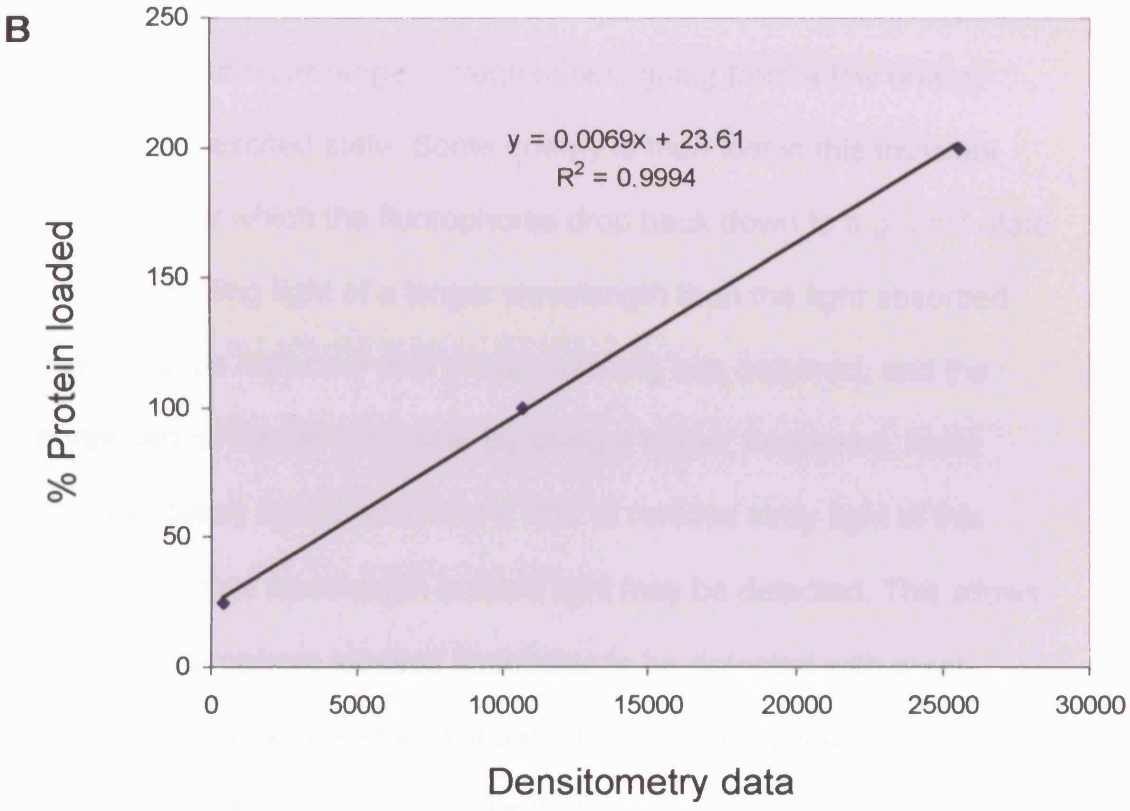

Figure 4.2: Demonstration of linear response from 25%-200% protein loading Recognition of linearity/prevention of saturation in densitometry data Western Blots. (A) raw densitometry data from b-actin blot in figure 4.1. (B) Protein concentration vs. densitometry data – linearity demonstrated from 25%-200% of protein loaded in each well.

Study 1iii: Flow Cytometry

Flow cytometry allows measurement of cells or particles individually, as they pass a sensing point. Light from a laser (or arc-lamp) is scattered by the cell as it passes the detection point: light transmitted forwards, or scattered sideways can be collected. This allows particles to be separated by size and their scattering properties. Fluorescence is the process whereby fluorophores absorb light of a particular range of frequencies, going from a low energy ground state to an excited state. Some energy is then lost in this transient excited phase, after which the fluorophores drop back down to a ground state in the process emitting light of a longer wavelength than the light absorbed. This process can be repeated until photobleaching has occurred, and the fluorophores can no longer fluoresce. By using a higher frequency, lower wavelength excitatory light source and a filter to remove stray light of this frequency, only longer wavelength emitted light may be detected. This allows the signal from fluorophore labelled antibodies to be detected with great sensitivity (e.g. fluorescein isothyocyanate – FITC). Cells labelled this way can then be counted. This technique requires that the tissue specimen be converted to a cell suspension (see below). The antigen expressed by the cells in question can then be detected by using an appropriate antibody labelled with an appropriate fluorophore, and excited with an appropriate wavelength of light, by measuring light emitted at the appropriate emission spectra.

Unfortunately antibodies can also bind non-specifically. By using an isotype control, non-specific binding can be measured, allowing this to be subtracted from the total binding, giving a measurement of specific antibody/antigen binding. This allows the binding of the antibody to be measured in terms of signal strength and number of positive cells. A positive control is used in which cells known to express the target antigen are exposed to the primary antibody.

Generating a cell suspension. Bladders were harvested at E14, E18 and postnatally as described above. These whole bladders were immersed in a known volume of dispersal solution containing collagen, dispase, DNase (CDD). This solution was composed of medium (DMEM/F12 with Insulin, selenium and transferrin supplements (ITS)), with 1.4 mg/ml collagenase A (103 578 Roche), 4 mg/ml of Dispase (17105 GIBCO), and 0.1 mg/ml of Dnase I (1 284 932 Roche). The collagenase A is derived from *Clostridium histolyticum*, and besides acting as a collagenase, has some clostripain, trypsin and protease activity. Ineffective disaggregation may be due to DNA release from digested cells, so DNase I was added. Dispase, a metalloenzyme produced by *Bacillus polymyxa*, separates epithelium form underlying substrate by cleaving the basement membrane zone, leaving the cells viable. Large bladders were minced using sterile scissors. The bladders were then repeatedly aspirated in and out of using large bore pipettes (1ml pipette with tip cut-off), then medium bore pipettes (intact 1ml pipette). This process of repeated aspiration used the shear forces as the suspension passed through the tip of the pipette to break the tissue down into component cells. The solution was then incubated at 37°C for 30 minutes in a water bath.

Repeated aspiration was repeated with medium bore pipettes, and then with fine bore pipettes (200 µl volume). The solution was again incubated for 30 minutes at 37°C. A final trituration was performed using fine bore pipettes. The cell suspension was then spun down in a desktop centrifuge at x3,000 g for 5 minutes. The CDD solution was discarded and the cell pellet resuspended in twice the volume of normal DMEM F-12 medium, producing a cell suspension of cells from whole bladders.

Labelling cells. Cell suspensions containing 1-4 x 10^5 cells in a 1 ml volume were made from E14, E18, day1 and 6 week mouse bladders as above. These were spun down in a desk top centrifuge at x3,000 g for 5 minutes and then resuspended in 1ml of FACS buffer. (FACS buffer contained 5% fetal calf serum in phosphate buffered saline, containing 0.02% sodium azide.) This was repeated twice.

This part of the experiment was performed by Mrs Vanita Shah, research assistant. Using a 96 well plate, 200 µl of cell suspension was loaded per well. The plate was placed in a centrifuge and spun down using a centrifuge for 5 minutes at 3,000g. The supernatant was discarded and the cells resuspended in 20 µl of 50 mg/ml primary antibody (mouse anti-integrin α7 monoclonal antibody 3C12 – MBL, Japan) and allowed to incubate for 30 minutes at 4°C , or with 20µl of isotype control mouse IgG (50µg/ml). The cells were washed three times by spinning down the suspensions (5 minutes at 2,000 rpm) and resuspending them in 200 µl FACS buffer. The secondary antibody was added (20 µl of 50 µg/ml solution), and incubated for 30 minutes at 4°C. The cells were then washed once more three times by spinning down at 2,000 rpm

for 5 minutes and resuspending in FACS buffer. The suspensions were then transferred to flow cytometry tubes and read on the flow cytometry performed.

FACS analysis. Control cell suspensions without antibody were used to set a gate on a dot-plot of forward versus sideways scatter data. Using a dot-plot of the FITC reading against the sideways scatter quadrants were set for each control suspension (i.e. the upper limit for the non-specific binding of the isotype control), and then the number of cells specifically labelled by the primary antibody and FITC labelled secondary antibody could be obtained. Numbers of positive cells are given as percentage of total cell numbers, and expressed as a mean, ± standard error of the mean, and analysed using ANOVA, where $p<0.05$ was taken as statistically significant. For this experiment because 3 separate cell suspensions from 3 different litters were prepared for E14, E18 and day1 time-points and for 3 adults for the 6 week suspensions, n was taken as 3.

Study 2: Adhesion blocking experiments

The experimental strategy for this experiment was to produce a cell suspension containing DSM from whole just-harvested bladders, and then to measure the adhesion of these cells to a fibronectin substrate. This provided an assay for the effectiveness of the blocking agents, but also tested whether the cells at that particular time-point expressed receptors for the substrate used.

Generating a cell suspension.

Bladders were harvested at E14, E18 and postnatally as described above, and cell suspensions were generated as described above.

Quantification of cell counts.

A haemocytometer was used to count the cell density in the cell solution. In the haemocytometer used (Sigma Brightline Z35,962-9) the floor of the slide is etched, dividing the area into 9 squares. Nine µl of cell suspension is pippetted onto the slide. With a coverslip in place each of these 9 squares has a volume of 0.1 mm^3, or 10^{-4} ml. Averaging the cell counts from the 4 outer squares will give the number of cells per 10^{-4} ml. Multiplying by 10,000 will give the cell density per millilitre (ml). In order for the counts to be reliable: 1) cells touching the top or left borders were counted, 2) cells touching the

bottom or right sides were not counted, 3) The average count of the 4 corner squares should be in the range 25-100.

Cell viability

Cell viability was ascertained by exclusion of Trypan blue. Trypan blue (Sigma T-8154) is a blue dye that is taken up by dead cells. An equal volume of cell suspension and Trypan blue is mixed in a tube. Living cells exclude the dye and appear refractile and colourless in comparison. The cell viability is given by the number of unstained living cells divided by the total number of cells present (stained and unstained), and expressed as a percentage.

Coating of slides with fibronectin

Mouse fibronectin is not commercially available in a preparation for coating slides. Rat plasma fibronectin has therefore been used (Sigma F0635). This is a lyophilised extract of rat plasma. It is reconstituted with sterile water, and must not be excessively agitated, or vortexed during this process. This stock solution had a concentration of 1mg/ml, and was stored in 50 µl (50 µg) aliquots. Dilute working solutions using Hanks balanced salt solution (HBSS) can be prepared up to 0.01% of the original stock solution. To coat slides an appropriate volume was made up to allow 1-5 $\mu g/cm^2$ of fibronectin to be deposited. Lab-tek 4 or 8 chamber slides (177399) were used in the adhesion experiments. Each 4-well slide has a culture area of 1.8 cm^2 with a suggested working volume of 0.5-0.9 ml. Two hundred and fifty µl of diluted fibronectin in HBSS was allowed to coat wells of the 4 chamber slides (125 µl for the 8 well

slides) overnight, at 4°C under sterile circumstances. The next morning (approximately 16 hours later) the excess liquid was tipped off, and the slides allowed to air dry.

Adhesion experiment

A homogenous suspension of cells from whole bladders was prepared. This was diluted aiming for 200-400,000 cells per ml, 250 µl of cell suspension (5-10x10^4 cells) being loaded per well on 4-well plates and 125 µl (2.5-5x10^4 cells) for 8-well plates. Two controls were compared to each blocking strategy: 1) cell suspension without additives – blank control; 2) control compound e.g. non-immune immunoglobulin G (IgG) for blocking antibodies. The blocking compound or the control compound were thoroughly mixed with the cell suspensions by vortexing, and then left to stand for 15 minutes at room temperature. The blank control cell suspensions were simply vortexed and left to stand. The cell suspensions were then applied to the slides in 250 µl aliquots, complete coverage of each well being ensured by agitation of the slide. The slides were incubated at 37°C in a 5% CO_2/air atmosphere in a humidified incubator for 4 hours. At the end of that time the cell suspension was tipped off the slides. The chambers were removed as was the sealing gasket. Any non-adherent cells were washed off by rinsing twice using PBS solution at room temperature. Cells were initially counted after staining with methylene blue as described below, or were counted using phase contrast microscopy. For methylene blue staining slides were fixed by immersion in acetone at -20°C for 10 minutes. Following this the slides were rinsed in PBS

3 times, then the adherent cells were stained with methylene blue (Sigma 180-8, diluted 10 fold in deionised water) for 20 minutes at room temperature. These were then rinsed in running water and dehydrated using ascending alcohols, finally placed in histoclear for 2 minutes. Coverslips were mounted using DPX.

For cell adhesion experiments, bladders were minced using sterile blades, and then dispersed to single cell suspensions using solution containing collagenase A (1.4 mg/ml) (103 578; Roche Diagnostics GMBH, Mannheim, Germany) dispase (4 mg/ml) (17105; Gibco BRL, Invitrogen Ltd, Paisley, UK), and DNase I (0.1 mg/ml) (1 284 932; Roche) in 'culture medium', composed of Dulbecco's modified Eagles medium/F-12 medium (DMEM/F12) (31330-038; Gibco BRL) with insulin, selenium and transferrin supplements (I3146). $2.5x10^4$ cells in culture medium were placed in each well of 8-chambered glass slides (Lab–Tek, Fisher Scientific UK, Loughborough, UK). Some wells were coated with rat plasma fibronectin (F0635) at concentrations from 5 to 20 µg/ml in Hanks balanced salt solution (HBSS; 14170-088; Gibco BRL) overnight at 4°C, control wells were incubated with HBSS alone. In some experiments blocking RGD, or negative control RAD peptides were added to the cell suspensions and incubated for 15 minutes; the oligopeptide concentration used was 20 µg/ml after testing doses from 10-40 µg/ml, based on published studies on other cell systems (Romanov and Goligorsky 1999). Suspended cells were allowed to adhere for 1 hour, at 37°C, in a 5% CO_2/air humidified atmosphere. Culture medium was decanted, and the slides gently washed twice with PBS. Adherent cells were counted using either phase contrast microscopy of unfixed cells, or using fixed cells (see below). For each

well, four medium power fields were randomly selected and adherent cells counted; the average was then used for subsequent analysis. Cell morphology assumed either a round, or spread appearance, and therefore we were able to express results as 'total', 'spread', and 'round'. Some slides were fixed in acetone at -20°C for 10 minutes, rinsed in PBS, permeabilised with NP40 (0.5%) and probed, for 30 minutes at room temperature, with the following primary antibodies: α-SMA, CD31, cytokeratin-18, desmin, integrin α5, integrin β1. Primary antibodies were detected with appropriate secondary antibodies using HRP/DAB, and slides were counter-stained with hematoxylin. Proliferation was assessed by 5-bromo-2-deoxyuridine (BrdU) incorporation as described in a commercially available kit (1444611, Roche) (See below). BrdU was added for 1 hour, before the experiment was terminated at 1 hour and 12 hours after the cells were plated either on to fibronectin coated plates or uncoated controls; the proliferation experiments were repeated twice, both with 10% fetal bovine serum (FCS) added to the medium, and without. Data were presented as mean±SEM. Parallel experiments on the same cell suspensions were analysed by paired Student's t-tests. Comparison over multiple conditions were performed using analysis of variance (ANOVA), with $p<0.05$ taken as significant. Analyses were performed using Microsoft Excel.

Analysis

Phase contrast microscopy was performed using an Olympus IX70 inverted microscope. The fixed slides were photographed using the computer controlled Zeiss Axiophot 2 microscope, and Photoshop 5 software. Four

medium power fields were counted per well, and averaged. The number of adherent cells in each well was then compared, using ANOVA, with a Bonferroni post-hoc test of significance.

Quantification of proliferation

In the adhesion experiments proliferation was measured by PCNA expression and, BrdU uptake. For PCNA expression, immunocytochemistry was performed, as described above.

When 5-bromo-2'-deoxy-uridine is added to cell culture, proliferative cells incorporate it into DNA in place of thymidine. Monoclonal antibodies to BrdU (either peroxidase conjugated or fluorescent conjugated) can then be used to detect cells in which BrdU has been incorporated – and so used as a marker of proliferation. This technique provided an alternative to the use of radioactive thymidine incorporation without the risk of radiation exposure.

In order to measure BrdU incorporation, cell cultures were exposed to BrdU (10μM) for 1 hour, i.e. BrdU was added at the start of the adhesion experiment for the 1 hour slides and at 11 hours for the 12 hour adhesion studies. At the end of the experimental period, slides were rinsed twice with PBS three times (room temperature) and then fixed in acetone at -20°C. PCNA immunocytochemistry was performed as described above. For BrdU detection cells were washed three times in PBS containing 10% FCS. The slides were then incubated with nucleases for 30 minutes at 37°C, and washed again, three times more with PBS/ FCS. The wash medium was

removed and anti-BrdU peroxidase labelled antibody (200 mU/ml in Washing Buffer with 10% FCS) was incubated for 30°C at 37°C (5-Bromo-2deoxyuridine labelling and detection kit 1444611, Roche Diagnostics GMBH, Mannheim, Germany). The antibody was then washed off using the washing buffer, and DAB added. The reaction of the peroxidase was terminated after 5 minutes by washing in tap water and the slides counter-stained with haematoxylin (30 secs), washed once more, and dehydrated using ascending alcohols (30secs each), then histoclear 5 minutes, twice. Coverslips were mounted using DPX, and the slides photographed when the DPX had dried.

Quantification of Apoptosis

TUNEL test

Apoptosis or programmed cell death (PCD) are terms used to describe an active form of 'suicide' in response to local signals, or lack of those signals. There are 3 processes involved in activation of apoptosis: initiation, regulation and execution (Renehan et al 2001). Apoptosis may be triggered by either the death receptor pathway or by the mitochondrial pathway. The death receptor pathway is activated by binding of Fas ligand to Fas (CD95), or tumour necrosis factor (TNF) to TNF receptor-1. This leads to receptor clustering and formation of a death inducing signalling complex. Fas-associated death domain protein (FADD) is recruited and multiple procaspase-8 molecules are bound. The close proximity of these molecules leads to caspase-8 activation (Hengartner 2000). Execution occurs after caspase 3, 6 and 7 are activated, with DNA fragmentation (by caspase activated DNase (CAD), which results in

DNA-ladder visulaised upon electrophoresis), chromatin condensation after cleavage of nuclear lamins, and surface alterations ('blebbing') (Hengartner 2000). Alternatively, the mitochondrial pathway can be initiated by a variety of factors: growth factor deprivation, steroids, DNA damage leading to upregulation of p53, loss of adhesion to a substrate (Michel 2003). These lead to mitochondrial membrane permeabilization by inactivation of anti-apoptotic Bcl-2 family members such as Bcl-2, and activation of pro-apoptotic Bcl-2 proteins such as Bax, with release of proteins such as cytochrome-c. This combines with Apaf-1 and procaspase-9 to form the apoptosome, which is then capable of activating caspase-3 and starting the execution programme (Hengartner 2000).

Apoptotic cells shrink, chromatin condenses and endonucleases cut the DNA into 180-200 bp fragments, nuclei become pyknotic, cytoplasmic membrane blebs and then apoptotic bodies form containing cytoplasm, organelles, and nuclear fragments. These apoptotic bodies are then phagocytosed.

Apoptosis can be detected by:

Propidium iodide staining of cell nuclei: apoptotic nuclei are pyknotic, then fragmented.

DNA laddering, DNA can be observed to form a series of bands on agarose gel electrophoresis.

Terminal deoxynucleotidyl transferase mediated deoxyuridine triphosphate biotin nick end labelling (TUNEL) test labels the cut ends of the DNA in-situ. Using recombinant terminal deoxynucleotidyl transferase (rTDT), either

biotinylated nucleotides (Promega DeadEnd colorimetric system G7360 Promega), or fluorescein labelled nucleotides (ROCHE Fluorescent detection kit – 1 684 795) are incorporated at 3' –OH ends of the DNA. These can then be identified either through chromagenic detection with DAB, using an avidin-biotin detection system linked to horse radish peroxidase (HRP), or by fluorescent microscopy.

Chromagenic TUNEL test in immunocytochemistry

Parallel E18 bladder cell suspensions were prepared as described above. Each suspension was incubated with RAD, RGD oligopeptides and HBSS, then and plated onto slides coated with fibronectin at 10µg/ml, and allowed to adhere for 1 hour. These slides were washed and then the slides were fixed using acetone at -20°C as described above. Slides were rinsed twice with PBS and then permeabilised with 0.2% Triton X-100 in PBS for 5 minutes. These were then rinsed in PBS for 5 minutes, repeated twice. Slides were incubated in equilibration buffer (G7360 Promega) for 5 minutes. The adherent apoptotic cells were then labelled using TUNEL reaction mixture incorporating equilibration buffer (contained 40 mM potassium cacodylate, 25 mM Tris, 0.2 mM DTT, 0.25 mg/ml BSA and 2.5 mM cobalt chloride - 100 µl of reaction mixture contained 98µl of equilibration buffer, 1 µl rTDT and 1 µl biotinylated nucleotide mix and was applied to each well). A negative control was provided by making a control mixture without rTDT. The reaction was allowed to proceed for 1 hour at 37°C. The reaction was then terminated by washing the slides in SSC for 15 minutes at room temperature. (SSC

contained 0.3M sodium chloride and 0.34M sodium citrate at pH 7.2- Part G3297 Promega). The slides were rinsed three times in PBS for 5 minutes, before endogenous peroxidase was quenched using 0.3% H_2O_2 for 3 minutes at room temperature. Streptavidin labelled horse radish peroxidase (1 ng/ml) was then allowed to ligate the biotinylated nucleotides for 30 minutes at room temperature. Slides were again washed three times in PBS. Finally the Streptavidin-HRP was detected by the application of DAB – chromagenic reaction was allowed to run for 10 minutes before being terminated by rinsing in water. The slides were counter-stained in Meyer's haematoxylin for 20 seconds, and then rinsed with running water for 2 minutes. The slides were dehydrated by passing through ascending alcohols, and then histoclear for 2 minutes, twice. Coverslips were mounted with DPX and adherent cells were counted. The results were recorded as total adherent cells and TUNEL positive cells. No false positive staining was seen in the control wells (no rTdT present). Four medium power fields were counted per well, and averaged. Results were then compared between same suspensions under different conditions using paired t-test.

Measurement of cell death using LDH assay

This assay was a colorimetric quantification of cell death and lysis as opposed to apoptosis. This assay is based on measuring the activity of lactate dehydrogenase (present in all cells) released from dying cells into a supernatant. This enzyme is stable. LDH detection is a two-step process whereby LDH catalyses the reduction of NAD+ to NADH+ as lactate is

oxidised to pyruvate. The second stage, catalysed by diaphorase) involves the transfer of H/H+ to a (yellow) tetrazolium salt, reducing it to a (red) formazan salt. This reaction can be followed by absorption at 500nm of this formazan salt. I used a commercially available cytotoxicity detection kit (Roche 1 644 793).

The cell suspensions from 1 hour adhesion experiments using no block, or RGD, or RAD, with and without substrate were aspirated and spun down at 13,000 rpm (desk top centrifuge) for 30 minutes at 4°C. The reaction mixture was made up by mixing 250 µl of solution 1 (catalyst) with 11.25 ml solution 2 (dye mixture). The supernatant was retained and subsequently used in the LDH assay. 10 µl of supernatant was added to 100 µl of reaction mixture in an ELISA plate. This was incubated for 30 minutes at 18°C, and covered to protect it from light. The absorbance of the wells in the plate was read at 490 nm. Each reaction was repeated in triplicate for 4 parallel cell suspensions.

Study 3: Organ Culture Experiment

The experimental strategy for this experiment was to generate an embryonic model of explant bladder growth, starting at organ inception at E14. I have investigated the functional effect of fibronectin/integrin α5β1 interactions on DSM maturation, by attempting to block fibronectin itself with a polyclonal antibody raised to mouse fibronectin (Chemicon), as described by Moursi et al (1997) in osteoblast culture.

Generating the model.

I generated a model of bladder development that started with murine bladders harvested at E14.This is the first time-point that murine bladders are a discrete structure which can easily be dissected. These were dissected under aseptic conditions and grown on Millipore filters (0.4 μm pore size), using serum-free, defined media (DMEM/F-12 supplemented with insulin (10 μg/ml), transferrin (5.5 μg/ml) and selenium (5 ng/ml)) (Figure 4.3A and B). Up to five explants are grown on each filter in an air/5% $C0_2$ atmosphere, at 37 C. Bladder explants were collected for analysis at the start of the experiment (E14 bladders), after 3 and 6 days in culture. One bladder from each plate was taken for frozen section, and the rest were dissociated into single cell suspensions as described above. The read-outs from this experiment were an assessment of growth, by cell numbers, weight and total protein; an assessment of bladder morphology by examination of explant histology; differentiation, by immunostaining and Western blot of smooth muscle

markers α-smooth muscle actin (α-SMA) and desmin, and proliferation, by PCNA IHC, which also allowed quantification by counting the proportion of proliferative cells present, as well as by western blot.

Embryonic bladder explant experiments using anti-fibronectin antibody

Bladders were harvested from 3-4 litters at E14 and dissected from the embryos, as described above. Two bladders from each litter were taken and weighed, then a cell suspension was created from them, cell numbers counted and protein extracted from the cell suspensions, again as described above.

In a 6 well plate (figure 4.4), the left hand wells were harvested at 3 days, and the right hand wells at 6 days. The top row were grown in the growth medium without any added immunoglobulin (ITS), the second row were grown in the presence of isotype control immunoglobulin (IgG), and the bottom row were exposed to the anti-fibronectin antibody. Bladders from each litter were placed on placed on the Millipore filters, such that each different experimental condition had (as evenly as possible) bladders from each litter allotted to it.

When harvested the bladders were weighed, dissociated into a cell suspension and cell numbers counted, and then protein was extracted. A bladder chosen at random from each filter (i.e. experimental condition) was mounted in OCT for frozen section and subsequent immunohistochemistry.

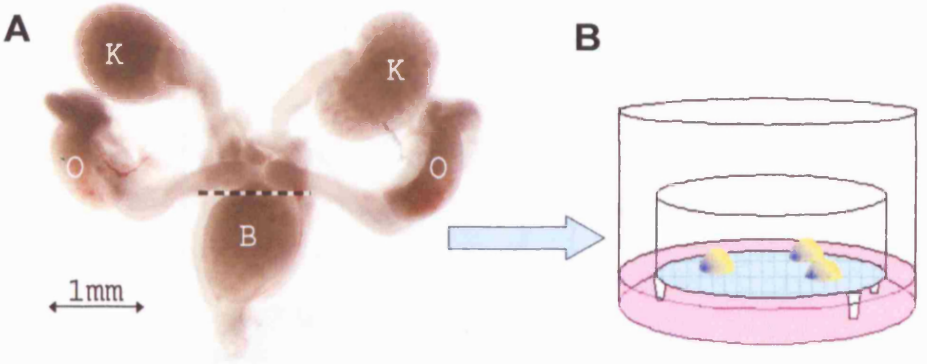

Figure 4.3: Generating fetal murine bladder explant model. (A) Embryonic day 14 mouse urogenital tract . (B) Diagrammatic representation of explant culture with bladders (Yellow), growing on filter (blue), resting in and in contact with defined medium DMEM/F-12 (pink). K - kidney; O - ovary; B - Bladder

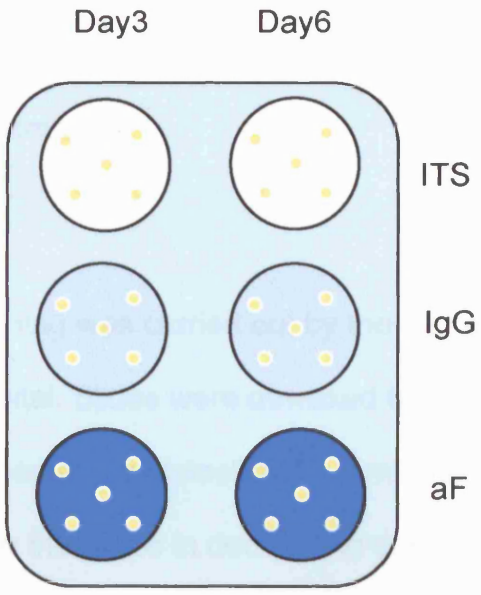

Figure 4.4: Setting up explant blocking experiment using immunoglobulins (yellow dots are bladders).

Study 4: Human fetal immunohistochemistry, morphometric analyses

Paraffin Sections

Slides were cut from formalin-fixed, paraffin-embedded blocks at 0.4μm thickness using a microtome.

Masson's trichrome

This histological staining was carried out by the histology laboratory at Great Ormond Street Hospital. Slides were dewaxed by incubating at 60°C for 5 minutes then by placement in histoclear for 5 minutes twice. Rehydration was performed by placing the slides in decreasing concentrations of alcohol (100%, 90%, 80%, 70%, 50%) for 1 minute each, then rinsing in water for 5 minutes. Slides were pre-treated in 3% potassium dichromate for 1 hour at 60°C. Nuclei were stained with Mayer's Haematoxylin, slides were washed in water. Slides were stained with Chromotrope green mixture (Chromotrope 2R 0.6g, Fast Green FCF 0.3g, Phosphotungstic acid 0.6g, glacial acetic acid 1 ml, dissolved in 100ml of distilled water), for 10 minutes at room temperature, then rinsed in 0.2% acetic acid. The slides were blotted dry, then dehydrated by passing through increasing concentrations of alcohol, then xylene and then coverslips were mounted using DPX. Muscle and fibrin was stained red, as were red blood cells. Collagen was stained green. Nuclei were stained black.

Quantification of the percentage area of muscle present was performed by measuring the area of the section stained red, and measuring the total area of the lamina propria and detrusor in each section (figure 4.5). These

measurements were performed by using ImageJ software: each image was converted into an image stack consisting of hue, saturation and brightness. Thresholds were set to detect the red staining (equivalent to 185 to 255) and the area measured. The total area of the lamina propria was also measured, so that the area of muscle could also be expressed as a proportion of the total area (muscle percentage of surface area) (figure 4.5C).

This method of quantification was similar to that employed by previous authors, except that these authors described it as area density (Workman and Kogan 1990;Kim et al 1991b, a;Freedman et al 1997).

The thickness of the bladder wall (urothelium, lamina propria and detrusor) was measured, using ImageJ, on each section at 3 different points as was the lamina propria thickness, and the detrusor thickness. The average of all three measurements for thickness was then used in subsequent analyses (figure 4.6). (All measurements were converted into millimetres (mm)).

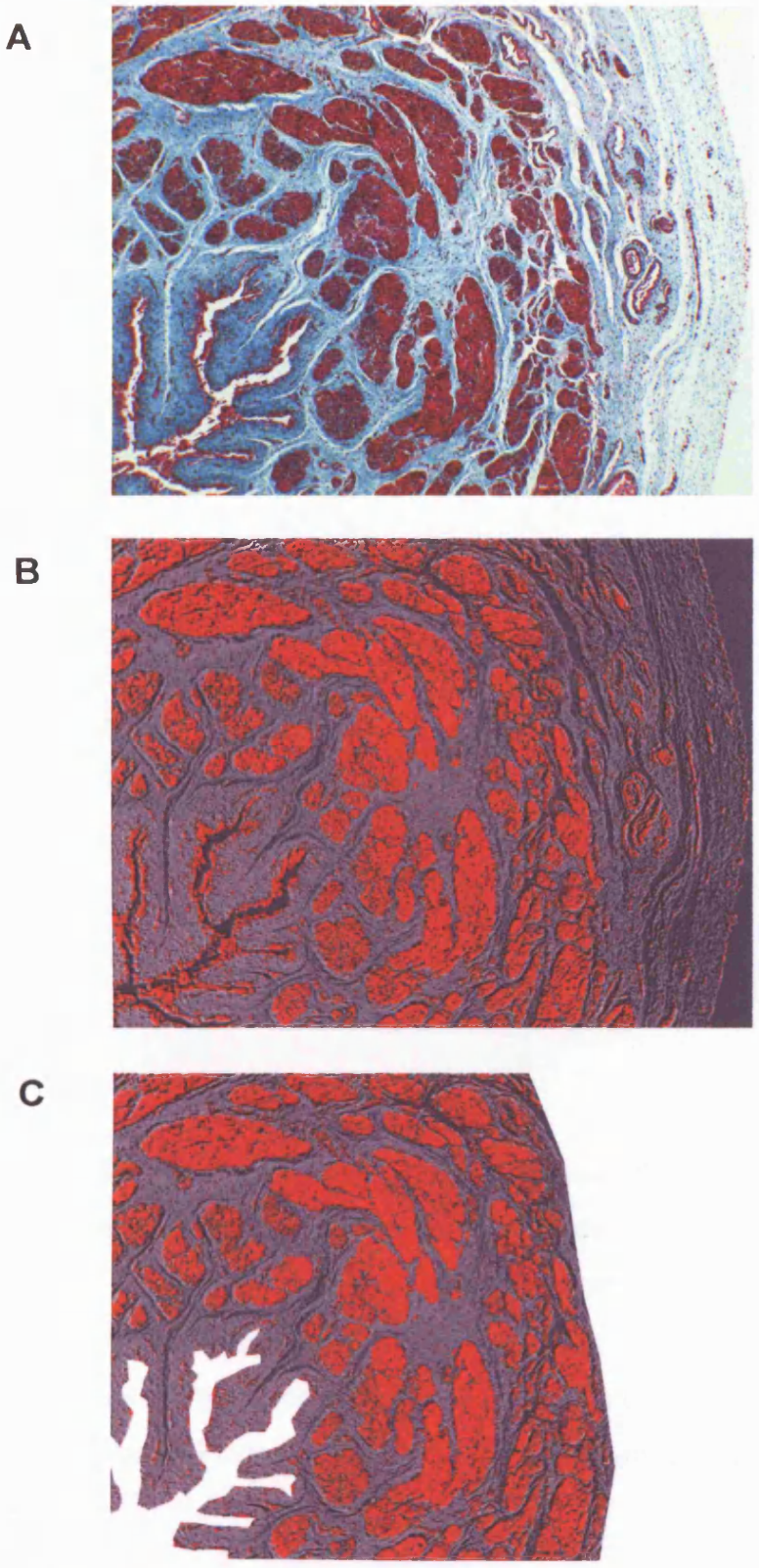

Figure 4.5: Muscle area measurement using ImageJ . (A) Masson's Trichrome staining of bladder (B) Image with thresholds set to detect red staining of muscle in ImageJ (C) ImageJ image trimmed of serosa. This is the image used to calculate area of muscle and total lamina propria and detrusor area.

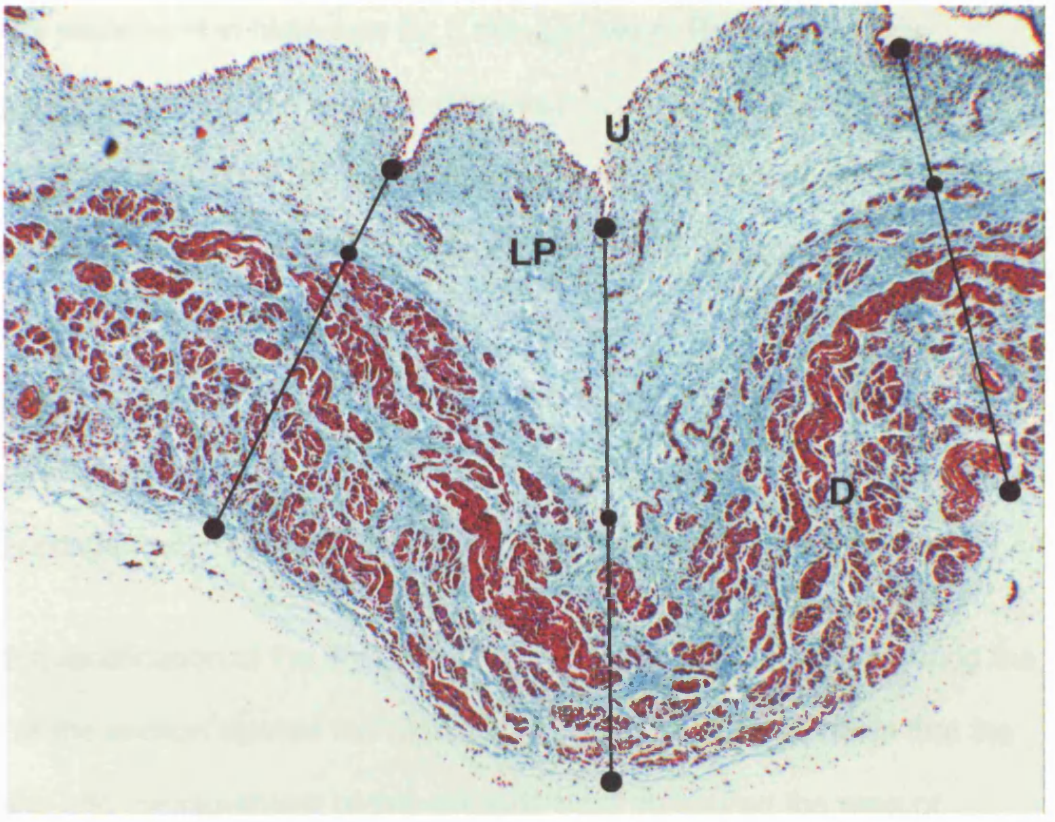

Figure 4.6: Morphometric analysis of bladder wall thickness . Minimum distance lines connecting mucosa to the outside of the detrusor layer were drawn in 3 places on each section. The total wall thickness as well as the lamina propria thickness and detrusor thickness were measured. The average of each was taken as the wall thickness of that bladder. This was a 20 week gestation normal male fetus. U urothelium; LP lamina propria; D detrusor.

Van Gieson stain

This procedure was carried out by the histology laboratory at Great Ormond Street Hospital. Slides were dewaxed by incubating at 60°C for 5 minutes then by placement in histoclear for 5 minutes twice. Rehydration was performed by placing the slides in decreasing concentrations of alcohol (100%, 90%, 80%, 70%, 50%) for 1 minute each, then rinsing in water for 5 minutes. Slides were stained with Celestin blue for 5 minutes, then Mayer's haematoxylin for 5 minutes, followed by rinsing in water. Sections were then counter-stained with Van Gieson stain. Slides were blotted dry, the dehydrated and coverslips mounted as described above. Nuclei were stained blue; collagen red; muscle, RBCs and cytoplasm were stained yellow.

Again quantification of the area of collagen was performed by measuring the area of the section stained red (figure 4.7). A close–up view shows that the staining and measurement of this collagen area measured the area of collagen fibres (figure 4.8). A measurement was generated of the collagen percentage of surface area (%) (Collagen area divided by total cross-sectional area of urothelium, lamina propria and detrusor, expressed as a percentage).

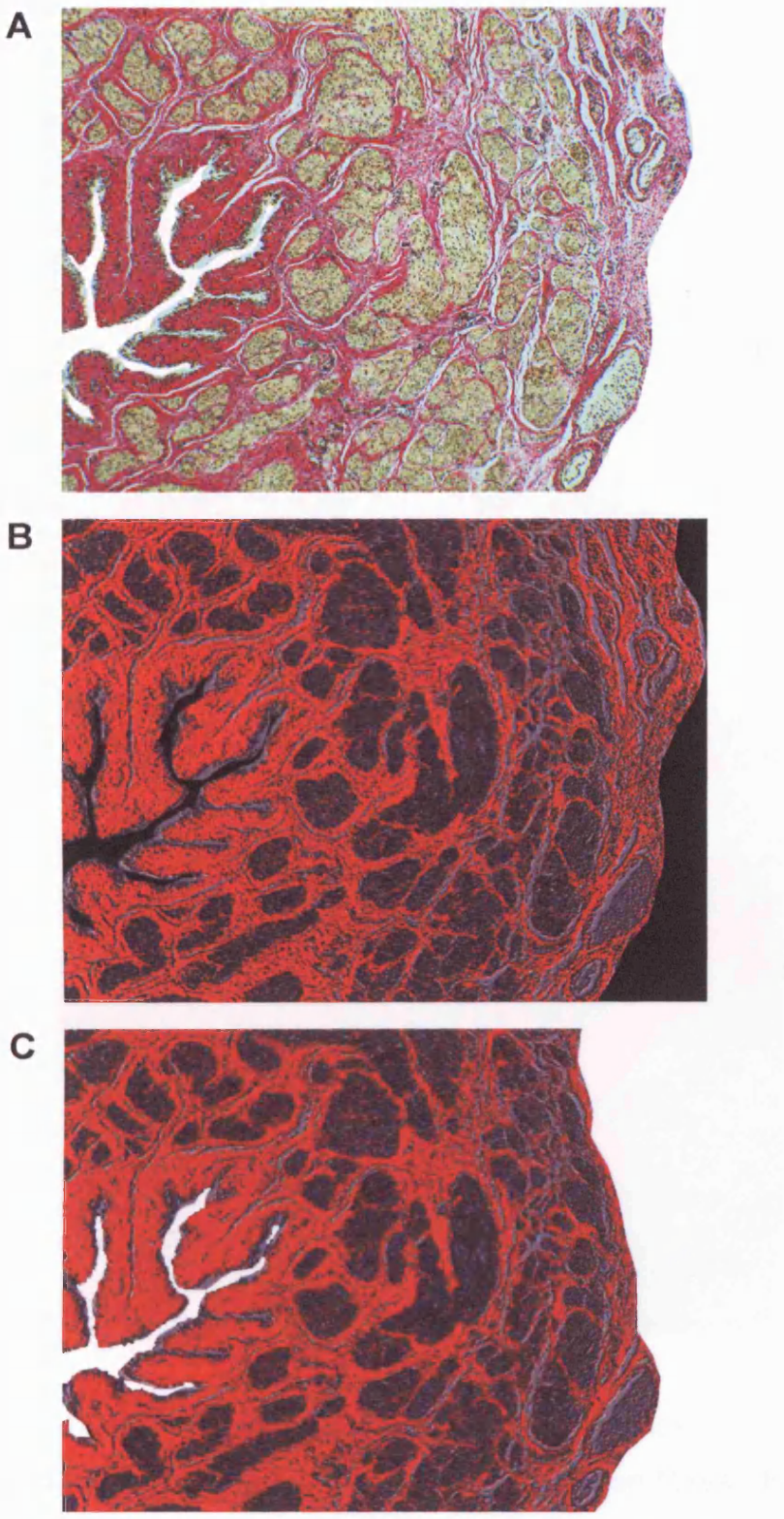

Figure 4.7: Measurement of Collagen proportion of surface area of sections of bladder using ImageJ. (A) Van Gieson staining of bladder (B) Image with thresholds set to detect red staining of collagen in ImageJ (C) ImageJ image trimmed of serosa. This is the image used to calculate area of collagen and total lamina propria and detrusor area.

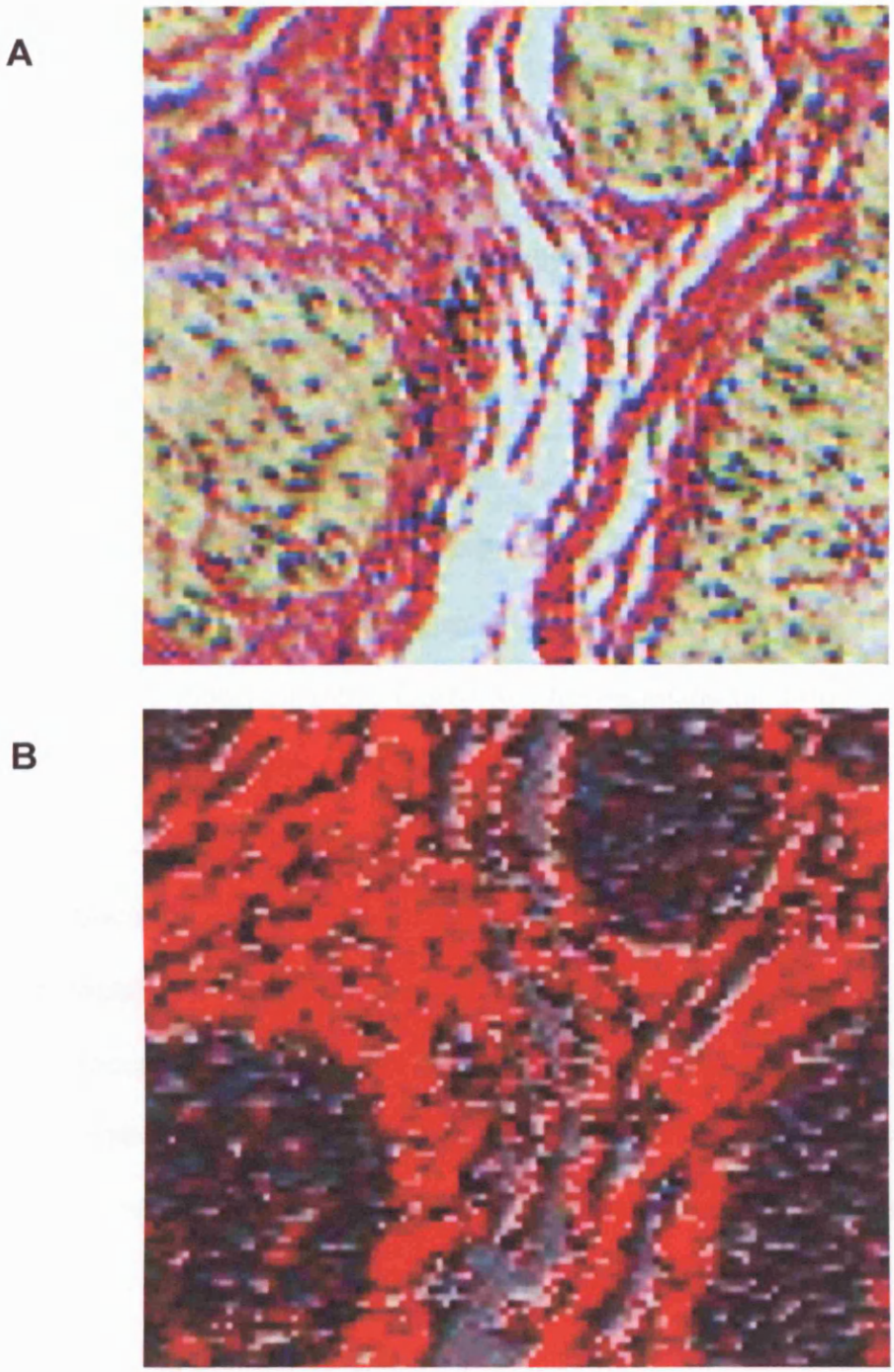

Figure 4.8: High power view of collagen fibres .(A) Close-up of van Gieson stain of bladder showing staining of collagen fibres. (B) Threshold image where red colour represents region to be measured.

Immunohistochemistry

Slides were dewaxed by incubating at 60°C for 5 minutes then by placement in histoclear for 5 minutes twice. Rehydration was performed by placing the slides in decreasing concentrations of alcohol (100%, 90%, 80%, 70%, 50%) for 1 minute each, then rinsing in water for 5 minutes. Antigen retrieval was performed by treating slides with citrate (2.1 g/l) at pH6, and micro-waving for 6 minutes at full power (750W). Slides were rinsed in PBS with 0.02% NP40 (PBS/NP40). Peroxidase block was applied for 5 minutes at room temperature, then rinsed off with PBS/NP40. Non-specific binding was prevented by incubating with 0.1% bovine serum albumin (BSA) 0.02% Triton X-100 block for 20 minutes at room temperature. Slides were then rinsed once more. Sections were then incubated with the following primary antibodies: rabbit anti-human fibronectin (1/2000) dilution, Ki67 MEB-1 monoclonal mouse anti-human (1/50), and mouse anti-human desmin-HRP conjugated antibody (1/4) overnight at 4°C. These antibodies were detected using DAKO Envision kit (anti mouse labelled polymer, or anti-rabbit IgG labelled polymer as appropriate). Conjugated horse radish peroxidase caused a brown colour change in diaminobenzidene (DAB), allowing detection of the primary antibodies. Slides were rinsed in water, and then counter-stained with haematoxylin, dehydrated, finally coverslips mounted using DPX.

Once again, quantification of the fibronectin area present was made by measuring the area of the section occupied by immunostained fibronectin. However in this case the quantification was done separately in the lamina

propria or detrusor layers, and expressing this as a proportion of the total area of lamina propria or detrusor respectively (figure 4.9). This was done because the fibronectin expression data from the mouse model described previously was for the detrusor layer alone, and so this was the most appropriate comparison. The resultant measurements were: 1) the total fibronectin area for lamina propria; 2) lamina propria fibronectin percentage of surface area; 3) detrusor fibronectin area; and 4) detrusor fibronectin percentage of surface area.

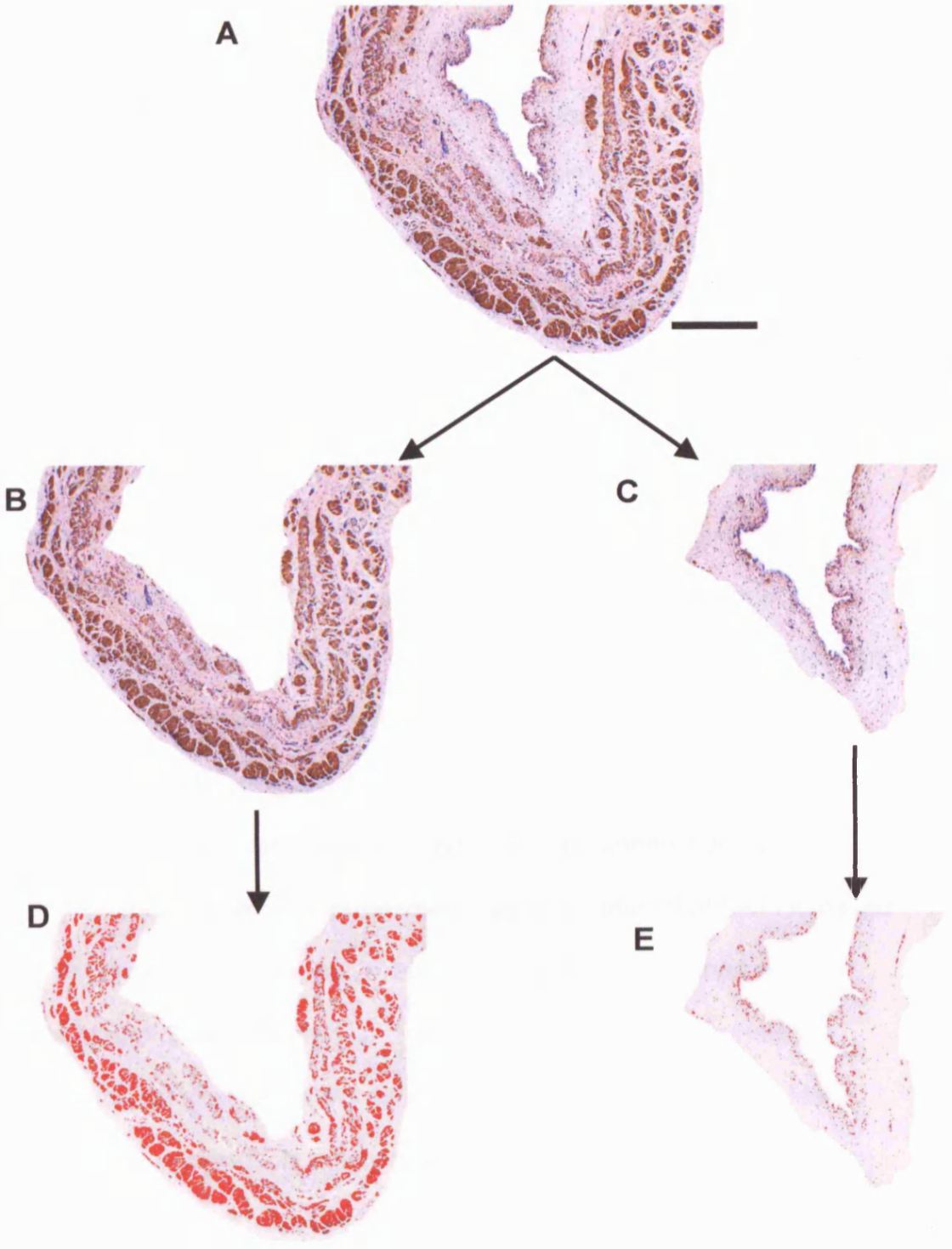

Figure 4.9: Semi–quantification of fibronectin expression in fetal bladders. (A) Immunostaining of fibronectin, detected with DAB – brown colour. (B) Detrusor 'cut–out' of image in (A). (C) lamina propria and urothelium 'cut–out' from image (A). (D) ImageJ thresholds set to detect brown colour of fibronectin immunostaining in detrusor layer. (E) same thresholds as used in (D), but for lamina propria layer.

Desmin-fibronectin colocalization.

Immunofluorescent microscopy using FITC conjugated anti-rabbit secondary antibody to detect anti-fibronectin antibody, and TRITC labelled anti-mouse secondary to detect mouse anti-human desmin antibody allowed colocalization of smooth muscle cells and fibronectin to be seen.

Muscle morphology ('Muscle dysmorphology' score)

Muscle morphology was graded from 0 to 2, by 3 different observers who were blinded to the details of each specimen (These were Professor AS Woolf, Dr P Winyard, and Mr D. Jenkins. Each observer was experienced in examining histological sections of fetal urinary tract). Muscle fibre morphology could be divided into normal fibres where each fibre was complete. Each observer was asked to compare the specimen to the high power views shown in figure 4.10. '0' represented muscle bundles with no connective tissue present within the bundles, '1' represented muscle bundles that had increased amounts of connective tissue, but in which muscle bundle outlines were recognizable and '2' represented completely disrupted muscle bundles, lacking any normal muscle bundle definition. The scores for each bladder were totalled giving a 'muscle dysmorphology' score ranging from 0 (normal) to a maximum of 6, as advised by the statistical support unit at ICH.

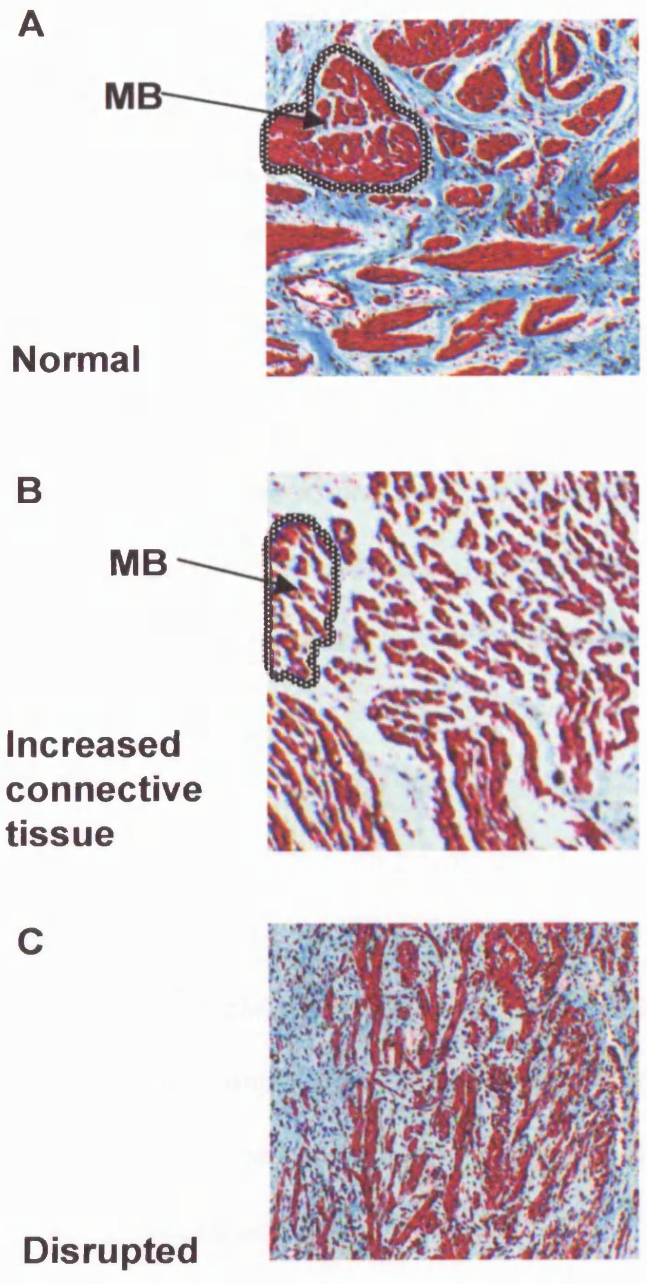

Figure 4.10: Muscle dysmorphology score. Each observer was blinded to all details about the bladders. They were asked to grade the detrusor muscle morphology in each of the bladders on a three point scale where 0 was normal (A). Muscle bundles (MB – outlined with dotted black and white line) were easily identified, with minimal connective tissue replacement. Or graded 1, where muscle bundles were identifiable but there was increased connective tissue expression (B). Muscle morphology was graded 2 where the detrusor muscle bundles was disrupted, with no identifiable muscle bundles and increased connective tissue (C).

Renal dysplasia

Three observers, blinded to the details of each specimen, independently graded the severity of kidney malformation of all the normal and obstructed fetal kidneys (again these were experts used to examining fetal kidneys, Professor AS Woolf, Dr P Winyard and Dr R. Scott). The score ranged from 0 for normal kidneys to 5 for the most dysplastic kidneys (figure 4.11). The kidneys associated with fetal presumed BOO showed a spectrum of abnormalities from fibrosis of the medulla to sub-cortical cysts, loss of the nephrogenic zone and dilatation of the renal tubules with pelvi-calyceal dilatation (Woolf et al 2004). Kidney morphology was assessed by three blinded experts in fetal kidney histology. They graded each kidney from 0 – normal, to 5 – most dysplastic. Medium power views of cortex and medulla from each fetus were provided for assessment, but no further information was given. There was very high concordance in grading between all 3 observers ($p<0.001$ Spearman nonparametric test for all comparisons between observers). The dysplasia score was therefore given as a sum of all 3 observers' scores for each bladder.

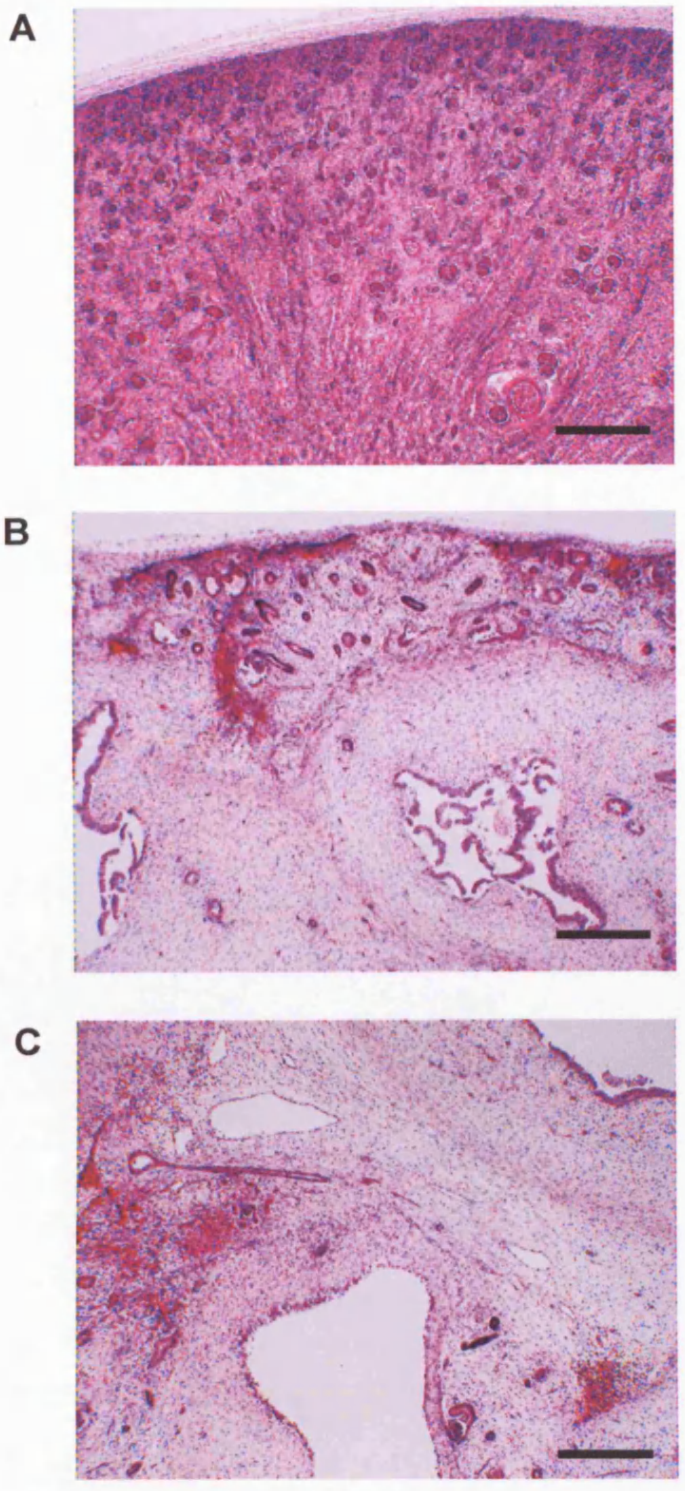

Figure 4.11: Renal dysplasia associated with congenital bladder outflow obstruction. This ranged from normal (dysplasia score 0) (A), to severe dysplasia (score 5) (B,C).(B) cortex, (C) medulla. Scale Bar 400 μm.

Pulmonary hypoplasia

From the post mortem reports the following information was obtained: fetal weight, weight of each lung, and presence of oligohydramnios. The percentage of fetal weight represented by total lung weight allowed an estimate of pulmonary hypoplasia to be made ≤1.5% taken to mean significant pulmonary hypoplasia (Scott and Goodburn 1995).

Proliferation in human fetal tissues

Immunohistochemistry was performed as described above. Preliminary test experiments were performed by myself. The tonsillar tissue produced the expected proliferation in the lymphoid follicles, and a positive result was seen in the human fetal tissue. This IHC was repeated by the Histology department of Great Ormond Street Hospital for all the slides.

Immunofluorescent TUNEL assay

The TUNEL test labelled the cut ends of the DNA in-situ. Using recombinant terminal deoxynucleotidyl transferase (rTDT), fluorescein labelled nucleotides (ROCHE Fluorescent detection kit – 1 684 795) were incorporated at 3' –OH ends of the DNA. These were then be identified by fluorescent microscopy. Nuclei were counter-stained by propidium iodide.

Images were captured using Axiophot computer controlled microscope, and Photoshop 6.0 software. Quantification of the expression of collagens, muscle and fibronectin was performed by analysing the proportion of surface area of the section that these represented. This calculation was done using ImageJ

(NIH) software, the results being expressed as a percentage of the total surface area for the section for collagens and muscle, but as a proportion of lamina propria and detrusor for fibronectin. For Ki67 and TUNEL quantification, 6 separate images of each bladder were captured (3 detrusor and lamina propria, 3 detrusor), and positive cells were counted for each compartment as well as total numbers of cells being estimated. The result was given as the percentage of positive cells for that compartment. For each fetus, these 3 numbers were averaged, and then used in further analysis.

Statistical analyses

Data were presented as means plus or minus standard error of the mean (SEM). Where 2 populations have been compared Student's t-test was employed where $p<0.05$ was taken as significant. Parallel experiments allowed the use of paired analyses, and the paired t-test was used in these analyses. Comparison of multiple groups over multiple time-points was performed using analysis of variance (ANOVA), again with $p<0.05$ taken as significant. Bonferroni post-hoc tests of significance were performed to differentiate between different groups as appropriate. Analyses were performed using Microsoft Excel and SPSS v11.

In analysing the human fetal bladder material, statistical advice was obtained from the Statistical Support Unit at ICH. For correlations between data, where data were parametric, then the Pearson correlation coefficient was determined using SPSS v11.5. If the data were not parametric, ie for scales

where the data were more correctly described as ordinal, then a non-parametric rank correlation (Spearman) was performed. These results were taken to be statistically significant if $p<0.05$.

Chapter 5. Analysis of expression of adhesion molecules fibronectin and laminin-1/2 and their candidate receptors during fetal mouse bladder development

Hypothesis

During murine bladder development, the candidate fibronectin receptor integrin $\alpha5\beta1$ may be expressed by detrusor smooth muscle cells (DSMC), and that laminin 1/2 candidate receptor integrin $\alpha7$ may be expressed by DSMC.

Background

In order for a ligand and receptor to interact, their expression should temporally and spatially overlap, i.e. they need to be in the same place (DSMC surface and surrounding basal lamina) at the same time to allow a response to occur. If these putative ligands (fibronectin and laminin-1 or lamini-2) are not expressed in the basal lamina of the DSMC, and these DSMC do not express the putative receptors (integrin $\alpha5\beta1$ and $\alpha7\beta1$) then the hypothesis can have no basis.

Aims

1) Seek potential expression of the fibronectin receptor integrin $\alpha5\beta1$. 2) Describe if the α-subunits of laminin-1 and laminin-2 (laminin $\alpha1$ and $\alpha2$

respectively) are expressed in the basal lamina of murine DSMC; and seek potential expression of the candidate laminin receptor (integrin α7β1).

Results

Fibronectin and candidate fibronectin receptor expression

For the immunohistochemistry, blocks of OCT embedded bladders were used that included positive control tissue (paw), surrounded by bladders: 6-8 bladders at E14, E18 and D1, with 3-4 bladders at 6wks. Each slide contained 4 sections – 3 were immunostained with primary antibody, one was the negative control section.

The expression of fibronectin was examined by using frozen sections, from organ inception at embryonic day 14 to maturity at 6 wks (figure 5.1). Throughout the stages examined fibronectin was expressed in the lamina propria and the detrusor layer, surrounding muscle cells. No immunostaining was seen at any time-point in the urothelium.

Immunohistochemistry was performed to look at the pattern of expression of fibronectin receptor integrin α5β1 (figure 5.2). Figure 5.3 shows the control sections performed at the same time, using non-immune rabbit antibody of the same isotype. At the start of organ development at embryonic day 14 there was no detectable immunostaining for integrin α5. By E16, there was expression in what will become the detrusor layer, which appeared to peak neonatally, and then decreased somewhat postnatally. The expression of the α5 integrin subunit appeared to be on the cell membranes of the fetal smooth muscle cells in the detrusor layer, but the presence of non-specific staining in

the DSM of the postnatal time-points makes the integrin α5 immunostaining of the DSM more ambiguous.

For the Western blot data each sample contained protein from multiple bladders (urothelium was dissected off the DSM and discarded, as described by Smeulders et al (2002)): E14 each sample was composed of the DSM of 16 bladders, E16 similarly, E18 approximately 8 bladders, 8 postnatal day1 bladders, and 8 from 6 week time-point, as described by (Smeulders et al 2002). Multiple samples were used, as described below, for subsequent statistical analysis.

Western blot data (Sample n=4 for E14, n=6 for E16, E18, Day1, and 6weeks), showed firstly a band at the expected size (140kD) (Hynes et al 1989) and when densitometry was performed a marked increase in expression of α5 integrin from organ inception during in utero development (ANOVA $p < 0.0001$ –figure 5.4). During post-natal development (D1 to 6wks) there was no change in the expression of integrin α5. Bonferroni post-hoc test of significance showed that there was significant upregulation of integrin α5 between E14 and postnatal time-points DI and 6wks ($p=0.001$ both comparisons), and between E16 and 6 wks ($p=0.001$), but no difference between E14, E16, and E18, and between D1 and 6wks. This Western blot data confirmed the presence of integrin α5 subunit in the DSM throughout bladder development from E14 to 6wks.

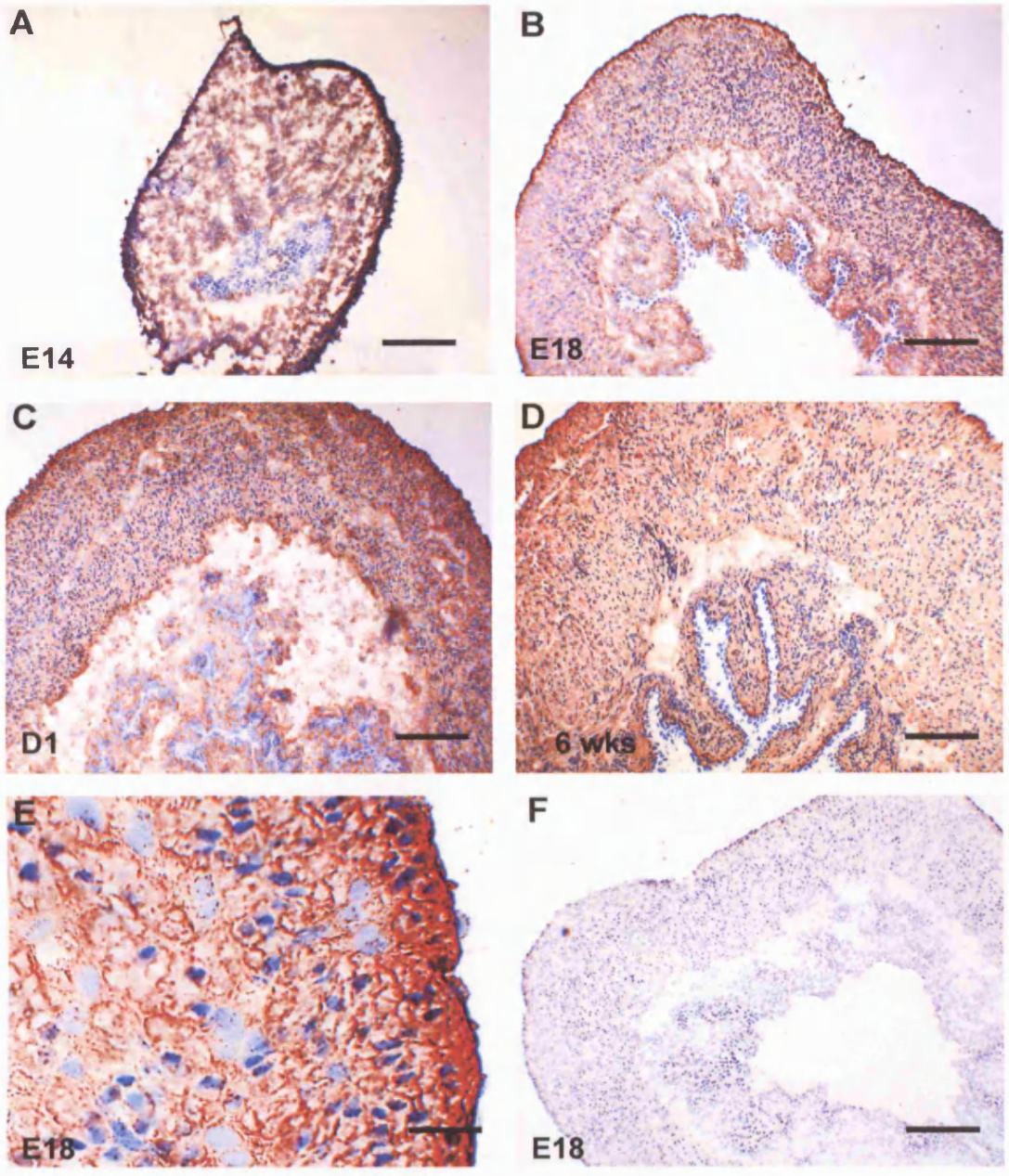

Figure 5.1 Fibronectin expression E14 to 6 wks postnatal. (A) Fibronectin assessed by immunohistochemistry (brown) at embryonic day 14 (E14), at E18 (B), at day1 neonatally (C) and at 6 weeks (D). Close-up of E18 detrusor reveals basal lamina staining around fetal smooth muscle cells (E). Control slide of E18 using isotype rabbit immunoglobulin – showing no staining (F). The black scale bar is 200 μm in A-D,F and 25 μm in (E).

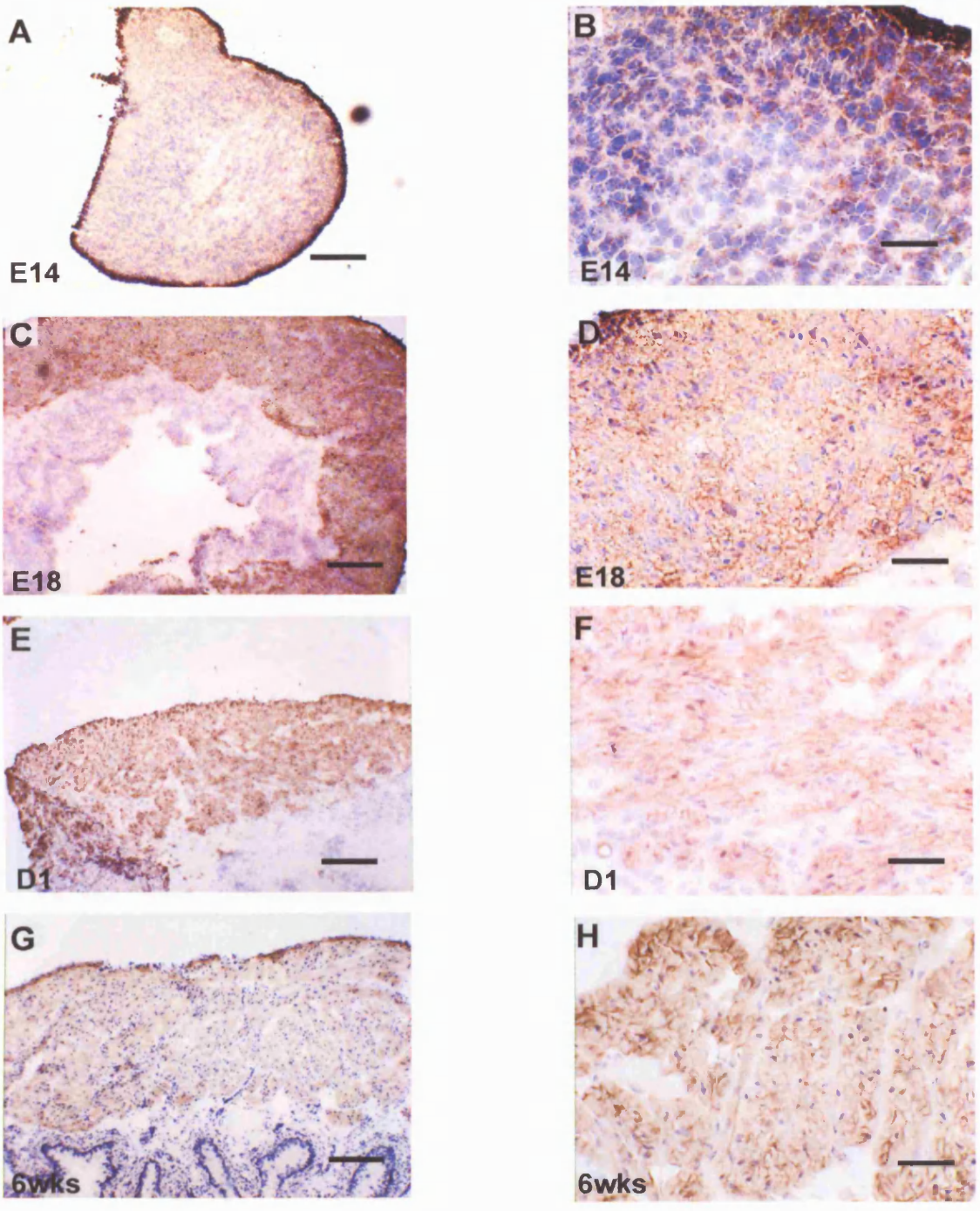

Figure 5.2: Integrin $\alpha 5$ expression E14 to 6 wks postnatal (Integrin $\alpha 5\beta 1$ is a fibronectin receptor): Expression from E14 (A and B), E18 (C and D), day1(E and F), 6 Weeks (G and H). A,C,E and G low power view of bladder wall (scale bar 200 μm), B,D,F and H high power view detrusor (scale bar 50 μm).

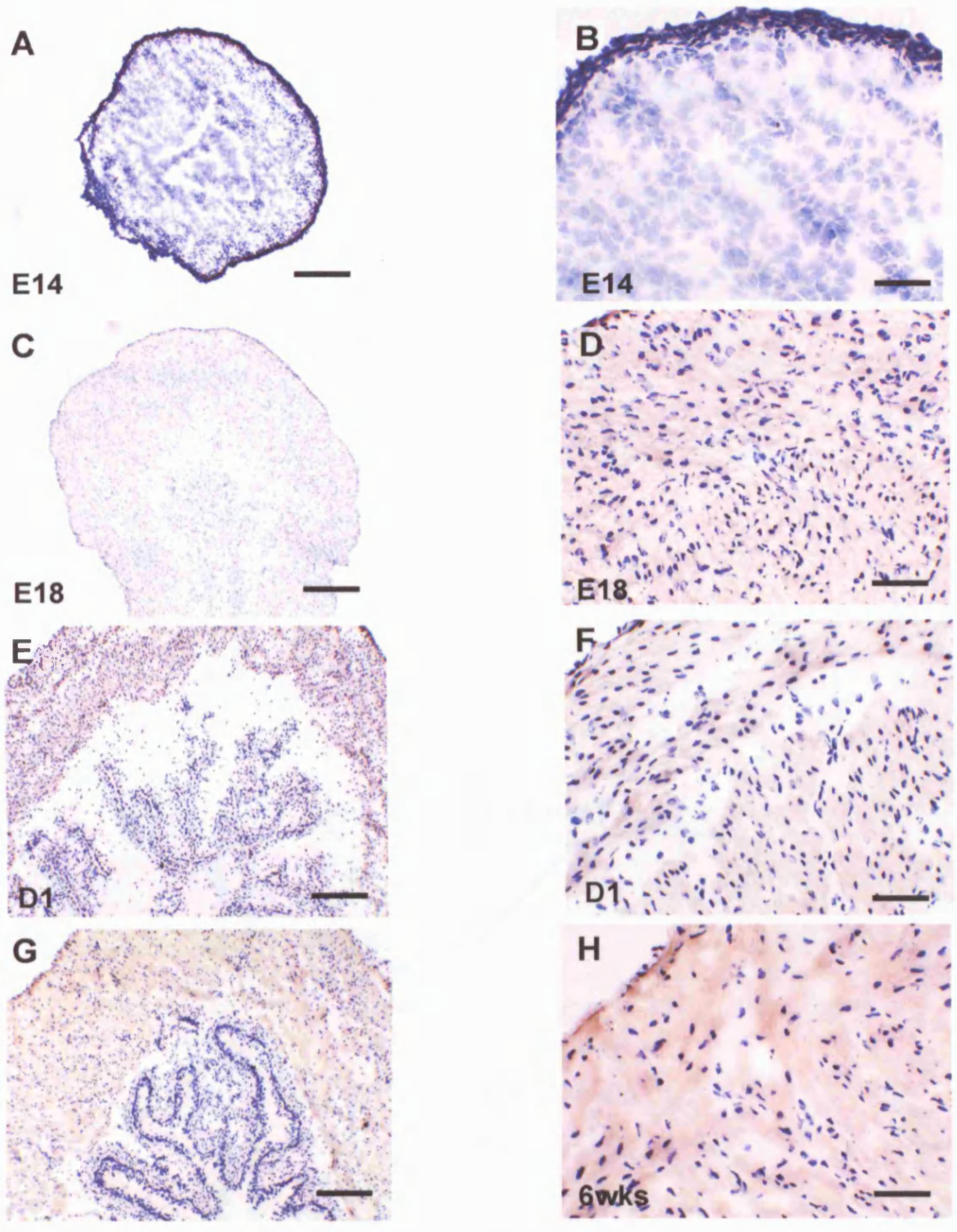

Figure 5.3 Rabbit isotype control antibody E14 to 6wks postnatal : Non-specific immunostaining from E14 (A and b), E18 (c and d), day1(e and f), 6 Weeks (g and h). A,C,E and G low power view (scale bar 200microns), B,D,F and H high power view (scale bar 50 microns).

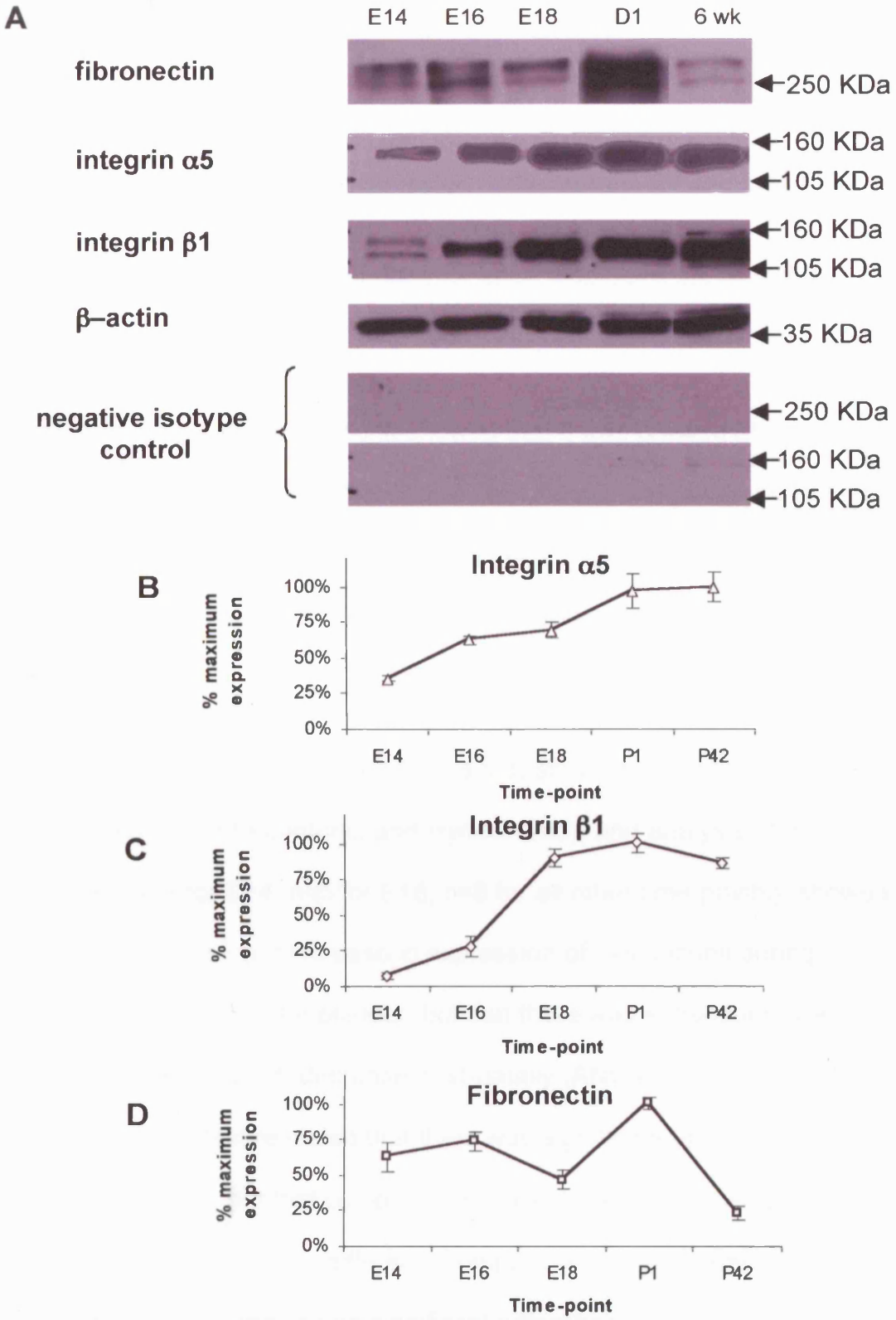

Figure 5.4: Quantification of fibronectin and fibronectin receptor by WB. (A) Representative blots for fibronectin, integrin α5, integrin β1, β-actin, and pre-immune rabbit IgG. (B) Integrin α5 levels factored for β-actin. Data expressed as mean±SEM (n=4 for E14, n=6 for other time-points), given as a percentage of the maximum level of integrin α5 expression. (C) Integrin β1 levels. (D) Fibronectin levels.

Figure 5.5 shows the pattern of expression of the integrin β1 subunit.

Multiple replicants were immunostained for each time-point, as described above for integrin α5 subunit.

Expression of the β1 integrin subunit showed that it was present at the periphery of the bladder at the start of bladder development, but by E18 there was marked immunostaining of the detrusor layer which persisted throughout development. In contrast to the α5 staining, β1 was also present in the urothelium.

Western blot data for the β1 subunit (figure 5.3) showed a band was present at the expected size (Marcantonio and Hynes 1988), and analysis of the densitometry (n=3 for E14, n=5 for E16, n=6 for all other time-points), showed that there was a significant increase in expression of this subunit during antenatal development of the bladder, but that there was subsequently a (non-statistically significant) decrease post-natally (ANOVA $p<0.01$). Bonferroni post-hoc test revealed that there was significant upregulation between E14 and D1, but that comparisons of expression between E14, E16 and E18 were not significantly different. Comparisons of postnatal expression between D1 and 6wks showed no significant difference.

These data show that the integrin sub-units α5 and β1 were expressed by the fetal and mature smooth muscle cells in the same spatial arrangement as

each other, in an appropriate pattern to act as a fibronectin receptor during the development of the bladder smooth muscle.

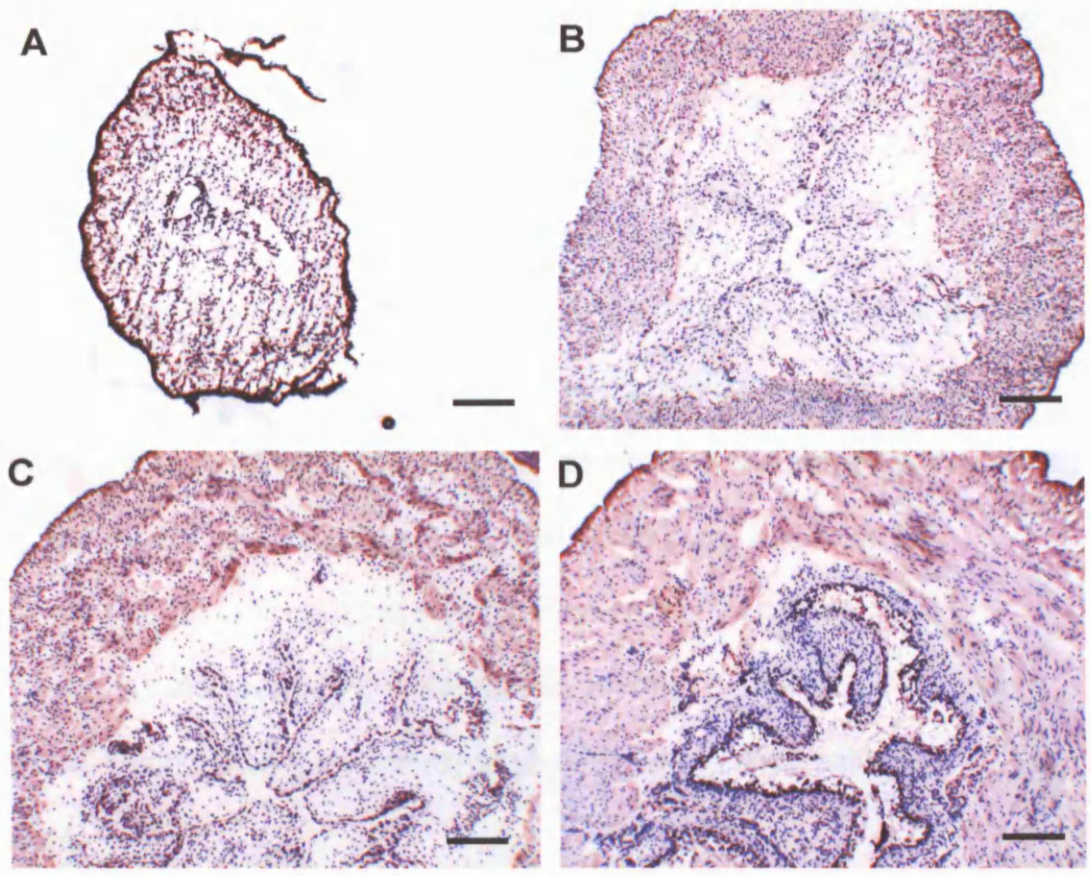

Figure 5.5: Integrin β1 expression E14 to 6wks post natal murine bladders. Expression from E14 (A), E18 (B) , day1(C), 6 Weeks (D). A,C low power view (scale bar 200 μm), B,D high power view (scale bar 50 μm).

Laminin and laminin binding integrins

Expression of specific laminin α sub-units (α1 and α2) was studied, because these are components of laminin-1 and laminin-2/4 respectively.

As described above multiple replicants were used for each time-point.

Laminin-1: (Laminin α1β1γ1) Expression of this laminin sub-type was present at the start of bladder development at E14, at the interface between the epithelium and mesenchyme. By E18, the laminin was expressed in the basal lamina of the developing detrusor layer and in the basal lamina of the urothelium, but not in the lamina propria. Post-natally this pattern was maintained, but with apparently less intense staining (figure 5.6). No western blot data is available as the antibody did not bind its antigen using this technique

Laminin-2 and 4: (Laminin α2β1γ1, lamininα2β2γ1 respectively). Expression of this laminin sub-type appeared at a latter stage than laminin-1, and was expressed in the same spatial pattern as laminin-1 thereafter, being present in the basal lamina of the detrusor layer, and of the urothelium, but not the lamina propria. Similarly no western blot data is available as the antibody did not bind its antigen using this technique (figure 5.7).

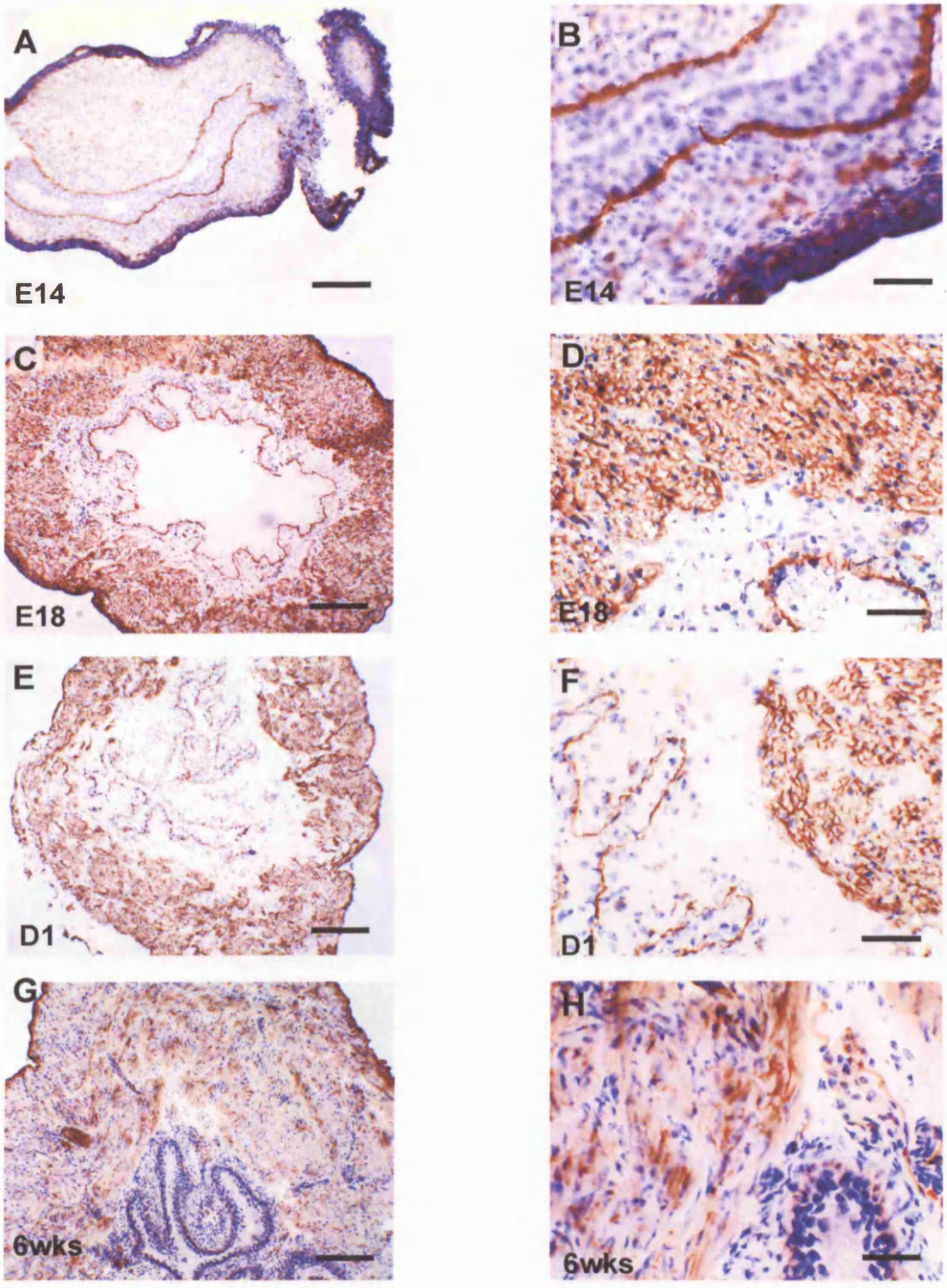

Figure 5.6:Laminin α1 expression E14 to 6wks post natal murine bladders. Laminin α1 (laminin–1): Expression from E14 (A and B), E18 (C and D), day1(E and F), 6 Weeks (G and H). A,C,E and G low power view (scale bar 200 μm), B,D,F and H high power view (scale bar 50 μm).

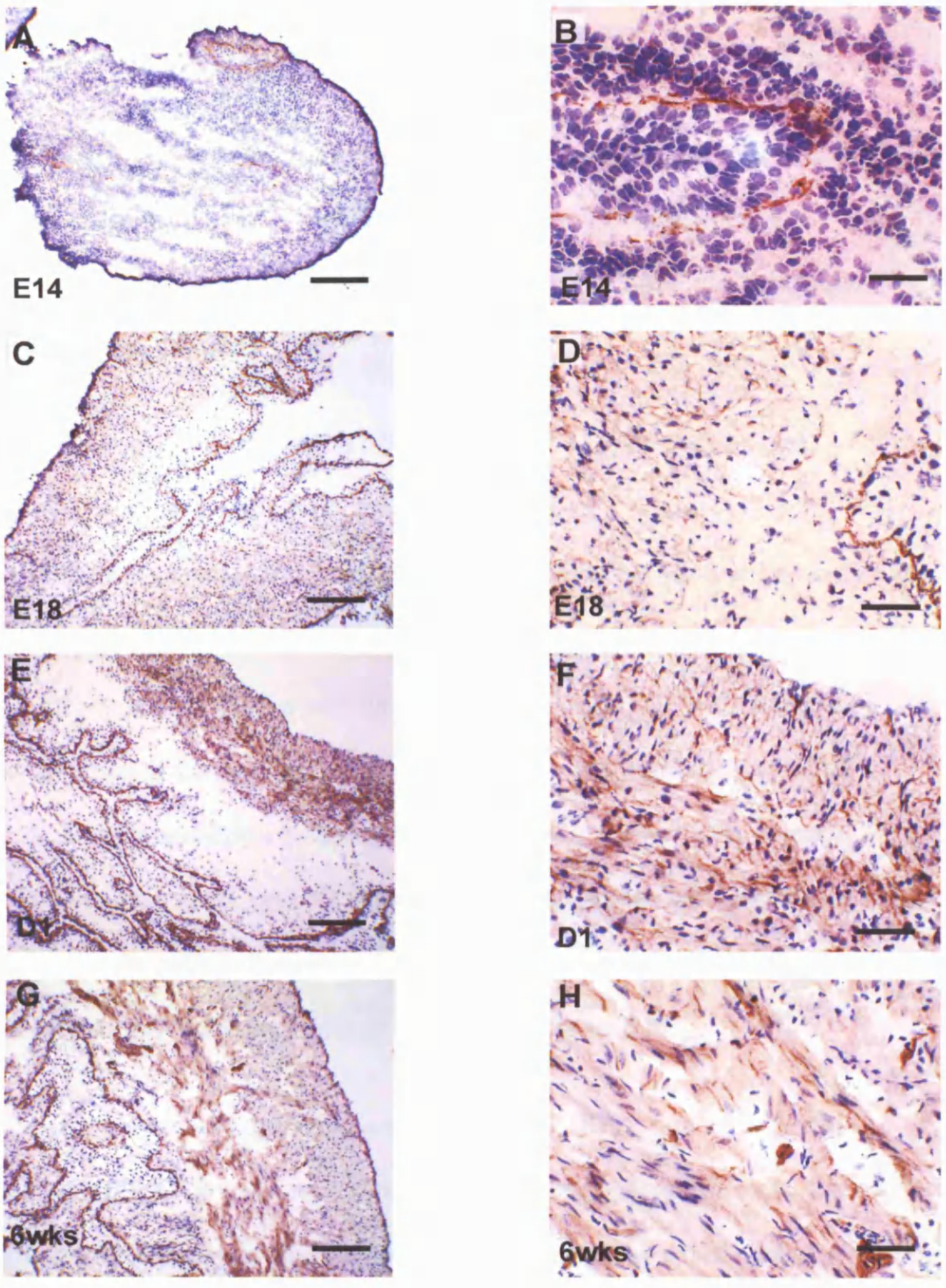

Figure 5.7: Laminin α2 expression E14 to 6wks post natal murine bladders Laminin α2 (laminin–2/4): Expression from E14 (a and b), E18 (c and d), day1(e and f), 6 Weeks (g and h). A,C,E and G low power view (scale bar 200 μm), B,D,F and H high power view (scale bar 50 μm).

Candidate Laminin receptor: Integrin α7β1

On preliminary immunohistochemistry integrin α6 expression was present in the urothelium, and also in the basal lamina of blood vessels in the lamina propria and detrusor. It was not expressed by fetal or adult smooth muscle cells (Appendix 1: figure 1.2).

Once fixation and the use of the ARK kit had been optimised, integrin α7 immunostaining could be easily detected (Appendix 1 figures 1.3-1.7). Positive control tissue in the form of myoblasts could be seen immunostained with this probe (which was originally generated by inoculating α7 null mutant mice with myoblasts from a wild type mouse). Integrin α7, in contrast, was highly expressed by adult smooth muscle cells in the detrusor and blood vessels. Fetal expression by smooth muscle precursors or fetal smooth muscle cells was weak on IHC (figure 5.8). A high power view of mature smooth muscle cells in 6 week old mouse bladder showed the integrin expressed in the cell membrane of these cells (figure 5.8E).

The only commercially available antibodies (MBL 3C12 and MBL 6A11) against integrin α7 are not recommended for probing Western blots, but are recommended for use in for flow cytometry. Three parallel cell suspensions were prepared from whole bladders, for the time-points E14, E18 and day1 from 3 separate litters, and from 3 separate individuals for 6 weeks. Flow cytometry was performed by Mrs V. Shah (Research Assistant, Institute of Child Health) as described above. This data is included in appendix 1 figure 1.8 and table 1.6. These analyses were performed with the technician blinded

to the nature of the samples. The pattern of expression of the laminin receptor integrin α7 increased from E14 to E18, by FACS, remained constant until day 1 and then doubled with maturation at 6 weeks (n=3, ANOVA p=0.0001), and was undetectable at E14 by IHC, with weak immunostaining in the detrusor at E18 and D1, but with strong immunostaining of the DSMC at 6 wks, figure 5.8F. Bonferroni post-hoc tests of significance revealed that upregulation of integrin α7 between E14 and E18 and D1 was significant ($p<0.005$, both comparisons), with no significant difference between E18 and D1, but that there was significant upregulation from D1 to 6 wks ($p<0.001$). Comparing E14 to 6 wks there was an upregulation of integrin α7 that was significant ($p<0.001$).

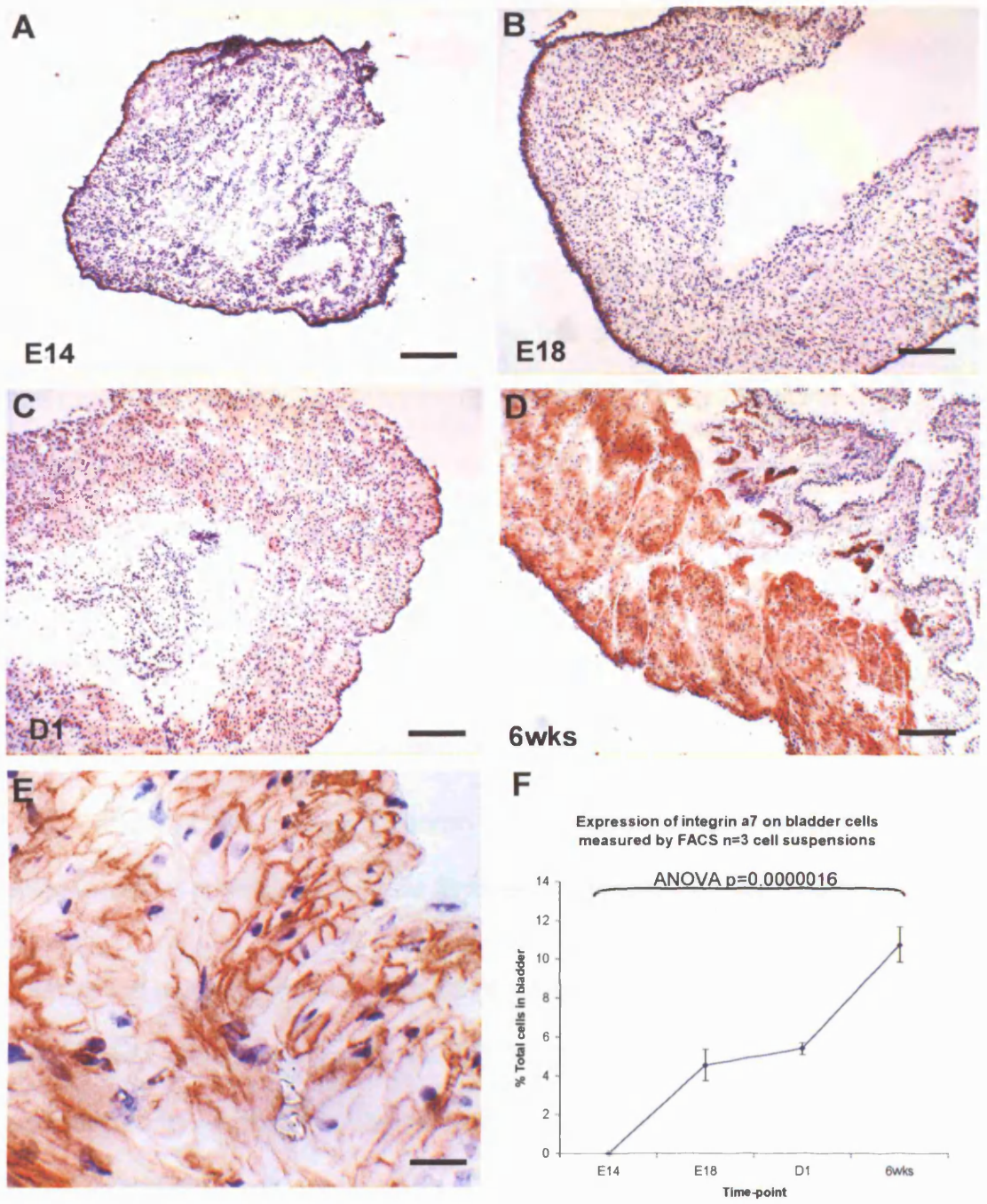

Figure 5.8: Integrin $\alpha 7$ expression E14 to 6wks post natal. Expression from E14 (A), E18 (B) , day1(C), 6 Weeks (D). (E) High power view of detrusor muscle at 6 weeks. (F) FACS data for integrin $\alpha 7$ (n=3 for each time–point). A-D low power view (scale bar 200 μm); E high power view (scale bar 25 μ m).

Discussion

Fibronectin and integrin α5β1 (a candidate DSMC fibronectin receptor)

The candidate integrin fibronectin receptor components α5 and β1 are both expressed by cells in the detrusor layer of the bladder. It has been demonstrated that there is an antenatal upregulation of these receptor components that parallels the temporal expression of fibronectin described by (Smeulders et al 2003) – the data from the current study is illustrated in figure 5.9. The pattern of fibronectin expression was in close agreement to that which found when fibronectin Western blots were performed for this study (figure 5.4).

This is the first report of changing pattern of expression of fibronectin, in association with a possible candidate fibronectin receptor, integrin $\alpha5\beta1$.

This part of the descriptive work supports the hypothesis that fibronectin and its integrin $\alpha5\beta1$ receptor is expressed in forming DSM of the embryonic mouse bladder. In other words the ligand and its receptor are in the right place at the right time to have an effect. The postnatal IHC for integrin $\alpha5$ subunit is more equivocal because of the high background staining seen, however the Western blot data is more convincing. In the future immuno-electron microscopy could be performed to define to sites of expression of fibronectin inside and outside fetal DSMC. Wilson et al (1996) describe a similar pattern of expression of integrin α5 and β1 in the adult human bladder, corresponding with detrusor fibronectin expression. When fibronectin is down

regulated post-natally, however, no striking down-regulation of integrin α5β1 was found. The error bars from the Western blot data mean that it is possible that there may be a smaller degree of down-regulation of this integrin or indeed no down-regulation at all.

There are many integrin receptors described that can ligate fibronectin. These include α4β1, α5β1, αvβ3, α8β1, αIIbβ3 (predominantly a platelet expressed integrin although ectopic expression has been described in tumours), as discussed in the Introduction. Other potential RGD-binding, fibronectin receptors have been described in DSMC, integrin αvβ3 expression has been described in stretched bladder DSMC using by RT-PCR (Upadhyay et al 2003), and IHC studies in human bladders have demonstrated both integrin α5β1 and β3 integrin expression in DSMC (Wilson et al 1996). Any signalling effect due to fibronectin may therefore be mediated by these alternative receptors. However, of note it is integrin α5β1 that is present in fibrillar adhesions associated with fibronectin fibrillogenesis (Pankov et al 2000), and blockade of integrin α5β1 inhibits many of the biological effects of culturing fibroblasts in 3-d culture (Cukierman et al 2001). A full assessment of the potential fibronectin receptors in developing detrusor would require an assessment of expression of all the potential receptors described above perhaps by a combination of IHC, Western blot and RT-PCR as has been described for laminin sub-type expression in the ureter (Hattori et al 2003).

Conversely, integrin α5β1 is capable of ligating other ECM molecules. The study of ECM and integrin interactions is complicated by the redundancy of these systems, whereby an ECM component can be replaced by another

molecule, or a receptor can be knocked out and its function taken over by another integrin, as reviewed by (De Arcangelis and Georges-Labouesse 2000). In order to demonstrate that fibronectin interacts with integrin $\alpha5\beta1$ in a functionally important manner, functional tests of this interaction are necessary. A possible technique to investigate this immunohistochemically would be to examine the activation state of the integrins present, using antibodies that detect the active conformation of integrin $\beta1$ (e.g. Chemicon MAB2079Z, mouse anti-human active conformation $\beta1$ integrin), as described by (Luque et al 1996). Similarly integrin activation could be assessed by immunostaining for activated, phosphorylated FAK, and examining for colocalization of this to focal adhesions containing integrin $\alpha5\beta1$ (e.g. anti-FAK phospho-Y397 antibody ab4803, Abcam) (Sieg et al 2000).

A functional assessment of fibronectin-integrin interactions forms the next part of this thesis.

Does this failure of down-regulation of the candidate receptor integrin $\alpha5\beta1$ have any significance?

No significance can be drawn form this, but possible explanations include the presence of unligated integrin $\alpha5\beta1$ on the cell membrane of DSMC; or, the integrin is ligated to an alternative ECM component; or fibronectin is in great excess of the integrin $\alpha5\beta1$ receptor transiently (perhaps ligated to another integrin receptor), and that all the integrin $\alpha5\beta1$ is in fact ligated to fibronectin.

It is possible to speculate that if the ligand is no longer present to stimulate its receptor then there is no signal, but that potential for this signalling

mechanism remains present in fully differentiated DSMC. It is possible that the presence of α5β1 integrins on the cell membranes of mature SMCs would then allow a proliferative response to the provisional fibronectin matrix laid down as a result of tissue damage (Okada et al 1985). This might be a mechanism of response to fetal bladder outflow obstruction (BOO).

Alternatively, there are is evidence to suggest that unligated integrins can actively cause down-stream signalling effects: (Varner et al 1995) and have shown that unligated integrin α5β1 activates signalling pathways, including growth arrest specific gene-1 (gas-1), which positively inhibit proliferation, and similarly tumorigenicity of hepatocellular carcinoma in mice is inhibited by over-expression of integrin α5β1 (Zhou et al 2000).

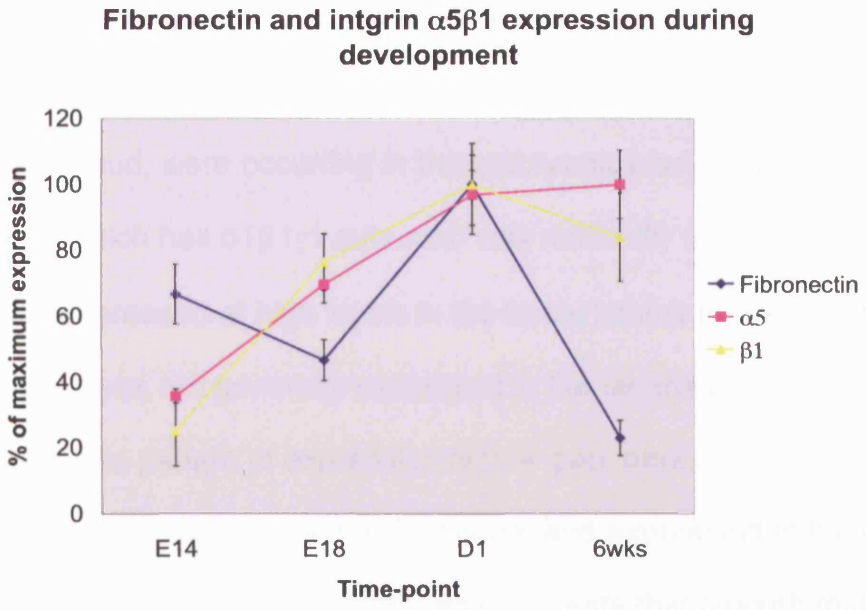

Figure 5.9: Relative trends in fibronectin and fibronectin receptor expression expression (western blot densitometry), plotted against trends in relative expression for the fibronectin receptor integrin α5β1. All data from this thesis.

Laminin and integrin α7β1 (laminin receptor)

Preliminary IHC on the expression of laminin α1 shows that it was present at the interface between the primitive urothelium and the mesenchyme at the start of bladder development. The means that it is possible that mesenchymal/epithelial interactions, described by Schuger et al (1997) for the developing lung bud, were occurring in the embryonic bladder. Laminin α1 (and laminin-1 which has α1β1γ1 subunits) was markedly upregulated by E18, and remained expressed at high levels in the basal lamina of the detrusor layer. Laminin-1 was not generally expressed in the lamina propria, except by blood vessels. This pattern of expression with a 'gap' between the laminin-1 expressed in the basal lamina of the urothelium and expression in the DSM layer is not seen in the developing lung, and suggests that smooth muscle myogenesis after initiation in the bladder is not following the same pattern as the lung bud (Schuger et al 1997). I was unable to get Western blots to work with this antibody, so quantification of the relative changes in expression during DSMC development are limited to interpretation of the IHC data only. These data are not so robust as the data for integrin sub-types discussed above. In general, integrin antibodies are not useful Western blot probes if the antigen to which the antibody is raised is an extracellular epitope (personal communication from Dr Kairbaan Hodivala-Dilke).

Laminin α2, present in laminin-2/4, followed a similar pattern of expression to laminin-1.

In this study expression of the integrin α7 sub-unit is specific for smooth muscle cells in the bladder, and that the two components of this receptor (α7 and β1) are both expressed in the mature bladder on the cell membranes of mature smooth muscle cells where they would be able to act as receptors for laminins in the surrounding basal lamina. The temporal pattern of expression of this integrin as assessed by flow cytometry is very similar to that described by (Smeulders et al 2003) for generic laminins– the fits of the data form this thesis and Smeulders et al (2003) are compared in figure 5.10. Expression of integrin α7 by mature mouse bladder detrusor has been previously described by (Yao et al 1997), with a similar pattern to these observations.

This pattern is what was expected from the previous lines of evidence described in the Introduction. It would also fit with an initial mesenchymal phenotype, with a paucity of fibronectin surrounding it, which then changes into the fetal smooth muscle phenotype with a large component of fibronectin. Finally, a second change in phenotype with down-regulation of fibronectin, loss of proliferation and final differentiation to the contractile mature smooth muscle phenotype. Similarly the laminins were expressed at low levels at E14, then upregulated at E18 coincidental with the fetal smooth muscle cell phenotype, as was the laminin receptor integrin α7β1. Both laminins and α7β1 remained at the same level of expression, until a final change in phenotype to the mature smooth muscle phenotype in the adult bladder.

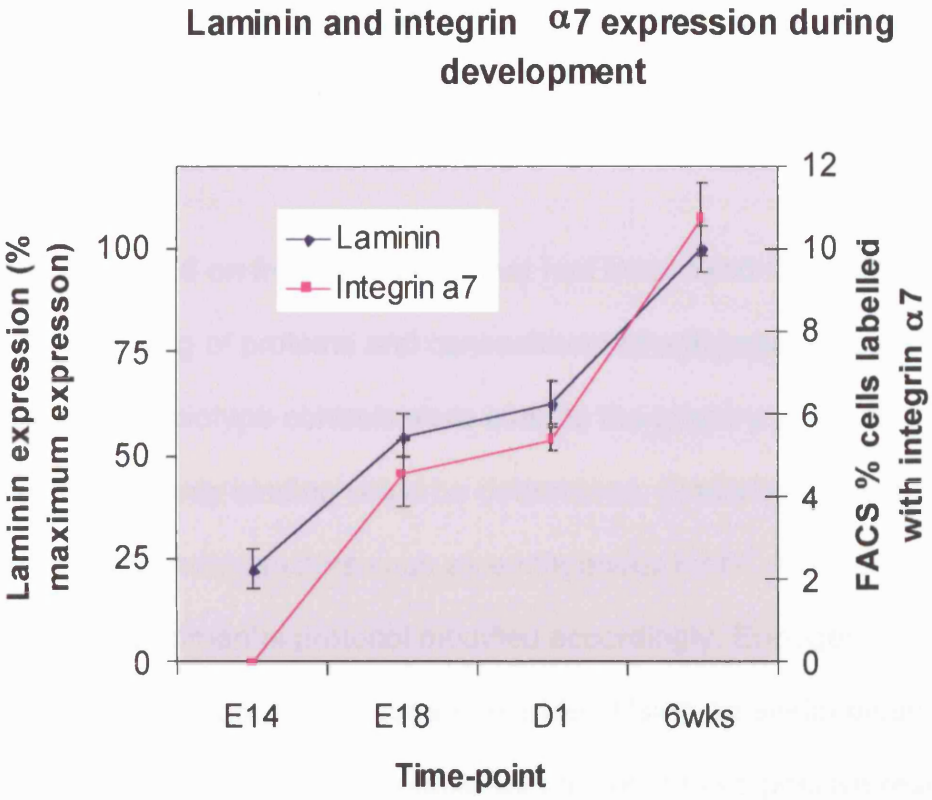

Figure 5.10: Western blot expression laminins versus Integrin α7 flow cytometry plotted against flow cytometry data (% positively staining cells) for integrin α7. (FACS data from this thesis, generic laminin data Smeulders et al, 2003),

The strengths of this descriptive work are firstly that expression has been assessed first by IHC, and then secondly quantified by an alternative technique, either western blot or flow cytometry. That these different techniques produce similar results makes interpretation of the results more reliable and robust.

IHC was performed on frozen sections that had been fixed using acetone at -20°C. Cross-linking of proteins and concealment of antigenic epitopes was therefore limited. Isotype controls were used to the primary antibodies so that non-specific antibody binding could be determined. Similarly, in the integrin α7 IHC, other confounding factors such as endogenous biotin and IgG were present and experimental protocol modified accordingly. Endogenous biotin is produced by the mature renal tract and bladder. Using an avidin-biotin detection system is therefore unreliable with a risk of false-positive results (Wang and Pevsner 1999;Banks et al 2003). This was detected in my IHC experiments and a biotin blocking kit (Vector) was used. Similarly the use of mouse primary antibodies would have produced marked false positive results unless the animal research kit (ARK-Dako) had been used.

The antibodies used in Western blot experiments were the same antibodies used in IHC. Western blots were performed using several controls. Successful electroblotting was assessed by Ponceau S staining; reliability of loading, electroblotting and probing of WB filters was demonstrated by reliable and consistent β-actin levels. Any loading errors that could have biased the results

were discounted by only analysing WB densitometry data once it was controlled for by β-actin expression for that protein sample lane. Statistical reliability was ensured by using separate litters to prepare the protein samples for E14, E16, E18 and neonatal day 1 time-points, and separate individuals for the 6 week time-point.

For the flow cytometry quantification of integrin α7 both negative and positive controls were included in every run. An isotype mouse immunonoglobulin G (IgG) was used, as was a positive control – adult bladder cell suspensions were run in parallel to all the fetal time-points. For statistical reliability, each suspension represented either a separate litter (E14, E18 and day1), or separate individuals (6weeks). Three parallel suspensions were run at each time, each with its own positive and negative control. Furthermore the cells suspensions were prepared by myself, but the identity of each suspension was blinded from the technician who ran the flow cytometry experiments.

Co-localization of the integrin α and β sub-units was strongly suggested by IHC of similar serial sections of bladder, but no formal co-localization has been performed. Similarly, serial/similar sections of bladder show ligand and receptor temporo-spatial parallels in expression, but again no true co-localization studies have been done.

Western blots are, at best, only semi-quantitative, providing only information about relative changes in expression for a particular protein. Comparisons between different proteins are therefore limited to examination of relative changes over the same time-points. An increase in the densitometry of a western blot band can occur as a consequence of either an increase in

expression of that protein by all cells from which the protein sample is made, or by an increase in a sub-population of cells that uniquely express the protein, or by some combination of the two. Flow cytometry is therefore a useful complementary approach as the number of cells expressing the antigen can be counted. A weakness for the quantification performed in this study is that flow cytometry has not been repeated for all the integrin sub-units. However when the IHC and western blot data are examined together, then a progressive upregulation of integrin expression by substantial number of cells in the detrusor is the most likely explanation.

Conclusion

First, this study is consistent with the contention that the candidate fibronectin receptor integrin α5β1 could mediate instructive signals from a fibronectin-rich matrix. Second, upregulation of integrin α7β1 harmonised with the upregulation of laminin and DSMC maturation, allowing for the possibility that these molecules may interact, perhaps modulating a muscle differentiation signal.

Chapter 6. Mouse bladder cell culture and adhesion blocking experiments

Hypothesis

In Vitro DSMC may adhere to fibronectin, possibly modifying cell behaviour, and that this adherence may be mediated by the candidate fibronectin receptor integrin $\alpha5\beta1$.

Background

That fibronectin is present in ECM of fetal DSMC during murine bladder development has been shown by (Smeulders et al 2003). Furthermore bovine DSMC are capable of secreting fibronectin in cell culture (Baskin et al 1993b). In cell culture vascular SMC adhere to fibronectin and become proliferative and synthetic on this substrate (Morla and Mogford 2000; Thyberg and Hultgardh-Nilsson 1994). Bourdoulous et al (1998) has shown that for endothelial cells and fibroblasts, fibronectin is necessary for cell cycle progression and proliferation. Hornberger et al (2000) has shown that adhesion dependent EGF stimulated growth of human fetal myocytes is enhanced by stimulation of integrin $\alpha5\beta1$. Nguyen et al (2005) have shown that $\beta1$ integrins including integrin $\alpha5\beta1$ are important in airway smooth muscle growth on collagen I, or fibronectin substrate. From chapter 5 upregulation of fibronectin in the ECM surrounding DSMC occurs in a similar spatial and temporal pattern as expression of the candidate fibronectin receptor integrin $\alpha5\beta1$. This leads to the question of whether there is a

functional interaction between the fibronectin and fibronectin receptor integrin $\alpha5\beta1$, and modulation of proliferation of these murine DSMC.

The strategy of this chapter was to use whole bladders disaggregated into a bladder cell suspension. Using this heterogenous suspension (presumably initially a mixture of detrusor, connective tissue, vascular and urothelial cells) the following aspects could be examined: 1) did fetal bladder cells stick to fibronectin? 2) what is the nature of these cells? (this would be examined by immunocytochemistry: are DSMC cells adhering, as demonstrated by smooth muscle markers such as αSMA and desmin; and do these cells express the candidate integrin receptor $\alpha5\beta1$?) 3) what is the nature of the effect of fibronectin adhesion on these cells with regards proliferation? 4) can adhesion of these cells be inhibited either by antibody blocking the fibronectin, or by use of RGD oligopeptides to block the integrin binding site for fibronectin.

Aims

Use in-vitro dissociated cells to study adhesion to defined substrates, examine effect substrates have on adherent cells, and to further investigate the mechanism of adhesion through functional blockade of integrin receptors.

Aims: 1) to examine adhesion of disaggregated bladder cells from fetal and mature murine bladders to a fibronectin substrate; 2) characterise these adherent cells; 3) examine any proliferative effect that fibronectin adhesion may have on fetal bladder cells; 4) examine any effect blockade of fibronectin/integrin interaction may have on adhesion of cells from whole bladder suspensions.

Results

Cell adhesion to fibronectin substrate

E18 whole bladder cell suspensions were plated on top of glass slides, with and without fibronectin coating. Phase contrast microscopy revealed that on uncoated slides, adherent cells adhered did not spread, remaining in a 'rounded' state (figure 6.1A). On fibronectin coated slides, a greater proportion of plated cells adhered, and they adopted a 'spread' morphology (figure 6.1B).

Preliminary experiments determined 1) the optimum duration for the adhesion experiments (figure 6.1 below); 2) the fibronectin coating concentration that should be used (appendix 2: figure 2.1 and table 2.1).

A test experiment comparing cell adhesion of uncoated slides to fibronectin coated slides with either 10 µg/ml (giving a maximum concentration of 1.4 $\mu g/cm^2$), or 20 µg/ml (2.8 $\mu g/cm^2$), or 40 µg/well (5.6 $\mu g/cm^2$) was performed, to find the most appropriate concentration of fibronectin for subsequent blocking experiments. E18 bladder cell suspensions of 200,000 - 400,000 cells/ml in DMEM/F-12 with supplemental ITS were used, 250 µl loaded onto 4-well slides (50-100,000 cells) and 125 µl loaded onto 8-well slides (25-50,000 cells). These were incubated at 37°C in 5%CO_2/air in a humidified incubator for 30 minutes to 4 hours. The non-adhesive cells were rinsed off using PBS, the adherent cells fixed with acetone, and stained with methylene blue, and counted. In terms of length of culture period there was no further

increase in total cell adhesion after 1 hour (Figure 6.1), although there was a change in ratio of spread to round cells.

With regards fibronectin coating concentration, the data of E18 cell suspensions is described in Appendix 2: table 2.1, and illustrated in Appendix 2: figure 2.1. This showed a 3-3.5 fold increase in adhesion of cells on fibronectin (20 µg/ml) versus uncoated slides (n=3, ANOVA $p<0.05$), over 4 hours, with no increase thereafter. The middle of this range was therefore used for adhesion experiments (5-20 µg/ml coating concentration of fibronectin).

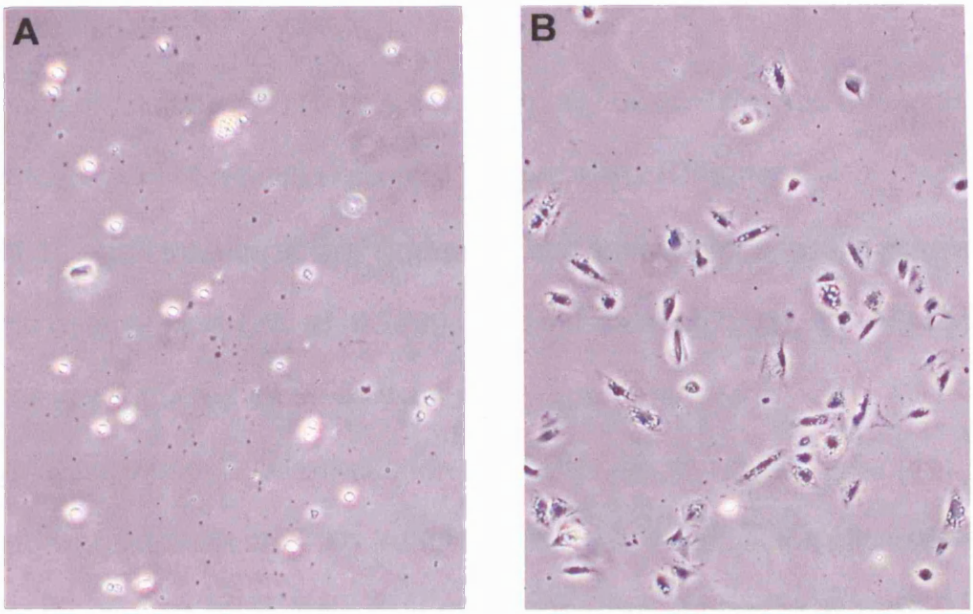

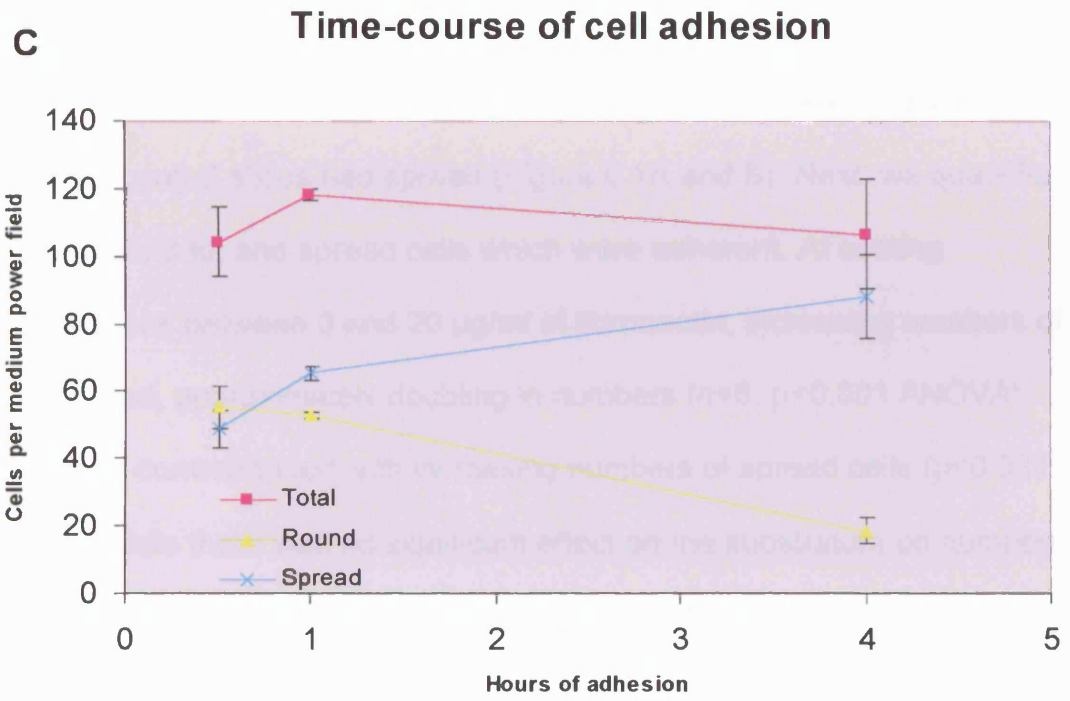

Figure 6.1: Adherence of whole bladder cell suspensions to fibronectin . (A) Some adherence, no spreading on uncoated glass. (B) More adherence, cell spreading on fibronectin coated slides

For cell adhesion studies E18 bladders were mainly used. This was due to the proven expression of fibronectin receptor integrin α5β1 (Chapter 5 – experiment 1), and because at this time-point, cell suspensions would include fetal smooth muscle cells (Wu et al 1999a;Smeulders et al 2002). E14 bladder suspensions were studied as these were most representative of mesenchymal cells prior to differentiation into fetal smooth muscle cells (Wu et al 1999a; Smeulders et al 2002). Adult bladder cell suspensions allowed the study of the mature phenotype (Wu et al 1999a; Smeulders et al 2002).

In the typical experiment, one hour after cells were plated, most adherent cells on uncoated slides were rounded, whereas most adherent cells on fibronectin coated slides had spread (Figure 6.1A and B). Next, we quantified the total, rounded, and spread cells which were adherent. At coating concentrations between 0 and 20 μg/ml of fibronectin, increasing numbers of cells adhered, approximately doubling in numbers ($n=6$, $p<0.001$ ANOVA); this entirely corresponded with increasing numbers of spread cells ($p<0.001$, ANOVA), while there was no significant effect on the substratum on numbers of rounded cell (Figure 6.2A, Appendix 2: figure 2.1).

Using numbers of spread adherent cells as a read-out, fibronectin coating also had a significant effect when dissociated cells from E14, and adult bladders were studied, numbers of adherent cells increasing 250% for these time points ($n=3$, $p<0.001$ and $p<0.05$ respectively, ANOVA) (Figure 6.2B).

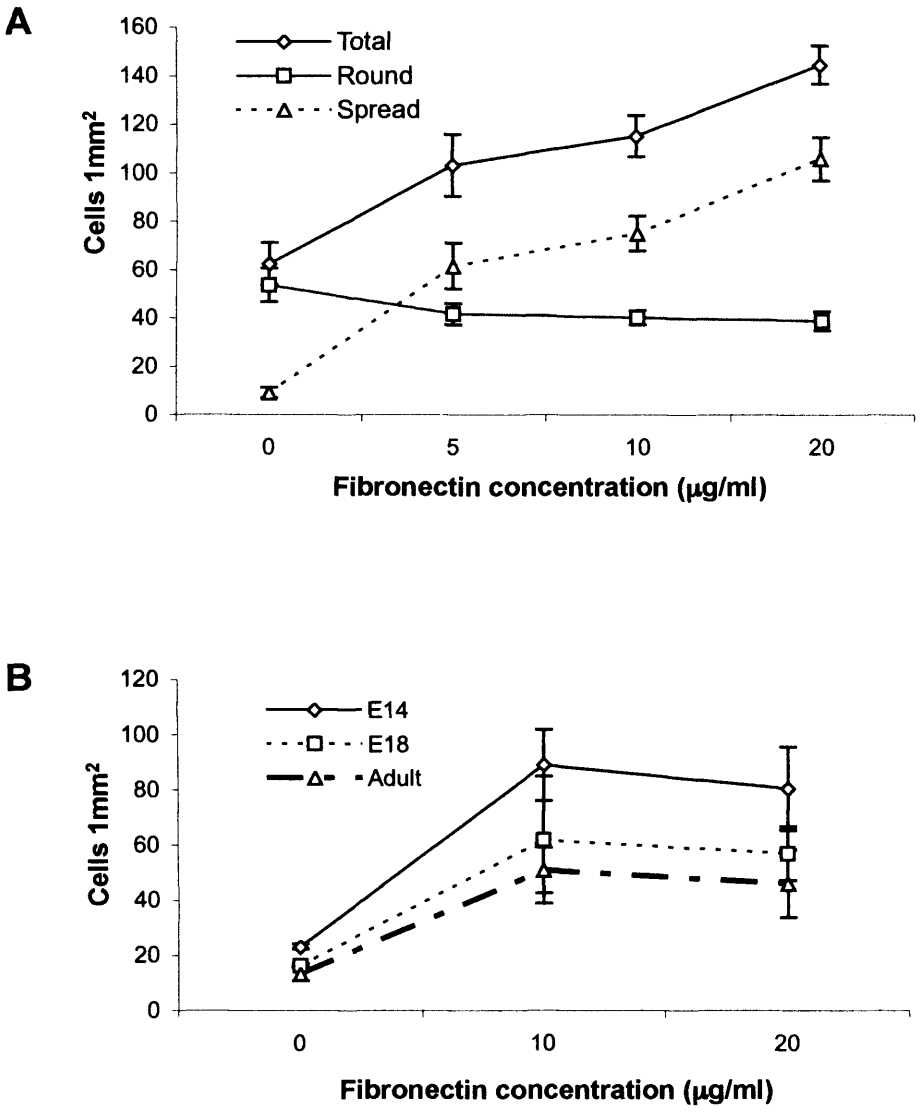

Figure 6.2: Adhesion of bladder cell suspensions to fibronectin. (A) E18 whole bladder suspensions (n=9) allowed to adhere for 1 hour. (B) numbers of adherent and spread cells in embryonic day 14 (E14), embryonic day (18) and adult cells.

Characterisation of adherent cells

Using E18 bladder cell suspensions plated onto fibronectin coated slides, immunocytochemistry was performed (figure 6.3 A-D): 79±12% of all cells which adhered to fibronectin were positive for integrin α5; and 80±4% were positive for integrin β1; 82±2% of all adherent cells were desmin positive – with similar results for α-SMA (α-SMA immunostaining during murine bladder development E14 to 6wks is shown Appendix 2: figure 2.7, α-SMA immunocytochemistry is shown Appendix 2: figure 2.8). Only 3% of cells adhering to uncoated slides were desmin positive (n=10 uncoated slides, n=4 fibronectin 5-10 μg/ml and n=6 fibronectin 20 μg/ml, $p<0.001$ ANOVA). Less than 2% of all adherent cells on fibronectin substrate were found to express CD31 or cytokeratin 18.

CD31 is expressed by endothelial cells, positive control immunostaining of umbilical artery is shown Appendix 2: figure 2.2. CD31 immunostaining in developing mouse bladders from E14 to 6 wks is shown in Appendix 2: figure 2.3; and CD31 immunocytochemistry for the E18 bladder cell suspension adhesion experiment is shown Appendix 2: figure 2.4.

Cytokeratin 18 is expressed by developing murine epithelium (Baskin et al 1996c). Cytokeratin 18 immunostaining during mouse bladder development from E14 to 6 wks is shown in Appendix 2: figure 2.5. Cytokeratin 18 immunostaining of adherent cells from E18 bladder cell suspension is shown in Appendix 2: figure 2.6.

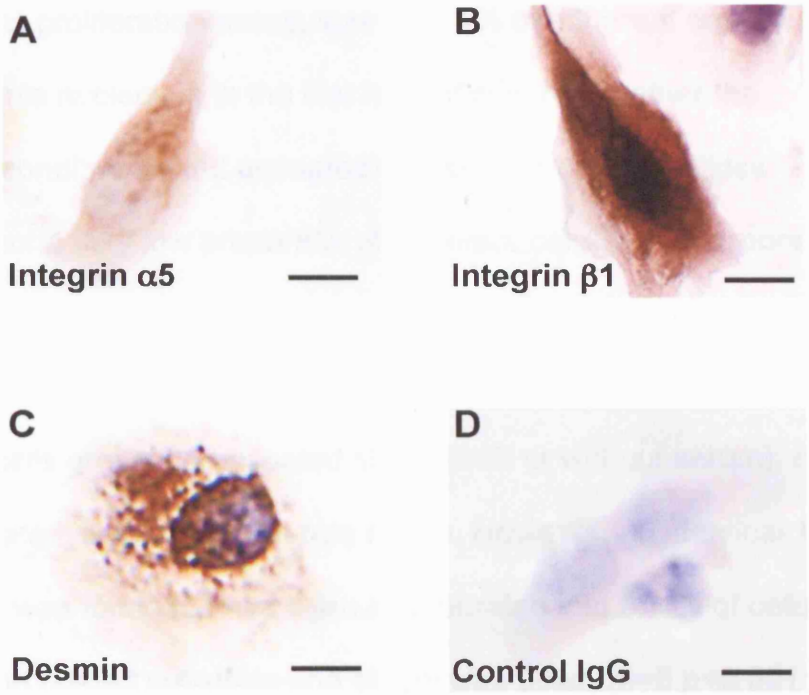

Figure 6.3: Immunocytochemistry of adherent cells. (A) Integrin α5. (B) Integrin β1. (C) Desmin. (D) Negative control using pre-immune rabbit IgG. Bars are 10μm.

Effect of fibronectin on proliferation

Using the BrdU proliferation assay, less than 1% of adherent cells had incorporated this nucleotide in the first hour of culture, whether the experimental conditions used uncoated or fibronectin coated slides; in addition the same very low proportion of adherent cells had incorporated BrdU when serum-supplemented media was used. If cells were maintained in culture for 12 hours, BrdU incorporation remained very low (on average, less than 2%) for cells grown on uncoated slides (with or without serum), or on fibronectin coated slides in serum-free media. However, an identical 1 hour pulse of BrdU was found to have been incorporated into 9±1% of cells when both fibronectin coated substrate and serum was used, ($n=6$ $p<0.001$ ANOVA) figure 6.4). (Data shown in appendix 2). Bonferroni post-hoc test of significance showed that proliferation after 12 hours of adhesion on fibronectin, in the presence of serum, was significantly different to all the other 7 groups ($p<0.001$, all comparisons). There was no significant difference between any of the other groups.

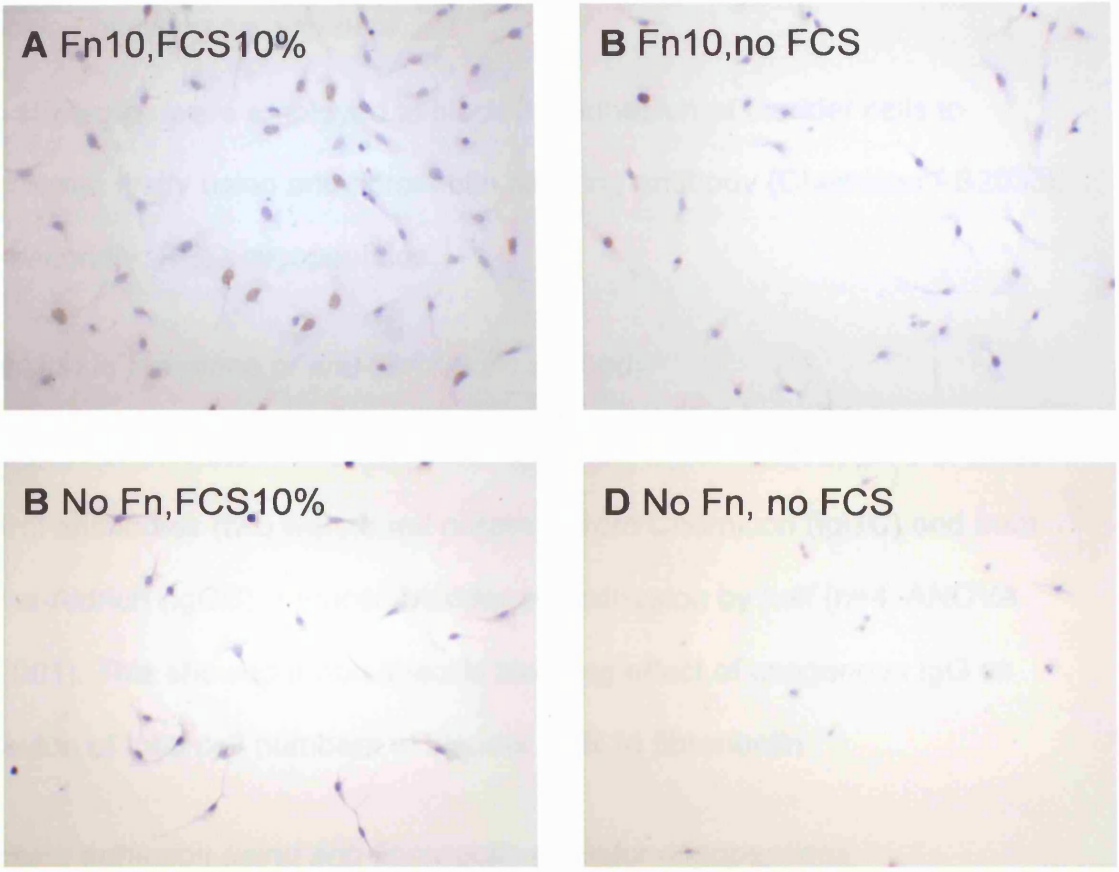

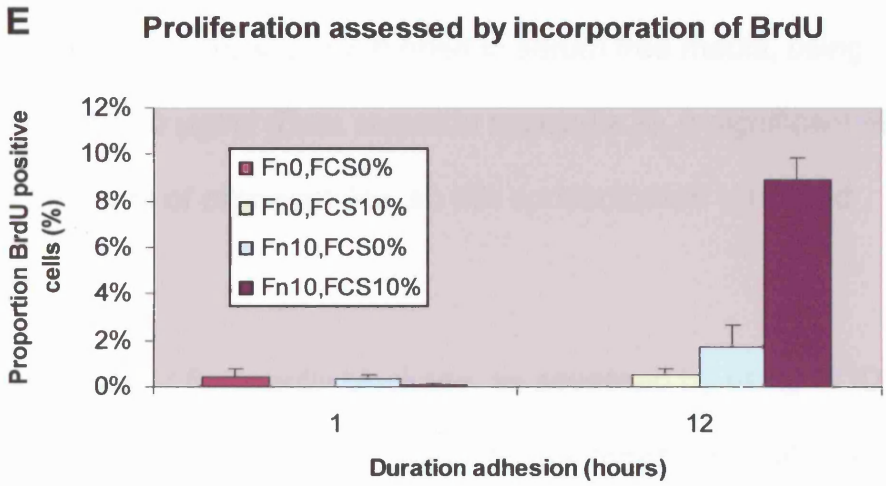

Figure 6.4:BrdU incorporation by Adherent E18 Cells. (A-D) BrdU uptake in E18 Cells over 12 hours. (A) Fibronectin 10mcg/ml, FCS 10%.(B) Fibronectin 10 mcg/ml, no FCS.(C) No fibronectin, FCS(10%). (D) No fibronectin, no FCS. (E) Proliferation as assessed by BrdU uptake. Data plotted as mean±SEM.

Adhesion blocking experiments

Two strategies were employed to block the adhesion of bladder cells to fibronectin: firstly using anti-fibronectin blocking antibody (Chemicon AB2033); and secondly, RGD oligopeptides.

Adhesion in presence of anti-fibronectin antibody

Figure 6.5 shows the results obtained: anti-fibronectin antibody (aF) or isotype control antibodies (two were used obtained from Chemicon (IgGC) and from Sigma-Aldrich (IgGS)) reduced bladder cell adhesion by half (n=4, ANOVA $p<0.001$). This showed a non-specific blocking effect of exogenous IgG on adhesion of total cell numbers of bladder cells to fibronectin.

Blocking adhesion using anti-fibronectin receptor oligopeptides.

Test adhesion experiments were performed in serum free media, using oligopeptides at 10-40 µg/ml (Data shown in appendix 2). A significant effect was seen at 20 µg/ml of oligopeptides, so this concentration was used subsequently.

The potential effects of fibronectin blockade, as assessed by using RGD peptides (20 µg/ml), were explored by quantifying different populations of adherent E18 cells. RGD oligopeptides significantly reduced adherent cells which were desmin positive at 10 and 20 µg/ml of fibronectin coating, compared to both the control peptide (RAD) and no additives (figure 6.6A): 71±9% of adherent cells expressed desmin in the presence of RAD oligopeptide; whereas the number was 48±9%, significantly fewer (n=6, $p<0.01$), in the presence of RGD.

Examination of the morphology of all adherent cells on fibronectin 10 μg/ml in the presence of RGD or RAD showed that there was a significant change in morphology associated with RGD integrin blockade (figure 6.6B). In the presence of RAD, 63±4% of cells were spread, whereas 54±4% spread in the presence of RGD, significantly less ($n=6$, $p<0.001$). In the presence of RAD, 37±4% of cells were rounded, whereas the number with RGD (46±4%) was significantly increased ($n=6$, $p<0.001$) (figure 6.6B).

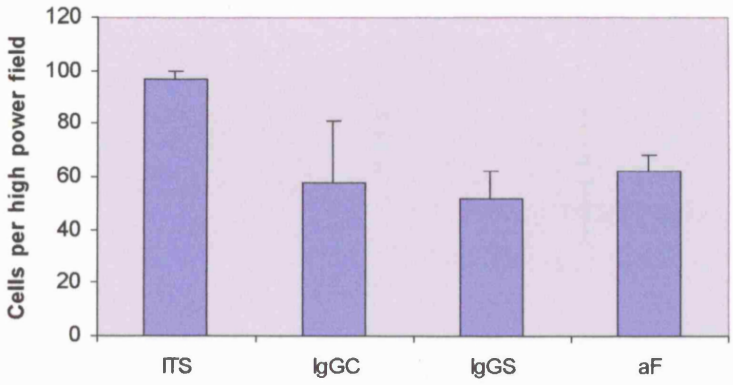

Figure 6.5: Non-specific effect of immunoglobulin on E18 whole bladder cell suspensions. ITS, DMEM/F12 supplemented with insulin, transferrin, selenium. IgGC, rabbit isotype control IgG from Chemicon. IgGS, rabbit isotype control IgG from Sigma. aF, rabbit anti-mouse fibronectin antibody (Chemicon AB2033)

A

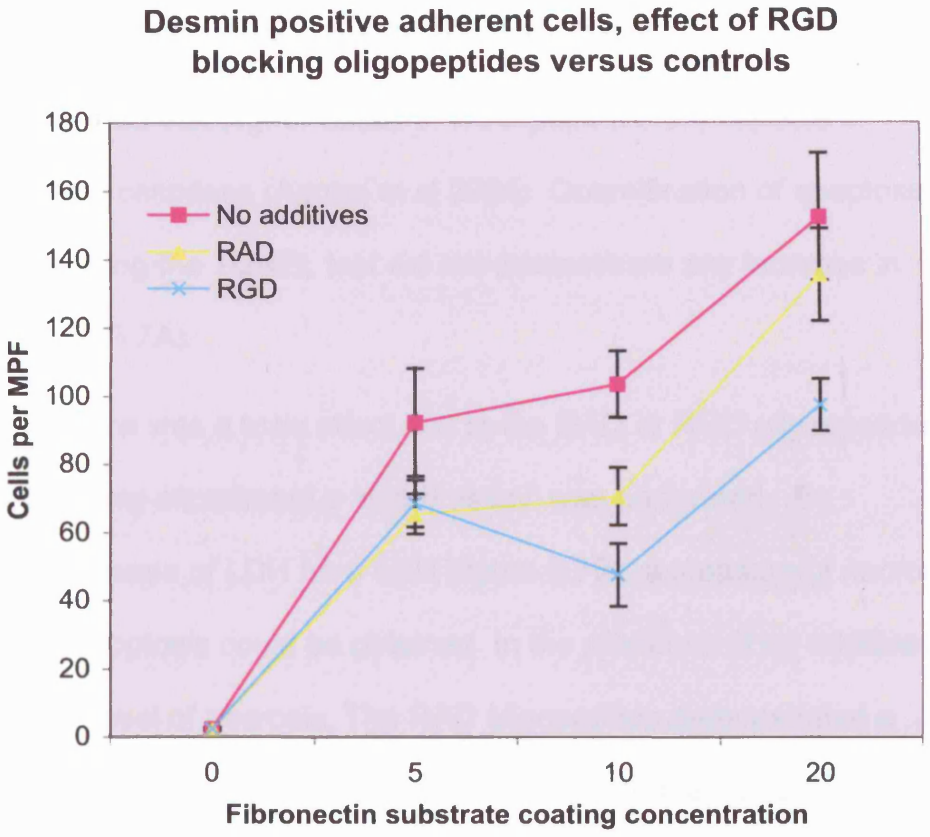

B

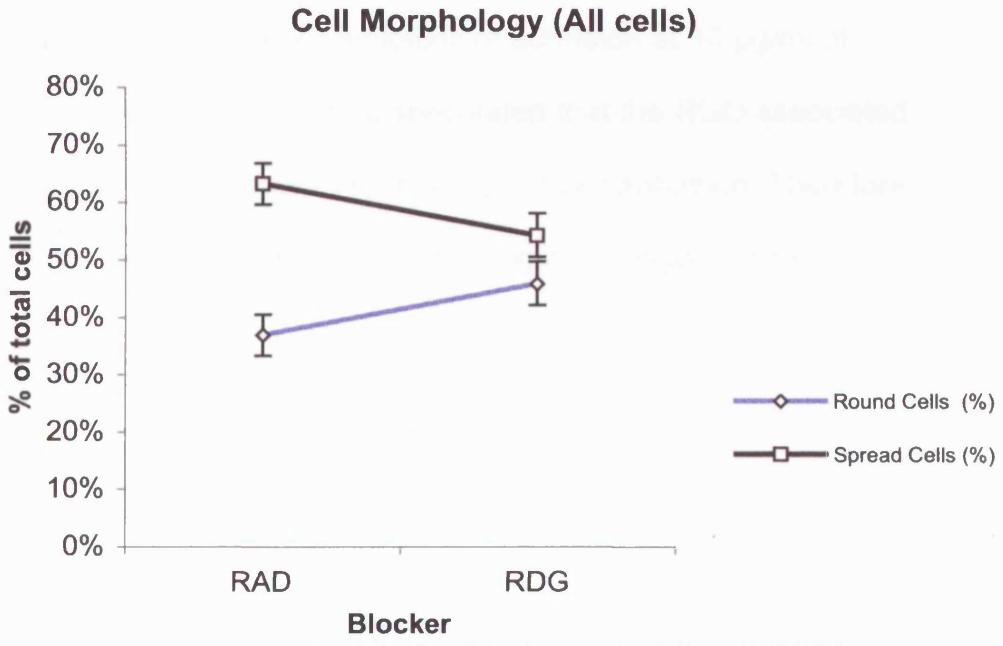

Figure 6.6: RGD oligopeptide adhesion blocking experiments. (A) adhesion of desmin positive cells. MPF medium power field (x20 objective on axiophot computer controlled microscope) Fibronectin coating concentration in mcg/ml). (B) Morphology of all adherent cells.

RGD/RAD oligopeptide apoptosis activation and toxicity

It has been reported that higher doses of RGD peptides are capable of directly activating caspases (Aguzzi et al 2004). Quantification of apoptosis in adherent cells using the TUNEL test did not demonstrate any increase in apoptosis (figure 6.7A).

To examine if there was a toxic effect due to the RAD or RGD oligopeptides used in the blocking experiment a 'death assay' was performed. By measuring the release of LDH from cells (figure 6.7B), a measure of necrosis as opposed to apoptosis could be obtained. In the presence of no additives there was a low level of necrosis. The RAD oligopeptide demonstrated a fibronectin independent toxicity, whereas the RGD cell-death doubled as the fibronectin substrate doubled, $p<0.01$ paired t-test, $n=4$. (From figure 6.6A it can be seen that there was a larger inhibition of adhesion at 10 µg/ml of fibronectin, than at 5 µg/ml). It could be speculated that the RGD associated death was therefore perhaps related to inhibition of cell adhesion. Therefore experiments were limited to using a dose of 20 µg/ml or oligopeptides.

Discussion

Whether fibronectin could indeed modify the behaviour of differentiating DSMC was explored by studying the potential effects of this ECM molecule in a cell adhesion model. Firstly it has been shown that the number of adherent cells from dissociated E18 bladders was strikingly increased on fibronectin

substrate in a concentration dependent manner; this effect was explained by an increase in spread versus rounded cells. Furthermore, similar effects were found using dissociated E14 and adult bladders. Because whole bladders (our starting material) contained urothelial, endothelial and fibroblast cells as well as DSMC, and because fibronectin is known to alter the behaviour of endothelia (Shono et al 2001), the phenotype of the adherent cells in our experiments was investigated by immunocytochemistry. On a fibronectin substrate, the great majority (80%) expressed desmin and α-SMA, whereas only a small minority (less than 2%) expressed the urothelial marker cytokeratin 18 or the endothelial marker CD31. Collectively, these support the hypothesis that fibronectin is a functional substrate for differentiating DSMC. This also explains why the proportion of cells exhibiting a smooth muscle marker in the fibronectin adhesion experiments was found to be far higher than the proportion of cells expressing integrin α7 in the FACS experiment described in the previous chapter: DSMC preferentially adhere to fibronectin, so the proportion of DSMC in the fibronectin adhesion experiment is enriched compared to the number of smooth muscle cells in an in vivo bladder.

Fibronectin has been implicated in enhancing proliferation (Thyberg and Hultgardh-Nilsson 1994), and was therefore assessed in this model system. It was found that at 1 hour after initial plating of cells, at a point when the fibronectin substrate was shown to have a profound effect on adhesion and particularly on cells which expressed smooth muscle markers, this adhesion molecule had no effect on proliferation as assessed by BrdU incorporation. On the other hand, when cell culture was prolonged to 12 hours, it was observed that the fibronectin substrate appeared to have a synergistic effect

on proliferation in the presence of serum. Interestingly it has been shown that, using vascular smooth muscle cells, fibronectin enhanced entry into G1, but that serum was necessary for completion of the cell cycle (Roy et al 2002).

This data also demonstrated that, as assessed by immunocytochemistry, the majority of the adherent cells expressed integrin α5 and integrin β1, the components of the integrin fibronectin receptor. Other integrin sub-types were not examined, however, so other integrin-fibronectin interactions are possible. The RGD motif of fibronectin has been shown to be important in the ligation of integrins (Pytela et al 1985b), so blocking peptides to the RGD motif were next used in this cell culture model. Versus RAD negative control peptides, it was observed that the RGD peptides reduced absolute numbers of desmin positive adherent cells by about 40%, and that this was accompanied by a shift in the appearance within the whole population of adherent cells from a spread to rounded phenotype. These data link the processes of adhesion, cell shape change and the expression of a muscle differentiation marker namely desmin. This is consistent with other work that supports a fundamental role for cell shape in determining cell fate. Smooth muscle differentiation has been shown to be at least in part dependent on cell shape, and specifically cell spreading by Yang et al (1999). They demonstrated that mesenchymal cells from lung, intestine and kidney all differentiated into smooth muscle lineage cells if given sufficient space to spread, whereas cells in identical but restricted conditions were inhibited from this pattern of differentiation. That fibronectin and β1 and β3 integrins have a role in geometric control of cell shape, and that these fibronectin/integrin interactions influence cell fate, has been shown by Chen et al (1997).

Although the above data does strongly suggest that the RGD motif is functionally important in these fetal DSMC, peptide blockade did not abolish all adhesion. There are at least two possible explanations for this. First, the degree of RGD blockade may have been incomplete. Second, adhesion could be occurring by a non RGD-dependent mechanism. The RGD motif is one of several mechanisms of fibronectin integrin interaction (Pankov and Yamada 2002). Hence other fibronectin domains would need to be blocked to elicit a more complete biological effect.

It has been reported that higher doses of RGD peptides are capable of directly activating caspases (Aguzzi et al 2004). Measurement of apoptosis in adherent cells using the TUNEL test did not demonstrate any increase in apoptosis (figure 6.7A). A death assay was also performed by measuring the release of LDH from cells (figure 6.7B), a measure of necrosis as opposed to apoptosis. In the presence of no additives there was a low level of necrosis. The RAD oligopeptide demonstrated a fibronectin independent toxicity, whereas the RGD cell-death doubled as the fibronectin substrate doubled, $p<0.01$ paired t-test, $n=4$. (From figure 6.6A it can be seen that there was a larger inhibition of adhesion at 10 µg/ml of fibronectin, than at 5 µg/ml) The RGD associated death was therefore presumably related to inhibition of cell adhesion. Therefore the dose of RGD/RAD was limited in the blocking experiments to a dose of 20 µg/ml.

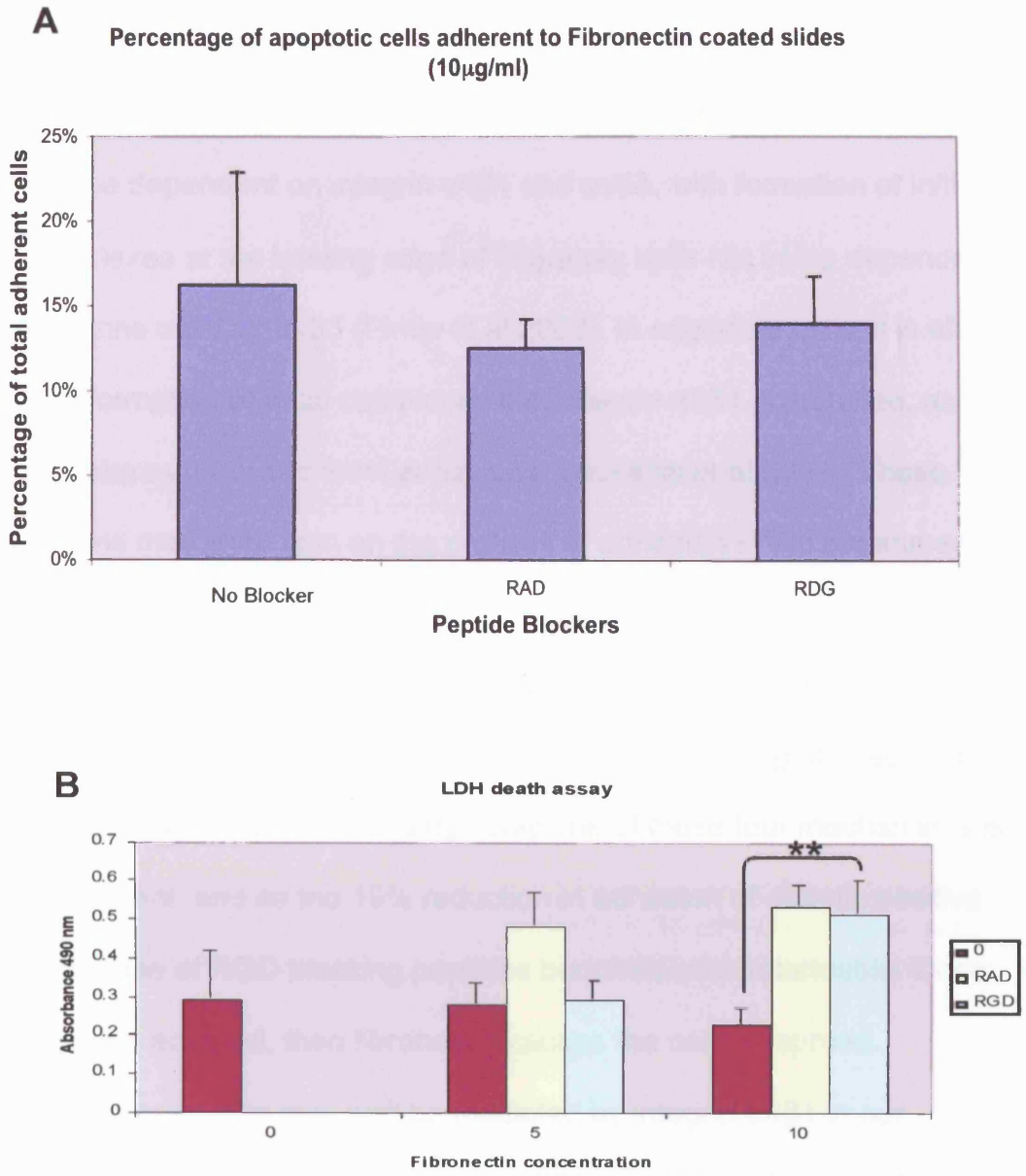

Figure 6.7:Apoptosis and death associated with RGD oligopeptides (A) Apoptosis of adherent cells. (B) Necrosis measured by 'Death assay'.**, $p<0.01$.

Different integrin fibronectin interactions may have different functions in the process of adhesion and cell spreading. Lamellipodia extension has been shown to be dependent on integrin α4β1 and αvβ3, with formation of initial focal complexes at the leading edge of migratory cells not being dependent on RGD integrins α5β1 or αvβ3 (Pinco et al 2002). In migratory cells, it is after this initial formation of focal complexes that integrin α5β1 is recruited, as the focal complexes grow into focal adhesions (Laukaitis et al 2001). These observations may shed light on the process of adhesion in the experiments reported here: a rounded, floating cell may initially adhere through RDG binding (fibronectin III10), by synergy sequence (fibronectin III9), or amino-terminal fibronectin I1-9 and fibronectin II2-3 repeats binding of integrin α5β1, or by integrin α4β1 mediated binding. Only one of these four mechanisms is RGD dependent, and so the 19% reduction in adhesion of desmin positive cells by the use of RGD blocking peptides becomes understandable. Once the cells have adhered, then fibronectin causes the cells to spread. Lamellipodia extension may well be mediated by integrin α4β1 in our experiments, with recruitment of integrin α5β1 occurring subsequently – stabilising the spread shape (figure 6.8).

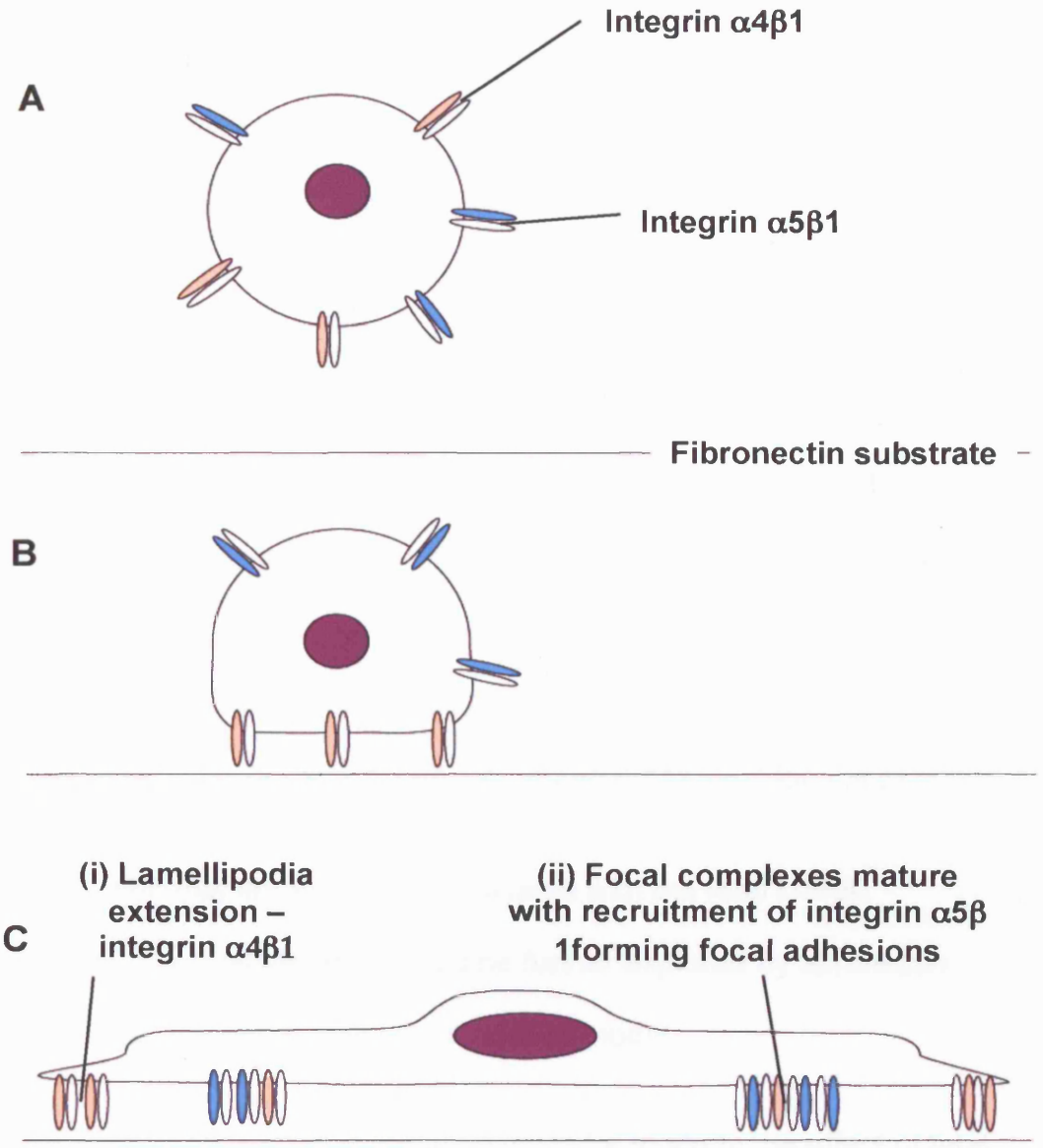

Figure 6.8: Hypothetical model of cell adhesion and spreading on fibronectin. (A) Cell in suspension. (B) initial adhesion through integrin $\alpha 4\beta 1$ 'round cell'. (C) Cell spreading takes place with (i) lamellipodia extension involving $\alpha 4\beta 1$ integrin adhesion, (ii) maturation of focal complexes with recruitment of integrin $\alpha 5\beta 1$ forming focal adhesions, to produce 'spread cell'.

It can be speculated that, in vivo, fibronectin is associated with the fetal DSMC differentiation and proliferation. Furthermore, at least some of this effect is mediated by RGD integrins such as integrin α5β1. This could have been further explored by using antibodies specific for the activated state of integrin β1: if these colocalized with integrin α5 on the surface of the adherent cells this would provide more evidence for an active signalling effect (e.g. Chemicon MAB2079Z, mouse anti-human active conformation β1 integrin), as described by (Luque et al 1996). Similarly, integrin activation could be assessed by immunostaining for activated, phosphorylated FAK, and examining for colocalization of this to focal adhesions containing integrin α5β1 (e.g. anti- FAK phospho-Y397 antibody ab4803, Abcam) (Sieg et al 2000).

The contention that fibronectin is associated with the fetal DSMC differentiation and proliferation could be further explored by fibronectin blockade in a fetal embryonic bladder organ model.

Another avenue for further exploration could be to study the effect of fetal DSMC in response to stretch because, in mice, the first vascularized and hence filtering glomeruli are evident from E15 and so the fetal bladder undergoes physiological cycles of filling and emptying from this time onwards.

There are problems with the use of whole bladder cell suspensions in the adhesion experiments: the population of cells would be mixed, and cells could have been damaged by the process of generating the cells suspension. The cell types present could include urothelium, cells of smooth muscle lineage,

endothelial cells and fibroblasts, as well as a small number of neural cells amongst others. In the adhesion experiments so far performed, the adhesive cells may be of several different types, and therefore might well be expected to express a different pattern of integrin receptors. From the IHC described above SMCs whether fetal or adult in phenotype express integrin α5β1, but fibroblasts from the lamina propria would not be expected to have this integrin, as no immunostaining could be demonstrated for the integrin α5 subunit in the lamina propria at any age. Fibronectin however was expressed in the lamina propria throughout development, so some fibronectin receptor might reasonably be expected to be present on cells from this compartment – for example integrin αvβ3. The use of RGD oligopeptides to block integrin receptors would be a useful strategy, as all integrin fibronectin receptors would be blocked by them.

These adhesion experiments have demonstrated that E18 bladder cells adhered to fibronectin. This suggests that a functional role for fibronectin is possible.

As described above, all immunoglobulins, whether anti-fibronectin, or non-immune IgG, had a large inhibitory effect on the adhesion of bladder cells to fibronectin. This non-specific effect has not previously been reported. Reasons for this occurring in this cell adhesion system include: 1) the dose of blocking antibody had not been optimised, perhaps any effect was overwhelmed by adding too much antibody and therefore swamping the specific effect with a non-specific effect; 2) the blocking antibody used simply did not have an adequate specific fibronectin blocking action. This could have

been tested by using a different model system, for example that described using osteoblast maturation (Moursi et al 1997); 3) This may be because fibronectin itself will bind IgG molecules, as described by (Rostagno et al 1996). It is not an effect reported in the literature however, so this mechanism is speculative. The fibronectin blocking experiment did not however advance our knowledge of the mechanism of adhesion involved

Conclusion

Fibronectin facilitated adherence and spreading of DSMC harvested from the developing bladder. These fetal DSMC expressed integrin α5, β1 and desmin. Blocking integrin receptors using RGD oligopeptides not only modestly but significantly decreased adherent cells which expressed desmin, but also reduced cell spreading. Fibronectin and serum had a synergistic effect on proliferation of bladder cells. Thus, integrin $\alpha 5\beta 1$ is probably one factor that mediates adhesion of fetal DSMC to fibronectin, and could potentially mediate a proliferative signal from fibronectin to these cells.

Chapter 7. Mouse fetal bladder explant culture

Hypothesis

Fibronectin-integrin interactions in ex vivo fetal bladders may be important in modulating DSMC development.

Background

Fibronectin is upregulated in the ECM of fetal murine DSMC (Smeulders et al 2003), which are proliferative (Smeulders et al 2002). A putative fibronectin receptor, integrin $\alpha5\beta1$, is also upregulated antenatally in these DSMC (chapter 5). Desmin positive cells from E18 bladders adhere to fibronectin and express integrin $\alpha5\beta1$, a process at least in part modulated by RGD integrins such as integrin $\alpha5\beta1$. Fibronectin adhesion is synergistic with serum in promoting proliferation. The environment of a fetal DFSMC in a developing fetal bladder is far more complex than this. Cells in 3-d culture behave differently to those in 2-D culture (Cukierman et al 2001). Furthermore mesenchymal-epithelial reciprocal induction is important in the differentiation of both the detrusor and urothelium (Baskin et al 1996b). Similarly there are other ECM proteins present (Chapter 5) (Smeulders et al 2003), as well as cell-cell interactions, the local growth factor and cytokine environment, and mechanical forces (stretch of the bladder), all of which contribute to the signals that control proliferation and differentiation of these cells. To examine the role of fibronectin and its receptor in normal bladder development by generating a homozygous knockout mouse mutant would be an ideal way of preserving the other factors, but both the fibronectin null mutants and integrin $\alpha5$ null mutants are lethal before bladder development as a discrete organ is

present in the mouse. By using an explant model the interaction between fibronectin and its putative receptor integrin $\alpha5\beta1$ could be investigated (Sakai et al 2003).

The first part of the strategy would be to generate the explant model, the second part would be to perform blocking experiments of ligand/and or integrin receptor.

Aims

First, generate a fetal bladder explant model which recapitulates at least some of the differentiation features seen in vivo; second, use this model to investigate the possible role of fibronectin-integrin interactions on fetal bladder DSMC development by attempting to blocking the function of the ligand using antibodies.

Results

Generating the explant model.

Preliminary experiments showed that addition of either antibiotics and FCS, or FCS alone inhibited growth and these were subsequently avoided (FCS data shown in figure 7.2A and B, comparison FCS and antibiotics, versus FCS only vs ITS only is in appendix 3: figure 3.1 and table 3.1). In serum-free and antibiotic-free culture E14 explants, which were initially composed simply of mesenchyme and epithelium, differentiated into three distinct morphological layers, with DSM, lamina propria and urothelium; moreover, DSM maturation was indicated by upregulation of αSMA (Figure 7.1 C and D). It was also observed that the bladders physiologically and functionally matured so that

they began to undergo spontaneous contractions in this milieu. Growth was prominent, as assessed by total cell numbers and total protein, in the first three days, while differentiation continued throughout the six days of culture. Dissociation of bladders was performed as described in Chapter 4 (n=4 at each time-point). Cell counts more than doubled by day 6 (ANOVA $p<0.05$), with evidence of continuing cell division in-vitro as assessed by proliferating cell nuclear antigen. Using the BCA protein assay (described above), protein was measured for each bladder (N=4 at each time-point), and again showed a significant increase ($P<0.01$ using ANOVA).

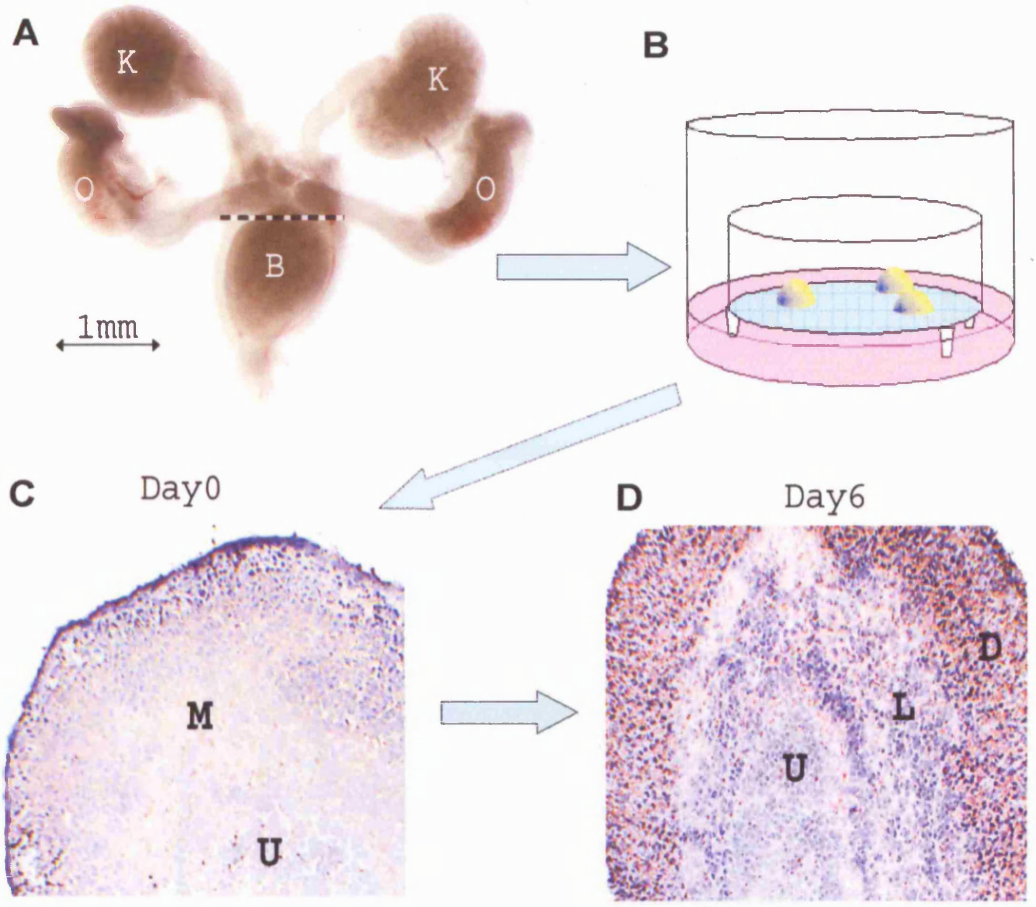

Figure 7.1: Generating explant model of fetal bladder development. (A) Genito-urinary tract dissected from E14 mouse (K=kidney; B=bladder; U=ureter; O=ovary; Dots=line of dissection of bladder). (B) Bladders are grown on Millipore filters - capillary action draws medium through filter and forms a meniscus over the bladder explant. (C) α-SMA immunolocalised at low levels in undifferentiated mesenchyme (M) at day 0 of culture; U=urothelium (D) Day 6 explant with upregulated αSMA expression in DSM; note that the three main layers of bladder have differentiated (D=detrusor, L=Lamina Propria, U=Urothelium)

A

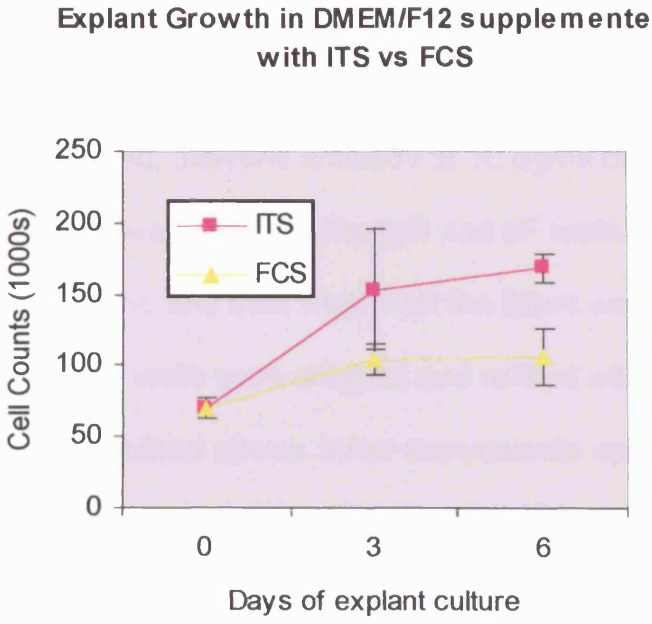

B

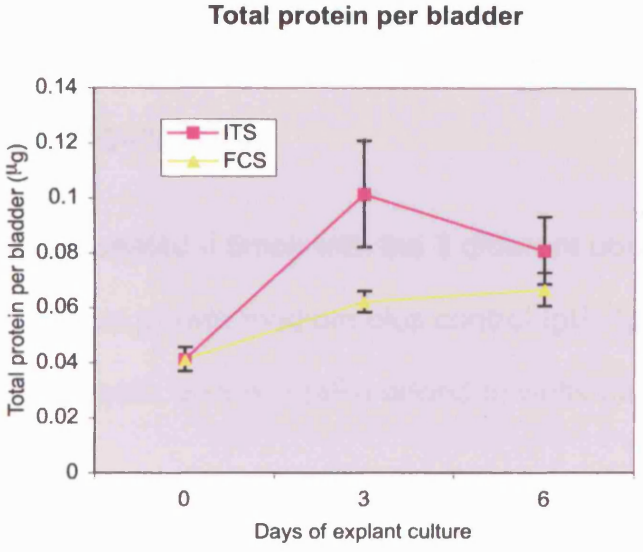

Figure 7.2: Inhibitory effect of fetal calf serum on explant growth (A) Dissociation of bladders (n=explant experiment) showed a significant increase of cell numbers in culture for explants grown in ITS (P=0.008 using ANOVA). (B) Using BCA assay, total protein content was measured for each bladder (n=6-8 for each time-point), and again showed an increase (P=0.008 using ANOVA) for explants grown in ITS.

Explant growth in presence of fibronectin blocking antibody.

For this experiment filtered, dialysed antibody at 10 µg/ml of control IgG, or anti-fibronectin antibody was added to the IgG and aF wells respectively, at the start of the experiment, and then when half the filters were harvested at 3 days, then the remaining wells were emptied and refilled with new growth medium with ITS as described above. Initial experiments using the rabbit anti-mouse polyclonal antibody AB2033 (Chemicon), and the control rabbit IgG (purified rabbit IgG PP64 Chemicon) both caused the explants to shrink. All antibodies were therefore filtered using a 0.2 µm filter and dialysed against the normal growth medium using a 10,000 RMW dialysis membrane overnight. (A western blot confirmed that the immunoglobulin was not lost by filtration and dialysis – figure 7.3A).

This experiment was repeated 4 times with the 3 different conditions (growth medium only (ITS) versus growth medium plus control IgG (IgG) and growth medium plus anti-fibronectin antibody (aF)) added to wells on the same plate (figure 7.3 B).

There was a large amount of biological variation between bladders, the majority of which was variation within a litter as opposed to variation between litters (figure 7.4A,B). There was no sex difference between male and female bladders (figure 7.4 C)

A

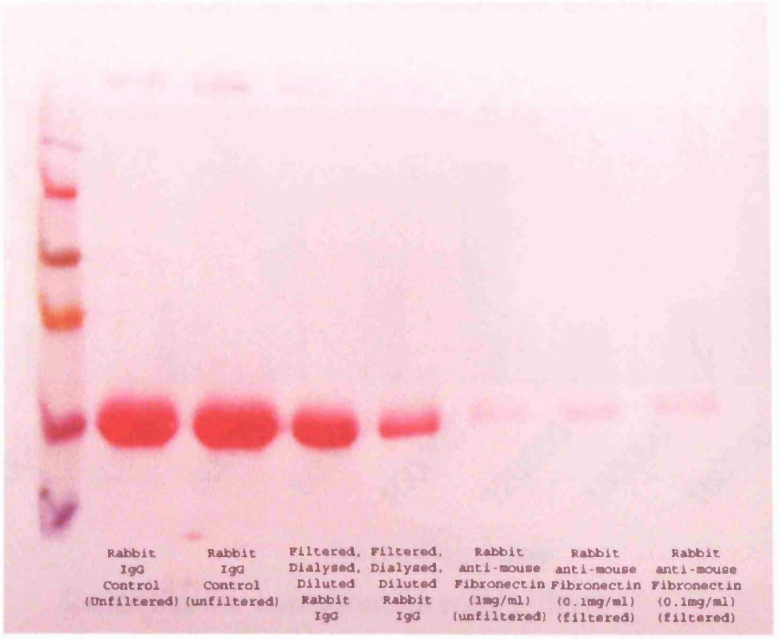

B

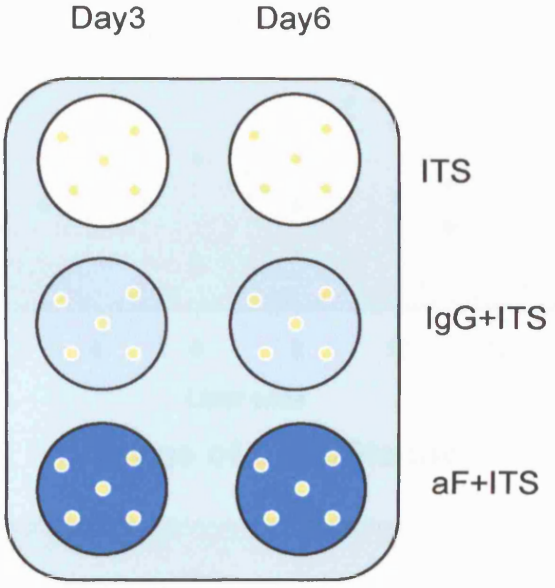

Figure 7.3: Filtration and dialysis of IgG, Explant experimental layout (A): Immunoglobulin (control) and anti-fibronectin, was filtered through 0.2μm membrane, then dialysed against DMEM/F-12 with ITS. The first 2 tracks are antibody prior to filtration. The third and fourth tracks are after filtering and dialysing the control antibody. The fifth track is the blocking antibody (Chemicon AB2033) diluted (to make a large enough volume to filter and dialyse), the sixth and seventh tracks show that the antibody is still present after filtration. (B): Layout of 6 well plates for explant blocking experiments (yellow dots are bladders).

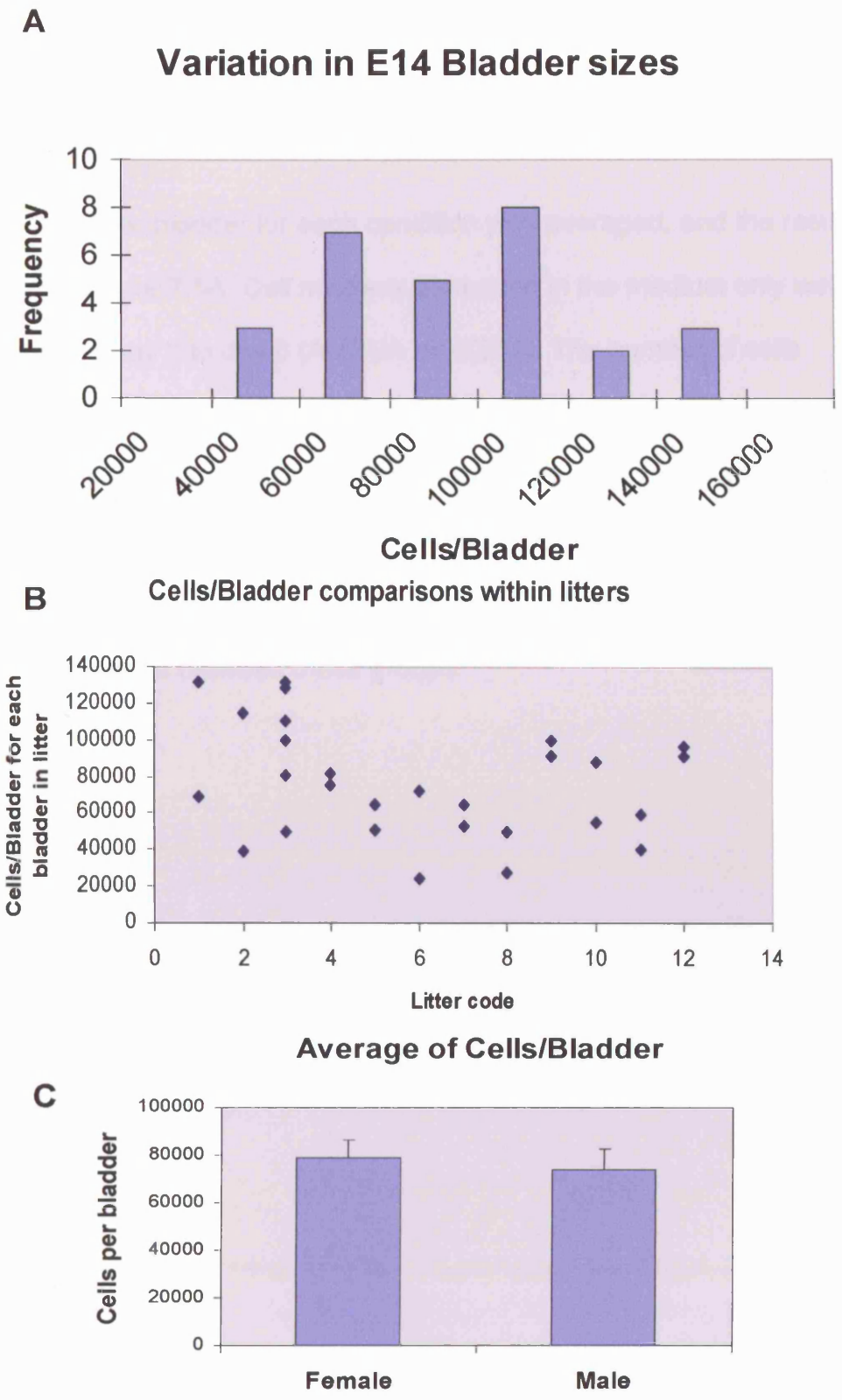

Figure 7.4: Bladder variation at the start of the explant experiments. (A) Histogram of bladder cell numbers, from bladders harvested at embryonic day14. (B) Within litter and between litter variation is illustrated. Each vertical column represents 1 litter. (c) Male:female variation in bladder size.

Explant growth

The cell count per bladder for each condition was averaged, and the results are shown in figure 7.5A. Cell numbers increased in the medium only wells (ITS) from 0 to day 3 to day 6 (ANOVA $p= 0.017$). The number of cells increased more in the control IgG and anti-fibronectin media, relative to the start of the experiment, ANOVA $p<0.05$ respectively. Bladder explants in the anti-fibronectin media grew more than those in the control media, which in turn grew more than those in the control media (ITS)-figure 7.5. There was no statistical difference between these groups.

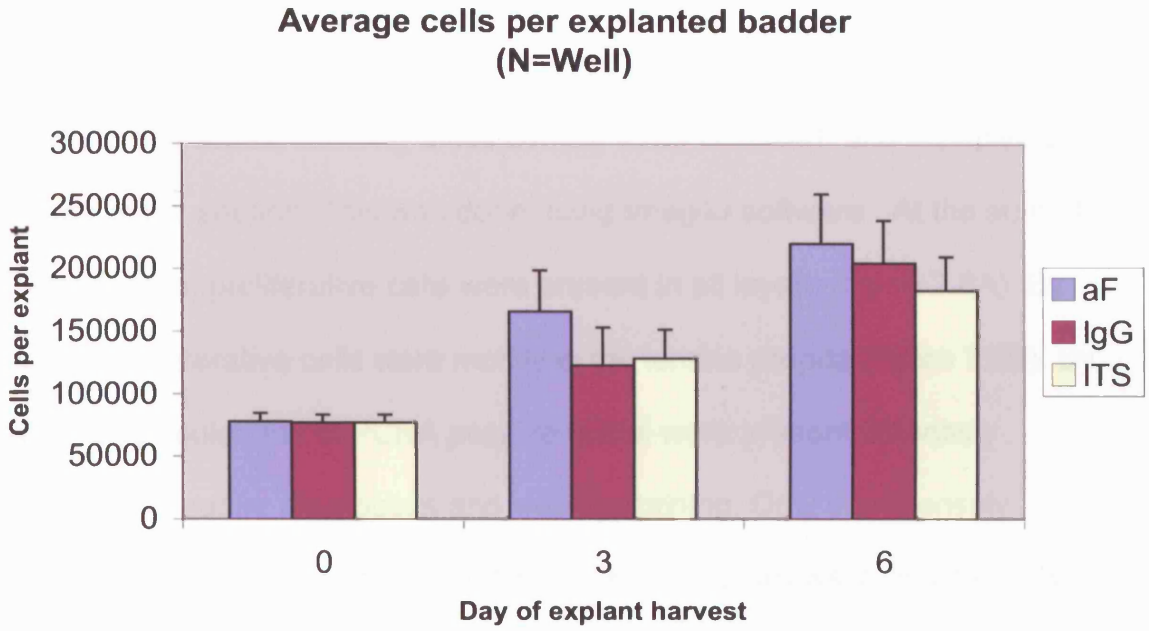

Figure 7.5: Outcome of explant growth in presence of anti-fibronectin antibody vs. isotype control IgG vs. ITS. Absolute cell numbers (mean+SEM).

Explant proliferation

Proliferation was assessed by expression of proliferative cell nuclear antigen (PCNA) using biotinylated mouse anti-human IgG (555567, Pharmingen), as described in chapter 4. This produced a clean signal on IHC (figure 7.6), allowing quantification of proliferation by counting PCNA positive cells, and estimating the total number of cells in each bladder from an average of 4 representative areas, allowing a cell density to be obtained, and multiplying by the area of the section. This was done using ImageJ software. At the start of explant culture, proliferative cells were present in all layers (figure 7.6A). By day 3 the proliferative cells were mostly in the lamina propria (figure 7.6B). By day 6, two populations of PCNA positive nuclei were present: intensely staining as at earlier time-points and weakly staining. Only the intensely staining nuclei have been counted (figure 7.6C). The arrows in figures 7.6B and C also highlight that the proliferative cells were concentrated in a single region of the lamina propria, in a 'proliferative centre', which was not evident on IHC of in-vivo bladders over E14, E16 and E18 time-points. The patterns for the IgG and fibronectin blocking antibodies were similar to this.

Western blots for PCNA expression were not sensitive enough for quantification of the tiny amounts of protein extracted from these explanted organs. Quantification was therefore performed by counting PCNA positive cells. Only intensely stained cells were included – as described above. Over 6

days of organ culture PCNA expression, and by implication proliferation, decreased 70% in control explants (ANOVA $p=0.05$), whereas it decreased by 86% (ANOVA $p<0.05$) for control IgG treated organs and 87% (ANOVA $p<0.05$) for those exposed to fibronectin blocking antibodies. Both immunoglobulins had a strikingly similar effect, but were not significantly different from the ITS medium alone.

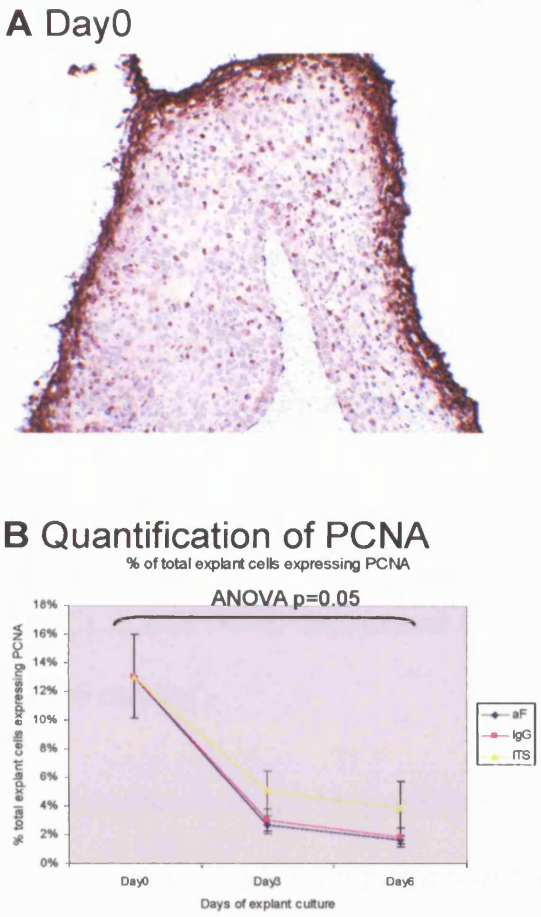

Figure 7.6: PCNA expression in explants. At the start of explant culture the PCNA positive cells (dark brown) are present throughout the bladder (A)– the results for medium alone (ITS), control IgG (IgG) and blocking antibody (aF) are shown for day0 (start of explant experiment), day3 and day6 (D).

Differentiation

Detrusor muscle differentiation was assessed by expression of desmin on IHC (figure 7.7). There was virtually no expression of desmin at E14 at the start of explant culture. By day 3, desmin had been unregulated and could be seen at the periphery of the organ, but was also expressed by some cells throughout what would become the lamina propria. By day 6, there was prominent desmin staining throughout the detrusor, but also staining of cells subjacent to the urothelium (figure 7.7C). It was never expressed in the urothelium (as befits a smooth muscle cell marker).

Western blotting was not sensitive enough to quantify desmin expression, so quantification was made by measuring the proportion of the surface area of each section from an explant staining positively for this antigen. This was performed using ImageJ 1.30 software. The explant experiment had been repeated 3 times, so n=3 for these comparisons. In explants grown in medium without immunoglobulins (ITS), desmin was progressively upregulated, with a 10–fold increase by day 6 (ANOVA p=0.008). IgG and aF treated explants showed a similar initial upregulation of desmin to day 3, but this then tailed off. There was a significant difference between ITS and aF explants by day6 (t–test p=0.02), but no such significance for IgG due to the wider error bars. The over–all effect of both the control IgG and the blocking antibody on desmin expression was the same.

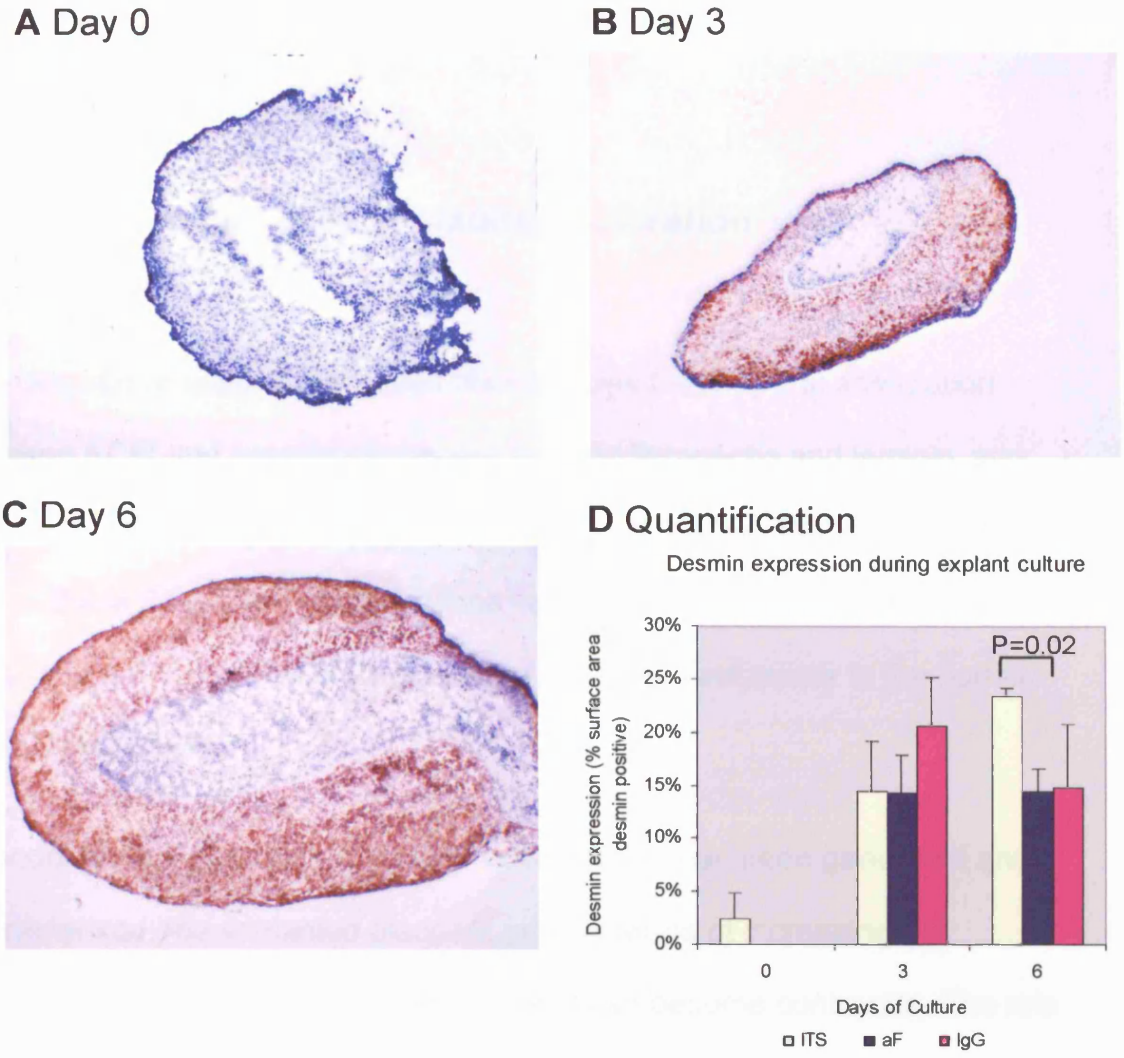

Figure 7.7: Desmin expression during explant culture: at the start of explant culture (E14) there was very little desmin expression (A). By 3 days there was definite expression at the periphery of the detrusor, but also some expression throughout what would become the lamina propria (B). After 6 days in culture desmin was well expressed by the outer detrusor layer of the bladder explant, but also by cells subjacent to the urothelium (C). Quantification was performed by measuring the proportion of the explant surface area on IHC, positive for desmin (D).

Discussion

An ex-vivo model of fetal bladder maturation

The descriptive work as described above showed a temporal association between ECM and integrin expression both for fibronectin and laminin, and their respective receptors integrins α5β1 and α7β1. However the functional role of these ECM/integrin interactions has not been demonstrated in the context of normal spatial arrangement of cell types and matrix in the normal fetal murine bladder.

A model for early embryonic bladder development has been generated and characterised: the explanted bladders grow in terms of increasing cell numbers and total protein, differentiate, and can become contractile. The role of mesenchymal /epithelial interactions in reciprocal induction of urothelial and mesenchymal maturation have been demonstrated in chimeric rat embryonic bladder explant constructs (Liu et al 2000), but smooth muscle contraction, as was noted in my experiments, has not been previously described. Similarly this experimental strategy has been employed to investigate the role of integrins and extracellular matrix in instructing development in ex-vivo culture of kidneys (Zent et al 2001).

The optimal conditions to maximise embryonic bladder explant growth included the use of DMEM/F-12. This is similar to the optimal growth conditions described by Gupta et al (2003) for metanephric explant culture.

However, the best metanephric growth was achieved in the presence of 5% fetal calf serum (FCS), whereas in this study bladder explants grew best when supplemented by insulin, transferrin and selenium (ITS). The use of antibiotics (gentamicin, penicillin and streptomycin) has also been demonstrated to inhibit growth of metanephroi in culture (Gilbert et al 1994). This is similar to the inhibitory effect found with the use of antibiotics (penicillin and streptomycin) and anti-fungals (amphotericin) on ex-vivo embryonic bladder growth. However the organs grew better in serum free, antibiotic free culture (appendix 3: table 3.1 and figure 3.1). This model has now been used to study the effect of VEGF on fetal bladder development (Burgu et al 2006). In this model explant growth was significantly increased by the addition of VEGF, as assessed by the following parameters: detrusor smooth muscle area; percentage increase in surface area; total cells per explant; total number of α-SMA expressing cells per explant; total number of CD31 positive cells per explant; protein per explant; DNA per explant; lamina propria and detrusor smooth muscle proliferative index; urothelial proliferative index. Lamina propria and detrusor apoptotic index, and urothelial apoptotic index were however significantly reduced (Burgu et al 2006). Growth was therefore a combination of increased proliferation and increased survival (decreased apoptosis).

Embryonic bladder explants more than doubled their cell number, but this growth did not match that of in-vivo bladders – figure 7.8. The organs did however undergo maturation, becoming trilaminar structures with expression of desmin and α-SMA in the detrusor layer. That this reflected smooth muscle differentiation was best illustrated by the onset of spontaneous contractions

from 4 days of culture onwards in some explants. By assessing proportion of the cross-sectional area that became converted to smooth muscle, and using αSMA and desmin expression as markers for this, an assessment of differentiation was possible. The morphology of the explants most closely matched neonatal bladders – figure 7.9.

Percentage of PCNA positivity was used as a measure of proliferation. This is a standard technique, however PCNA is present in cells as they go into S1 phase, and remains present after mitosis has occurred. PCNA is therefore present in cells about to undergo proliferation, proliferating cells and in cells that have recently replicated (Mathews et al 1984; Morris and Mathews 1989). PCNA can be detectable in some model systems up to 3 days after proliferation has stopped (Wijsman et al 1992). Use of PCNA immunostaining therefore leads to an overestimate of the population of cells actually undergoing proliferation at any one moment (Wijsman et al 1992). Measuring uptake of BrdU would have been a more sensitive technique to use.

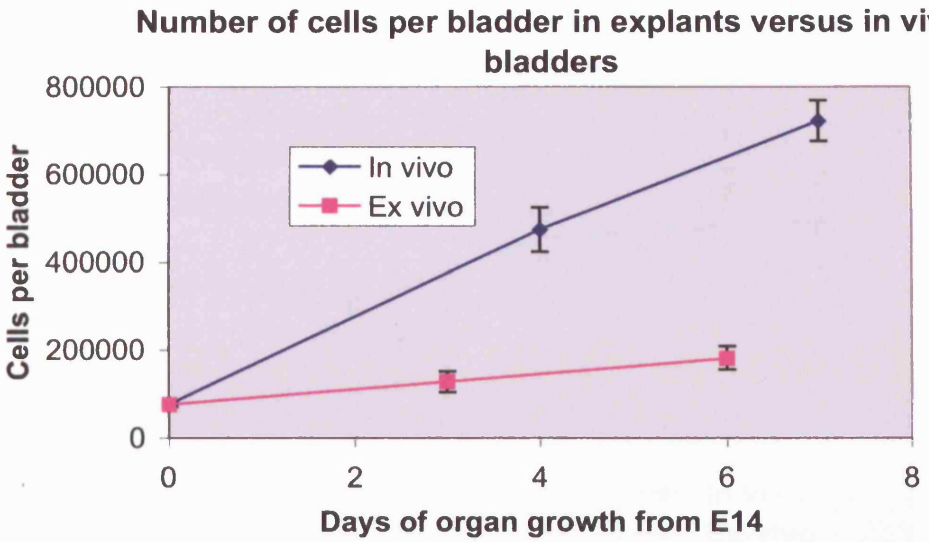

Figure 7.8: Explant growth in cell numbers versus in vivo bladders
Increase in cell numbers in explants (pink) as compared to in-vivo bladders (blue). The in-vivo data are from 3 parallel suspensions, prepared from whole litters at E14 (day0), E18 (day 4) and neonatal mouse pups (day7). This illustrates that although ex vivo bladders did grow in culture, the growth was not at a normal rate.

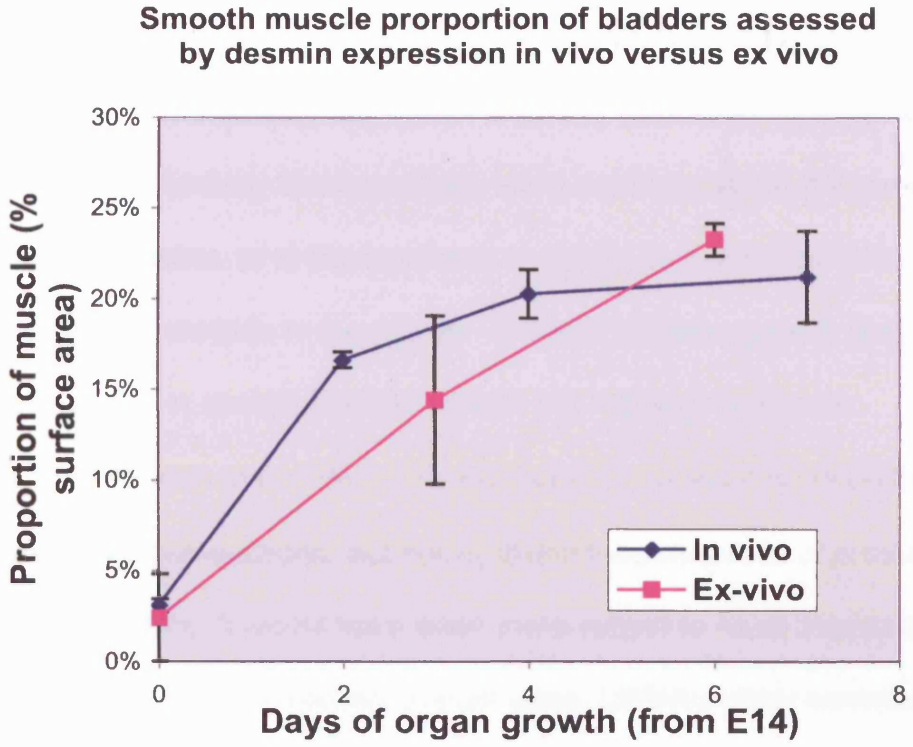

Figure 7.9: Smooth muscle maturation of explants versus in vivo bladders. The proportion of bladder surface area that has differentiated into smooth muscle has been assessed by examining the proportion of the surface area of histological sections that expressed desmin. N=3 for each time-point (separate bladders stained at the same time). This allowed comparison to be made against the proportion of smooth muscle differentiation that has occurred in the ex vivo bladders.

Growing embryonic bladders ex-vivo is obviously not a normal process. The bladders had no blood supply, needing to receive all their nutrients by diffusion from the fluid surrounding them, and exchange gases across their surface area, rather than at a capillary level. The diffusion distance would therefore have been markedly increased. That this should limit growth should not be a surprise. Similarly these explants were not exposed to the growth factors present in urine, or to the mechanical stretch by urine that occurs from embryonic day 16 onwards in the mouse. The role of these growth factors and mechanical stretch in normal bladder growth are however unknown. Quantitation of desmin and αSMA was assessed by measuring proportions of surface area on cross-sections, but not by direct measurement of protein levels by western blot. It would have been more robust to have measured PCNA and smooth muscle markers in both ways. Unfortunately samples were not pooled and the tiny amounts of protein extracted from individual bladders were too small to perform WB with.

Despite these limitations ex vivo embryonic bladder culture provides a model which recapitulates key steps in detrusor smooth muscle differentiation providing a tool for interventional studies to examine development ex-vivo, even though it is not per se a good model for normal growth. This model has been used to explore the effect of exogenous VEGF on explant bladder growth (Burgu et al 2006). The addition of VEGF to the explanted bladders in this study might have improved their growth, perhaps making a perturbing effect (such as the use of the anti-fibronectin antibody) more marked.

Unfortunately the first strategy employed to block fibronectin function using a polyclonal antibody to fibronectin, as has been successfully described by Moursi et al (1997) and Sakai et al (2003) - the latter in mouse salivary gland explants - did not prove successful. In this explant experiment the control IgG appeared to have the same effect as the blocking antibody. In the adhesion blocking experiment (discussed below), all three IgG's, whether control or function blocking, had a large effect – reducing cell adhesion by 50% when added to explant growth media at 10 µg/ml (final concentration).

Is there a mechanism that can explain these somewhat surprising results? There are several possible explanations: 1) the blocking antibody was not effective, and non-specific effects of IgG swamped any specific anti-fibronectin action; 2) the outcome measures were crude, and it may have been with more accurate techniques, such as the use of FACS as described by Burgu et al (2006), that a difference between the control and blocked group could have been found; 3) perhaps if growth of the explants had been optimised by the addition of VEGF Burgu et al (2006), then the blocking effect of the anti-fibronectin antibody might have been detectable. 4) a speculative possibility is that IgG generically interacts with fibronectin (Rostagno et al 1989; Rostagno et al 1996; Rostagno et al 2002), and has a blocking function. This effect has not been described in previous cell culture (Moursi et al 1996; Moursi et al 1997), or organ culture work (Sakai et al 2003).

Conclusion

In order to further explore possible roles for fibronectin in the whole developing bladder, rather than isolated cells, an explant embryonic organ culture model was established in mice which recapitulated at least some of the differentiation features seen in vivo. This model was used to investigate the possible effects of presumed 'fibronectin-blocking' antibodies on parameters of growth and differentiation: however, no specific effects could be demonstrated. Time did not allow the testing of possible effects of RGD oligopeptides.

Chapter 8. Fibronectin expression in normal and pathological development of human fetal bladders

Hypotheses

Fibronectin is expressed during normal human fetal DSMC development, furthermore altered fibronectin expression may be implicated in human BOO detrusor smooth muscle pathology.

Background

Fibronectin is upregulated in the ECM of fetal murine DSMC (Smeulders et al 2003), which are proliferative (Smeulders et al 2002). A putative fibronectin receptor, integrin $\alpha5\beta1$, is also upregulated antenatally in these DSMC (chapter 5). Desmin positive cells from E18 bladders adhere to fibronectin and express integrin $\alpha5\beta1$, a process at least in part modulated by RGD integrins such as integrin $\alpha5\beta1$. Fibronectin adhesion is synergistic with serum in promoting proliferation (Chapter 6).

This leads to questions about the expression of fibronectin in human bladders; 1) is fibronectin expressed in the basal lamina of fetal human bladders? 2) What the pattern of expression of fibronectin and the morphology of these bladders in obstruction? 3) How does normal development and development of the urinary tract (kidneys and bladder) in obstruction differ? In order to be able to compare the normal and obstructed kidneys and bladders a measure of renal dysplasia (renal dysplasia score) needs to be generated, as does a scoring scheme for muscle abnormality in the bladder (muscle dysmorphology

score). The strategy would therefore be to obtain ethical committee approval to identify normal and abnormal human fetuses (diagnosed as having presumed congenital bladder outflow obstruction on post mortem) from the human embryo bank held at UCH by Dr R Scott. Using the information from the post mortem certificates, from IHC examination of the urinary tracts (bladders and kidneys) to answer these questions.

Aims

1) Demonstrate the normal pattern of fibronectin expression in human fetal bladders, and to correlate this with gestational age, and measures of cell turnover such as proliferation (by Ki67 expression) and apoptosis (using TUNEL test). 2) Describe the fibronectin expression in fetal bladders with presumed BOO and to compare this with normal development.

Results

Normal development:

Muscle

At 16 weeks the human fetal bladder had three recognisable morphological layers on histology section: first, urothelium; second, lamina propria; and third, detrusor; surrounded by a serosa composed of loose areolar tissue. The detrusor layer (stained red by Masson's trichrome in figure 8.1A) had well defined recognised muscle bundles, but those on the medial and lateral side

of this layer are smaller. As gestation proceeds the overall thickness of the detrusor layer increases, with the muscle bundles become much larger and more homogenous in size throughout the detrusor layer (figure 8.1B-F).

Serial sections immunostained with mouse anti-human desmin antibody revealed a similar pattern of muscle distribution to that shown by the Masson's trichrome stain (Figure 8.2).

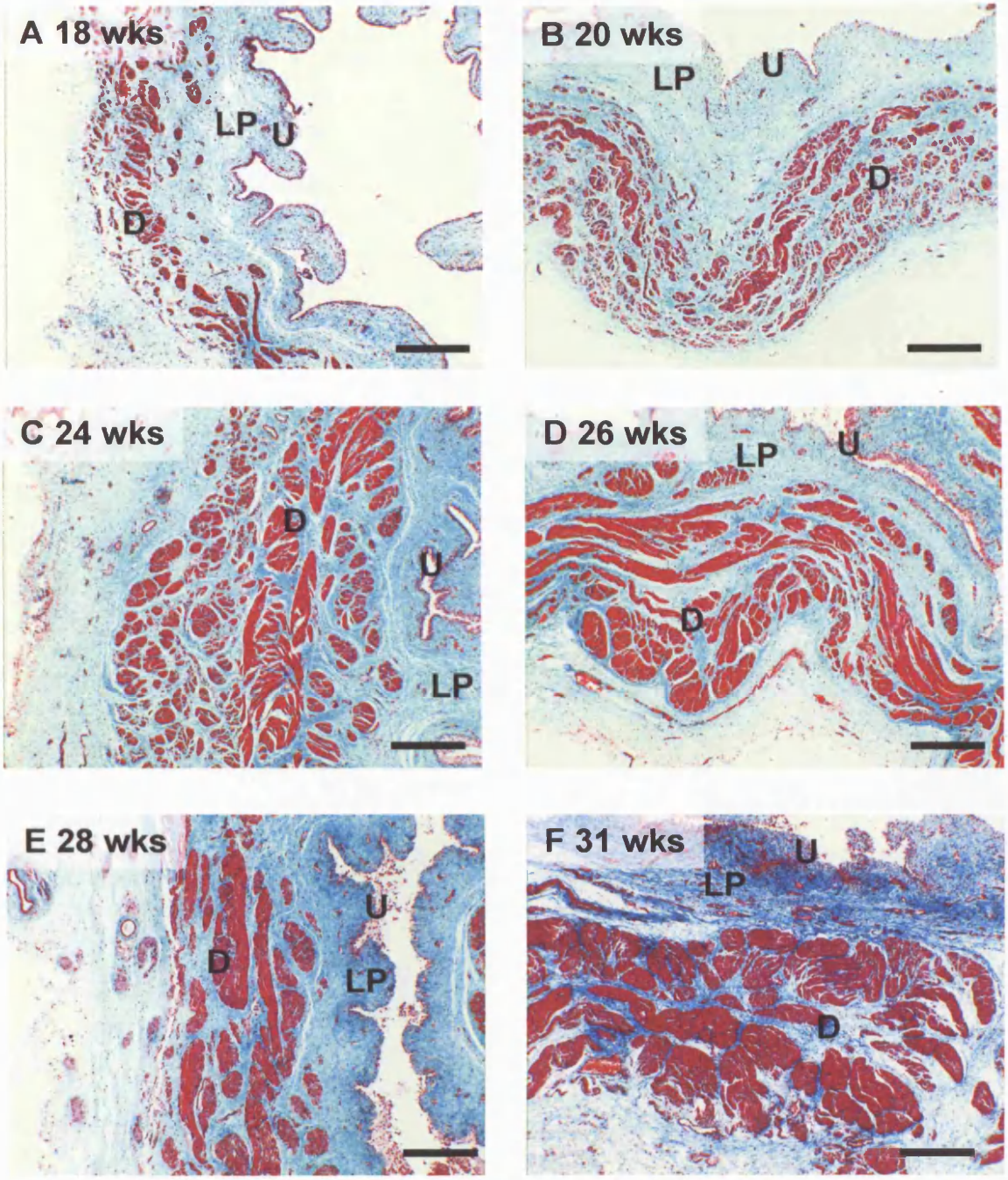

Figure 8.1: Masson's trichrome staining of normal human fetal bladders from 14 weeks of gestational age to 31 weeks. (A) 18 wks, (B) 20 wks, (C) 24 wks, (D) 26 wks, (E) 28 wks, (F) 31 wks. Scale bar 400μm.

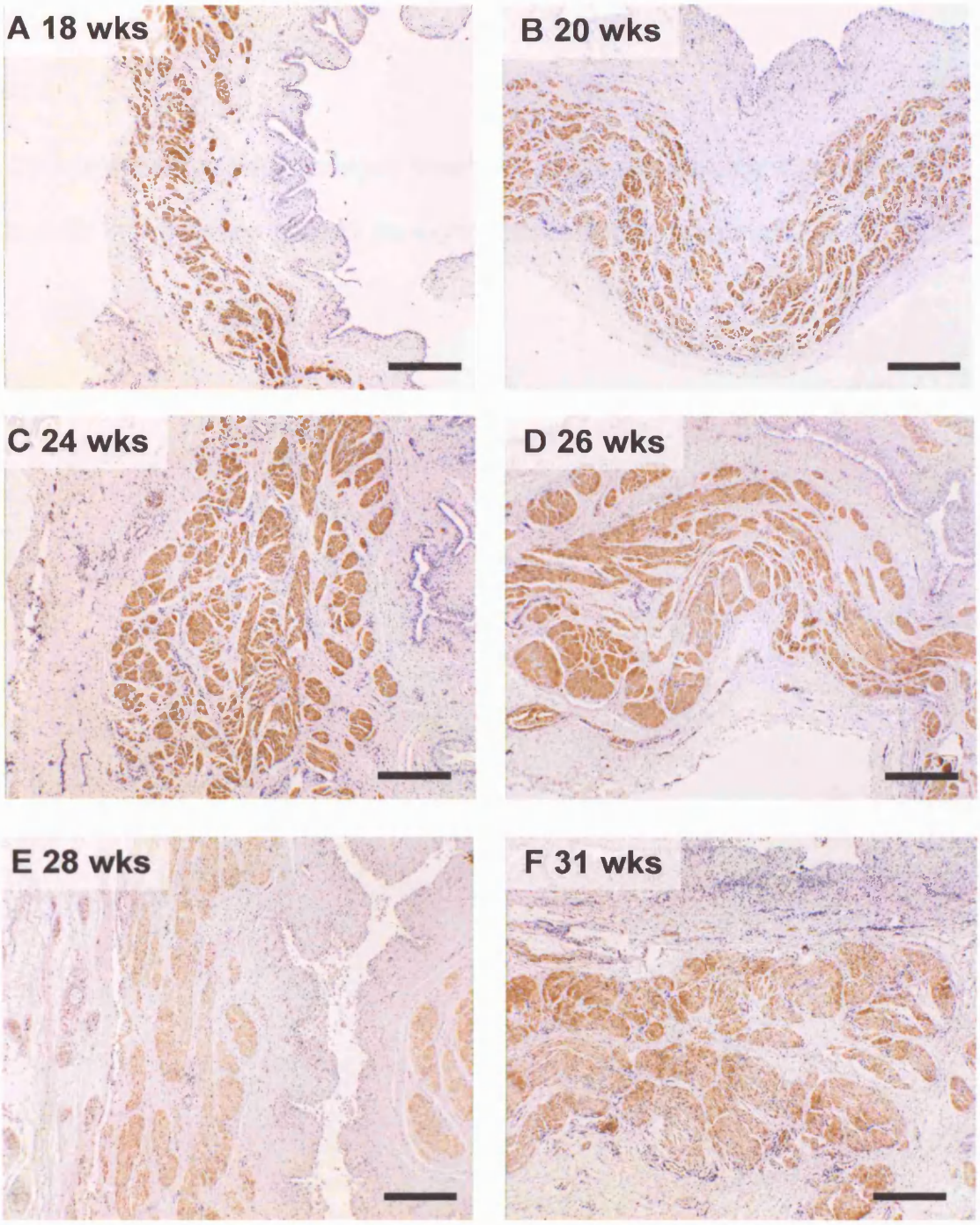

Figure 8.2: Desmin immunostaining of normal human fetal bladders from 14 weeks of gestational age to 31 weeks, counter-stained with haematoxylin. (A) 18 wks, (B) 20 wks, (C) 24 wks, (D) 26 wks, (E) 28 wks, (F) 31 wks. Scale bars 40 μm.

Collagen

Van Gieson staining stains collagen fibres red. Collagen staining was present persistently in the lamina propria throughout development (figure 8.3).

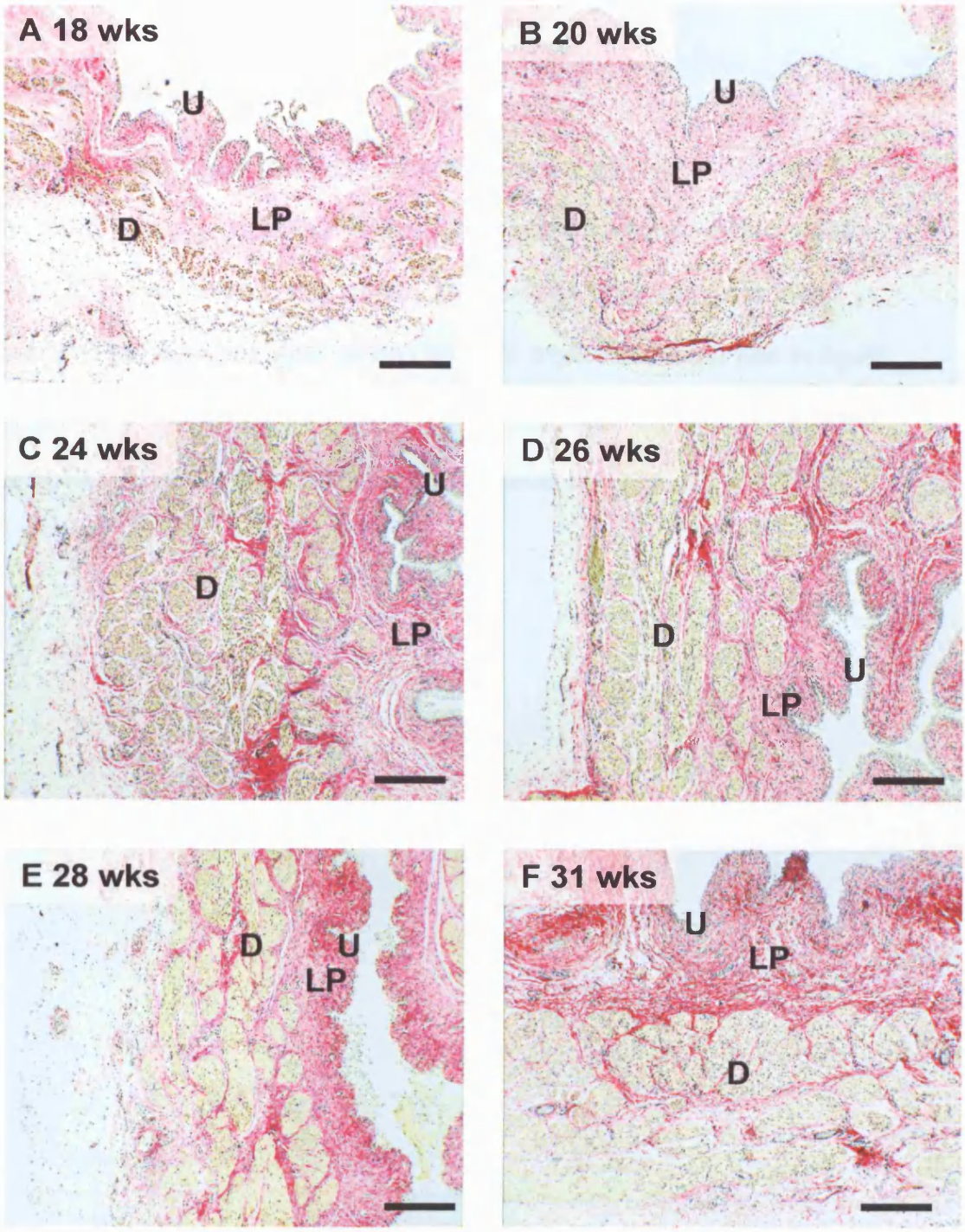

Figure 8.3: Van Gieson staining of normal human fetal bladders from 14 weeks of gestational age to 31 weeks. (A) 18 wks, (B) 20 wks, (C) 24 wks, (D) 26 wks, (E) 28 wks, (F) 31 wks. Scale bar 40 μm.

Wall thickness

For normal bladders the total wall thickness increased over gestation from 16 weeks to 32 weeks (figure 8.4A). This was a statistically significant, r=0.89 p=0.001, 2–tailed Pearson correlation. Most of this apparent growth was in thickness of the detrusor layer as can be seen from the scatter plot in figure 8.4B. Growth in detrusor thickness correlated significantly with gestational age, r=0.74 p< 0.01 2–tailed Pearson correlation.

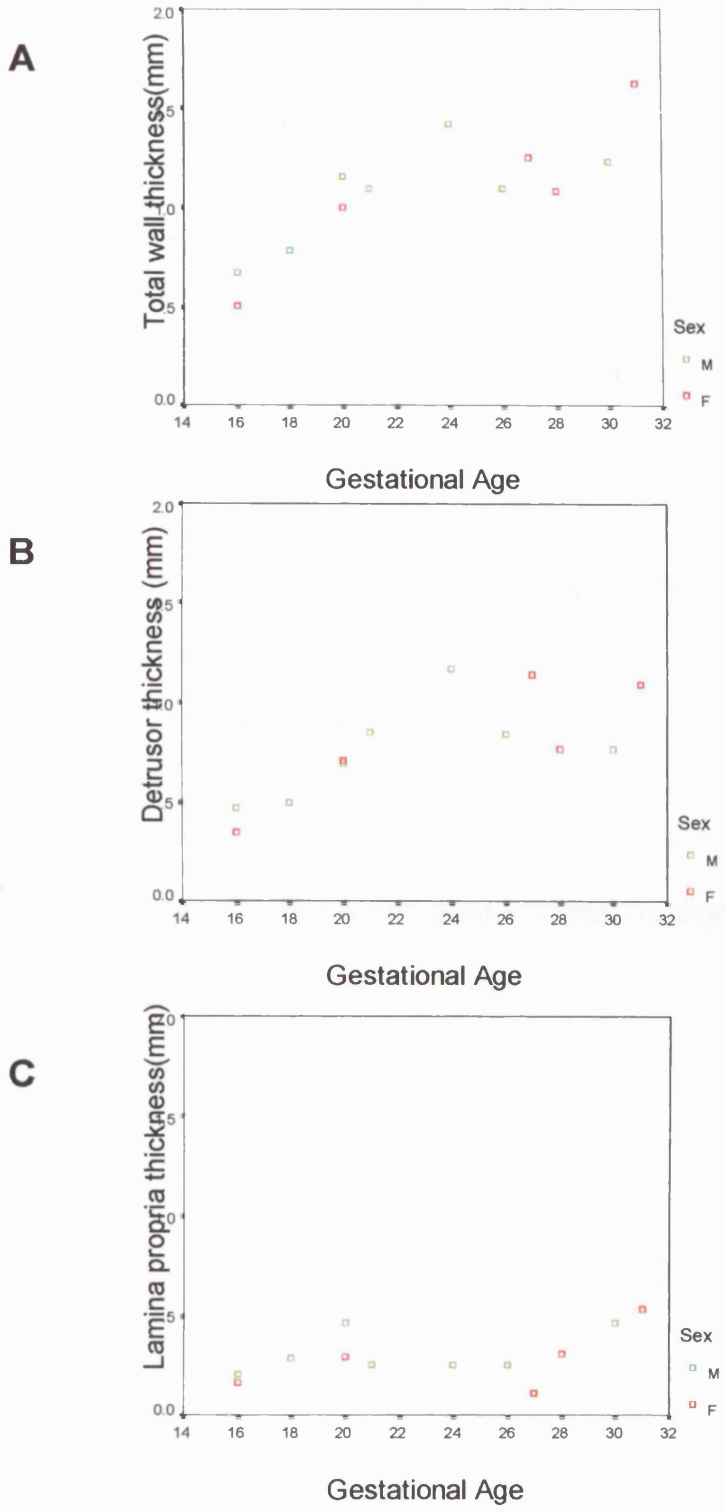

Figure 8.4: Morphometry of normal human fetal bladders. Wall thickness (mm) as measured on sections of normal fetal bladders using ImageJ. (A) total wall thickness in normal bladders compared with gestational age. (B) detrusor thickness versus gestational age (C) lamina propria thickness compared to gestational age. Males are green boxes, females are red boxes.

Fibronectin

Fibronectin, as assessed by IHC, was expressed predominantly in association with the fetal smooth muscle cells of the detrusor (figure 8.5). As gestation progressed, the thickness of the detrusor muscle increased, as did the area of associated fibronectin expression - assessed qualitatively by examination of the slides (figure 8.5). Colocalization of desmin and fibronectin examined using confocal microscopy revealed the close relationship between fetal smooth muscle cells and fibronectin in the fetal detrusor (figure 8.6).

Quantification of detrusor fibronectin percentage of surface area (%) positively correlated with gestational age, $r=0.62$ $p<0.05$ Pearson 2–tailed test. Quantification of the lamina propria fibronectin area showed no significant change related to gestational age.

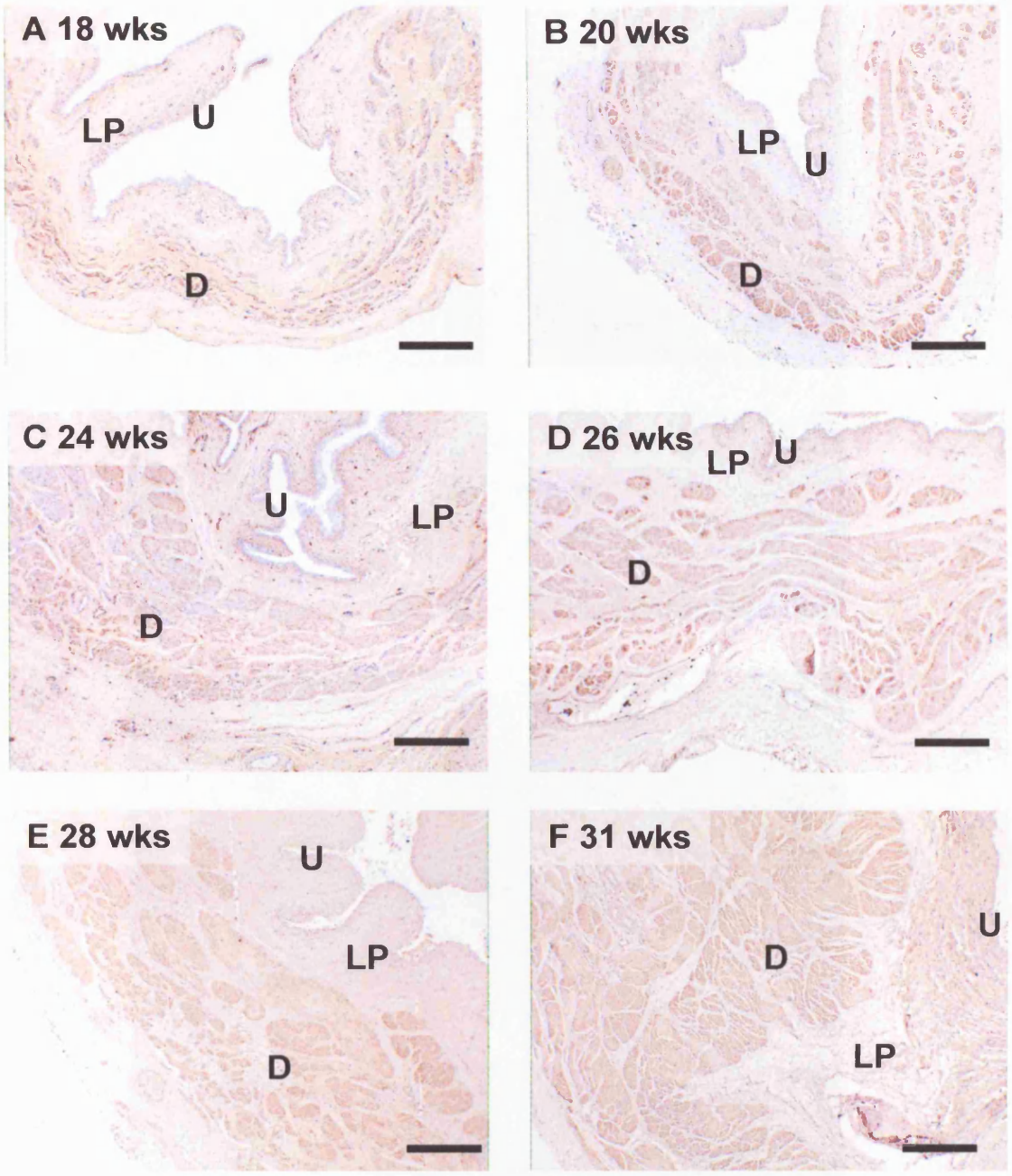

Figure 8.5: Fibronectin immunostaining of normal human fetal bladders from 14 weeks of gestational age to 31 weeks. Counter–stained with haematoxylin. (A) 18 wks, (B) 20 wks, (C) 24 wks, (D) 26 wks, (E) 28 wks, (F) 31 wks. Scale bar 40μm. Positive and negative controls for anti-human fibronectin antibody (A0245, DAKO) are shown in Appendix 4: figure 4.1.

A

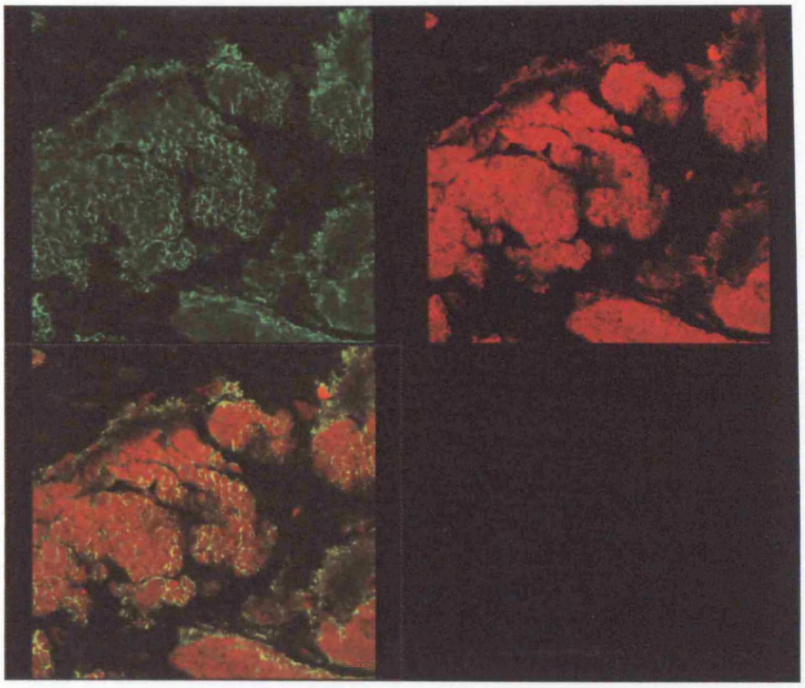

B

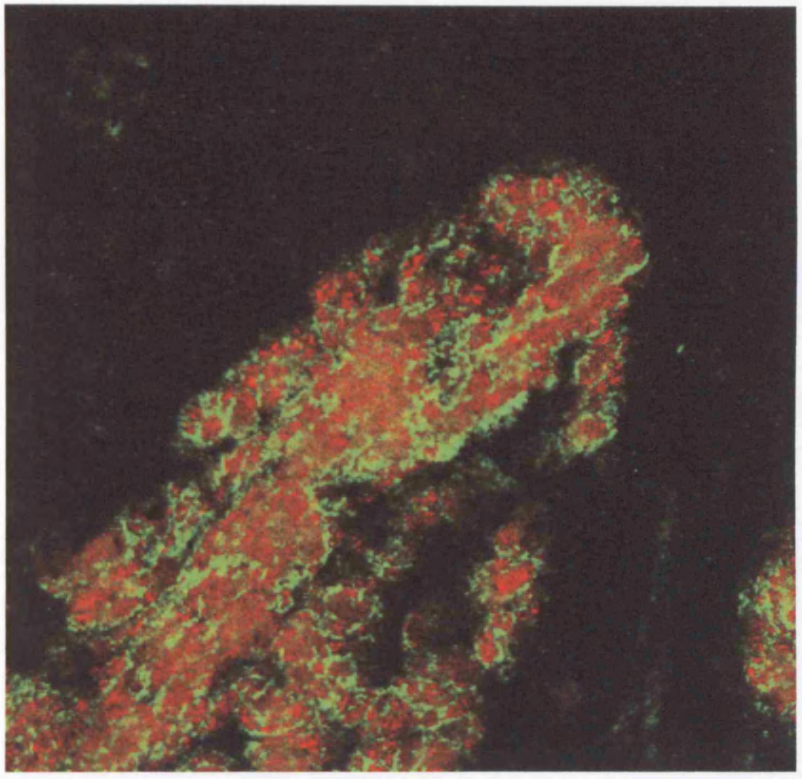

Figure 8.6: Desmin and fibronectin double immunostaining in normal bladders (18 weeks gestational age) . Green (FITC) fibronectin, red (TRITC) desmin. (A) x20 FITC, immunofluorescence staining of Fibronectin (green). TRITC, immunfluorescent staining desmin (red) and combined image, (B) x99 High power view of detrusor with FITC and TRITC signals superimposed.

Cell turnover in normal bladder development

There was no significant correlation between gestational age and proliferation as measured by percentage of Ki67 positive nuclei in the urothelium, lamina propria and detrusor, data tabulated in Appendix 4: table 4.2. Similarly no correlation between apoptosis, as measured by TUNEL positive cells as a percentage of total cells in each layer, and gestational age was apparent, data tabulated in Appendix 4: table 4.2. The results for each layer of the bladder for all gestational ages were averaged (figure 8.7). Although the lamina propria appeared to be a more active compartment both in terms of proliferation, as assessed by Ki67, and apoptosis, this was not statistically significant. However the most actively proliferating bladders were most proliferative in all 3 compartments: urothelial proliferation correlated with lamina propria proliferation and detrusor proliferation ($r=0.81$ $p=0.005$, and $r=0.71$ $p<0.05$) and between lamina propria and detrusor proliferation ($r=0.87$ $p<0.001$). Detrusor fibronectin density did both correlate significantly, but inversely with downregulation of proliferation in the detrusor layer ($r=-0.694$ $p=0.012$).

Comparison of normal male and female fetal bladders

In none of the analyses were there any significant differences between normal male and female fetal bladders. All bladders were therefore analyzed as one group.

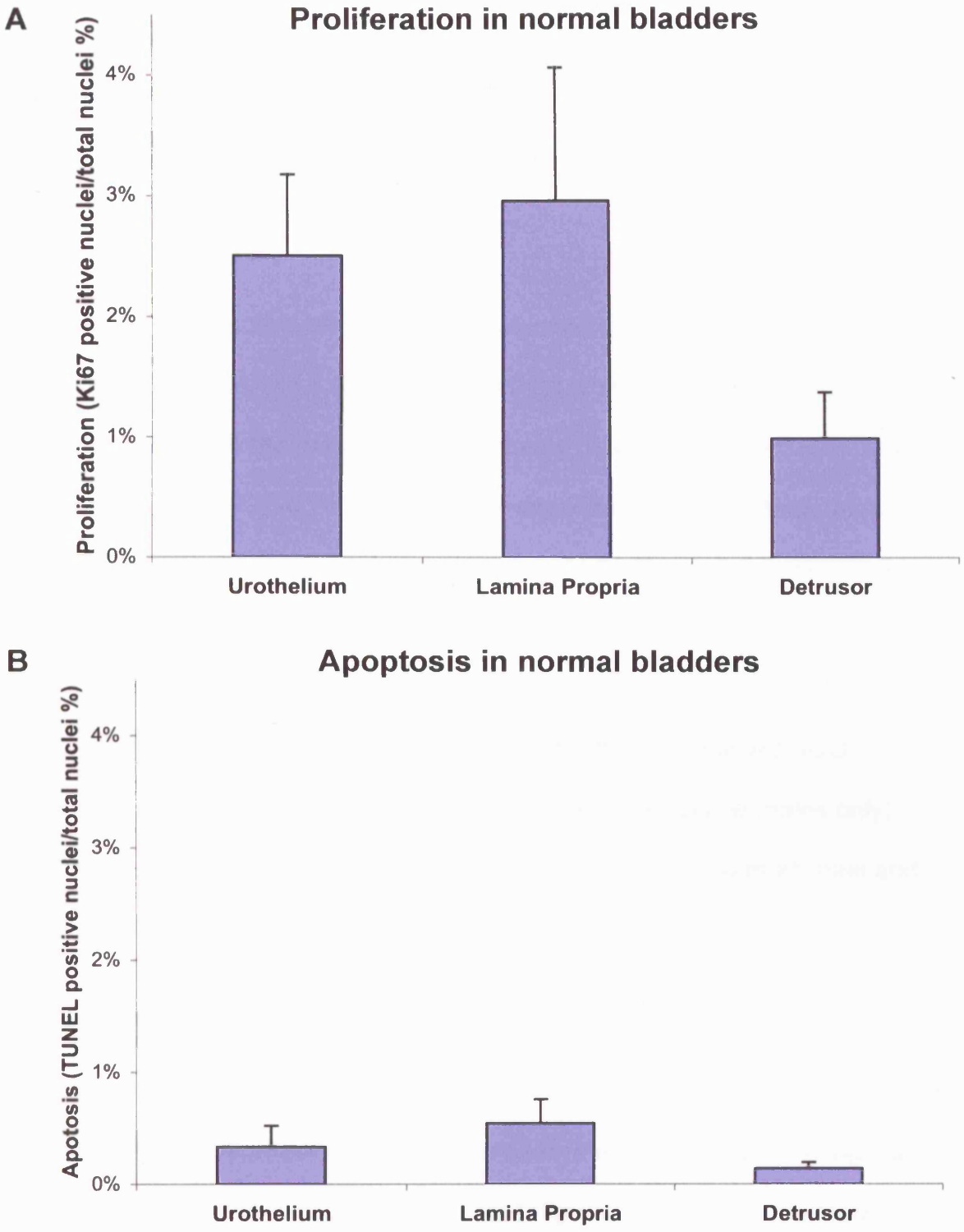

Figure 8.7: Proliferation and apoptosis in normal fetal bladders. (Bars mean±SEM)

Bladders from fetuses with presumed bladder outflow obstruction

Muscle

The amount of muscle present in the presumed congenitally obstructed bladders varied across a spectrum from thick walled, to intermediate muscles, to bladders where the muscle was attenuated (figure 8.8). The thickness of the lamina propria also varied, but in the opposite direction: a thick detrusor layer was associated with a thinner lamina propria (figure 8.8 A,B), and thin detrusor was associated with a thicker apparent lamina propria (figure 8.8 E,F). These results are plotted against gestational age and normal bladders in figure 8.9. Analysis was performed by comparing the presumed BOO bladders (all male) against age and sex matched normals (ie males only), against age matched controls (male and female) and also with all male and female normals (with similar results).

Muscle morphology

Examination of the morphology of the muscle bundles in the detrusor showed a spectrum of abnormality, varying form near normal (with easily recognised bundles with no excess connective tissue) (figure 8.10 A,B); to bladders where the detrusor muscle bundles were still recognisable, but with increased collagen (figure 8.10 C); to bladders where the amount of muscle was reduced, but also where the muscle bundles were no longer recognisable, with large amounts of connective tissue (figure 8.10 D,E,F).

Decrease in the area density of muscle in these bladders correlated positively with increasing muscle dysmorphology score ($r=0.49$ $p<0.05$, 2–tailed Spearman non–parametric rank correlation). Only one quarter the variation in the dysmorphology score can be explained by differences in muscle density.

Collagen

The amount of collagen present varied in a spectrum in these bladders also: the thicker walled bladders had relatively little collagen, whereas the intermediate bladders had more, collagen between and within the muscle bundles of the detrusor, and the 'disrupted/attenuated' bladders had less muscle and more general connective tissue infiltration (Figure 8.8).

Muscle/Collagen ratios are tabulated in Appendix 4: table 4.1, and results discussed in Appendix 4.

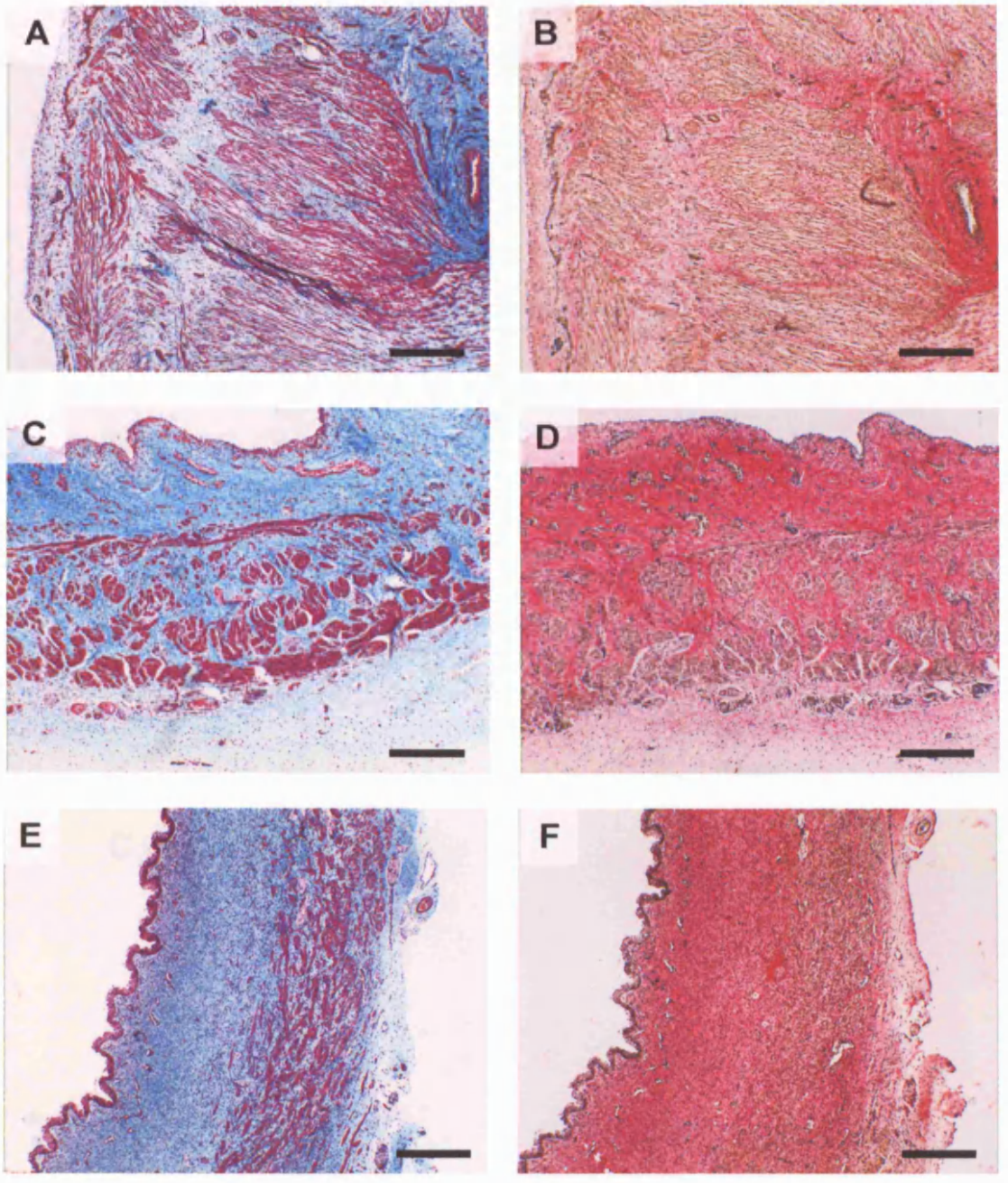

Figure 8.8: Fetal bladder outflow obstruction Masson's trichrome and van Gieson stains . (A,C,E) Masson's Trichrome. (B,D,F) Van Gieson stain. (A,B) thicker walled bladder, (B,C) intermediate-walled bladder, (E,F) thinner -walled bladder with disrupted detrusor. Scale bar 400μm.

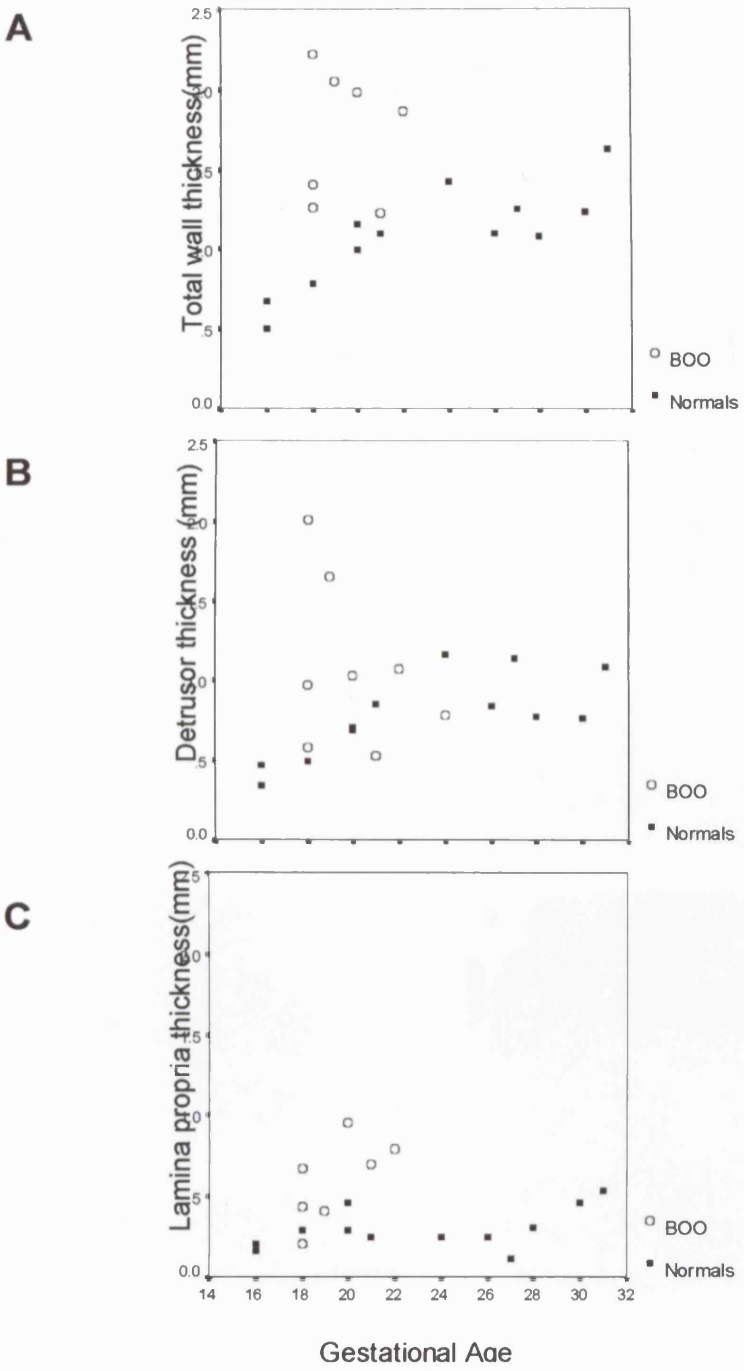

Figure 8.9: Morphometry of fetal presumed bladder outflow obstruction (A) Total wall thickness, (B) detrusor wall thickness and (C) lamina propria thickness versus gestational age for presumed obstructed (Open circles, BOO) and all normal bladders (Black circles, Normals).

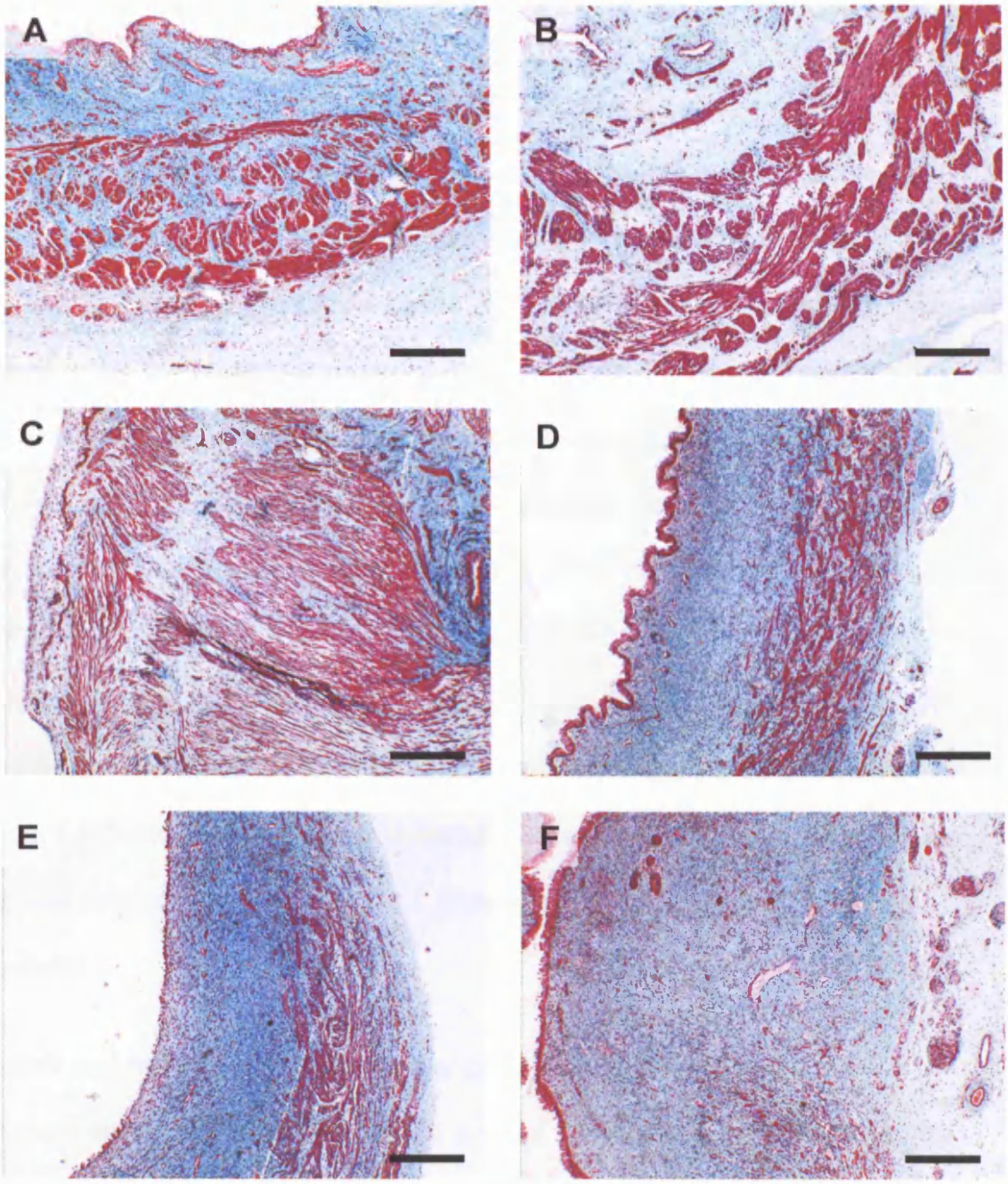

Figure 8.10: Muscle dysmorphology in presumed fetal bladder outlet obstruction . (A) Muscle dysmorphology score 2, MC ratio 0.45.(B) Muscle dysmorphology 2, MC ratio0.84. (C) Muscle morphology 5, MC ratio 0.77. (D) Muscle Morphology 5 MC ratio 0.27 (E) Muscle morphology score 6, MC ratio 0.23. Scale bar 400μm. MC is muscle/collagen ratio, discussed in Appendix 4.

Fibronectin

Fibronectin area in congenitally obstructed bladders was maximal on immunostaining the most morphologically normal bladders with intermediate wall thickness (figure 8.11A). These bladders also had the most normal muscle morphology. In the thick-walled obstructed bladders, fibronectin was present in the basal lamina around the detrusor smooth muscle cells, but the immunostaining was apparently reduced as assessed qualitatively by examination of the slides (figure 8.11 C). These bladders had intermediate muscle morphology. Double immunostaining using confocal microscopy showed that fibronectin was present in thick walled bladders, in the basal lamina of smooth muscle cells (figure 8.12), but that this was lost in bladders with disruption of muscle morphology (figure 8.13). Figure 8.14 shows that the bladders with the most normal architecture were associated with fibronectin in the basal lamina, whereas disrupted architecture was associated with less fibronectin.

The detrusor fibronectin area inversely correlated with the muscle dysmorphology score ($r=-0.54$ $p<0.05$ 2-tailed Spearman rank correlation) for all bladders both presumed BOO and normal (with no change whether males and females were included or not).

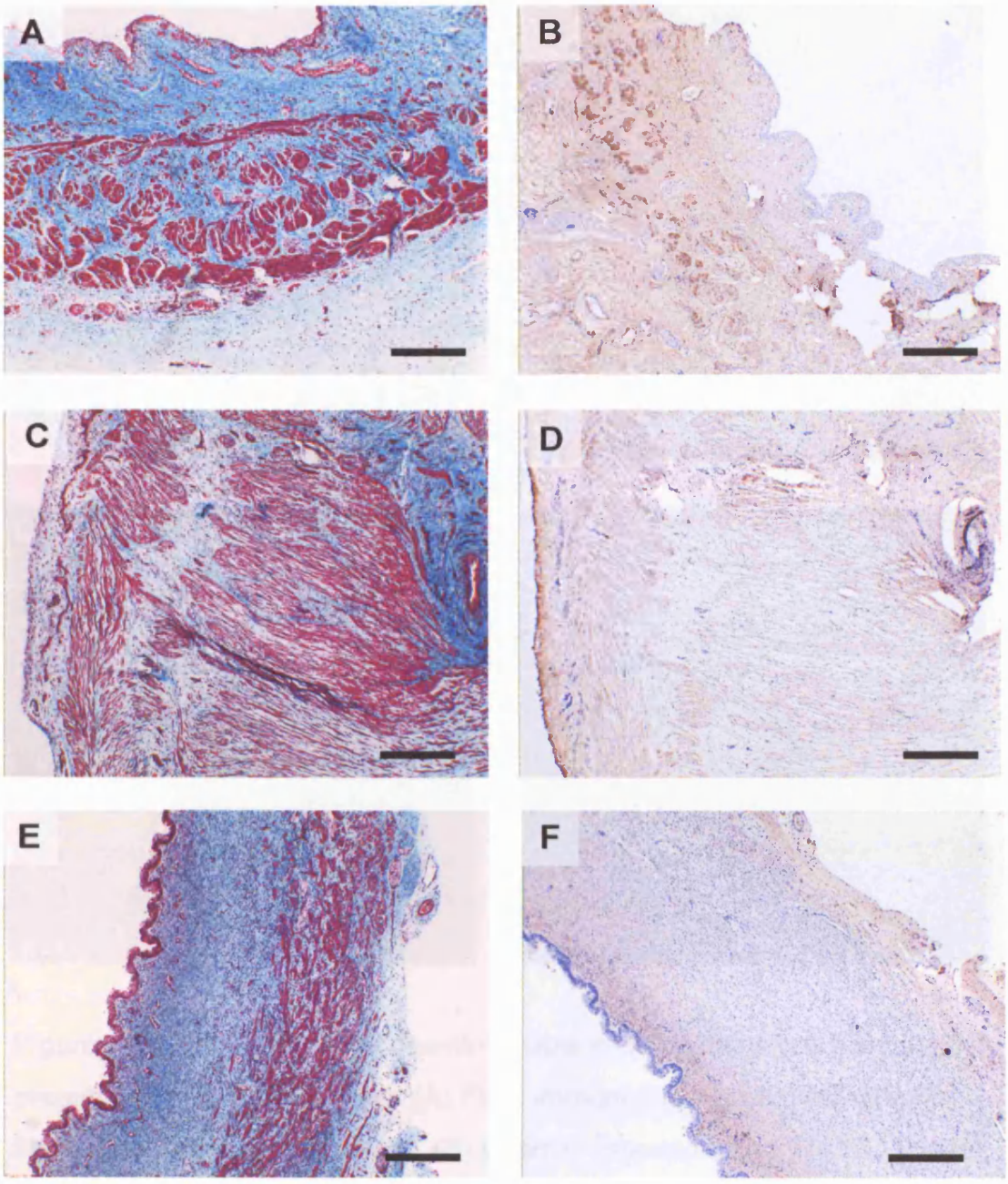

Figure 8.11: Fibronectin expression compared to muscle morphology in fetal presumed BOO. (A,C,E) Masson's Trichrome; (B,D,F) fibronectin immunostaining. (A,B) Muscle morphology minimally affected, (CD) moderately affected morphology (E,F) bladder disrupted detrusor. Scale bar 400μm.

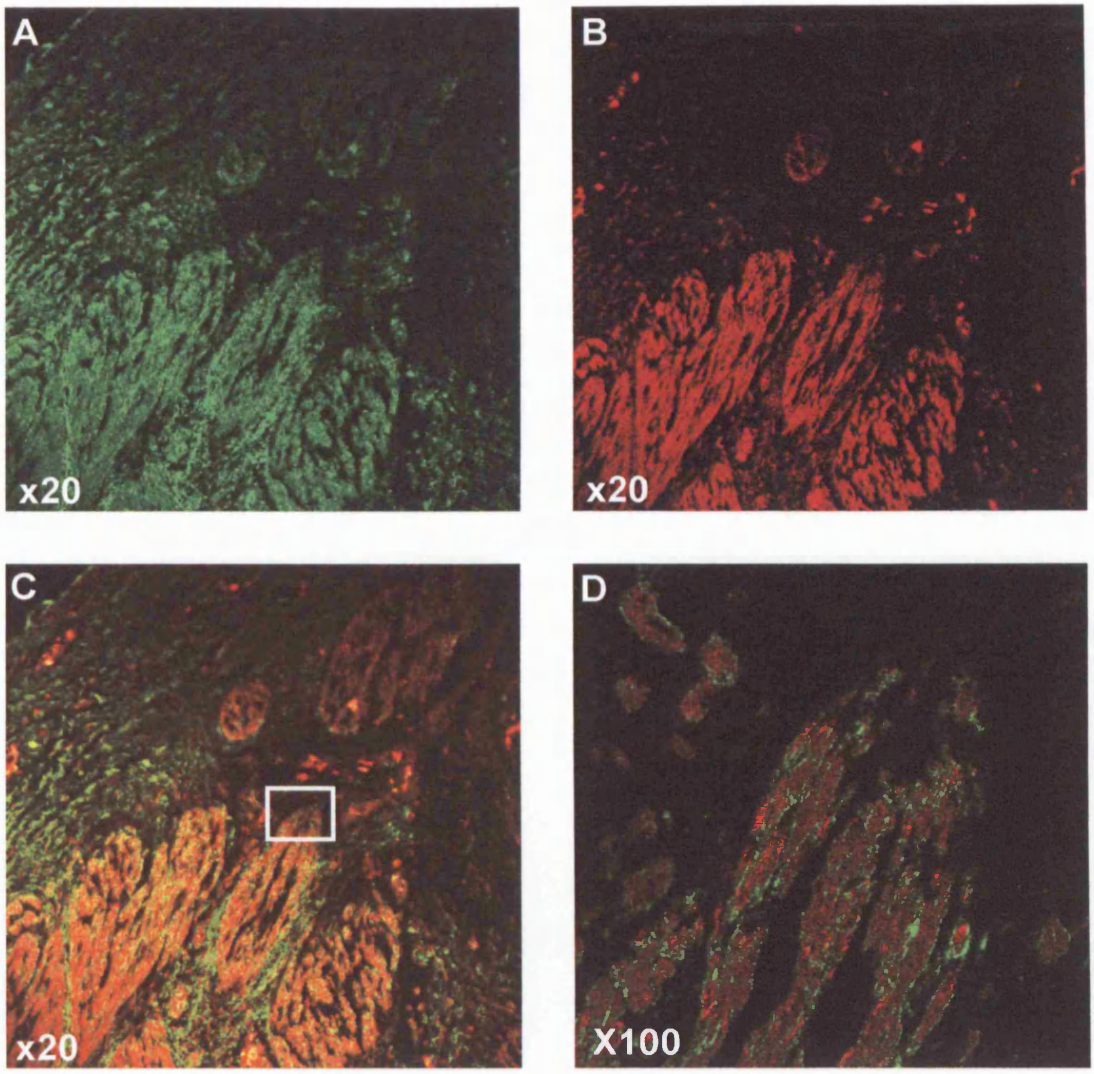

Figure 8.12: Fibronectin and desmin double immunostaining in thick–walled presumed obstructed bladder. (A) FITC immunofluoresecent staining of fibronectin in the detrusor layer. (B) Desmin detected using TRITC labelled antibodies in detrusor layer. (C) Combined FITC/TRITC (desmin/fibronectin) expression. (D) high power view of area in white box in C, showing desmin expression of DSMCs, with surrounding fibronectin in the basal lamina. Magnification (A-C) x20. Magnification (D) x100.

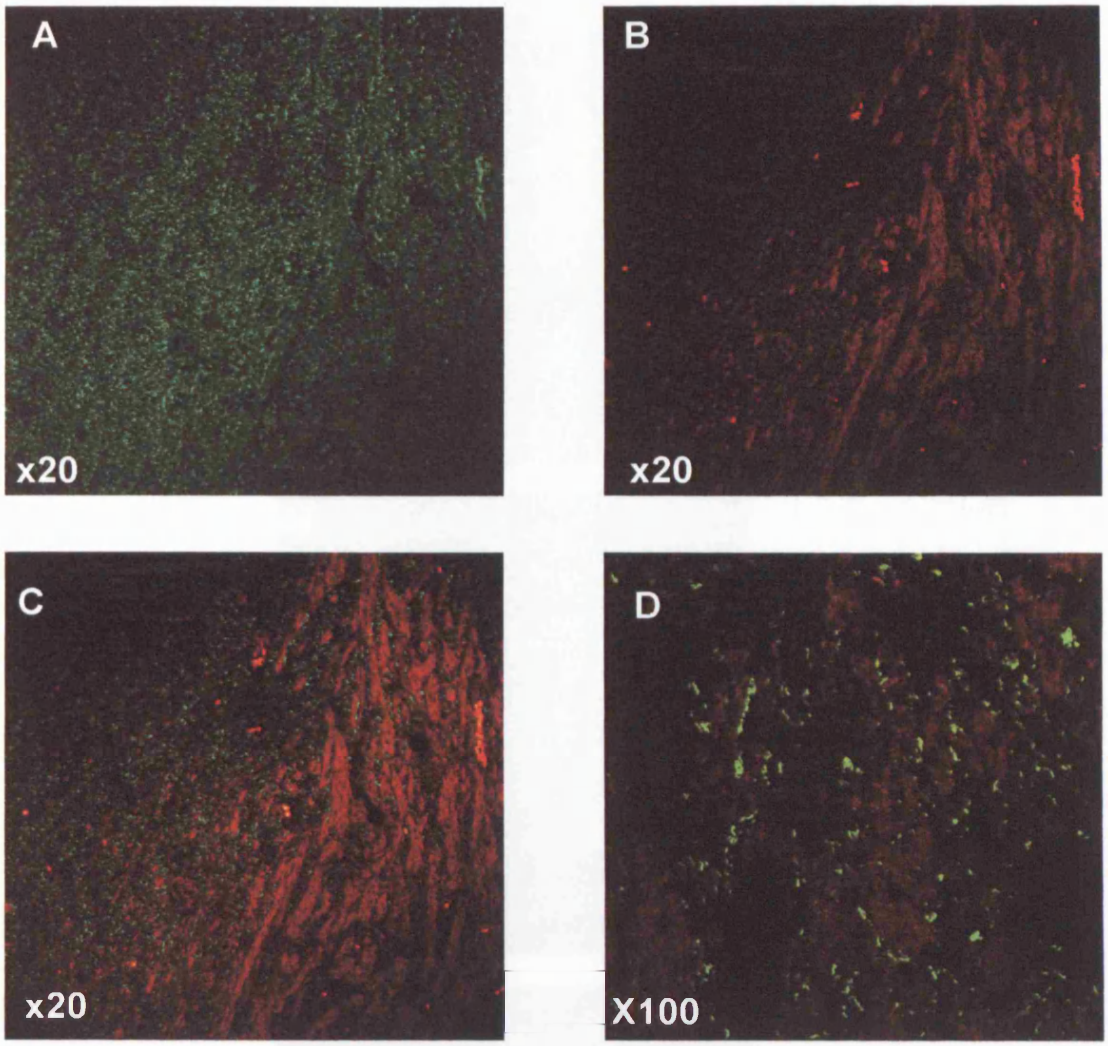

Figure 8.13: Fibronectin and desmin double immunostaining in disrupted, thin-walled presumed obstructed bladder. (A) FITC immunofluoresecent staining of fibronectin in the detrusor layer. (B) Desmin detected using TRITC labelled antibodies in detrusor layer. (C) Combined FITC/TRITC (desmin/fibronectin) expression. (D) high poer view of area in white box in C, showing desmin expression of DSMCs, with surrounding fibronectin in the basal lamina. Magnification (A-C) x20. Magnification (D) x100.

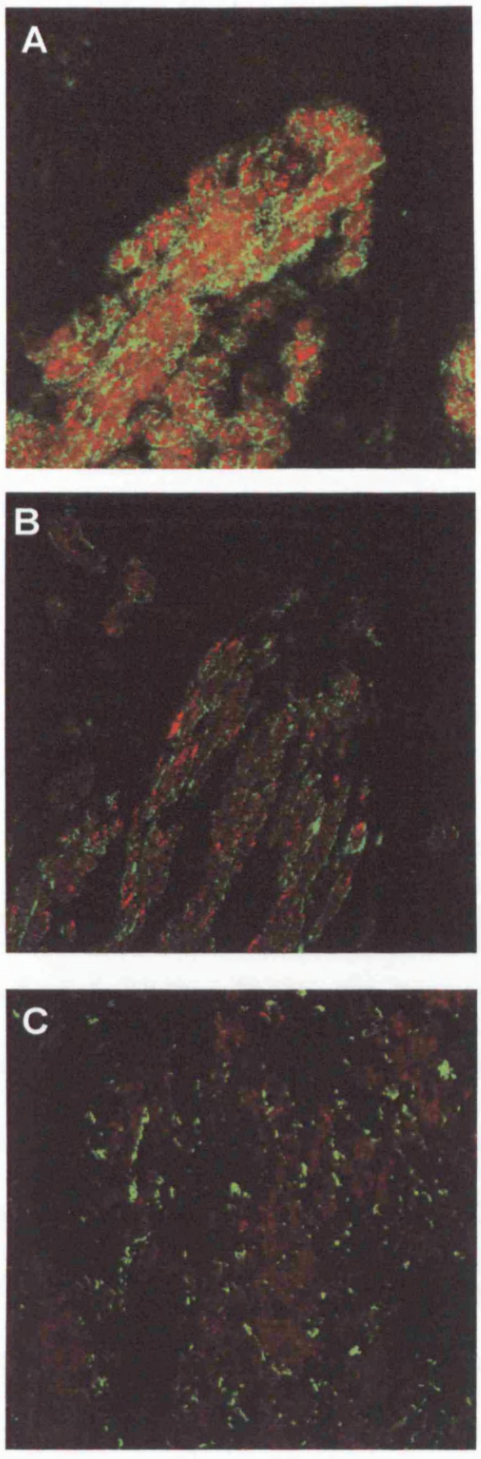

Figure 8.14: Fibronectin and desmin double immunostaining in the detrusor of normal, thick walled, disrupted detrusor. Comparison of (a) normal detrusor fibronectin desmin colocalization; (b) thick walled, presumed obstructed bladder showing loss of fibronectin; (c) disrupted detrusor with loss of fibronectin.

Renal dysplasia, muscle dysmorphology and fibronectin expression

The most normal bladders from presumed BOO cases, were associated with the most normal kidneys (figure 8.15 A,B). Moderately disrupted thick-walled bladders were associated with marked renal malformations (figure 8.15 C,D). The most abnormal muscle morphology was associated with the most abnormal kidneys (figure 8.15 E,F). The muscle dysmorphology positively score correlated with the renal dysplasia score ($r=0.823$ $p<0.001$, 2-tailed Spearman rank correlation).

Similarly, the same comparison was made between the fibronectin expression of these bladders and the degree of kidney abnormality (figure 8.16). A greater degree of fibronectin immunostaining was associated with more normal kidneys (figure 8.16 A,B); less fibronectin immunostaining was associated with more dysplastic appearance of the kidneys (figure 8.16 C,D); Absence of fibronectin in the most severely affected bladders was associated with severe renal dysplasia (figure 8.16 E,F). Detrusor fibronectin area (%) significantly negatively correlated with renal dysplasia score ($r=-0.573$ $p<0.05$, Spearman rank correlation coefficient). Similarly decreasing detrusor fibronectin area (%) correlated with an increasing muscle dysmorphology score, detrusor fibronectin area (%) versus muscle dysmorphology score($r=-0.61$ $p<0.05$, Spearman rank correlation).

In summary greater detrusor fibronectin immunostaining was associated with more normal muscle morphology, more muscle and less collagen, and the

most normal kidneys. Lower detrusor fibronectin immunostaining was associated with disrupted muscle morphology, loss of muscle and increased fibrosis, and with increased renal abnormalities.

Lamina propria fibronectin area or density showed no association with increasing fibrosis, or the degree of kidney malformation.

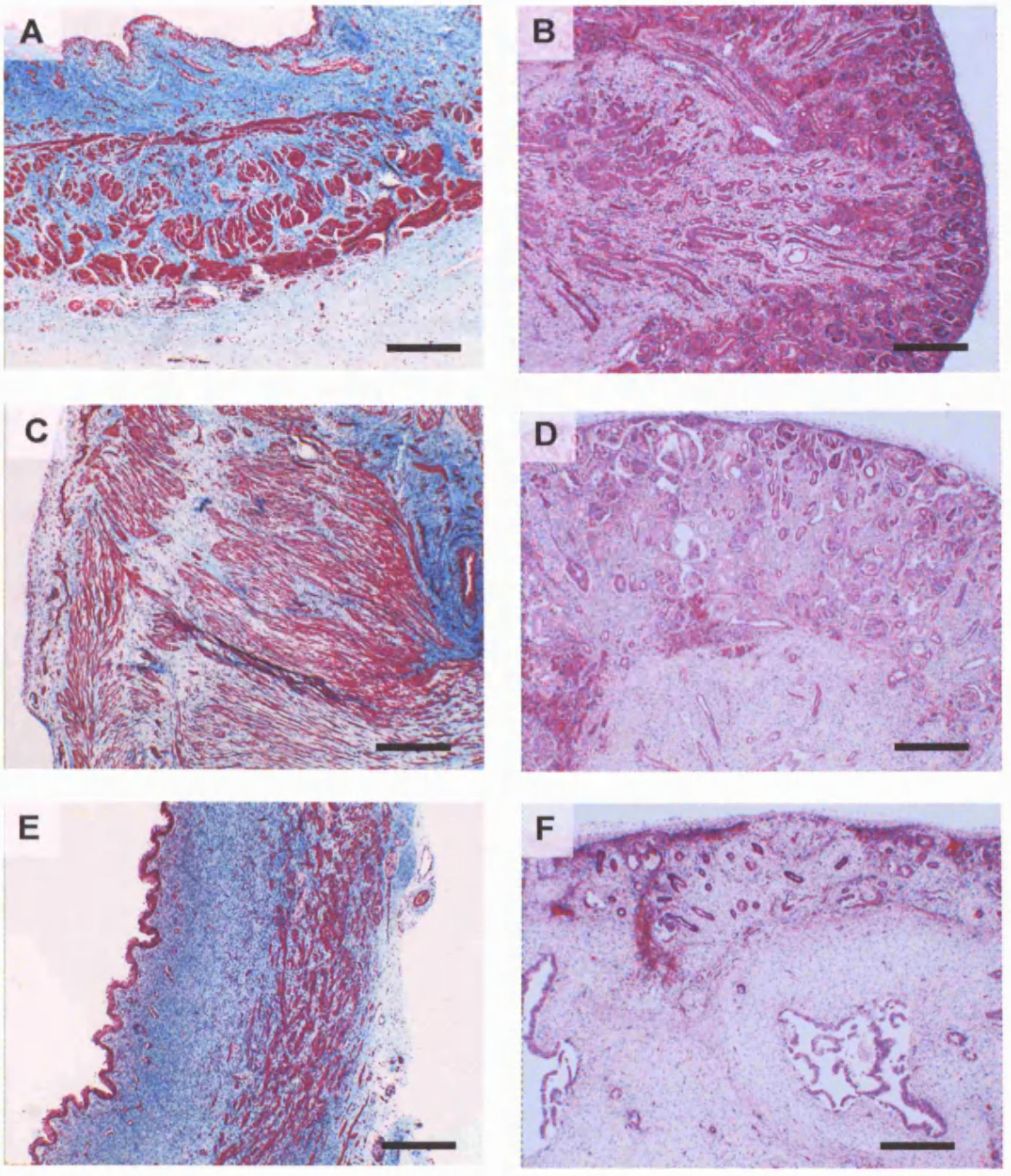

Figure 8.15: Detrusor muscle morphology and renal dysplasia. (A,C,E) Masson's Trichrome; (B,D,F) Haematoxylin and eosin staining of the fetal kidneys from the same fetuses. (A,) Muscle morphology minimally affected, (C) moderately affected morphology (E) bladder disrupted detrusor. Scale bar 40μm.

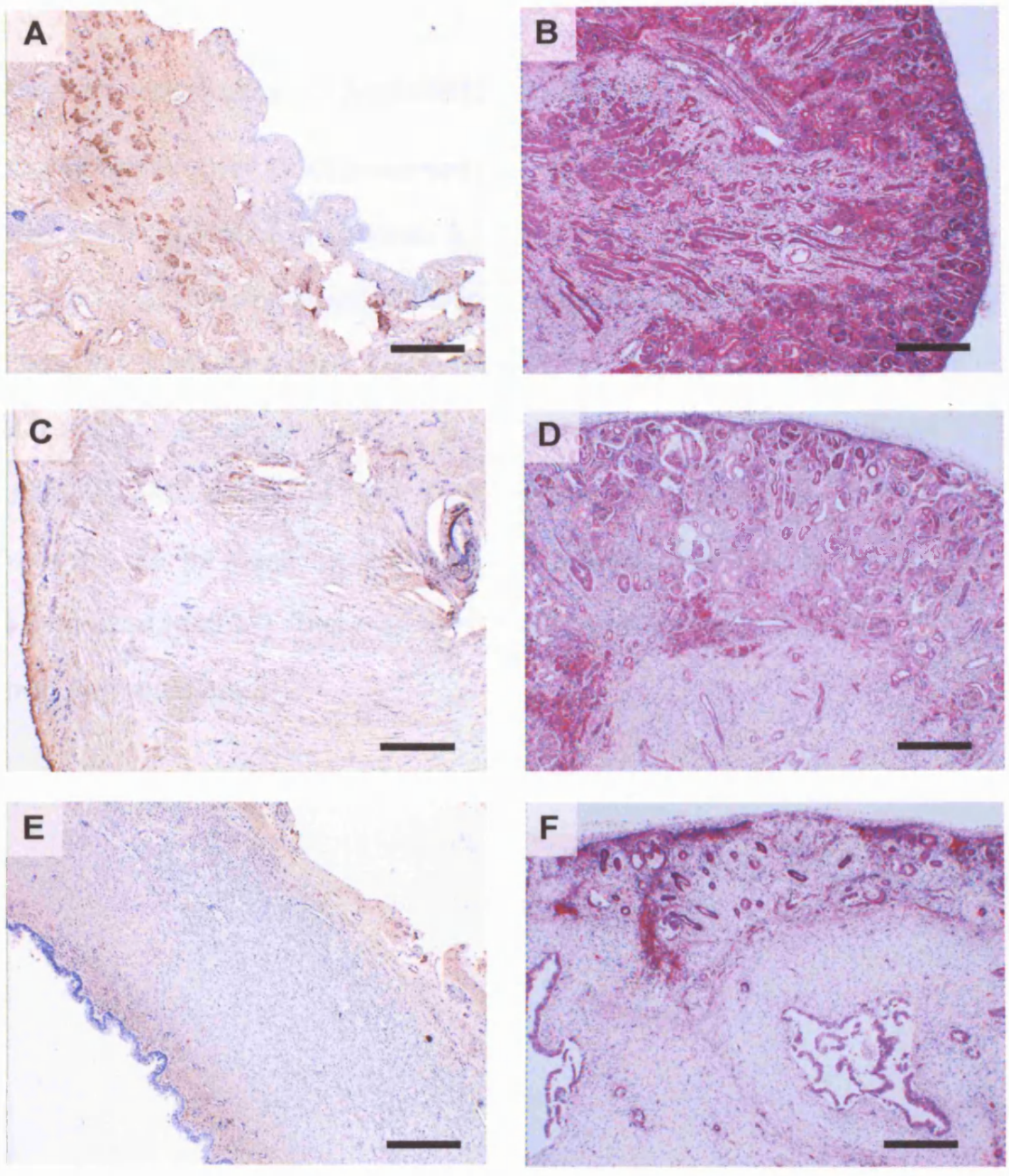

Figure 8.16: Detrusor fibronectin immunostaining and renal dysplasia. (A,C,E) Masson's trichrome; (B,D,F) Haematoxylin and eosin staining of the fetal kidneys from the same fetuses. (A) Muscle morphology minimally affected, fibronectin expressed strongly in detrusor muscle bundles. (C) moderately affected morphology, with fibronectin weakly expressed in detrusor muscle bundles. (E) bladder with disrupted detrusor muscle bundles, no fibronectin. Scale bar 40μm.

Proliferation and apoptosis in presumed obstructed fetal bladders

Averaging cell turnover for all presumed BOO bladders the urothelium showed similar incidence of apoptotic 3.7±2.4% (mean±SEM) and proliferative cells (3.5±1.2%), not significantly different to that found in the normal bladders. In the lamina propria, proliferation (5.3±1.5%) was not significantly greater than in the normals ($p=0.31$), but apoptosis was significantly reduced (0.1±0.02%), $p<0.05$ 2–tailed t–test if all normal bladders were considered, however this did not reach significance if only age and sex matched controls were compared ($p=0.17$). There were no significant differences in the cell turnover for the detrusor.

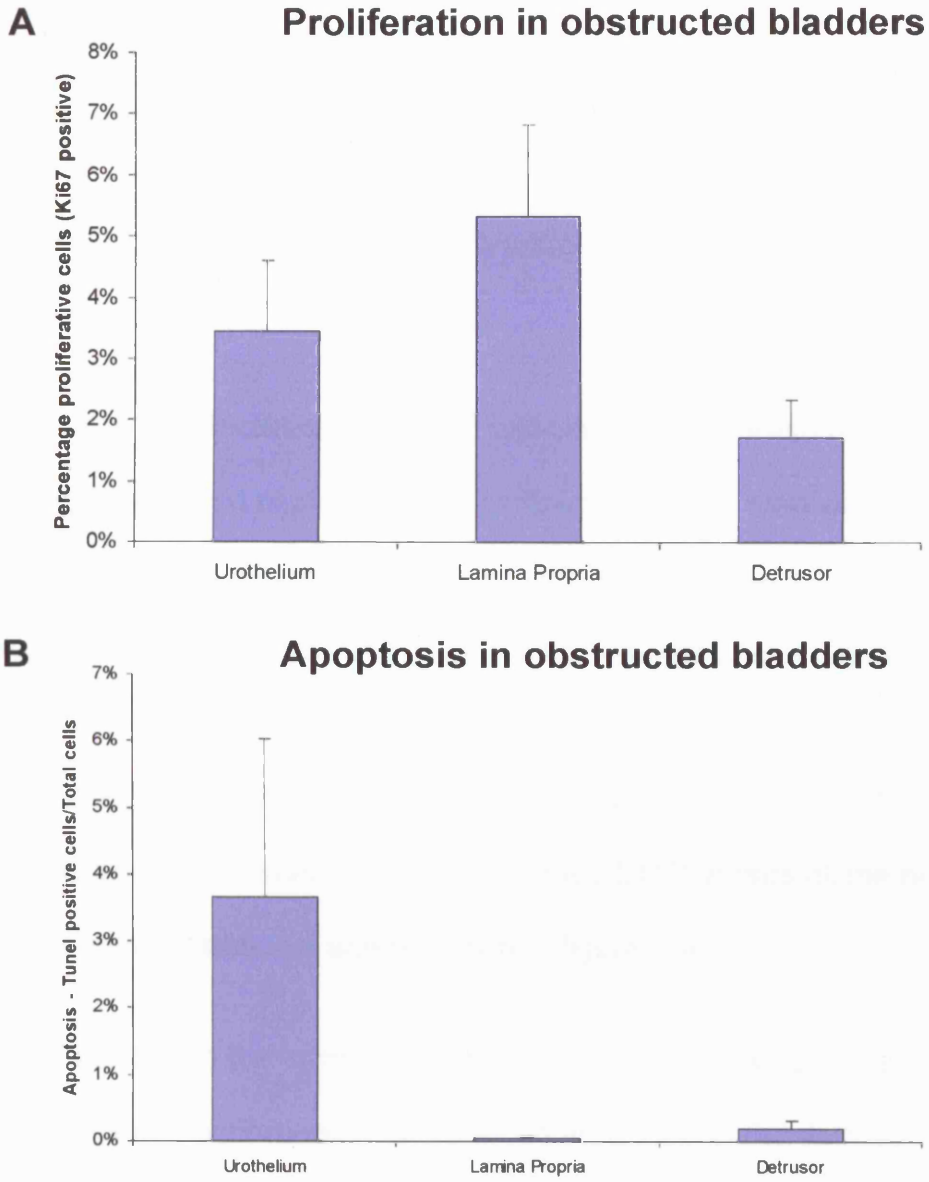

Figure 8.17: Proliferation and apoptosis in presumed BOO bladders. Bars show mean±SEM of counts for bladders.

Comparisons between normal fetal bladders and presumed obstructed fetal bladders

The presumed congenitally obstructed bladders were compared to all the normal bladders.

Examination of wall thickness however revealed that the presumed congenitally obstructed bladders had significantly greater total wall thicknesses ($p=0.001$ 2–tailed t–test), and that this increase was mainly due to an apparent increase in lamina propria thickness ($p=0.003$) (figure 8.18 A,B). The difference between presumed BOO and normal groups did not reach significance for the detrusor thickness (figure 8.18 C). A scatter-plot between the wall thicknesses for fetal presumed BOO versus all the normal bladders against gestational age is shown in figure 8.4.

Comparison between the normal group and presumed BOO group showed that the expression of fibronectin (fibronectin area (%)) in the detrusor was significantly reduced in the presumed obstructed (8.4±2.9%) versus normal bladders (18.4±1.9%), $p<0.01$ 2–tailed t–test unequal variance (figure 8.19A). The obstructed bladders similarly had a greater muscle morphology score (17±1.5) versus normals (9.5±0.9), $p<0.05$ 2–tailed t–test unequal variance (figure 8.19B). Renal dysplasia was higher in the presumed BOO group (10±1) compared to the normal fetal bladders (1±0.5), $p<0.05$ 2–tailed t–test unequal variance. Comparisons of the muscle/collagen ratios showed a reduction in the presence of obstruction, but this was not significant (figure

8.19C). Similarly the decrease of lung/weight ratios in the presence of oligohydramnios did not reach significance.

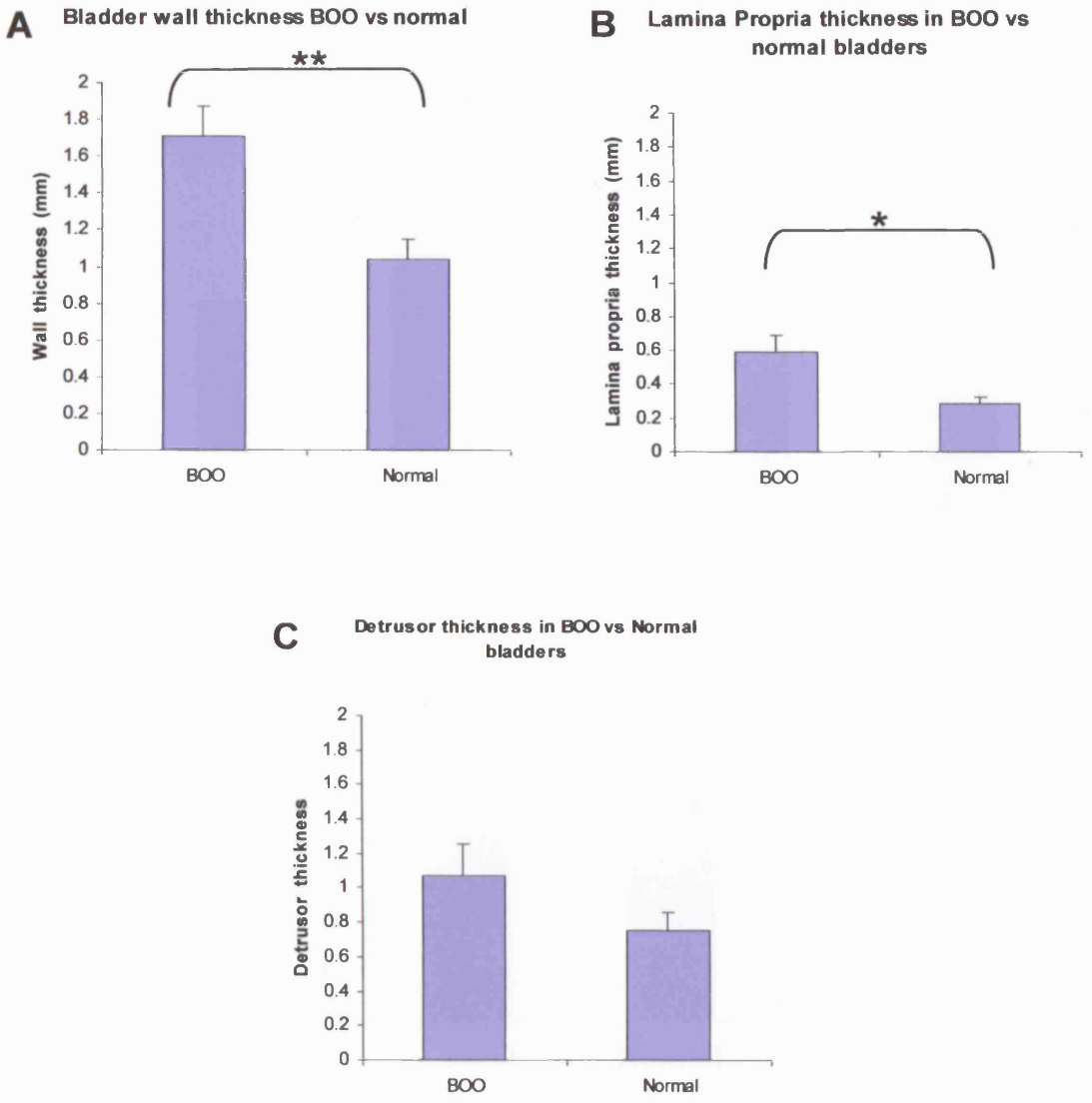

Figure 8.18: Comparisons of wall thickness between fetal presumed BOO bladders and normal controls. (A) Total wall thickness was significantly bigger. (B) Lamina propria thickness was significantly greater in BOO bladders. (C) Detrusor thickness was not significantly larger in BOO bladders. *, $p<0.05$; **,$p<0.01$. Data plotted as mean±SEM.

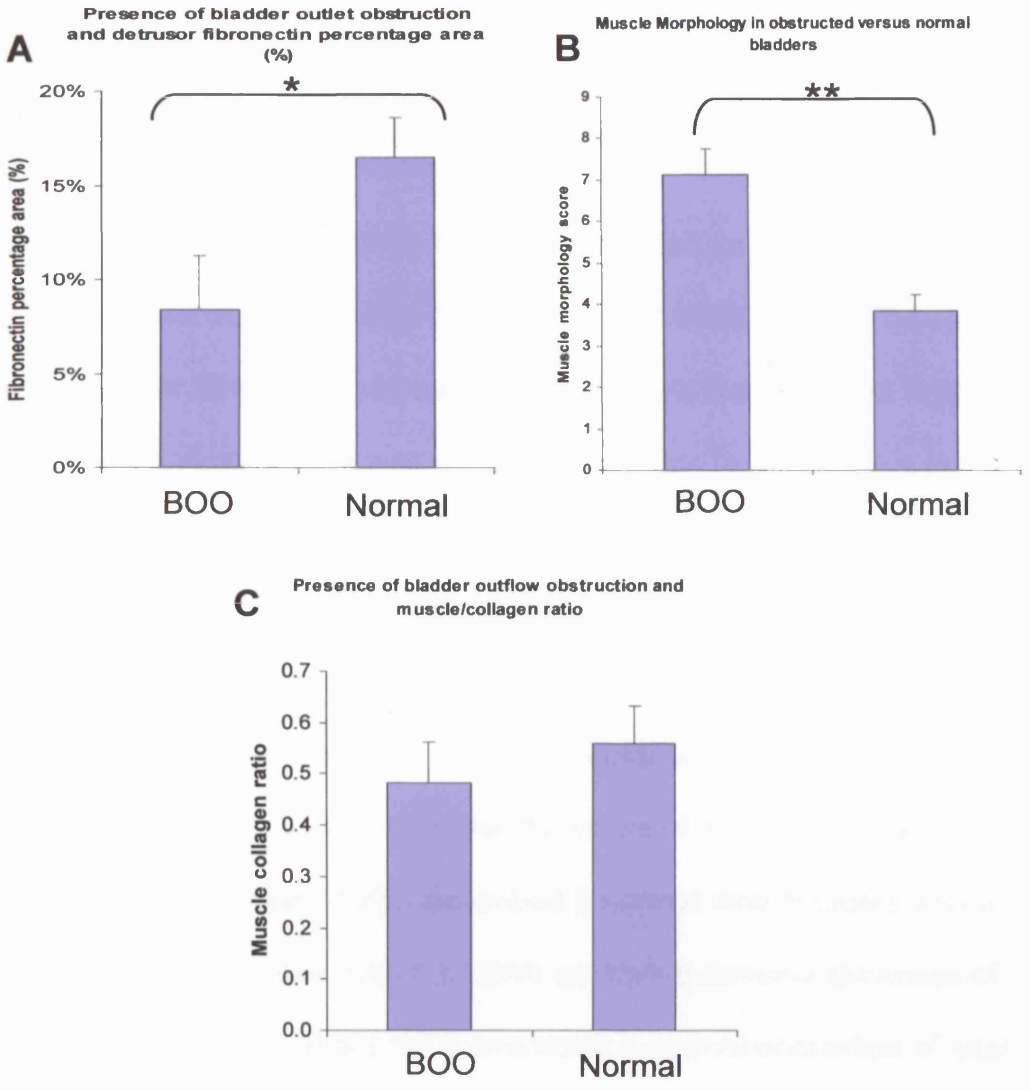

Figure 8.19: Comparisons between fetal presumed BOO and normal controls. (A) detrusor fibronectin area percentage was down-regulated. (B) Muscle morphology score was upregulated. (C) Muscle/Collagen ratio was not significantly different. *, $p<0.05$; **,$p<0.01$. Data plotted as mean±SEM.

Discussion

Normal development of the human fetal bladder

In normal fetal bladder the wall of the bladder underwent an approximate doubling in thickness from 0.5 mm to 1.2 mm, from 16 to 24 weeks. Thereafter there was no further increase. Total wall thickness more than doubled, which was statistically significant. This was almost entirely due to an increase in thickness of the muscle layer which increased from 0.3 to 1.0 mm from 16 to 24 weeks and thereafter plateaued. The lamina propria thickness did not increase. Similar results were obtained in previous studies: 15 normal male and female bladders in the age range 19 to 40 weeks, with a mean gestational age of 27 weeks had a detrusor thickness of 1 mm (Kim et al 1991a); Workman and Kogan (1990) described 5 normal fetal bladders with a gestational age of 27±4 weeks (mean ± SEM) as having detrusor thickness of 0.9±0.2 mm; and Freedman et al (1997) described a normal population of fetal bladders <30 weeks gestational age with a detrusor thickness of 1.1±0.8 mm, and >30 weeks 1.8±0.1 mm. This again is in close agreement with the detrusor thickness described in our series. No data has been described for the thickness of the lamina propria in other series.

In normal bladders at 16 weeks, the muscle bundles were poorly developed, and thin, but demonstrated a progressive increase in size until mature large muscle bundles were present by 30 weeks (figures 8.1, 8.2). This morphological change has also been described by (Kim et al 1991a). The amount of muscle present (muscle area), but not the percentage of surface

area of muscle present (muscle surface area (%)), significantly increased in our series, as was described by (Kim et al 1991a). In our series the muscle/collagen ratio doubled significantly during gestation ($p<0.05$ 2–tailed Pearson correlation), and again, Kim et al reported a similar finding (Kim et al 1991a). Bladder wall thickness is dependent on the state of filling of the bladder. In this series, only sections of the dome were fixed, so the bladders wall thickness is that for relaxed bladders. Sections of bladder dome were obtained in another series (Freedman et al 1997), and then fixed, so the wall was relaxed in a comparable manner to our series. In other studies, the bladders were fixed in distension (Workman and Kogan 1990;Kim et al 1991b, a).

Fibronectin expression was immunolocalised mainly to the detrusor layer and increased with gestational age (fibronectin area (%)), $r=0.62$ $p<0.05$, as did the detrusor thickness ($r=0.74$ $p<0.01$). The area of muscle correlated with the area of fibronectin as can be seen by comparing figures 8.1, 8.2, 8.6; and the confocal images highlight that fibronectin appeared to be in the basal laminae of the DSMC. The area of muscle correlated with the area of fibronectin for the normal bladders, $r=0.76$ $p<0.01$ (Data appendix 4). In normal human fetal bladders fibronectin is immunostaining increases with growth of the DSMC (figure 8.6). This increase in normal detrusor fibronectin has not previously been reported.

Cell turnover has not previously been described in the fetal human bladder. There was a significant inverse association between fibronectin area and density (%), and downregulation of proliferation in all layers of the normal

human fetal bladder. This could mean either that fibronectin was acting as a maturation factor in this case, or that some other mechanism was inhibiting the proliferative signal from the fibronectin. This observation agreed with the data described by Smeulders et al where increasing fibronectin in the detrusor antenatally was actually associated with a progressive decrease in proliferation in the detrusor (Smeulders et al 2002, 2003). There was however a marked decrease in postnatal fibronectin expression in murine bladders, associated with a further decrease in proliferation of DSMC, and an increase in maturation, as assessed by desmin IHC and Western blot.

Fetal bladder outlet obstruction

Comparisons were made between the presumed BOO bladders and the normal bladders (there was no difference in outcome if the comparisons were made by comparing all the normals, or age-matched, or age and sex-matched controls), using Students t-test e.g. for wall thickness, fibronectin expression, renal dysplasia score etc. Correlations were also drawn for the whole group for measurements that varied continuously from normality to abnormality. This allowed correlation between muscle morphology (dysmorphology score) and renal abnormality (renal dysplasia score), for example, to be made.

Comparisons between presumed BOO and normals revealed that the presumed BOO bladders were generally thicker walled than the normal bladders, averaging 70% thicker. This was significant, $p<0.01$ unpaired t–test. The absolute increase in wall thickness was also described in previous human fetal series (Workman and Kogan 1990;Kim et al 1991b;Freedman et al 1997). However in these series the detrusor muscle thickness was significantly increased. This was not found in this series, where it was the doubling in width of the lamina propria in the obstructed group that resulted in the overall difference in total wall thickness. Comparisons between the normal and presumed BOO groups in this study, with regards muscle and collagen area and density (%) were not significant (data in appendix 4). This was because the obstructed group included members with a higher than 'normal' muscle area (perhaps compensated bladders), and at the other extreme members with a lower than normal muscle area (possible decompensated

bladders). Similar observations applied to collagen expression. This wider range averaged out to similar mean values for muscle area, collagen area, and muscle/collagen ratio as for the normal controls (figure 8.21 and below for further discussion of hypothetical mechanisms of bladder dysgenesis). Again these results agreed with series previously described (Freedman et al 1997). Fibronectin expression as measured by percentage of surface area (%) in the presumed BOO bladders was halved in comparison to the normal male fetal bladders. Other differences between the groups that were significant included a marked increase in the dysmorphology scores and renal dysplasia scores in the presumed BOO bladders compared to the normals.

Comparisons within the group of obstructed bladders showed that this was a heterogenous group. Some bladders had thick muscular walls, some had almost no muscle left at all. If the muscle/collagen ratio was examined some were much more muscular than normal bladders, whereas some were much more fibrotic. Increased detrusor fibronectin was associated with more normal muscle morphology, more muscle and less collagen, and the most normal kidneys. Reduced detrusor fibronectin was associated with disrupted muscle morphology, loss of muscle and increased fibrosis, and with increased renal abnormalities. Fibronectin was lost with increasing severity of obstruction.

From this study it is not possible to quantify the degree of obstruction, but the most abnormal human bladders had a histological appearance similar to rabbit models of decompensation, and adult human decompensated bladders (Buttyan et al 1997).

Reliability of methods of quantification

It would have been much more powerful to have had descriptive immunohistochemistry compared with an independent measure of the amount of protein by Western blot, or ELISA (eg Desmin as smooth muscle marker), collagen and fibronectin. Unfortunately this was a retrospective study using tissue that had been stored in paraffin blocks. No protein samples were available for independent analysis by, for example, Western blot. The significance of the area quantifications made should not be over-interpreted, but simply used as supporting evidence for the immunohistochemistry.

The immunohistochemical observations in this study were backed up by morphometric analyses of the thickness of the bladder walls in these human fetal bladders. The results obtained were in agreement with previous series of human data. The area and area (%) of muscle, collagen and fibronectin in these human fetal bladders measured. This was a modification of the methods used by previous authors (Workman and Kogan 1990;Kim et al 1991a, b;Freedman et al 1997). In these papers the authors measured wall thickness, but then at medium to high power measured the area of muscle, connective tissue or collagen in multiple defined small areas. This produced a two--dimensional density measurement used as a surrogate for 'the amount' of eg muscle present. Freedman et al called this the 'density (%)' (Freedman et al 1997). In this thesis, however the total area of, for example muscle, in a section has been measured, as well as the total area of the section so that not just a density measurement (the term percentage surface area is used as an alternative to area density (%) in this thesis), but also a total area measurement. These values have different advantages and disadvantages,

so a consideration of both is useful. Figure 8.20 describes in cartoon form the relationship between the linear morphometric data, area data, and implications for comparison with mouse data where independent western blot data was available.

Area measurements will vary according to the square of the linear measurements. Area measurements give a guide as to how much of a protein, or muscle is present, but this is not the same as the mass (intuitively the mass would be 'the amount present') of a particular protein. Mass varies with the cube of the linear measurement. As such the area measurements are a guide to the mass present. Western blot data gives relative information to changes of a protein concentration. The limitation of this is that if one were to measure for example desmin in this way, if the amount of desmin per milligram of muscle were to be constant, then the actual total amount of muscle could double, or halve and the desmin concentration as it would be constant would not change- and neither would the western blot data. Concentration measurements are therefore independent of total mass present. In a similar way measuring the total area of for example muscle in these sections is a guide to the total mass present, whereas the density measurement is not. Density measurements however do have a built in advantage. There would be variations in total area due to randomness in the selection of fields to be photographed, boxes P,Q,R in the cartoon figure 8.20B. Multiple fields could be averaged as a way of reducing this error. Alternatively the area density could be compared which gives information that is area independent, all be it with loss of a measurement that is related to absolute quantities. It is area density that is the 2-D equivalent of measuring

relative changes in protein concentration that is western blot data. Measuring a ratio of area densities of 2 different materials e.g. collagen and muscle would be a way to arrive at a number that described the total bladder that was area independent. Variations in choice of fields examined would cancel out. The muscle/collagen ratio was therefore measured in this study for this reason, and was similarly measured by Freedman et al (1997), although the authors in this study quote collagen/muscle ratios.

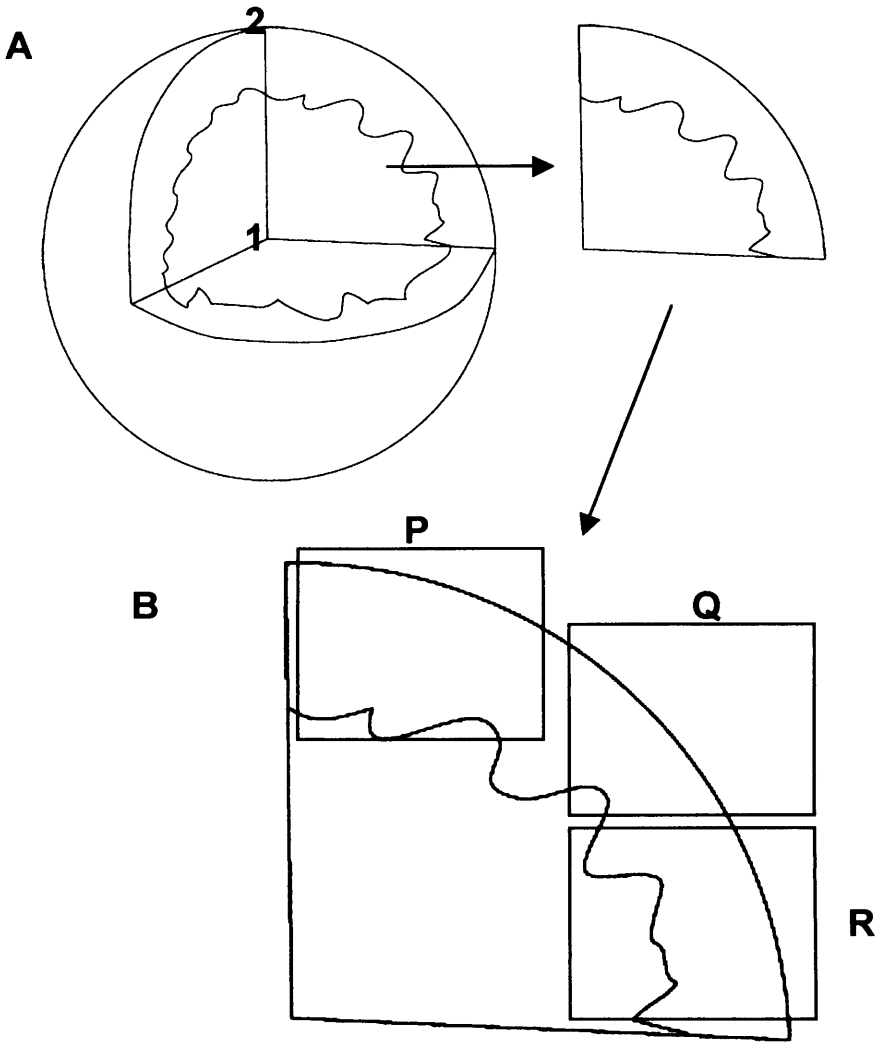

	Absolute 'amount'	Relative 'amount'
1 dimension	Linear measurement	Ratio lengths
2 dimensions	Area measurement	Area density (% surface area)
3 dimensions	Volume/mass measurement	Concentration (Western Blot)

Figure 8.20: What has been measured? (A) linear measurements of bladder wall thickness. (B) Area measurements – positioning of region-of-interest will affect total area measurement. Area density is not so affected.

Variation in the intensity of expression in the immunohistochemistry slides obviously occurred. However for the purpose of area measurements this variation in intensity was lost, simply a measure of presence or absence taking place. Area measurements were therefore an approximation to expression seen on direct examination of slides.

Absolute numbers were however measured for cell turnover and apoptosis. These results were given in terms of number of positive cells as a percentage of total cells in each compartment, where 3 fields of each fetal specimen were counted. This data was therefore robust.

The most subjective data were the scores for muscle morphology and renal dysplasia. Bias in these scores was avoided by having three independent, blinded observers. That there were very close correlations between scores by each of these observers demonstrates the reproducibility and reliability of these scores. What is less certain is how linear the relationship is between an increase in muscle morphology score and the disruption in the fetal bladders. Because these are relative numbers generated from an ordinal scale, and possibly non-linear, the analysis of the correlations of these scores with absolute variables has been entirely by non-parametic statistical tests (Spearman's rank correlation).

What does the muscle 'dysmorphology score' describe? Similar changes documented in human obstructed adult bladders with 'infiltration' of smooth muscle bundles by connective tissue (Gosling and Dixon 1980). Similar findings have been reported in a rat model of partial bladder outflow obstruction (Hanai et al 2002) and in a fetal sheep model of bladder outflow

obstruction (Thiruchelvam et al 2003). In decompensated obstructed bladders disruption and loss of smooth muscle have been reported in humans, and animal models (Levin et al 2000). This score therefore recapitulates this progression. It also correlated well with the severity of renal dysplasia, $p<0.05$ Spearman rank correlation.

Is renal dysplasia a marker for severity of bladder outlet obstruction?

That there was a spectrum of mild to severely abnormal renal dysplasia in the fetal presumed BOO group is not in question. However there are two possible explanations for the dysplasia and muscle dysmorphology; either there is a failure of normal development that encapsulates both the bladder and kidney, i.e. a 'field change' – as has been postulated to occur with severe vesico-ureteric reflux and kidney dysplasia (Godley et al 2001); or the bladder is obstructed and back pressure on the kidney results in dysplasia. This has been demonstrated in animal models (Peters et al 1992a; Nyirady et al 2002), but has also been suggested as the pathogenesis in human fetuses (Shimada et al 2003).

Study groups: presumed fetal bladder outlet obstruction and normal fetuses

Presumed BOO was defined clinically in this series by the appearance at the time of post-mortem, in a similar manner to previous series reported in the literature (Workman and Kogan 1990; Kim et al 1991a, b; Freedman et al 1997). Direct examination of the posterior urethra was limited to describing if

the posterior urethra is dilated. No attempt to identify an infravesical obstruction was routinely carried out as part of the postmortem examination at UCH, either by histology, or by radiology. Histology was not done as the yield of identifying the obstruction is low because of difficulties with aligning sections for cutting. These specimens were identified retrospectively, and as the diagnosis therefore was on the appearance of secondary signs of BOO, these specimens have at best a presumed diagnosis of bladder outflow obstruction.

Presumed congenital BOO fetuses which had evidence of prune belly syndrome were excluded, as were isolated urethral atresias. The remaining group therefore most probably represented posterior urethral valves, and was a much more homogenous study group than in other series. In previously studied series PUV, urethral atresia and PBS were variously included. In comparison to the previously published series my pathologically obstructed group was on average much younger (Workman and Kogan 1990; Kim et al 1991a, b; Freedman et al 1997).

Similarly the 'normal' group were all morphologically normal fetuses, as opposed to simply those which had normal genitourinary tracts as described in the published series (Workman and Kogan 1990; Kim et al 1991a, b; Freedman et al 1997). However normal fetuses do not die in utero or spontaneously abort. The control group in our series overlapped well with those in other series. An alternative would have been to use fetuses aborted for other congenital abnormalities.

The combination of a more normal study group and a more homogenous obstructed group has made comparison easier between the two groups, with reduced variation within the groups, than in previously published series.

Implications

The obstructed bladders in this group were not just from earlier gestational ages but also appeared to be much more abnormal than the bladders in previous human series, where thick-walled bladders, due to increased detrusor thickness, predominated. In this series there was a spectrum of thicker muscle to attenuated muscle, but the 'decompensated' appearance as described by Levin et al predominated (Levin et al 2000). The appearance in extreme cases being similar to that described in the fetal ovine obstruction model, after 30 days of obstruction (Thiruchelvam et al 2003). A shorter duration of obstruction (9 days) appears to produce a thick-walled, hypertrophic bladder (Farrugia et al 2006a, b). The muscle/collagen ratio in the obstructed bladders straddled the normals, a similar result to that described by (Freedman et al 1997).

In adult rabbit bladders exposed to partial bladder outflow obstruction, an initial hypertrophic phase has been described, followed by a period of compensated function, followed by decompensation (Buttyan et al 1997). Similar changes appear to happen in adult men with BOO (Levin et al 2000).

It could be speculated that the bladders with presumed BOO represented a spectrum from compensated to decompensated bladders with loss of

fibronectin, increased muscle dysmorphology and worsening renal dysplasia. It is however also possible that these bladders actually were a human analogue of the two forms of decompensation described in the rabbit model by Levin et al (2000): myogenic failure with a large, compliant flaccid thin-walled bladder; or, myogenic failure with a thick-walled, non-compliant, small volume bladder. Other immunohistochemical markers for decompensation that might be instructive in this situation would be acetyl cholinesterase, or another neuronal marker such as PGP 9.5, or S100: this has been shown to be significantly downregulated in decompensated human bladders (Buttyan et al 1997), with a reduction in expression of neuronal markers also seen in the fetal ovine bladder outflow obstruction model described by (Nyirady et al 2002). This could help resolve the question as whether all of these bladders were in fact decompensated or whether some were still compensated.

In normal human bladders the detrusor smooth muscle was closely associated with fibronectin. That there was reduced fibronectin in the presumed obstructed group was explained by this group having relative disruption and loss of muscle also. It can be further speculated that fetal DSMC and fibronectin are interdependent.

Fibronectin immunostaining was not increased in the lamina propria in presumed obstruction. This may be indirect evidence that activation of myofibroblasts as has been described in cutaneous wound healing (Serini and Gabbiani 1999) – with their dependence on fibronectin – was not taking place in these bladders. Or, it could be that fibrosis was taking place due to a different mechanism than other forms of fibrosis (Gabbiani 2003).

In the obstructed bladders in this series the apparent lamina propria was thickened. There are two possible mechanisms that could explain this: either, obstruction inhibits myogenesis in the detrusor layer, but stimulates the growth of the lamina propria instead; or, the thickened lamina propria seen in the presumed BOO group may represent in part degenerated DSM, which has lost cells with the typical smooth muscle markers looked for in this study i.e. it is only apparent lamina propria. Thickening of the lamina propria has not previously been described and may become a clinically useful marker for severely affected obstructed bladders in the future as higher resolution ultrasound and MRI become available.

Hypothetical models of response of human fetal bladders to obstruction

1) Compensation/decompensation

It is possible that the pattern of compensation, followed at a variable time later by decompensation is a good model for the changes in the human bladder. In this model the initially relatively normal bladder (with a normal muscle/collagen ratio) compensates by hypertrophy and hyperplasia of the detrusor smooth muscle cells – with increased expression of fibronectin. The muscle collagen ratio rises and then at a variable time later the bladder decompensates in one of 2 ways – thin walled, or thick walled (figure 8.21A).

2) Progressive bladder dysplasia – Prune belly type

The bladders may never start as normal having always been partially obstructed. Some become progressively thick walled and decompensate (muscle/collagen ratio rises to above normal). Other bladders never undergo

normal smooth muscle myogenesis and become progressively more fibrotic, with poorly developed detrusor layer (figure 8.21B).

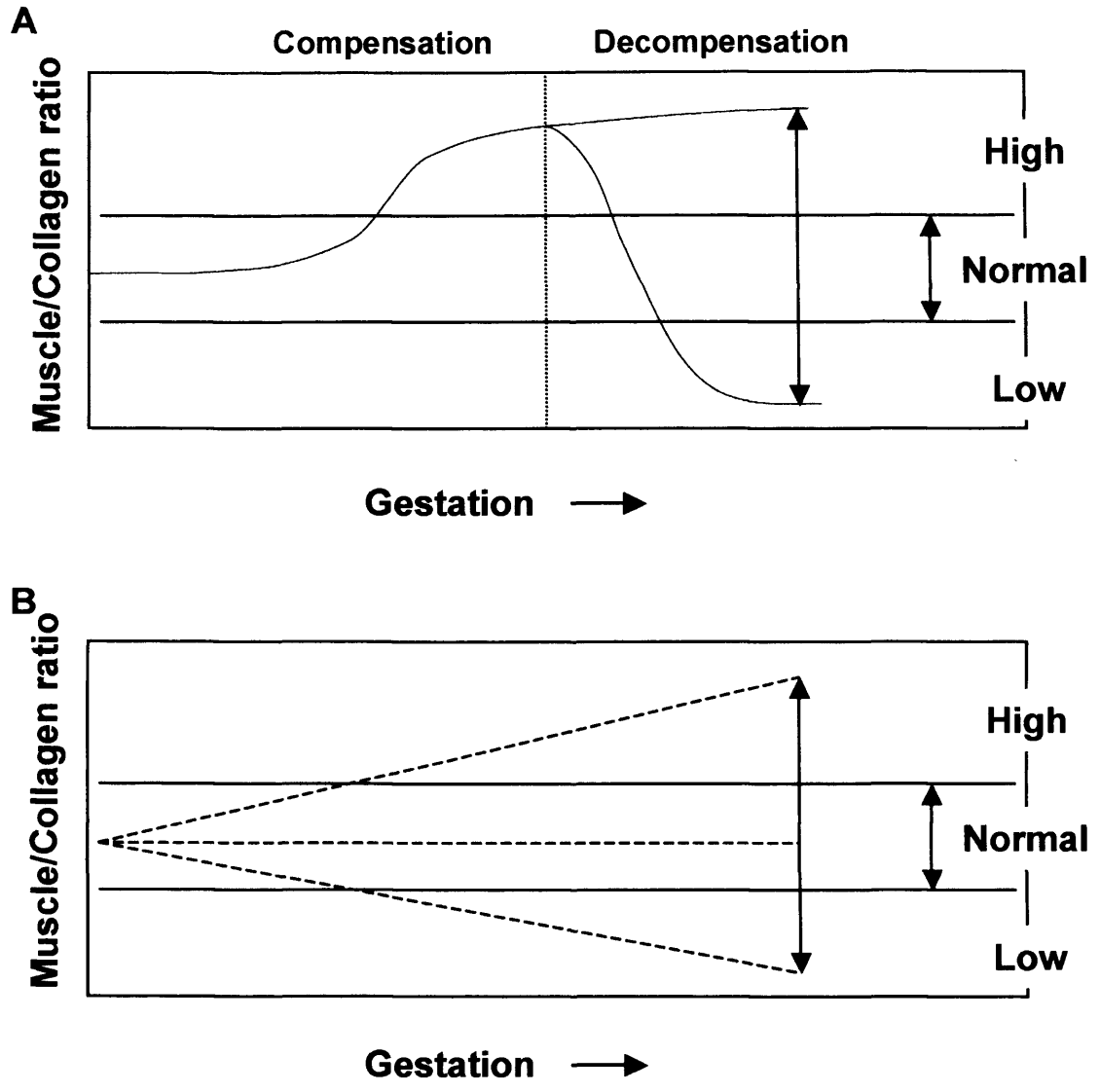

Figure 8.21: Hypothetical models of bladder dysgenesis resulting from fetal bladder outlet obstruction : (A) Levin compensation-decompensation. (B) Woolf Prune belly-type dysplasia. Normal = normal muscle/collagen ratio, high = excess muscle vs. collagen; low = reduced muscle vs. collagen.

The data we have simply represent snap-shots. No inference about what has gone before can be made, but would be a pointer towards future work.

Conclusion

With regards the hypotheses tested by this comparison of normal and fetally obstructed human bladders, the following conclusions can be drawn:

1) During normal human bladder development detrusor thickens and fibronectin is expressed proportionally to the increase in muscle tissue. However, the proliferative synergy between fibronectin substrate and fetal calf serum, seen in the mouse bladder cell suspension experiments described in Chapter 6, did not appear to happen. Increasing fibronectin instead being associated with increased maturation, and decreased proliferation.

2) In human fetal bladders with presumed BOO, there is a spectrum of phenotypes: at one extreme, some of these bladders had fibronectin expression, muscle morphology and renal histology which resembled normal controls. At the other extreme, reduced detrusor fibronectin was associated with disrupted muscle morphology and with increased renal abnormalities.

3) In severely affected fetal bladder outlet obstruction, the lamina propria was apparently thickened.

Chapter 9. Final discussion and future work

A hypothetical cell biology model for bladder development

The studies presented here provide further descriptive, and hence circumstantial, evidence that ECM/integrin interactions are important in normal bladder development; however, further studies are warranted to resolve the apparently conflicting organ and cell culture data to unravel possible functional roles for fibronectin and its receptors. The studies also provide the first evidence that fibronectin expression is abnormal in human congenital bladder anomalies.

First, the descriptive work on normal murine bladder development is consistent with the contention that integrin α5β1 could mediate instructive signals from a fibronectin-rich matrix. Second, upregulation of integrin α7β1 harmonised with the upregulation of laminin and DSMC maturation, suggesting that these molecules could modulate a muscle differentiation signal.

Second, the cell adhesion experiments showed that fibronectin allowed adherence and spreading of DSMC in the developing bladder. These fetal DSMC predominantly expressed integrin α5, β1 and desmin. Blocking integrin receptors using RGD oligopeptides not only decreased desmin positive cell adhesion, but also reduced cell spreading. Fibronectin and serum had a synergistic effect on proliferation of bladder cells. Thus, integrin α5β1 could

mediate adhesion of fetal DSMC to fibronectin, and could potentially mediate a proliferative signal from fibronectin to these cells.

Based on the descriptive work presented in this thesis, and the results of previous studies (Baskin et al 1993a, b and c; Schuger et al 1997; Relan et al 1999; Yang et al 1999; Smeulders et al 2002 and 2003), a scheme has been generated to explain DSMC differentiation (McCarthy et al 2003). The smooth muscle differentiation occurs at the periphery first. Two possible hypotheses can explain the pattern of DSM maturation:

1) Centripetal hypothesis This requires an initial signalling event between the urothelium and primitive mesenchyme, which causes the mesenchyme to start differentiating at the periphery of the bladder. Baskin et al (1996b) propose a role for the serosa, sensitising the peripheral cells to subsequent epithelial signals. These smooth muscle pre-cursor cells then differentiate and acquire the markers of the smooth muscle phenotype: (αSMA, desmin, myosin, vimentin) Baskin et al (1996c). These cells proliferate, the zone of differentiation spreading 'centripetally' towards the centre of the bladder. The bladder of figure 1 would appear with differentiated smooth muscle cells extending from the periphery towards the lamina propria.

2) Centrifugal hypothesis Mesenchymal/epithelial interaction induces laminin-1 expression in the basement membrane. This causes spreading and proliferation of mesenchymal cells in a similar way to myogenesis in the lung-bud (Schuger et al 1997). These mesenchymal 'stem cells' would proliferate producing a 'transit amplifying' population of smooth muscle precursor cells. These would be pushed 'centrifugally', outwards, by continued production of

more smooth muscle precursor cells by the mesenchymal 'stem cells' underneath them. Mesenchymal-epithelial interaction therefore has acted locally to induce mesenchymal proliferation; cells proliferate causing centrifugal/outwards movement of the most mature of these, which then differentiate at the periphery of the bladder. It is at the periphery that smooth muscle markers first become detectable. These ultimately will mature into adult smooth muscle cells, from the periphery inwards. This fits with the progressive thinning of the lamina propria layer we see as maturation progresses. It can be speculated that the transit amplifying cells in the lamina propria are not exposed to the same differentiation signals as those in the detrusor layer and so differentiate into fibroblasts. Similarly those cells in the interfascicular regions, between the muscle bundles of the detrusor may experience different cues and become fibroblasts.

Role of Fibronectin

Whether these cells arrived by a centrifugal or centripetal pattern of growth, it can be hypothesized that the fetal smooth muscle cell phenotype is dependent on fibronectin expression. These cells are capable of further proliferation, particularly in response to stretch, and synthesis of more basal lamina components. As they mature the DSM cells change from the fetal to the adult phenotype with a loss of synthetic capability, become non-proliferative, and increasingly contractile. Associated with this is a replacement of the basal lamina fibronectin by laminin reinforcing this

phenotype switch to a fully differentiated form. Integrins mediate this ECM ligand signal to the muscle cells.

This hypothetical model for the role of extracellular matrix in bladder development might also shed light on the pathological changes in congenital bladder outflow obstruction.

In congenital bladder outflow obstruction, the bladder wall is 'over-stretched' and damaged. It can be speculated that fibronectin is deposited at the site of tissue damage. From the cell culture experiments described in the introduction this would encourage the fetal smooth muscle cells to maintain this phenotype: that is a synthetic, proliferative phenotype that continues to produce ECM components and more smooth muscle cells. The result could be the thick walled, fibrotic, poorly compliant, dysfunctional valve bladder that is commonly seen in posterior urethral valves.

This could led on to a further questions:

Is fibronectin expression increased in bladder outflow obstruction?

In the human fetal bladder outflow obstruction fetuses examined, loss of smooth muscle cells in the most severely abnormal bladders was associated with loss of the basal lamina fibronectin. It was not possible to comment on whether detrusor hyperplasia and hypertrophy might be associated with increased fibronectin expression in the basal lamina, in an initial response to BOO.

Are the adult smooth muscle cells capable of proliferation?

This could be tested by generating primary cultures of adult mouse bladders and characterising the phenotypes of the cells that become proliferative, when these cells are grown on an appropriate substrate (e.g. fibronectin) in an appropriate growth medium.

Normal and pathological human fetal bladder development

During normal human bladder development DSMC proliferate and hypertrophy in close association with fibronectin. However the proliferative synergy between fibronectin substrate and FCS does not appear to happen, the increasing fibronectin instead being associated with increased maturation.

In human fetal bladder outlet obstruction, there is a spectrum of bladder responses: at one extreme, increased detrusor fibronectin was associated with more normal muscle morphology, and the most normal kidneys. Reduced detrusor fibronectin was associated with disrupted muscle morphology and with increased renal abnormalities. In could be speculated that this spectrum of abnormalities may represent a progression from compensation to decompensation.

Future work

The role of fibronectin in maintenance of fetal smooth muscle cell phenotype needs elucidating. Using the explant model of fetal bladder maturation might allow this to be determined using other strategies such as the use of RGD / RAD oligopeptides to block fibronectin receptors, and the use of RNA interference techniques to 'turn off' fibronectin expression – as described by Sakai et al (2003), or downregulate integrin α5, or indeed α7 expression.

What happens on maturation of the detrusor post-natally? How does the change from a fibronectin rich basal lamina to a laminin rich milieu occur, and does this influence DSM maturation?

What is the biochemical pathway that leads to bladder decompensation? Is this a result of increasing ischaemia in the bladder wall? Perhaps the ex-vivo fetal bladder explants could elucidate the mechanism. Work subsequently has shown that vascular endothelial growth factor (upregulated in ischaemia), increases the smooth muscle mass of fetal murine bladders by a combination of increasing proliferation and inhibiting apoptosis (Burgu et al 2006).

Is the pattern of fetal bladder growth in response to presumed BOO compensation / decompensation or is it a progressive dysplasia? A dynamic fetal animal model, demonstrating if compensation followed by decompensation does occur in the fetal bladder, would be necessary (Nyirady et al 2002; Thiruchelvam et al 2003; Farrugia et al 2006b, a). This model may allow an evaluation of the effect of timing of a fetal intervention such as

vesico-amniotic shunt placement – on renal preservation and recovery, or otherwise of fetal bladder function

Prospective studies to identify failing bladders, is lamina propria thickness a marker? Use of high resolution cross-sectional imaging may in the future be able to use the increase in thickness of the lamina propria as a marker for worsening bladder state.

Conclusion

The extracellular matrix has a hierarchical structure: structural collagens link to the basal lamina, which in turn connects to the cell surface via integrins. Components of the basal lamina such as laminin and fibronectin have not just a supportive function but are also have an instructive role in determining smooth muscle differentiation in the bladder. This signal is mediated by integrins. ECM, growth factors and integrins are an essential part of the story, and epithelial mesenchymal interactions, irrespective of how they are mediated, are crucial to this process. In human fetal bladder outlet obstruction, there is a spectrum of bladder responses: at one extreme, increased detrusor fibronectin was associated with more normal muscle morphology, and the most normal kidneys. Reduced detrusor fibronectin was associated with disrupted muscle morphology, loss of muscle and increased fibrosis, and with increased renal abnormalities.

Specifically the following have been shown:

1) Fibronectin and the candidate integrin receptor (α5β1) used in this study change in a coordinated manner during mouse bladder maturation, allowing for a possible instructive role in development.
2) Laminins, specifically laminin-1 and laminin-2/4, are upregulated in very similar pattern to integrin α7- subunit, the candidate muscle laminin receptor, during mouse bladder development.
3) Fetal mouse DSMC expressed integrin α5, β1 and desmin. Blocking integrin receptors using RGD oligopeptides not only decreased desmin positive cell adhesion, but also reduced cell spreading. Fibronectin and serum had a synergistic effect on proliferation of bladder cells. Thus, integrin α5β1 could mediate adhesion of fetal DSMC to fibronectin, and could potentially mediate a proliferative signal from fibronectin to these cells.
4) Established serum free, antibiotic free defined culture conditions for ex-vivo fetal bladder explant differentiation.
5) During normal human bladder development DSMC are in close association with fibronectin.
6) In human fetal presumed bladder outlet obstruction, there is a spectrum of bladder phenotypes: at one extreme, more detrusor fibronectin was associated with more normal muscle morphology and the most normal kidneys. Less detrusor fibronectin was associated with disrupted muscle morphology, loss of muscle and increased fibrosis, and with increased renal abnormalities.
7) In fetal presumed BOO, the lamina propria is apparently disproportionately thickened.

References

Abbott JF, Levine D, and Wapner R. Posterior urethral valves: inaccuracy of prenatal diagnosis. *Fetal Diagn Ther* 13: 179-183, 1998.

Adair BD, Xiong JP, Maddock C, Goodman SL, Arnaout MA, and Yeager M. Three-dimensional EM structure of the ectodomain of integrin αVβ3 in a complex with fibronectin. *J Cell Biol* 168: 1109-1118, 2005.

Adams JC and Watt FM. Expression of β1, β3, β4, and β5 integrins by human epidermal keratinocytes and non-differentiating keratinocytes. *J Cell Biol* 115: 829-841, 1991.

Aguirre KM, McCormick RJ, and Schwarzbauer JE. Fibronectin self-association is mediated by complementary sites within the amino-terminal one-third of the molecule. *J Biol Chem* 269: 27863-27868, 1994.

Aguzzi MS, Giampietri C, De Marchis F, Padula F, Gaeta R, Ragone G, Capogrossi MC, and Facchiano A. RGDS peptide induces caspase 8 and caspase 9 activation in human endothelial cells. *Blood* 103: 4180-4187, 2004.

Akagi T, Murata K, Shishido T, and Hanafusa H. v-Crk activates the phosphoinositide 3-kinase/AKT pathway by utilizing focal adhesion kinase and H-Ras. *Mol Cell Biol* 22: 7015-7023, 2002.

Alberts B, Bray D, Lewis J, Raff M, Roberts K, and Watson J. Chapter 19: Cell Junctions, Cell Adhesion, and the Extracellular Matrix. In: *Molecular Biology of the Cell*: Garland Publishing, 1994, p. 950.

Alenghat FJ and Ingber DE. Mechanotransduction: all signals point to cytoskeleton, matrix, and integrins. *Sci STKE: 2002(119): PE6.*

Ali IU, Mautner V, Lanza R, and Hynes RO. Restoration of normal morphology, adhesion and cytoskeleton in transformed cells by addition of a transformation-sensitive surface protein. *Cell* 11: 115-126, 1977.

Amano M, Ito M, Kimura K, Fukata Y, Chihara K, Nakano T, Matsuura Y, and Kaibuchi K. Phosphorylation and activation of myosin by Rho-associated kinase (Rho-kinase). *J Biol Chem* 271: 20246-20249, 1996.

Andac Z, Sasaki T, Mann K, Brancaccio A, Deutzmann R, and Timpl R. Analysis of heparin, α-dystroglycan and sulfatide binding to the G domain of the laminin α1 chain by site-directed mutagenesis. *J Mol Biol* 287: 253-264, 1999.

Aota S, Nagai T, and Yamada KM. Characterization of regions of fibronectin besides the arginine-glycine-aspartic acid sequence required for adhesive function of the cell-binding domain using site-directed mutagenesis. *J Biol Chem* 266: 15938-15943, 1991.

Aslan AR and Kogan BA. The effect of bladder outlet obstruction on the developing kidney. *BJU Int* 92 Suppl 1: 38-41, 2003.

Aumailley M, Battaglia C, Mayer U, Reinhardt D, Nischt R, Timpl R, and Fox JW. Nidogen mediates the formation of ternary complexes of basement membrane components. *Kidney Int* 43: 7-12, 1993.

Aumailley M, Timpl R, and Sonnenberg A. Antibody to integrin α6 subunit specifically inhibits cell-binding to laminin fragment 8. *Exp Cell Res* 188: 55-60, 1990.

Backhaus BO, Kaefer M, Haberstroh KM, Hile K, Nagatomi J, Rink RC, Cain MP, Casale A, and Bizios R. Alterations in the molecular determinants of bladder compliance at hydrostatic pressures less than 40 cm. H2O. *J Urol* 168: 2600-2604, 2002.

Balaban NQ, Schwarz US, Riveline D, Goichberg P, Tzur G, Sabanay I, Mahalu D, Safran S, Bershadsky A, Addadi L, and Geiger B. Force and focal

adhesion assembly: a close relationship studied using elastic micropatterned substrates. *Nat Cell Biol* 3: 466-472, 2001.

Baneyx G, Baugh L, and Vogel V. Coexisting conformations of fibronectin in cell culture imaged using fluorescence resonance energy transfer. *Proc Natl Acad Sci USA* 98: 14464-14468, 2001.

Baneyx G, Baugh L, and Vogel V. Fibronectin extension and unfolding within cell matrix fibrils controlled by cytoskeletal tension. *Proc Natl Acad Sci USA* 99: 5139-5143, 2002.

Banks RE, Craven RA, Harnden PA, and Selby PJ. Use of a sensitive EnVision +-based detection system for Western blotting: avoidance of streptavidin binding to endogenous biotin and biotin-containing proteins in kidney and other tissues. *Proteomics* 3: 558-561, 2003.

Barcellos-Hoff MH, Aggeler J, Ram TG, and Bissell MJ. Functional differentiation and alveolar morphogenesis of primary mammary cultures on reconstituted basement membrane. *Development* 105: 223-235, 1989.

Baron MD, Davison MD, Jones P, and Critchley DR. The sequence of chick α-actinin reveals homologies to spectrin and calmodulin. *J Biol Chem* 262: 17623-17629, 1987.

Baskin L, Howard PS, and Macarak E. Effect of physical forces on bladder smooth muscle and urothelium. *J Urol* 150: 601-607, 1993a.

Baskin LS, Howard PS, Duckett JW, Snyder HM, and Macarak EJ. Bladder smooth muscle cells in culture: I. Identification and characterization. *J Urol* 149: 190-197, 1993b.

Baskin LS, Hayward SW, Sutherland RA, DiSandro MJ, Thomson AA, Goodman J, and Cunha GR. Mesenchymal-epithelial interactions in the bladder. *World J Urol* 14: 301-309, 1996a.

Baskin LS, Hayward SW, Young P, and Cunha GR. Role of mesenchymal-epithelial interactions in normal bladder development. *J Urol* 156: 1820-1827, 1996b.

Baskin LS, Hayward SW, Young PF, and Cunha GR. Ontogeny of the rat bladder: smooth muscle and epithelial differentiation. *Acta Anat (Basel)* 155: 163-171, 1996c.

Batourina E, Tsai S, Lambert S, Sprenkle P, Viana R, Dutta S, Hensle T, Wang F, Niederreither K, McMahon AP, Carroll TJ, and Mendelsohn CL. Apoptosis induced by vitamin A signaling is crucial for connecting the ureters to the bladder. *Nat Genet* 37: 1082-1089, 2005.

Beauboeuf A, Ordille S, Erickson DR, and Ehrlich HP. In vitro ligation of ureters and urethra modulates fetal mouse bladder explants development. *Tissue Cell* 30: 531-536, 1998.

Beck K, Dixon TW, Engel J, and Parry DA. Ionic interactions in the coiled-coil domain of laminin determine the specificity of chain assembly. *J Mol Biol* 231: 311-323, 1993.

Begg RC. The urachus: its anatomy, histology and development. *J Anatomy* 64: 170-183, 1930.

Belal M and Abrams P. Noninvasive methods of diagnosing bladder outlet obstruction in men. Part 2: Noninvasive urodynamics and combination of measures. *J Urol* 176: 29-35, 2006.

Bhatt A, Kaverina I, Otey C, and Huttenlocher A. Regulation of focal complex composition and disassembly by the calcium-dependent protease calpain. *J Cell Sci* 115: 3415-3425, 2002.

Bitgood MJ and McMahon AP. Hedgehog and Bmp genes are coexpressed at many diverse sites of cell-cell interaction in the mouse embryo. *Dev Biol* 172: 126-138, 1995.

Bosman FT and Stamenkovic I. Functional structure and composition of the extracellular matrix. *J Pathol* 200: 423-428, 2003.

Bourdoulous S, Orend G, MacKenna DA, Pasqualini R, and Ruoslahti E. Fibronectin matrix regulates activation of RHO and CDC42 GTPases and cell cycle progression. *J Cell Biol* 143: 267-276, 1998.

Brakebusch C and Fassler R. The integrin-actin connection, an eternal love affair. *EMBO J* 22: 2324-2333, 2003.

Brauer PR and Keller JM. Ultrastructure of a model basement membrane lacking type IV collagen. *Anat Rec* 223: 376-383, 1989.

Brotschi EA, Hartwig JH, and Stossel TP. The gelation of actin by actin-binding protein. *J Biol Chem* 253: 8988-8993, 1978.

Brown MC, Curtis MS, and Turner CE. Paxillin LD motifs may define a new family of protein recognition domains. *Nat Struct Biol* 5: 677-678, 1998.

Brown MC and Turner CE. Paxillin: adapting to change. *Physiol Rev* 84: 1315-1339, 2004.

Brown NH, Gregory SL, Rickoll WL, Fessler LI, Prout M, White RA, and Fristrom JW. Talin is essential for integrin function in Drosophila. *Dev Cell* 3: 569-579, 2002.

Brugnera E, Haney L, Grimsley C, Lu M, Walk SF, Tosello-Trampont AC, Macara IG, Madhani H, Fink GR, and Ravichandran KS. Unconventional Rac-GEF activity is mediated through the Dock180-ELMO complex. *Nat Cell Biol* 4: 574-582, 2002.

Bultmann H, Santas AJ, and Peters DM. Fibronectin fibrillogenesis involves the heparin II binding domain of fibronectin. *J Biol Chem* 273: 2601-2609, 1998.

Buoro S, Ferrarese P, Chiavegato A, Roelofs M, Scatena M, Pauletto P, Passerini-Glazel G, Pagano F, and Sartore S. Myofibroblast-derived smooth

muscle cells during remodelling of rabbit urinary bladder wall induced by partial outflow obstruction. *Lab Invest* 69: 589-602, 1993.

Burgeson RE, Chiquet M, Deutzmann R, Ekblom P, Engel J, Kleinman H, Martin GR, Meneguzzi G, Paulsson M, Sanes J, and et al A new nomenclature for the laminins. *Matrix Biol* 14: 209-211, 1994.

Burgu B, McCarthy LS, Shah V, Long DA, Wilcox DT, and Woolf AS. Vascular endothelial growth factor stimulates embryonic urinary bladder development in organ culture. *BJU Int* 98: 217-225, 2006.

Burkin DJ, Wallace GQ, Nicol KJ, Kaufman DJ, and Kaufman SJ. Enhanced expression of the $\alpha 7\beta 1$ integrin reduces muscular dystrophy and restores viability in dystrophic mice. *J Cell Biol* 152: 1207-1218, 2001.

Burridge K and Feramisco JR. Non-muscle αactinins are calcium-sensitive actin-binding proteins. *Nature* 294: 565-567, 1981.

Busby TF, Argraves WS, Brew SA, Pechik I, Gilliland GL, and Ingham KC. Heparin binding by fibronectin module III-13 involves six discontinuous basic residues brought together to form a cationic cradle. *J Biol Chem* 270: 18558-18562, 1995.

Buttyan R, Chen MW, and Levin RM. Animal models of bladder outlet obstruction and molecular insights into the basis for the development of bladder dysfunction. *Eur Urol* 32 Suppl 1: 32-39, 1997.

Calalb MB, Polte TR, and Hanks SK. Tyrosine phosphorylation of focal adhesion kinase at sites in the catalytic domain regulates kinase activity: a role for Src family kinases. *Mol Cell Biol* 15: 954-963, 1995.

Calderwood DA, Yan B, de Pereda JM, Alvarez BG, Fujioka Y, Liddington RC, and Ginsberg MH. The phosphotyrosine binding-like domain of talin activates integrins. *J Biol Chem* 277: 21749-21758, 2002.

Calderwood DA, Zent R, Grant R, Rees DJ, Hynes RO, and Ginsberg MH. The Talin head domain binds to integrin βsubunit cytoplasmic tails and regulates integrin activation. *J Biol Chem* 274: 28071-28074, 1999.

Capolicchio G, Aitken KJ, Gu JX, Reddy P, and Bagli DJ. Extracellular matrix gene responses in a novel ex vivo model of bladder stretch injury. *J Urol* 165: 2235-2240, 2001.

Caputi M, Melo CA, and Baralle FE. Regulation of fibronectin expression in rat regenerating liver. *Nucleic Acids Res* 23: 238-243, 1995.

Cary LA, Han DC, Polte TR, Hanks SK, and Guan JL. Identification of p130Cas as a mediator of focal adhesion kinase-promoted cell migration. *J Cell Biol* 140: 211-221, 1998.

Cattelino A, Albertinazzi C, Bossi M, Critchley DR, and de Curtis I. A cell-free system to study regulation of focal adhesions and of the connected actin cytoskeleton. *Mol Biol Cell* 10: 373-391, 1999.

Chang SL, Howard PS, Koo HP, and Macarak EJ. Role of type III collagen in bladder filling. *Neurourol Urodyn* 17: 135-145, 1998.

Chen CS, Mrksich M, Huang S, Whitesides GM, and Ingber DE. Geometric control of cell life and death. *Science* 276: 1425-1428, 1997.

Chen H, Huang XN, Stewart AF, and Sepulveda JL. Gene expression changes associated with fibronectin-induced cardiac myocyte hypertrophy. *Physiol Genomics* 18: 273-283, 2004.

Chen H and Mosher DF. Formation of sodium dodecyl sulfate-stable fibronectin multimers. Failure to detect products of thiol-disulfide exchange in cyanogen bromide or limited acid digests of stabilized matrix fibronectin. *J Biol Chem* 271: 9084-9089, 1996.

Cheng YS, Champliaud MF, Burgeson RE, Marinkovich MP, and Yurchenco PD. Self-assembly of laminin isoforms. *J Biol Chem* 272: 31525-31532, 1997.

Chicurel ME, Singer RH, Meyer CJ, and Ingber DE. Integrin binding and mechanical tension induce movement of mRNA and ribosomes to focal adhesions. *Nature* 392: 730-733, 1998.

Choquet D, Felsenfeld DP, and Sheetz MP. Extracellular matrix rigidity causes strengthening of integrin-cytoskeleton linkages. *Cell* 88: 39-48, 1997.

Christerson LB, Vanderbilt CA, and Cobb MH. MEKK1 interacts with α-actinin and localizes to stress fibers and focal adhesions. *Cell Motil Cytoskeleton* 43: 186-198, 1999.

Chrzanowska-Wodnicka M and Burridge K. Rho-stimulated contractility drives the formation of stress fibers and focal adhesions. *J Cell Biol* 133: 1403-1415, 1996.

Chung AE, Jaffe R, Freeman IL, Vergnes JP, Braginski JE, and Carlin B. Properties of a basement membrane-related glycoprotein synthesized in culture by a mouse embryonal carcinoma-derived cell line. *Cell* 16: 277-287, 1979.

Cilento BG, Jr., Bauer SB, Retik AB, Peters CA, and Atala A. Urachal anomalies: defining the best diagnostic modality. *Urology* 52: 120-122, 1998.

Clark TJ, Martin WL, Divakaran TG, Whittle MJ, Kilby MD, and Khan KS. Prenatal bladder drainage in the management of fetal lower urinary tract obstruction: a systematic review and meta-analysis. *Obstet Gynecol* 102: 367-382, 2003.

Colognato H, MacCarrick M, O'Rear JJ, and Yurchenco PD. The laminin α2-chain short arm mediates cell adhesion through both the α1β1 and α2β1 integrins. *J Biol Chem* 272: 29330-29336, 1997.

Colognato H, Winkelmann DA, and Yurchenco PD. Laminin polymerization induces a receptor-cytoskeleton network. *J Cell Biol* 145: 619-631, 1999.

Colognato H and Yurchenco PD. Form and function: the laminin family of heterotrimers. *Dev Dyn* 218: 213-234, 2000.

Chicurel ME, Singer RH, Meyer CJ, and Ingber DE. Integrin binding and mechanical tension induce movement of mRNA and ribosomes to focal adhesions. *Nature* 392: 730-733, 1998.

Choquet D, Felsenfeld DP, and Sheetz MP. Extracellular matrix rigidity causes strengthening of integrin-cytoskeleton linkages. *Cell* 88: 39-48, 1997.

Christerson LB, Vanderbilt CA, and Cobb MH. MEKK1 interacts with α-actinin and localizes to stress fibers and focal adhesions. *Cell Motil Cytoskeleton* 43: 186-198, 1999.

Chrzanowska-Wodnicka M and Burridge K. Rho-stimulated contractility drives the formation of stress fibers and focal adhesions. *J Cell Biol* 133: 1403-1415, 1996.

Chung AE, Jaffe R, Freeman IL, Vergnes JP, Braginski JE, and Carlin B. Properties of a basement membrane-related glycoprotein synthesized in culture by a mouse embryonal carcinoma-derived cell line. *Cell* 16: 277-287, 1979.

Cilento BG, Jr., Bauer SB, Retik AB, Peters CA, and Atala A. Urachal anomalies: defining the best diagnostic modality. *Urology* 52: 120-122, 1998.

Clark TJ, Martin WL, Divakaran TG, Whittle MJ, Kilby MD, and Khan KS. Prenatal bladder drainage in the management of fetal lower urinary tract obstruction: a systematic review and meta-analysis. *Obstet Gynecol* 102: 367-382, 2003.

Colognato H, MacCarrick M, O'Rear JJ, and Yurchenco PD. The laminin α2-chain short arm mediates cell adhesion through both the α1β1 and α2β1 integrins. *J Biol Chem* 272: 29330-29336, 1997.

Colognato H, Winkelmann DA, and Yurchenco PD. Laminin polymerization induces a receptor-cytoskeleton network. *J Cell Biol* 145: 619-631, 1999.

Colognato H and Yurchenco PD. Form and function: the laminin family of heterotrimers. *Dev Dyn* 218: 213-234, 2000.

Colognato-Pyke H, O'Rear JJ, Yamada Y, Carbonetto S, Cheng YS, and Yurchenco PD. Mapping of network-forming, heparin-binding, and α1β1 integrin-recognition sites within the α-chain short arm of laminin-1. *J Biol Chem* 270: 9398-9406, 1995.

Coppolino M, Leung-Hagesteijn C, Dedhar S, and Wilkins J. Inducible interaction of integrin α2β1 with calreticulin. Dependence on the activation state of the integrin. *J Biol Chem* 270: 23132-23138, 1995.

Costell M, Gustafsson E, Aszodi A, Morgelin M, Bloch W, Hunziker E, Addicks K, Timpl R, and Fassler R. Perlecan maintains the integrity of cartilage and some basement membranes. *J Cell Biol* 147: 1109-1122, 1999.

Cote PD, Moukhles H, Lindenbaum M, and Carbonetto S. Chimaeric mice deficient in dystroglycans develop muscular dystrophy and have disrupted myoneural synapses. *Nat Genet* 23: 338-342, 1999.

Cram EJ, Clark SG, and Schwarzbauer JE. Talin loss-of-function uncovers roles in cell contractility and migration in C. elegans. *J Cell Sci* 116: 3871-3878, 2003.

Crombleholme TM, Harrison MR, Golbus MS, Longaker MT, Langer JC, Callen PW, Anderson RL, Goldstein RB, and Filly RA. Fetal intervention in obstructive uropathy: prognostic indicators and efficacy of intervention. *Am J Obstet Gynecol* 162: 1239-1244, 1990.

Cukierman E, Pankov R, Stevens DR, and Yamada KM. Taking cell-matrix adhesions to the third dimension. *Science* 294: 1708-1712, 2001.

D'Amico M, Hulit J, Amanatullah DF, Zafonte BT, Albanese C, Bouzahzah B, Fu M, Augenlicht LH, Donehower LA, Takemaru K, Moon RT, Davis R, Lisanti MP, Shtutman M, Zhurinsky J, Ben-Ze'ev A, Troussard AA, Dedhar S, and Pestell RG. The integrin-linked kinase regulates the cyclin D1 gene through glycogen synthase kinase 3β and cAMP-responsive element-binding protein-dependent pathways. *J Biol Chem* 275: 32649-32657, 2000.

Dabrowska R, Goch A, Osinska H, Szpacenko A, and Sosinski J. Dual effect of filamin on actomyosin ATPase activity. *J Muscle Res Cell Motil* 6: 29-42, 1985.

Davis BJ. Disc Electrophoresis. Ii. Method and Application to Human Serum Proteins. *Ann N Y Acad Sci* 121: 404-427, 1964.

Dawid IB, Breen JJ, and Toyama R. LIM domains: multiple roles as adapters and functional modifiers in protein interactions. *Trends Genet* 14: 156-162, 1998.

De Arcangelis A and Georges-Labouesse E. Integrin and ECM functions: roles in vertebrate development. *Trends Genet* 16: 389-395, 2000.

de Kort LM, Uiterwaal CS, Beek EJ, Jan Nievelstein RA, Klijn AJ, and de Jong TP. Reliability of voiding cystourethrography to detect urethral obstruction in boys. *Urology* 63: 967-971, 2004.

De La Rosette J, Smedts F, Schoots C, Hoek H, and Laguna P. Changing patterns of keratin expression could be associated with functional maturation of the developing human bladder. *J Urol* 168: 709-717, 2002.

DeSimone DW, Norton PA, and Hynes RO. Identification and characterization of alternatively spliced fibronectin mRNAs expressed in early Xenopus embryos. *Dev Biol* 149: 357-369, 1992.

Dzamba BJ, Bultmann H, Akiyama SK, and Peters DM. Substrate-specific binding of the amino terminus of fibronectin to an integrin complex in focal adhesions. *J Biol Chem* 269: 19646-19652, 1994.

Eble JA, Wucherpfennig KW, Gauthier L, Dersch P, Krukonis E, Isberg RR, and Hemler ME. Recombinant soluble human $\alpha 3\beta 1$ integrin: purification, processing, regulation, and specific binding to laminin-5 and invasin in a mutually exclusive manner. *Biochemistry* 37: 10945-10955, 1998.

Elices MJ, Urry LA, and Hemler ME. Receptor functions for the integrin VLA-3: fibronectin, collagen, and laminin binding are differentially influenced by Arg-Gly-Asp peptide and by divalent cations. *J Cell Biol* 112: 169-181, 1991.

Engvall E and Ruoslahti E. Binding of soluble form of fibroblast surface protein, fibronectin, to collagen. *Int J Cancer* 20: 1-5, 1977.

Ewalt DH, Howard PS, Blyth B, Snyder HM, III, Duckett JW, Levin RM, and Macarak EJ. Is lamina propria matrix responsible for normal bladder compliance? *J Urol* 148: 544-549, 1992.

Eyden B. The myofibroblast: an assessment of controversial issues and a definition useful in diagnosis and research. *Ultrastruct Pathol* 25: 39-50, 2001.

Farrugia MK, Long DA, Godley ML, Peebles DM, Fry CH, Cuckow PM, and Woolf AS. Experimental short-term fetal bladder outflow obstruction: I. Morphology and cell biology associated with urinary flow impairment. *Journal of Pediatric urology* 2: 243-253, 2006a.

Farrugia MK, Long DA, Godley ML, Peebles DM, Fry CH, Cuckow PM, and Woolf AS. Experimental short-term fetal bladder outflow obstruction: II. Compliance and contractility associated with urinary flow impairment. *Journal of Pediatric urology* 2: 254-260, 2006b.

Ffrench-Constant C. Alternative splicing of fibronectin--many different proteins but few different functions. *Exp Cell Res* 221: 261-271, 1995.

Ffrench-Constant C and Hynes RO. Alternative splicing of fibronectin is temporally and spatially regulated in the chicken embryo. *Development* 106: 375-388, 1989.

Ffrench-Constant C, Van de Water L, Dvorak HF, and Hynes RO. Reappearance of an embryonic pattern of fibronectin splicing during wound healing in the adult rat. *J Cell Biol* 109: 903-914, 1989.

Fogerty FJ, Akiyama SK, Yamada KM, and Mosher DF. Inhibition of binding of fibronectin to matrix assembly sites by anti-integrin ($\alpha5\beta1$) antibodies. *J Cell Biol* 111: 699-708, 1990.

Fox JW, Mayer U, Nischt R, Aumailley M, Reinhardt D, Wiedemann H, Mann K, Timpl R, Krieg T, Engel J, and et al Recombinant nidogen consists of three globular domains and mediates binding of laminin to collagen type IV. *Embo J* 10: 3137-3146, 1991.

Freedman AL, Qureshi F, Shapiro E, Lepor H, Jacques SM, Evans MI, Smith CA, Gonzalez R, and Johnson MP. Smooth muscle development in the obstructed fetal bladder. *Urology* 49: 104-107, 1997.

Fukuda T, Yoshida N, Kataoka Y, Manabe R, Mizuno-Horikawa Y, Sato M, Kuriyama K, Yasui N, and Sekiguchi K. Mice lacking the EDB segment of fibronectin develop normally but exhibit reduced cell growth and fibronectin matrix assembly in vitro. *Cancer Res* 62: 5603-5610, 2002.

Gabbiani G. The myofibroblast in wound healing and fibrocontractive diseases. *J Pathol* 200: 500-503, 2003.

Galbraith CG, Yamada KM, and Sheetz MP. The relationship between force and focal complex development. *J Cell Biol* 159: 695-705, 2002.

Garcia AJ, Schwarzbauer JE, and Boettiger D. Distinct activation states of $\alpha5\beta1$ integrin show differential binding to RGD and synergy domains of fibronectin. *Biochemistry* 41: 9063-9069, 2002.

Garcia-Alvarez B, de Pereda JM, Calderwood DA, Ulmer TS, Critchley D, Campbell ID, Ginsberg MH, and Liddington RC. Structural determinants of integrin recognition by talin. *Mol Cell* 11: 49-58, 2003.

Gardner H, Kreidberg J, Koteliansky V, and Jaenisch R. Deletion of integrin $\alpha1$ by homologous recombination permits normal murine development but gives rise to a specific deficit in cell adhesion. *Dev Biol* 175: 301-313, 1996.

George EL, Georges-Labouesse EN, Patel-King RS, Rayburn H, and Hynes RO. Defects in mesoderm, neural tube and vascular development in mouse embryos lacking fibronectin. *Development* 119: 1079-1091, 1993.

Georges-Labouesse E, Messaddeq N, Yehia G, Cadalbert L, Dierich A, and Le Meur M. Absence of integrin α6 leads to epidermolysis bullosa and neonatal death in mice. *Nat Genet* 13: 370-373, 1996.

Ghafar MA, Anastasiadis AG, Olsson LE, Chichester P, Kaplan SA, Buttyan R, and Levin RM. Hypoxia and an angiogenic response in the partially obstructed rat bladder. *Lab Invest* 82: 903-909, 2002.

Giannone G, Jiang G, Sutton DH, Critchley DR, and Sheetz MP. Talin1 is critical for force-dependent reinforcement of initial integrin-cytoskeleton bonds but not tyrosine kinase activation. *J Cell Biol* 163: 409-419, 2003.

Gilbert T, Gaonach S, Moreau E, and Merlet-Benichou C. Defect of nephrogenesis induced by gentamicin in rat metanephric organ culture. *Lab Invest* 70: 656-666, 1994.

Gilpin SA, Gosling JA, and Barnard RJ. Morphological and morphometric studies of the human obstructed, trabeculated urinary bladder. *Br J Urol* 57: 525-529, 1985.

Ginsberg M, Pierschbacher MD, Ruoslahti E, Marguerie G, and Plow E. Inhibition of fibronectin binding to platelets by proteolytic fragments and synthetic peptides which support fibroblast adhesion. *J Biol Chem* 260: 3931-3936, 1985.

Glenney JR, Jr. and Zokas L. Novel tyrosine kinase substrates from Rous sarcoma virus-transformed cells are present in the membrane skeleton. *J Cell Biol* 108: 2401-2408, 1989.

Glick PL, Harrison MR, Golbus MS, Adzick NS, Filly RA, Callen PW, Mahony BS, Anderson RL, and deLorimier AA. Management of the fetus with congenital hydronephrosis II: Prognostic criteria and selection for treatment. *J Pediatr Surg* 20: 376-387, 1985.

Godley ML, Desai D, Yeung CK, Dhillon HK, Duffy PG, and Ransley PG. The relationship between early renal status, and the resolution of vesico-ureteric reflux and bladder function at 16 months. *BJU Int* 87: 457-462, 2001.

Gonzales ET, Walsh, Retick, Vaughan, and Wein. Posterior Urethral valves and other urethral anomalies. In: *Campbell's Urology*: Saunders, 2004.

Gonzalez R, De Filippo R, Jednak R, and Barthold JS. Urethral atresia: long-term outcome in 6 children who survived the neonatal period. *J Urol* 165: 2241-2244, 2001.

Gorlin JB, Yamin R, Egan S, Stewart M, Stossel TP, Kwiatkowski DJ, and Hartwig JH. Human endothelial actin-binding protein (ABP-280, nonmuscle filamin): a molecular leaf spring. *J Cell Biol* 111: 1089-1105, 1990.

Gosling JA and Dixon JS. Structure of trabeculated detrusor smooth muscle in cases of prostatic hypertrophy. *Urol Int* 35: 351-355, 1980.

Greenwood JA, Theibert AB, Prestwich GD, and Murphy-Ullrich JE. Restructuring of focal adhesion plaques by PI 3-kinase. Regulation by PtdIns (3,4,5)-p(3) binding to α-actinin. *J Cell Biol* 150: 627-642, 2000.

Grinnell F, Ho CH, Tamariz E, Lee DJ, and Skuta G. Dendritic fibroblasts in three-dimensional collagen matrices. *Mol Biol Cell* 14: 384-395, 2003.

Grossman HB, Lee C, Bromberg J, and Liebert M. Expression of the α6β4 integrin provides prognostic information in bladder cancer. *Oncol Rep* 7: 13-16, 2000.

Guo L, Sanders PW, Woods A, and Wu C. The distribution and regulation of integrin-linked kinase in normal and diabetic kidneys. *Am J Pathol* 159: 1735-1742, 2001.

Guo XD, Johnson JJ, and Kramer JM. Embryonic lethality caused by mutations in basement membrane collagen of C. elegans. *Nature* 349: 707-709, 1991.

Haberstroh KM, Kaefer M, DePaola N, Frommer SA, and Bizios R. A novel in-vitro system for the simultaneous exposure of bladder smooth muscle cells to mechanical strain and sustained hydrostatic pressure. *J Biomech Eng* 124: 208-213, 2002.

Haberstroh KM, Kaefer M, Retik AB, Freeman MR, and Bizios R. The effects of sustained hydrostatic pressure on select bladder smooth muscle cell functions. *J Urol* 162: 2114-2118, 1999.

Hagel M, George EL, Kim A, Tamimi R, Opitz SL, Turner CE, Imamoto A, and Thomas SM. The adaptor protein paxillin is essential for normal development in the mouse and is a critical transducer of fibronectin signaling. *Mol Cell Biol* 22: 901-915, 2002.

Han DC and Guan JL. Association of focal adhesion kinase with Grb7 and its role in cell migration. *J Biol Chem* 274: 24425-24430, 1999.

Hanai T, Ma FH, Matsumoto S, Park YC, and Kurita T. Partial outlet obstruction of the rat bladder induces a stimulatory response on proliferation of the bladder smooth muscle cells. *Int Urol Nephrol* 34: 37-42, 2002.

Handler M, Yurchenco PD, and Iozzo RV. Developmental expression of perlecan during murine embryogenesis. *Dev Dyn* 210: 130-145, 1997.

Hanks SK, Calalb MB, Harper MC, and Patel SK. Focal adhesion protein-tyrosine kinase phosphorylated in response to cell attachment to fibronectin. *Proc Natl Acad Sci U S A* 89: 8487-8491, 1992.

Hannigan GE, Leung-Hagesteijn C, Fitz-Gibbon L, Coppolino MG, Radeva G, Filmus J, Bell JC, and Dedhar S. Regulation of cell adhesion and anchorage-dependent growth by a new β1-integrin-linked protein kinase. *Nature* 379: 91-96, 1996.

Harte MT, Hildebrand JD, Burnham MR, Bouton AH, and Parsons JT. p130Cas, a substrate associated with v-Src and v-Crk, localizes to focal adhesions and binds to focal adhesion kinase. *J Biol Chem* 271: 13649-13655, 1996.

Hattori K, Mabuchi R, Fujiwara H, Sanzen N, Sekiguchi K, Kawai K, and Akaza H. Laminin expression patterns in human ureteral tissue. *J Urol* 170: 2040-2043, 2003.

Hayashi K, Madri JA, and Yurchenco PD. Endothelial cells interact with the core protein of basement membrane perlecan through β1 and β3 integrins: an adhesion modulated by glycosaminoglycan. *J Cell Biol* 119: 945-959, 1992.

Hayashi M, Schlesinger DH, Kennedy DW, and Yamada KM. Isolation and characterization of a heparin-binding domain of cellular fibronectin. *J Biol Chem* 255: 10017-10020, 1980.

Hayashi Y, Haimovich B, Reszka A, Boettiger D, and Horwitz A. Expression and function of chicken integrin β1 subunit and its cytoplasmic domain mutants in mouse NIH 3T3 cells. *J Cell Biol* 110: 175-184, 1990.

Hedin UL, Daum G, and Clowes AW. Disruption of integrin α5β1 signaling does not impair PDGF-BB-mediated stimulation of the extracellular signal-regulated kinase pathway in smooth muscle cells. *J Cell Physiol* 172: 109-116, 1997.

Heggeness MH, Ash JF, and Singer SJ. Transmembrane linkage of fibronectin to intracellular actin-containing filaments in cultured human fibroblasts. *Ann N Y Acad Sci* 312: 414-417, 1978.

Hengartner MO. The biochemistry of apoptosis. *Nature* 407: 770-776, 2000.

Hertle MD, Adams JC, and Watt FM. Integrin expression during human epidermal development in vivo and in vitro. *Development* 112: 193-206, 1991.

Hindermann W, Berndt A, Haas KM, Wunderlich H, Katenkamp D, and Kosmehl H. Immunohistochemical demonstration of the γ2 chain of laminin-5 in urinary bladder urothelial carcinoma. Impact for diagnosis and prognosis. *Cancer Detect Prev* 27: 109-115, 2003.

Hohenester E and Engel J. Domain structure and organisation in extracellular matrix proteins. *Matrix Biol* 21: 115-128, 2002.

Holmes N, Harrison MR, and Baskin LS. Fetal surgery for posterior urethral valves: long-term postnatal outcomes. *Pediatrics* 108: E7, 2001.

Hopf M, Gohring W, Kohfeldt E, Yamada Y, and Timpl R. Recombinant domain IV of perlecan binds to nidogens, laminin-nidogen complex, fibronectin, fibulin-2 and heparin. *Eur J Biochem* 259: 917-925, 1999.

Hopf M, Gohring W, Mann K, and Timpl R. Mapping of binding sites for nidogens, fibulin-2, fibronectin and heparin to different IG modules of perlecan. *J Mol Biol* 311: 529-541, 2001.

Hornberger LK, Singhroy S, Cavalle-Garrido T, Tsang W, Keeley F, and Rabinovitch M. Synthesis of extracellular matrix and adhesion through β1 integrins are critical for fetal ventricular myocyte proliferation. *Circ Res* 87: 508-515, 2000.

Huff S, Matsuka YV, McGavin MJ, and Ingham KC. Interaction of N-terminal fragments of fibronectin with synthetic and recombinant D motifs from its binding protein on Staphylococcus aureus studied using fluorescence anisotropy. *J Biol Chem* 269: 15563-15570, 1994.

Hughes AL. Evolution of the integrin α and β protein families. *J Mol Evol* 52: 63-72, 2001.

Humphries MJ. Insights into integrin-ligand binding and activation from the first crystal structure. *Arthritis Res* 4 Suppl 3: S69-78, 2002.

Hunter A, Kaufman MH, McKay A, Baldock R, Simmen MW, and Bard JB. An ontology of human developmental anatomy. *J Anat* 203: 347-355, 2003.

Hunter DD, Porter BE, Bulock JW, Adams SP, Merlie JP, and Sanes JR. Primary sequence of a motor neuron-selective adhesive site in the synaptic basal lamina protein S-laminin. *Cell* 59: 905-913, 1989.

Hutter H, Vogel BE, Plenefisch JD, Norris CR, Proenca RB, Spieth J, Guo C, Mastwal S, Zhu X, Scheel J, and Hedgecock EM. Conservation and novelty in

the evolution of cell adhesion and extracellular matrix genes. *Science* 287: 989-994, 2000.

Huuhtanen RL, Blomqvist CP, Wiklund TA, Bohling TO, Virolainen MJ, Tukiainen EJ, Tribukait B, and Andersson LC. Comparison of the Ki-67 score and S-phase fraction as prognostic variables in soft-tissue sarcoma. *Br J Cancer* 79: 945-951, 1999.

Hynes RO. Alteration of cell-surface proteins by viral transformation and by proteolysis. *Proc Natl Acad Sci U S A* 70: 3170-3174, 1973.

Hynes RO. Integrins: a family of cell surface receptors. *Cell* 48: 549-554, 1987.

Hynes RO. Cell adhesion: old and new questions. *Trends Cell Biol* 9: M33-37, 1999.

Hynes RO. Integrins: bidirectional, allosteric signaling machines. *Cell* 110: 673-687, 2002.

Hynes RO, Marcantonio EE, Stepp MA, Urry LA, and Yee GH. Integrin heterodimer and receptor complexity in avian and mammalian cells. *J Cell Biol* 109: 409-420, 1989.

Hynes RO and Zhao Q. The evolution of cell adhesion. *J Cell Biol* 150: F89-96, 2000.

Ingham KC, Brew SA, Huff S, and Litvinovich SV. Cryptic self-association sites in type III modules of fibronectin. *J Biol Chem* 272: 1718-1724, 1997.

Izaguirre G, Aguirre L, Hu YP, Lee HY, Schlaepfer DD, Aneskievich BJ, and Haimovich B. The cytoskeletal/non-muscle isoform of α-actinin is phosphorylated on its actin-binding domain by the focal adhesion kinase. *J Biol Chem* 276: 28676-28685, 2001.

Izaguirre G, Aguirre L, Ji P, Aneskievich B, and Haimovich B. Tyrosine phosphorylation of α-actinin in activated platelets. *J Biol Chem* 274: 37012-37020, 1999.

Jiang G, Giannone G, Critchley DR, Fukumoto E, and Sheetz MP. Two-piconewton slip bond between fibronectin and the cytoskeleton depends on talin. *Nature* 424: 334-337, 2003.

John T. Edsall, Foster JF, and Scheinberg H. Studies on Double Refraction of Flow. III. Human Fibrinogen and Fraction I of Human Plasma. *J Am Chem Soc* 69: 2731-2738, 1947.

Johnson KJ, Sage H, Briscoe G, and Erickson HP. The compact conformation of fibronectin is determined by intramolecular ionic interactions. *J Biol Chem* 274: 15473-15479, 1999.

Kaefer M, Keating MA, Adams MC, and Rink RC. Posterior urethral valves, pressure pop-offs and bladder function. *J Urol* 154: 708-711, 1995.

Kammerer RA, Schulthess T, Landwehr R, Schumacher B, Lustig A, Yurchenco PD, Ruegg MA, Engel J, and Denzer AJ. Interaction of agrin with laminin requires a coiled-coil conformation of the agrin-binding site within the laminin gamma1 chain. *Embo J* 18: 6762-6770, 1999.

Kanagawa M, Michele DE, Satz JS, Barresi R, Kusano H, Sasaki T, Timpl R, Henry MD, and Campbell KP. Disruption of perlecan binding and matrix assembly by post-translational or genetic disruption of dystroglycan function. *FEBS Lett* 579: 4792-4796, 2005.

Kang SH and Kramer JM. Nidogen is nonessential and not required for normal type IV collagen localization in Caenorhabditis elegans. *Mol Biol Cell* 11: 3911-3923, 2000.

Kaufman MH. *The atlas of mouse development*, 2003.

Kieffer JD, Plopper G, Ingber DE, Hartwig JH, and Kupper TS. Direct binding of F actin to the cytoplasmic domain of the α2 integrin chain in vitro. *Biochem Biophys Res Commun* 217: 466-474, 1995.

Kilicdag EB, Kilicdag H, Bagis T, Tarim E, and Yanik F. Large pseudocyst of the umbilical cord associated with patent urachus. *J Obstet Gynaecol Res* 30: 444-447, 2004.

Kim KM, Kogan BA, Massad CA, and Huang YC. Collagen and elastin in the normal fetal bladder. *J Urol* 146: 524-527, 1991a.

Kim KM, Kogan BA, Massad CA, and Huang YC. Collagen and elastin in the obstructed fetal bladder. *J Urol* 146: 528-531, 1991b.

Kimura K, Ito M, Amano M, Chihara K, Fukata Y, Nakafuku M, Yamamori B, Feng J, Nakano T, Okawa K, Iwamatsu A, and Kaibuchi K. Regulation of myosin phosphatase by Rho and Rho-associated kinase (Rho-kinase). *Science* 273: 245-248, 1996.

Kirkpatrick P and d'Ardenne AJ. Effects of fixation and enzymatic digestion on the immunohistochemical demonstration of laminin and fibronectin in paraffin embedded tissue. *J Clin Pathol* 37: 639-644, 1984.

Kiyokawa E, Hashimoto Y, Kurata T, Sugimura H, and Matsuda M. Evidence that DOCK180 up-regulates signals from the CrkII-p130(Cas) complex. *J Biol Chem* 273: 24479-24484, 1998.

Kiyoshima K, Oda Y, Kinukawa N, Naito S, and Tsuneyoshi M. Overexpression of laminin-5 gamma2 chain and its prognostic significance in urothelial carcinoma of urinary bladder: association with expression of cyclooxygenase 2, epidermal growth factor receptor [corrected] and human epidermal growth factor receptor [corrected] 2. *Hum Pathol* 36: 522-530, 2005.

Klemke RL, Leng J, Molander R, Brooks PC, Vuori K, and Cheresh DA. CAS/Crk coupling serves as a "molecular switch" for induction of cell migration. *J Cell Biol* 140: 961-972, 1998.

Koch M, Olson PF, Albus A, Jin W, Hunter DD, Brunken WJ, Burgeson RE, and Champliaud MF. Characterization and expression of the laminin gamma3

chain: a novel, non-basement membrane-associated, laminin chain. *J Cell Biol* 145: 605-618, 1999.

Kornblihtt AR, Umezawa K, Vibe-Pedersen K, and Baralle FE. Primary structure of human fibronectin: differential splicing may generate at least 10 polypeptides from a single gene. *Embo J* 4: 1755-1759, 1985.

Kramer RH, Vu MP, Cheng YF, Ramos DM, Timpl R, and Waleh N. Laminin-binding integrin $\alpha 7\ \beta 1$: functional characterization and expression in normal and malignant melanocytes. *Cell Regul* 2: 805-817, 1991.

Kureishi Y, Kobayashi S, Amano M, Kimura K, Kanaide H, Nakano T, Kaibuchi K, and Ito M. Rho-associated kinase directly induces smooth muscle contraction through myosin light chain phosphorylation. *J Biol Chem* 272: 12257-12260, 1997.

Laemmli UK. Cleavage of structural proteins during the assembly of the head of bacteriophage T4. *Nature* 227: 680-685, 1970.

Lariviere B, Rouleau M, Picard S, and Beaulieu AD. Human plasma fibronectin potentiates the mitogenic activity of platelet-derived growth factor and complements its wound healing effects. *Wound Repair Regen* 11: 79-89, 2003.

Larsen WJ. *Human Embryology*: Churchill Livingston, 2001.

Laukaitis CM, Webb DJ, Donais K, and Horwitz AF. Differential dynamics of $\alpha 5$ integrin, paxillin, and α-actinin during formation and disassembly of adhesions in migrating cells. *J Cell Biol* 153: 1427-1440, 2001.

Le Gat L, Gogat K, Van Den Berghe L, Brizard M, Kobetz A, Marchant D, Abitbol M, and Menasche M. The $\beta 3$ integrin gene is expressed at high levels in the major haematopoietic and lymphoid organs, vascular system, and skeleton during mouse embryo development. *Cell Commun Adhes* 10: 129-140, 2003.

Leahy DJ, Aukhil I, and Erickson HP. 2.0 A crystal structure of a four-domain segment of human fibronectin encompassing the RGD loop and synergy region. *Cell* 84: 155-164, 1996.

Levin RM, Haugaard N, O'Connor L, Buttyan R, Das A, Dixon JS, and Gosling JA. Obstructive response of human bladder to BPH vs. rabbit bladder response to partial outlet obstruction: a direct comparison. *Neurourol Urodyn* 19: 609-629, 2000.

Levin RM, Levin SS, Zhao Y, and Buttyan R. Cellular and molecular aspects of bladder hypertrophy. *Eur Urol* 32 Suppl 1: 15-21, 1997.

Levin RM, Wein AJ, Buttyan R, Monson FC, and Longhurst PA. Update on bladder smooth-muscle physiology. *World J Urol* 12: 226-232, 1994.

Li R, Mitra N, Gratkowski H, Vilaire G, Litvinov R, Nagasami C, Weisel JW, Lear JD, DeGrado WF, and Bennett JS. Activation of integrin αIIbβ3 by modulation of transmembrane helix associations. *Science* 300: 795-798, 2003.

Li S, Harrison D, Carbonetto S, Fassler R, Smyth N, Edgar D, and Yurchenco PD. Matrix assembly, regulation, and survival functions of laminin and its receptors in embryonic stem cell differentiation. *J Cell Biol* 157: 1279-1290, 2002.

Liao YF, Gotwals PJ, Koteliansky VE, Sheppard D, and Van De Water L. The EIIIA segment of fibronectin is a ligand for integrins α9β1 and α4β1 providing a novel mechanism for regulating cell adhesion by alternative splicing. *J Biol Chem* 277: 14467-14474, 2002.

Litynska A, Przybylo M, Pochec E, and Laidler P. Adhesion properties of human bladder cell lines with extracellular matrix components: the role of integrins and glycosylation. *Acta Biochim Pol* 49: 643-650, 2002.

Liu G, Guibao CD, and Zheng J. Structural insight into the mechanisms of targeting and signaling of focal adhesion kinase. *Mol Cell Biol* 22: 2751-2760, 2002.

Liu W, Li Y, Cunha S, Hayward G, and Baskin L. Diffusable growth factors induce bladder smooth muscle differentiation. *In Vitro Cell Dev Biol Anim* 36: 476-484, 2000.

Loo DT, Kanner SB, and Aruffo A. Filamin binds to the cytoplasmic domain of the β1-integrin. Identification of amino acids responsible for this interaction. *J Biol Chem* 273: 23304-23312, 1998.

Luo BH, Springer TA, and Takagi J. A specific interface between integrin transmembrane helices and affinity for ligand. *PLoS Biol* 2: e153, 2004.

Luque A, Gomez M, Puzon W, Takada Y, Sanchez-Madrid F, and Cabanas C. Activated conformations of very late activation integrins detected by a group of antibodies (HUTS) specific for a novel regulatory region (355-425) of the common β1 chain. *J Biol Chem* 271: 11067-11075, 1996.

Mackie GG and Stephens FD. Duplex kidneys: a correlation of renal dysplasia with position of the ureteral orifice. *J Urol* 114: 274-280, 1975.

Mann K, Deutzmann R, and Timpl R. Characterization of proteolytic fragments of the laminin-nidogen complex and their activity in ligand-binding assays. *Eur J Biochem* 178: 71-80, 1988.

Marcantonio EE and Hynes RO. Antibodies to the conserved cytoplasmic domain of the integrin β1 subunit react with proteins in vertebrates, invertebrates, and fungi. *J Cell Biol* 106: 1765-1772, 1988.

Martin KH, Boerner SA, and Parsons JT. Regulation of focal adhesion targeting and inhibitory functions of the FAK related protein FRNK using a novel estrogen receptor "switch". *Cell Motil Cytoskeleton* 51: 76-88, 2002.

Mathews MB, Bernstein RM, Franza BR, Jr., and Garrels JI. Identity of the proliferating cell nuclear antigen and cyclin. *Nature* 309: 374-376, 1984.

Matsuka YV, Medved LV, Brew SA, and Ingham KC. The NH2-terminal fibrin-binding site of fibronectin is formed by interacting fourth and fifth finger

domains. Studies with recombinant finger fragments expressed in Escherichia coli. *J Biol Chem* 269: 9539-9546, 1994.

Matsumoto S, Kogan BA, Levin RM, Howard PS, and Macarak EJ. Response of the fetal sheep bladder to urinary diversion. *J Urol* 169: 735-739, 2003.

Mayer U, Saher G, Fassler R, Bornemann A, Echtermeyer F, von der Mark H, Miosge N, Poschl E, and von der Mark K. Absence of integrin α7 causes a novel form of muscular dystrophy. *Nat Genet* 17: 318-323, 1997.

McCarthy LS, Smeulders N, and Wilcox DT. Cell biology of bladder development and the role of the extracellular matrix. *Nephron Exp Nephrol* 95: e129-133, 2003.

McKeown-Longo PJ and Mosher DF. Binding of plasma fibronectin to cell layers of human skin fibroblasts. *J Cell Biol* 97: 466-472, 1983.

McLellan DL, Gaston MV, Diamond DA, Lebowitz RL, Mandell J, Atala A, and Bauer SB. Anterior urethral valves and diverticula in children: a result of ruptured Cowper's duct cyst? *BJU Int* 94: 375-378, 2004.

Mesrobian HG, Zacharias A, Balcom AH, and Cohen RD. Ten years of experience with isolated urachal anomalies in children. *J Urol* 158: 1316-1318, 1997.

Mialhe A, Louis J, Pasquier D, Rambeaud JJ, and Seigneurin D. Expression of three cell adhesion molecules in bladder carcinomas: correlation with pathological features. *Anal Cell Pathol* 13: 125-136, 1997.

Michel JB. Anoikis in the cardiovascular system: known and unknown extracellular mediators. *Arterioscler Thromb Vasc Biol* 23: 2146-2154, 2003.

Miguelez J, Bunduki V, Yoshizaki CT, Sadek Ldos S, Koch V, Peralta CF, and Zugaib M. Fetal obstructive uropathy: is urine sampling useful for prenatal counselling? *Prenat Diagn* 26: 81-84, 2006.

Mo R, Kim JH, Zhang J, Chiang C, Hui CC, and Kim PC. Anorectal malformations caused by defects in sonic hedgehog signaling. *AmJPathol* 159: 765-774, 2001.

Monaghan E, Gueorguiev V, Wilkins-Port C, and McKeown-Longo PJ. The receptor for urokinase-type plasminogen activator regulates fibronectin matrix assembly in human skin fibroblasts. *J Biol Chem* 279: 1400-1407, 2004.

Mongiat M, Otto J, Oldershaw R, Ferrer F, Sato JD, and Iozzo RV. Fibroblast growth factor-binding protein is a novel partner for perlecan protein core. *J Biol Chem* 276: 10263-10271, 2001.

Monkley SJ, Zhou XH, Kinston SJ, Giblett SM, Hemmings L, Priddle H, Brown JE, Pritchard CA, Critchley DR, and Fassler R. Disruption of the talin gene arrests mouse development at the gastrulation stage. *Dev Dyn* 219: 560-574, 2000.

Morla AO and Mogford JE. Control of smooth muscle cell proliferation and phenotype by integrin signaling through focal adhesion kinase. *Biochem Biophys Res Commun* 272: 298-302, 2000.

Moro L, Venturino M, Bozzo C, Silengo L, Altruda F, Beguinot L, Tarone G, and Defilippi P. Integrins induce activation of EGF receptor: role in MAP kinase induction and adhesion-dependent cell survival. *Embo J* 17: 6622-6632, 1998.

Morris GF and Mathews MB. Regulation of proliferating cell nuclear antigen during the cell cycle. *J Biol Chem* 264: 13856-13864, 1989.

Mosher DF, Schad PE, and Vann JM. Cross-linking of collagen and fibronectin by factor XIIIa. Localization of participating glutaminyl residues to a tryptic fragment of fibronectin. *J Biol Chem* 255: 1181-1188, 1980.

Mostafavi-Pour Z, Askari JA, Whittard JD, and Humphries MJ. Identification of a novel heparin-binding site in the alternatively spliced IIICS region of fibronectin: roles of integrins and proteoglycans in cell adhesion to fibronectin splice variants. *Matrix Biol* 20: 63-73, 2001.

Mould AP, Askari JA, Aota S, Yamada KM, Irie A, Takada Y, Mardon HJ, and Humphries MJ. Defining the topology of integrin α5β1-fibronectin interactions using inhibitory anti-α5 and anti-β1 monoclonal antibodies. Evidence that the synergy sequence of fibronectin is recognized by the amino-terminal repeats of the α5 subunit. *J Biol Chem* 272: 17283-17292, 1997.

Mould AP and Humphries MJ. Identification of a novel recognition sequence for the integrin α4 β1 in the COOH-terminal heparin-binding domain of fibronectin. *Embo J* 10: 4089-4095, 1991.

Moursi AM, Damsky CH, Lull J, Zimmerman D, Doty SB, Aota S, and Globus RK. Fibronectin regulates calvarial osteoblast differentiation. *J Cell Sci* 109: 1369-1380, 1996.

Moursi AM, Globus RK, and Damsky CH. Interactions between integrin receptors and fibronectin are required for calvarial osteoblast differentiation in vitro. *J Cell Sci* 110 (Pt 18): 2187-2196, 1997.

Moyano JV, Carnemolla B, Dominguez-Jimenez C, Garcia-Gila M, Albar JP, Sanchez-Aparicio P, Leprini A, Querze G, Zardi L, and Garcia-Pardo A. Fibronectin type III5 repeat contains a novel cell adhesion sequence, KLDAPT, which binds activated α4β1 and α4β7 integrins. *J Biol Chem* 272: 24832-24836, 1997.

Muro AF, Chauhan AK, Gajovic S, Iaconcig A, Porro F, Stanta G, and Baralle FE. Regulated splicing of the fibronectin EDA exon is essential for proper skin wound healing and normal lifespan. *J Cell Biol* 162: 149-160, 2003.

Murshed M, Smyth N, Miosge N, Karolat J, Krieg T, Paulsson M, and Nischt R. The absence of nidogen 1 does not affect murine basement membrane formation. *Mol Cell Biol* 20: 7007-7012, 2000.

Newman J and Antonakopoulos GN. The fine structure of the human fetal urinary bladder. Development and maturation. A light, transmission and scanning electron microscopic study. *J Anat* 166: 135-150, 1989.

Nguyen TT, Ward JP, and Hirst SJ. β1-Integrins mediate enhancement of airway smooth muscle proliferation by collagen and fibronectin. *Am J Respir Crit Care Med* 171: 217-223, 2005.

Noakes PG, Miner JH, Gautam M, Cunningham JM, Sanes JR, and Merlie JP. The renal glomerulus of mice lacking s-laminin/laminin β2: nephrosis despite molecular compensation by laminin β1. *Nat Genet* 10: 400-406, 1995.

Nobes CD and Hall A. Rho, rac, and cdc42 GTPases regulate the assembly of multimolecular focal complexes associated with actin stress fibers, lamellipodia, and filopodia. *Cell* 81: 53-62, 1995.

Nyirady P, Thiruchelvam N, Fry CH, Godley ML, Winyard PJ, Peebles DM, Woolf AS, and Cuckow PM. Effects of in utero bladder outflow obstruction on fetal sheep detrusor contractility, compliance and innervation. *JUrol* 168: 1615-1620, 2002.

O'Toole TE, Katagiri Y, Faull RJ, Peter K, Tamura R, Quaranta V, Loftus JC, Shattil SJ, and Ginsberg MH. Integrin cytoplasmic domains mediate inside-out signal transduction. *J Cell Biol* 124: 1047-1059, 1994.

O'Toole TE, Mandelman D, Forsyth J, Shattil SJ, Plow EF, and Ginsberg MH. Modulation of the affinity of integrin αIIb β3 (GPIIb-IIIa) by the cytoplasmic domain of αIIb. *Science* 254: 845-847, 1991.

Ohashi T, Kiehart DP, and Erickson HP. Dynamics and elasticity of the fibronectin matrix in living cell culture visualized by fibronectin-green fluorescent protein. *Proc Natl Acad Sci U S A* 96: 2153-2158, 1999.

Ohashi T, Kiehart DP, and Erickson HP. Dual labeling of the fibronectin matrix and actin cytoskeleton with green fluorescent protein variants. *J Cell Sci* 115: 1221-1229, 2002.

Ohta Y, Suzuki N, Nakamura S, Hartwig JH, and Stossel TP. The small GTPase RalA targets filamin to induce filopodia. *Proc Natl Acad Sci U S A* 96: 2122-2128, 1999.

Okada M, Blomback B, Chang MD, and Horowitz B. Fibronectin and fibrin gel structure. *J Biol Chem* 260: 1811-1820, 1985.

Olski TM, Noegel AA, and Korenbaum E. Parvin, a 42 kDa focal adhesion protein, related to the α-actinin superfamily. *J Cell Sci* 114: 525-538, 2001.

Ornstein L. Disc Electrophoresis. I. Background and Theory. *Ann N Y Acad Sci* 121: 321-349, 1964.

Orsola A, Adam RM, Peters CA, and Freeman MR. The decision to undergo DNA or protein synthesis is determined by the degree of mechanical deformation in human bladder muscle cells. *Urology* 59: 779-783, 2002.

Owen JD, Ruest PJ, Fry DW, and Hanks SK. Induced focal adhesion kinase (FAK) expression in FAK-null cells enhances cell spreading and migration requiring both auto- and activation loop phosphorylation sites and inhibits adhesion-dependent tyrosine phosphorylation of Pyk2. *Mol Cell Biol* 19: 4806-4818, 1999.

Palmer EL, Ruegg C, Ferrando R, Pytela R, and Sheppard D. Sequence and tissue distribution of the integrin α9 subunit, a novel partner of β1 that is widely distributed in epithelia and muscle. *J Cell Biol* 123: 1289-1297, 1993.

Pankov R, Cukierman E, Katz BZ, Matsumoto K, Lin DC, Lin S, Hahn C, and Yamada KM. Integrin dynamics and matrix assembly: tensin-dependent translocation of α5β1 integrins promotes early fibronectin fibrillogenesis. *J Cell Biol* 148: 1075-1090, 2000.

Pankov R and Yamada KM. Fibronectin at a glance. *J Cell Sci* 115: 3861-3863, 2002.

Park JM, Borer JG, Freeman MR, and Peters CA. Stretch activates heparin-binding EGF-like growth factor expression in bladder smooth muscle cells. *Am J Physiol* 275: C1247-1254, 1998.

Parkhouse HF, Barratt TM, Dillon MJ, Duffy PG, Fay J, Ransley PG, Woodhouse CR, and Williams DI. Long-term outcome of boys with posterior urethral valves. *Br J Urol* 62: 59-62, 1988.

Patil S, Jedsadayanmata A, Wencel-Drake JD, Wang W, Knezevic I, and Lam SC. Identification of a talin-binding site in the integrin β3 subunit distinct from the NPLY regulatory motif of post-ligand binding functions. The talin n-terminal head domain interacts with the membrane-proximal region of the β3 cytoplasmic tail. *J Biol Chem* 274: 28575-28583, 1999.

Paul JI, Schwarzbauer JE, Tamkun JW, and Hynes RO. Cell-type-specific fibronectin subunits generated by alternative splicing. *J Biol Chem* 261: 12258-12265, 1986.

Paulsson M, Saladin K, and Landwehr R. Binding of Ca2+ influences susceptibility of laminin to proteolytic digestion and interactions between domain-specific laminin fragments. *Eur J Biochem* 177: 477-481, 1988.

Pavalko FM, Chen NX, Turner CH, Burr DB, Atkinson S, Hsieh YF, Qiu J, and Duncan RL. Fluid shear-induced mechanical signaling in MC3T3-E1 osteoblasts requires cytoskeleton-integrin interactions. *Am J Physiol* 275: C1591-1601, 1998.

Pelicci G, Lanfrancone L, Grignani F, McGlade J, Cavallo F, Forni G, Nicoletti I, Grignani F, Pawson T, and Pelicci PG. A novel transforming protein (SHC) with an SH2 domain is implicated in mitogenic signal transduction. *Cell* 70: 93-104, 1992.

Persad S, Attwell S, Gray V, Delcommenne M, Troussard A, Sanghera J, and Dedhar S. Inhibition of integrin-linked kinase (ILK) suppresses activation of protein kinase B/Akt and induces cell cycle arrest and apoptosis of PTEN-mutant prostate cancer cells. *Proc Natl Acad Sci U S A* 97: 3207-3212, 2000.

Persad S, Attwell S, Gray V, Mawji N, Deng JT, Leung D, Yan J, Sanghera J, Walsh MP, and Dedhar S. Regulation of protein kinase B/Akt-serine 473 phosphorylation by integrin-linked kinase: critical roles for kinase activity and

amino acids arginine 211 and serine 343. *J Biol Chem* 276: 27462-27469, 2001.

Peters CA, Bolkier M, Bauer SB, Hendren WH, Colodny AH, Mandell J, and Retik AB. The urodynamic consequences of posterior urethral valves. *J Urol* 144: 122-126, 1990.

Peters CA, Carr MC, Lais A, Retik AB, and Mandell J. The response of the fetal kidney to obstruction. *J Urol* 148: 503-509, 1992a.

Peters CA, Vasavada S, Dator D, Carr M, Shapiro E, Lepor H, McConnell J, Retik AB, and Mandell J. The effect of obstruction on the developing bladder. *JUrol* 148: 491-496, 1992b.

Pfaff M, Liu S, Erle DJ, and Ginsberg MH. Integrin β cytoplasmic domains differentially bind to cytoskeletal proteins. *J Biol Chem* 273: 6104-6109, 1998.

Piali L, Hammel P, Uherek C, Bachmann F, Gisler RH, Dunon D, and Imhof BA. CD31/PECAM-1 is a ligand for αv β3 integrin involved in adhesion of leukocytes to endothelium. *J Cell Biol* 130: 451-460, 1995.

Piechotta R, Milakofsky L, Nibbio B, Hare T, and Epple A. Impact of exogenous amino acids on endogenous amino compounds in the fluid compartments of the chicken embryo. *Comp Biochem Physiol A Mol Integr Physiol* 120: 325-337, 1998.

Pierschbacher MD and Ruoslahti E. Cell attachment activity of fibronectin can be duplicated by small synthetic fragments of the molecule. *Nature* 309: 30-33, 1984.

Pierschbacher MD, Ruoslahti E, Sundelin J, Lind P, and Peterson PA. The cell attachment domain of fibronectin. Determination of the primary structure. *J Biol Chem* 257: 9593-9597, 1982.

Pinco KA, He W, and Yang JT. α4β1 integrin regulates lamellipodia protrusion via a focal complex/focal adhesion-independent mechanism. *Mol Biol Cell* 13: 3203-3217, 2002.

Plow EF, Haas TA, Zhang L, Loftus J, and Smith JW. Ligand binding to integrins. *J Biol Chem* 275: 21785-8, 2000.

Pulkkinen L, Christiano AM, Airenne T, Haakana H, Tryggvason K, and Uitto J. Mutations in the gamma 2 chain gene (LAMC2) of kalinin/laminin 5 in the junctional forms of epidermolysis bullosa. *Nat Genet* 6: 293-297, 1994.

Pulkkinen L, Gerecke DR, Christiano AM, Wagman DW, Burgeson RE, and Uitto J. Cloning of the β3 chain gene (LAMB3) of human laminin 5, a candidate gene in junctional epidermolysis bullosa. *Genomics* 25: 192-198, 1995.

Pytela R, Pierschbacher MD, and Ruoslahti E. A 125/115-kDa cell surface receptor specific for vitronectin interacts with the arginine-glycine-aspartic acid adhesion sequence derived from fibronectin. *Proc Natl Acad Sci USA* 82: 5766-5770, 1985a.

Pytela R, Pierschbacher MD, and Ruoslahti E. Identification and isolation of a 140 kd cell surface glycoprotein with properties expected of a fibronectin receptor. *Cell* 40: 191-198, 1985b.

Reddy KB, Gascard P, Price MG, Negrescu EV, and Fox JE. Identification of an interaction between the m-band protein skelemin and β-integrin subunits. Colocalization of a skelemin-like protein with β1- and β3-integrins in non-muscle cells. *J Biol Chem* 273: 35039-35047, 1998.

Reef VB and Collatos C. Ultrasonography of umbilical structures in clinically normal foals. *Am J Vet Res* 49: 2143-2146, 1988.

Reinberg Y, Chelimsky G, and Gonzalez R. Urethral atresia and the prune belly syndrome. Report of 6 cases. *Br J Urol* 72: 112-114, 1993.

Reinberg Y, Shapiro E, Manivel JC, Manley CB, Pettinato G, and Gonzalez R. Prune belly syndrome in females: a triad of abdominal musculature deficiency and anomalies of the urinary and genital systems. *J Pediatr* 118: 395-398, 1991.

Relan NK, Yang Y, Beqaj S, Miner JH, and Schuger L. Cell elongation induces laminin α2 chain expression in mouse embryonic mesenchymal cells: role in visceral myogenesis. *J Cell Biol* 147: 1341-1350, 1999.

Renehan AG, Booth C, and Potten CS. What is apoptosis, and why is it important? *BMJ* 322: 1536-1538, 2001.

Renshaw MW, Price LS, and Schwartz MA. Focal adhesion kinase mediates the integrin signaling requirement for growth factor activation of MAP kinase. *J Cell Biol* 147: 611-618, 1999.

Renshaw MW, Ren XD, and Schwartz MA. Growth factor activation of MAP kinase requires cell adhesion. *Embo J* 16: 5592-5599, 1997.

Richter H, Seidl M, and Hormann H. Location of heparin-binding sites of fibronectin. Detection of a hitherto unrecognized transamidase sensitive site. *Hoppe Seylers Z Physiol Chem* 362: 399-408, 1981.

Ridley AJ and Hall A. The small GTP-binding protein rho regulates the assembly of focal adhesions and actin stress fibers in response to growth factors. *Cell* 70: 389-399, 1992.

Roberts DD, Rao CN, Magnani JL, Spitalnik SL, Liotta LA, and Ginsburg V. Laminin binds specifically to sulfated glycolipids. *Proc Natl Acad Sci U S A* 82: 1306-1310, 1985.

Rohrmann D, Monson FC, Damaser MS, Levin RM, Duckett JW, Jr., and Zderic SA. Partial bladder outlet obstruction in the fetal rabbit. *JUrol* 158: 1071-1074, 1997.

Romanic AM, Adachi E, Kadler KE, Hojima Y, and Prockop DJ. Copolymerization of pNcollagen III and collagen I. pNcollagen III decreases the rate of incorporation of collagen I into fibrils, the amount of collagen I incorporated, and the diameter of the fibrils formed. *J Biol Chem* 266: 12703-12709, 1991.

Romanov VI and Goligorsky MS. RGD-recognizing integrins mediate interactions of human prostate carcinoma cells with endothelial cells in vitro. *Prostate* 39: 108-118, 1999.

Rostagno A, Williams M, Frangione B, and Gold LI. Biochemical analysis of the interaction of fibronectin with IgG and localization of the respective binding sites. *Mol Immunol* 33: 561-572, 1996.

Rostagno AA, Frangione B, and Gold LI. Biochemical characterization of the fibronectin binding sites for IgG. *J Immunol* 143: 3277-3282, 1989.

Rostagno AA, Gallo G, and Gold LI. Binding of polymeric IgG to fibronectin in extracellular matrices: an in vitro paradigm for immune-complex deposition. *Mol Immunol* 38: 1101-1111, 2002.

Roy J, Tran PK, Religa P, Kazi M, Henderson B, Lundmark K, and Hedin U. Fibronectin promotes cell cycle entry in smooth muscle cells in primary culture. *Exp Cell Res* 273: 169-177, 2002.

Ruoslahti E, Hayman EG, Kuusela P, Shively JE, and Engvall E. Isolation of a tryptic fragment containing the collagen-binding site of plasma fibronectin. *J Biol Chem* 254: 6054-6059, 1979.

Ryan MC, Lee K, Miyashita Y, and Carter WG. Targeted disruption of the LAMA3 gene in mice reveals abnormalities in survival and late stage differentiation of epithelial cells. *J Cell Biol* 145: 1309-1323, 1999.

Sakai T, Larsen M, and Yamada KM. Fibronectin requirement in branching morphogenesis. *Nature* 423: 876-881, 2003.

Salmivirta K, Talts JF, Olsson M, Sasaki T, Timpl R, and Ekblom P. Binding of mouse nidogen-2 to basement membrane components and cells and its expression in embryonic and adult tissues suggest complementary functions of the two nidogens. *Exp Cell Res* 279: 188-201, 2002.

Sambrook J, Fritsch EF, and Maniatis T. *Molecular Cloning - a laboratory manual*: Cold Spring Harbour Laboratory Press, 1989.

Sampath R, Gallagher PJ, and Pavalko FM. Cytoskeletal interactions with the leukocyte integrin β2 cytoplasmic tail. Activation-dependent regulation of associations with talin and α-actinin. *J Biol Chem* 273: 33588-33594, 1998.

Saoncella S, Echtermeyer F, Denhez F, Nowlen JK, Mosher DF, Robinson SD, Hynes RO, and Goetinck PF. Syndecan-4 signals cooperatively with integrins in a Rho-dependent manner in the assembly of focal adhesions and actin stress fibers. *Proc Natl Acad Sci U S A* 96: 2805-2810, 1999.

Sasaki M, Kato S, Kohno K, Martin GR, and Yamada Y. Sequence of the cDNA encoding the laminin B1 chain reveals a multidomain protein containing cysteine-rich repeats. *Proc Natl Acad Sci U S A* 84: 935-939, 1987.

Schaller MD, Hildebrand JD, Shannon JD, Fox JW, Vines RR, and Parsons JT. Autophosphorylation of the focal adhesion kinase, pp125FAK, directs SH2-dependent binding of pp60src. *Mol Cell Biol* 14: 1680-1688, 1994.

Schaller MD, Otey CA, Hildebrand JD, and Parsons JT. Focal adhesion kinase and paxillin bind to peptides mimicking βintegrin cytoplasmic domains. *J Cell Biol* 130: 1181-1187, 1995.

Schiesser M, Lapaire O, Holzgreve W, and Tercanli S. Umbilical cord edema associated with patent urachus. *Ultrasound Obstet Gynecol* 22: 646-647, 2003.

Schnapp LM, Breuss JM, Ramos DM, Sheppard D, and Pytela R. Sequence and tissue distribution of the human integrin α8 subunit: a β1-associated αsubunit expressed in smooth muscle cells. *J Cell Sci* 108: 537-544, 1995a.

Schnapp LM, Hatch N, Ramos DM, Klimanskaya IV, Sheppard D, and Pytela R. The human integrin α8 β1 functions as a receptor for tenascin, fibronectin, and vitronectin. *J Biol Chem* 270: 23196-23202, 1995b.

Schuger L, Skubitz AP, Zhang J, Sorokin L, and He L. Laminin α1 chain synthesis in the mouse developing lung: requirement for epithelial-mesenchymal contact and possible role in bronchial smooth muscle development. *J Cell Biol* 139: 553-562, 1997.

Schwarzbauer JE, Patel RS, Fonda D, and Hynes RO. Multiple sites of alternative splicing of the rat fibronectin gene transcript. *Embo J* 6: 2573-2580, 1987.

Schwarzbauer JE, Spencer CS, and Wilson CL. Selective secretion of alternatively spliced fibronectin variants. *J Cell Biol* 109: 3445-3453, 1989.

Scott RJ and Goodburn SF. Potter's syndrome in the second trimester--prenatal screening and pathological findings in 60 cases of oligohydramnios sequence. *Prenat Diagn* 15: 519-525, 1995.

Scriven SD, Booth C, Thomas DF, Trejdosiewicz LK, and Southgate J. Reconstitution of human urothelium from monolayer cultures. *J Urol* 158: 1147-1152, 1997.

Sechler JL and Schwarzbauer JE. Coordinated regulation of fibronectin fibril assembly and actin stress fiber formation. *Cell Adhes Commun* 4: 413-424, 1997.

Sechler JL, Takada Y, and Schwarzbauer JE. Altered rate of fibronectin matrix assembly by deletion of the first type III repeats. *J Cell Biol* 134: 573-583, 1996.

Serini G and Gabbiani G. Mechanisms of myofibroblast activity and phenotypic modulation. *Exp Cell Res* 250: 273-283, 1999.

Sharma CP, Ezzell RM, and Arnaout MA. Direct interaction of filamin (ABP-280) with the β2-integrin subunit CD18. *J Immunol* 154: 3461-3470, 1995.

Shima Y, Hayashida M, Hayashi T, Kuwabara Y, and Araki T. Characteristic prenatal ultrasonographic findings of patent urachus: a case report. *J Nippon Med Sch* 70: 172-174, 2003.

Shimada K, Hosokawa S, Tohda A, Matsumoto F, and Johnin K. Histology of the fetal prune belly syndrome with reference to the efficacy of prenatal decompression. *Int J Urol* 7: 161-166, 2000.

Shimada K, Matsumoto F, Tohda A, and Ueda M. Histological study of fetal kidney with urethral obstruction and vesicoureteral reflux: a consideration on the etiology of congenital reflux nephropathy. *Int J Urol* 10: 518-524, 2003.

Shono T, Mochizuki Y, Kanetake H, and Kanda S. Inhibition of FGF-2-mediated chemotaxis of murine brain capillary endothelial cells by cyclic RGDfV peptide through blocking the redistribution of c-Src into focal adhesions. *Exp Cell Res* 268: 169-178, 2001.

Sieg DJ, Hauck CR, Ilic D, Klingbeil CK, Schaefer E, Damsky CH, and Schlaepfer DD. FAK integrates growth-factor and integrin signals to promote cell migration. *Nat Cell Biol* 2: 249-256, 2000.

Singer, II. The fibronexus: a transmembrane association of fibronectin-containing fibers and bundles of 5 nm microfilaments in hamster and human fibroblasts. *Cell* 16: 675-685, 1979.

Singh P, Reimer CL, Peters JH, Stepp MA, Hynes RO, and Van De Water L. The spatial and temporal expression patterns of integrin $\alpha 9\beta 1$ and one of its ligands, the EIIIA segment of fibronectin, in cutaneous wound healing. *J Invest Dermatol* 123: 1176-1181, 2004.

Skalli O, Ropraz P, Trzeciak A, Benzonana G, Gillessen D, and Gabbiani G. A monoclonal antibody against α-smooth muscle actin: a new probe for smooth muscle differentiation. *J Cell Biol* 103: 2787-2796, 1986.

Skorstengaard K, Holtet TL, Etzerodt M, and Thogersen HC. Collagen-binding recombinant fibronectin fragments containing type II domains. *FEBS Lett* 343: 47-50, 1994.

Smedts F, Ramaekers F, Troyanovsky S, Pruszczynski M, Link M, Lane B, Leigh I, Schijf C, and Vooijs P. Keratin expression in cervical cancer. *Am J Pathol* 141: 497-511, 1992.

Smeulders N, Woolf AS, and Wilcox DT. Smooth muscle differentiation and cell turnover in mouse detrusor development. *J Urol* 167: 385-390, 2002.

Smeulders N, Woolf AS, and Wilcox DT. Extracellular matrix protein expression during mouse detrusor development. *J Pediatr Surg* 38: 1-12, 2003.

Smith EA, Woodward JR, Walsh, Retik, Vaughan, and Wein. Prune-Belly Syndrome. Saunders, 2004.

Smith PK, Krohn RI, Hermanson GT, Mallia AK, Gartner FH, Provenzano MD, Fujimoto EK, Goeke NM, Olson BJ, and Klenk DC. Measurement of protein using bicinchoninic acid. *Anal Biochem* 150: 76-85, 1985.

Smyth N, Vatansever HS, Murray P, Meyer M, Frie C, Paulsson M, and Edgar D. Absence of basement membranes after targeting the LAMC1 gene results in embryonic lethality due to failure of endoderm differentiation. *J Cell Biol* 144: 151-160, 1999.

Solowska J, Guan JL, Marcantonio EE, Trevithick JE, Buck CA, and Hynes RO. Expression of normal and mutant avian integrin subunits in rodent cells. *J Cell Biol* 109: 853-861, 1989.

Sottile J and Chandler J. Fibronectin matrix turnover occurs through a caveolin-1-dependent process. *Mol Biol Cell* 16: 757-768, 2005.

Sottile J and Hocking DC. Fibronectin polymerization regulates the composition and stability of extracellular matrix fibrils and cell-matrix adhesions. *Mol Biol Cell* 13: 3546-3559, 2002.

Sottile J, Schwarzbauer J, Selegue J, and Mosher DF. Five type I modules of fibronectin form a functional unit that binds to fibroblasts and Staphylococcus aureus. *J Biol Chem* 266: 12840-12843, 1991.

Southgate J, Kennedy W, Hutton KA, and Trejdosiewicz LK. Expression and in vitro regulation of integrins by normal human urothelial cells. *Cell Adhes Commun* 3: 231-242, 1995.

Spinardi L, Ren YL, Sanders R, and Giancotti FG. The β4 subunit cytoplasmic domain mediates the interaction of α6 β4 integrin with the cytoskeleton of hemidesmosomes. *Mol Biol Cell* 4: 871-884, 1993.

Stum M, Davoine CS, Fontaine B, and Nicole S. Schwartz-Jampel syndrome and perlecan deficiency. *Acta Myol* 24: 89-92, 2005.

Sunada Y, Bernier SM, Utani A, Yamada Y, and Campbell KP. Identification of a novel mutant transcript of laminin α2 chain gene responsible for muscular dystrophy and dysmyelination in dy2J mice. *Hum Mol Genet* 4: 1055-1061, 1995a.

Sunada Y, Edgar TS, Lotz BP, Rust RS, and Campbell KP. Merosin-negative congenital muscular dystrophy associated with extensive brain abnormalities. *Neurology* 45: 2084-2089, 1995b.

Sung U, O'Rear JJ, and Yurchenco PD. Localization of heparin binding activity in recombinant laminin G domain. *Eur J Biochem* 250: 138-143, 1997.

Tachikawa M, Nakagawa H, Terasaki AG, Mori H, and Ohashi K. A 260-kDa filamin/ABP-related protein in chicken gizzard smooth muscle cells is a new component of the dense plaques and dense bodies of smooth muscle. *J Biochem (Tokyo)* 122: 314-321, 1997.

Tadokoro S, Shattil SJ, Eto K, Tai V, Liddington RC, de Pereda JM, Ginsberg MH, and Calderwood DA. Talin binding to integrin βtails: a final common step in integrin activation. *Science* 302: 103-106, 2003.

Takada Y, Wayner EA, Carter WG, and Hemler ME. Extracellular matrix receptors, ECMRII and ECMRI, for collagen and fibronectin correspond to VLA-2 and VLA-3 in the VLA family of heterodimers. *J Cell Biochem* 37: 385-393, 1988.

Takagi J, Strokovich K, Springer TA, and Walz T. Structure of integrin α5β1 in complex with fibronectin. *EMBO J* 22: 4607-4615, 2003.

Tamkun JW, DeSimone DW, Fonda D, Patel RS, Buck C, Horwitz AF, and Hynes RO. Structure of integrin, a glycoprotein involved in the transmembrane linkage between fibronectin and actin. *Cell* 46: 271-282, 1986.

Tarantal AF, Han VK, Cochrum KC, Mok A, daSilva M, and Matsell DG. Fetal rhesus monkey model of obstructive renal dysplasia. *Kidney Int* 59: 446-456, 2001.

Thiruchelvam N, Nyirady P, Peebles DM, Fry CH, Cuckow PM, and Woolf AS. Urinary outflow obstruction increases apoptosis and deregulates Bcl-2 and Bax expression in the fetal ovine bladder. *Am J Pathol* 162: 1271-1282, 2003.

Thomas DFM, Thomas DFM, Rickwood AMK, and Duffy PG. Embryology. In: *Essentials of Pediatric Urology*. London: Martin Dunitz, 2002, p. 1.

Thyberg J and Hultgardh-Nilsson A. Fibronectin and the basement membrane components laminin and collagen type IV influence the phenotypic properties of subcultured rat aortic smooth muscle cells differently. *Cell Tissue Res* 276: 263-271, 1994.

Tohyama Y, Katagiri K, Pardi R, Lu C, Springer TA, and Kinashi T. The critical cytoplasmic regions of the αL/β2 integrin in Rap1-induced adhesion and migration. *Mol Biol Cell* 14: 2570-2582, 2003.

Tolaymat LL, Maher JE, Kleinman GE, Stalnaker R, Kea K, and Walker A. Persistent patent urachus with allantoic cyst: a case report. *Ultrasound Obstet Gynecol* 10: 366-368, 1997.

Troussard AA, Costello P, Yoganathan TN, Kumagai S, Roskelley CD, and Dedhar S. The integrin linked kinase (ILK) induces an invasive phenotype via AP-1 transcription factor-dependent upregulation of matrix metalloproteinase 9 (MMP-9). *Oncogene* 19: 5444-5452, 2000.

Tu Y, Huang Y, Zhang Y, Hua Y, and Wu C. A new focal adhesion protein that interacts with integrin-linked kinase and regulates cell adhesion and spreading. *J Cell Biol* 153: 585-598, 2001.

Tu Y, Li F, Goicoechea S, and Wu C. The LIM-only protein PINCH directly interacts with integrin-linked kinase and is recruited to integrin-rich sites in spreading cells. *Mol Cell Biol* 19: 2425-2434, 1999.

Turner CE, Glenney JR, Jr., and Burridge K. Paxillin: a new vinculin-binding protein present in focal adhesions. *J Cell Biol* 111: 1059-1068, 1990.

Turner CE, Kramarcy N, Sealock R, and Burridge K. Localization of paxillin, a focal adhesion protein, to smooth muscle dense plaques, and the myotendinous and neuromuscular junctions of skeletal muscle. *Exp Cell Res* 192: 651-655, 1991.

Ulmer TS, Calderwood DA, Ginsberg MH, and Campbell ID. Domain-specific interactions of talin with the membrane-proximal region of the integrin β3 subunit. *Biochemistry* 42: 8307-8312, 2003.

Upadhyay J, Aitken KJ, Damdar C, Bolduc S, and Bagli DJ. Integrins expressed with bladder extracellular matrix after stretch injury in vivo mediate bladder smooth muscle cell growth in vitro. *J Urol* 169: 750-755, 2003.

Vaheri A, Ruoslahti E, Linder E, Wartiovaara J, Keski-Oja J, Kuusela P, and Saksela O. Fibroblast surface antigen (SF): molecular properties, distribution in vitro and in vivo, and altered expression in transformed cells. *J Supramol Struct* 4: 63-70, 1976.

Varner JA, Emerson DA, and Juliano RL. Integrin α5 β1 expression negatively regulates cell growth: reversal by attachment to fibronectin. *Mol Biol Cell* 6: 725-740, 1995.

Velling T, Risteli J, Wennerberg K, Mosher DF, and Johansson S. Polymerization of type I and III collagens is dependent on fibronectin and enhanced by integrins α11β1 and α2β1. *J Biol Chem* 277: 37377-37381, 2002.

Vinogradova O, Vaynberg J, Kong X, Haas TA, Plow EF, and Qin J. Membrane-mediated structural transitions at the cytoplasmic face during integrin activation. *Proc Natl Acad Sci U S A* 101: 4094-4099, 2004.

Vinogradova O, Velyvis A, Velyviene A, Hu B, Haas T, Plow E, and Qin J. A structural mechanism of integrin α(IIb)β(3) "inside-out" activation as regulated by its cytoplasmic face. *Cell* 110: 587-597, 2002.

Wang H and Pevsner J. Detection of endogenous biotin in various tissues: novel functions in the hippocampus and implications for its use in avidin-biotin technology. *Cell Tissue Res* 296: 511-516, 1999.

Wang N and Ingber DE. Probing transmembrane mechanical coupling and cytomechanics using magnetic twisting cytometry. *Biochem Cell Biol* 73: 327-335, 1995.

Wary KK, Mariotti A, Zurzolo C, and Giancotti FG. A requirement for caveolin-1 and associated kinase Fyn in integrin signaling and anchorage-dependent cell growth. *Cell* 94: 625-634, 1998.

Watson E, Mahaffey MB, Crowell W, Selcer BA, Morris DD, and Seginak L. Ultrasonography of the umbilical structures in clinically normal calves. *Am J Vet Res* 55: 773-780, 1994.

Wayner EA and Carter WG. Identification of multiple cell adhesion receptors for collagen and fibronectin in human fibrosarcoma cells possessing unique αand common βsubunits. *J Cell Biol* 105: 1873-1884, 1987.

Wayner EA, Garcia-Pardo A, Humphries MJ, McDonald JA, and Carter WG. Identification and characterization of the T lymphocyte adhesion receptor for an alternative cell attachment domain (CS-1) in plasma fibronectin. *J Cell Biol* 109: 1321-1330, 1989.

Weber K and Osborn M. The reliability of molecular weight determinations by dodecyl sulfate-polyacrylamide gel electrophoresis. *J Biol Chem* 244: 4406-4412, 1969.

Weber S, Mir S, Schlingmann KP, Nurnberg G, Becker C, Kara PE, Ozkayin N, Konrad M, Nurnberg P, and Schaefer F. Gene locus ambiguity in posterior urethral valves/prune-belly syndrome. *Pediatr Nephrol* 20: 1036-1042, 2005.

Welsh A, Agarwal S, Kumar S, Smith RP, and Fisk NM. Fetal cystoscopy in the management of fetal obstructive uropathy: experience in a single European centre. *Prenat Diagn* 23: 1033-1041, 2003.

Weng Z, Taylor JA, Turner CE, Brugge JS, and Seidel-Dugan C. Detection of Src homology 3-binding proteins, including paxillin, in normal and v-Src-transformed Balb/c 3T3 cells. *J Biol Chem* 268: 14956-14963, 1993.

Wijsman JH, Van Dierendonck JH, Keijzer R, van de Velde CJ, and Cornelisse CJ. Immunoreactivity of proliferating cell nuclear antigen compared with bromodeoxyuridine incorporation in normal and neoplastic rat tissue. *J Pathol* 168: 75-83, 1992.

Williamson RA, Henry MD, Daniels KJ, Hrstka RF, Lee JC, Sunada Y, Ibraghimov-Beskrovnaya O, and Campbell KP. Dystroglycan is essential for early embryonic development: disruption of Reichert's membrane in Dag1-null mice. *Hum Mol Genet* 6: 831-841, 1997.

Wilson CB, Leopard J, Cheresh DA, and Nakamura RM. Extracellular matrix and integrin composition of the normal bladder wall. *World J Urol* 14 Suppl 1: S30-37, 1996.

Woolf AS, Price KL, Scambler PJ, and Winyard PJ. Evolving concepts in human renal dysplasia. *J Am Soc Nephrol* 15: 998-1007, 2004.

Woolf AS and Thiruchelvam N. Congenital obstructive uropathy: Its origin and contribution to end- stage renal disease in children. *Adv Ren Replace Ther* 8: 157-163, 2001.

Workman SJ and Kogan BA. Fetal bladder histology in posterior urethral valves and the prune belly syndrome. *J Urol* 144: 337-339, 1990.

Wu C, Keivens VM, O'Toole TE, McDonald JA, and Ginsberg MH. Integrin activation and cytoskeletal interaction are essential for the assembly of a fibronectin matrix. *Cell* 83: 715-724, 1995.

Wu HY, Baskin LS, Blakey C, Goodman J, and Cunha GR. Ultrastructural smooth muscle ontogeny of the rat bladder. *Adv Exp Med Biol* 462: 93-102, 1999a.

Wu HY, Baskin LS, Liu W, Li YW, Hayward S, and Cunha GR. Understanding bladder regeneration: smooth muscle ontogeny. *J Urol* 162: 1101-1105, 1999b.

Xiong JP, Stehle T, Diefenbach B, Zhang R, Dunker R, Scott DL, Joachimiak A, Goodman SL, and Arnaout MA. Crystal structure of the extracellular segment of integrin αVβ3. *Science* 294: 339-345, 2001.

Xiong JP, Stehle T, Zhang R, Joachimiak A, Frech M, Goodman SL, and Arnaout MA. Crystal structure of the extracellular segment of integrin αVβ3 in complex with an Arg-Gly-Asp ligand. *Science* 296: 151-155, 2002.

Yang Y, Relan NK, Przywara DA, and Schuger L. Embryonic mesenchymal cells share the potential for smooth muscle differentiation: myogenesis is controlled by the cell's shape. *Development* 126: 3027-3033, 1999.

Yao CC, Breuss J, Pytela R, and Kramer RH. Functional expression of the α7 integrin receptor in differentiated smooth muscle cells. *J Cell Sci* 110: 1477-1487, 1997.

Yao CC, Ziober BL, Squillace RM, and Kramer RH. α7 integrin mediates cell adhesion and migration on specific laminin isoforms. *J Biol Chem* 271: 25598-25603, 1996a.

Yao CC, Ziober BL, Sutherland AE, Mendrick DL, and Kramer RH. Laminins promote the locomotion of skeletal myoblasts via the α7 integrin receptor. *JCell Sci* 109 (Pt 13): 3139-3150, 1996b.

Yosypiv IV, Schroeder M, and El-Dahr SS. Angiotensin II type 1 receptor-EGF receptor cross-talk regulates ureteric bud branching morphogenesis. *J Am Soc Nephrol* 17: 1005-1014, 2006.

Young HH, Frontz WA, and Baldwin JC. Congenital obstruction of the posterior urethra. *J Urol* 3: 289-365, 1919.

Yu J, Carroll TJ, and McMahon AP. Sonic hedgehog regulates proliferation and differentiation of mesenchymal cells in the mouse metanephric kidney. *Development* 129: 5301-5312, 2002.

Yurchenco PD, Amenta PS, and Patton BL. Basement membrane assembly, stability and activities observed through a developmental lens. *Matrix Biol* 22: 521-538, 2004a.

Yurchenco PD, Cheng YS, Campbell K, and Li S. Loss of basement membrane, receptor and cytoskeletal lattices in a laminin-deficient muscular dystrophy. *J Cell Sci* 117: 735-742, 2004b.

Yurchenco PD and Furthmayr H. Self-assembly of basement membrane collagen. *Biochemistry* 23: 1839-1850, 1984.

Yurchenco PD and Ruben GC. Basement membrane structure in situ: evidence for lateral associations in the type IV collagen network. *J Cell Biol* 105: 2559-2568, 1987.

Zaidel-Bar R, Ballestrem C, Kam Z, and Geiger B. Early molecular events in the assembly of matrix adhesions at the leading edge of migrating cells. *J Cell Sci* 116: 4605-4613, 2003.

Zent R, Bush KT, Pohl ML, Quaranta V, Koshikawa N, Wang Z, Kreidberg JA, Sakurai H, Stuart RO, and Nigam SK. Involvement of laminin binding integrins and laminin-5 in branching morphogenesis of the ureteric bud during kidney development. *Dev Biol* 238: 289-302, 2001.

Zervas CG, Gregory SL, and Brown NH. Drosophila integrin-linked kinase is required at sites of integrin adhesion to link the cytoskeleton to the plasma membrane. *J Cell Biol* 152: 1007-1018, 2001.

Zhou GF, Ye F, Cao LH, and Zha XL. Over expression of integrin $\alpha 5\beta 1$ in human hepatocellular carcinoma cell line suppresses cell proliferation in vitro and tumorigenicity in nude mice. *Mol Cell Biochem* 207: 49-55, 2000.

Appendix 1

Integrin α5 positive control

Positive staining of fetal skin (from mouse paw) is seen on this slide. Human keratinocytes have previously been shown to express integrin α5 (Adams and Watt 1991).

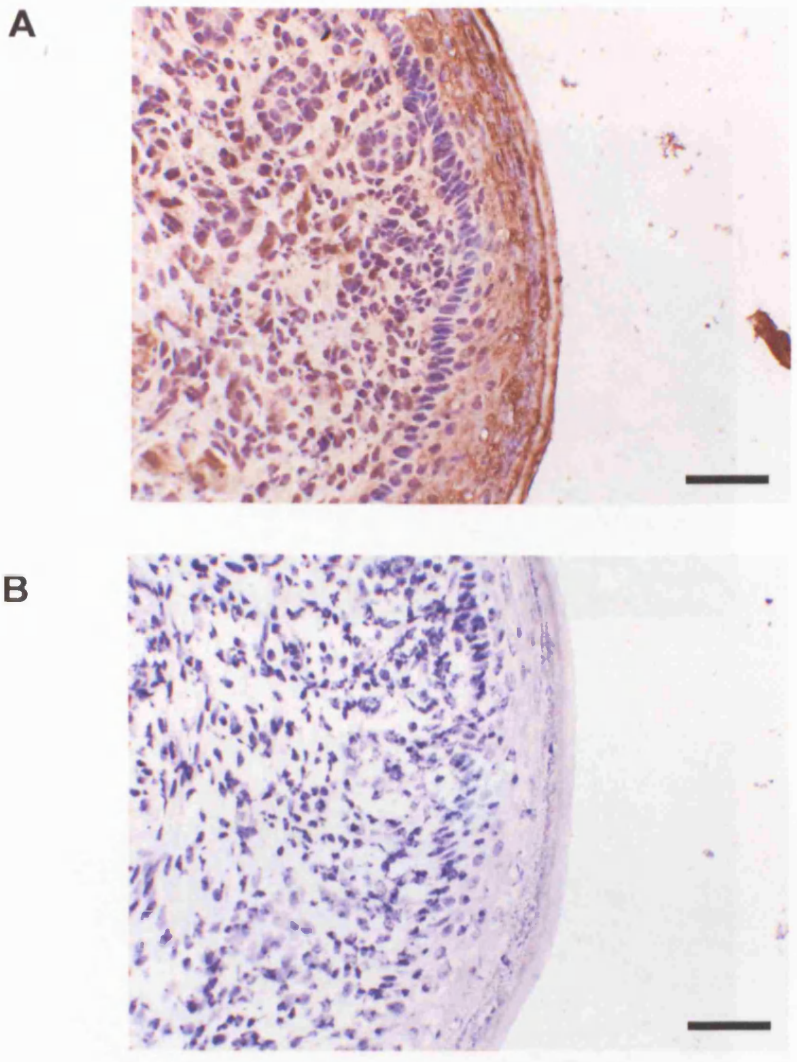

Appendix 1: Figure 1.1 Positive control for integrin α5. (A) integrin α5 immunostaining of positive control tissue – skin of E18 mouse paw. (B) Same section of mouse paw with isotype control rabbit IgG substituted for integrin α5 antibody. Scale bar 50μm

A

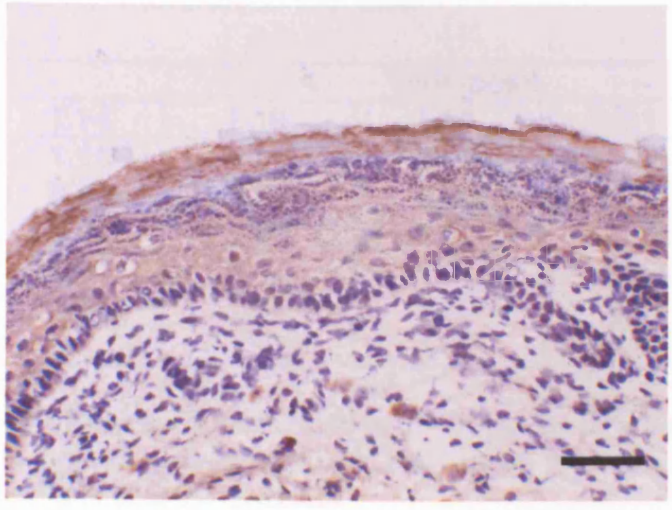

B

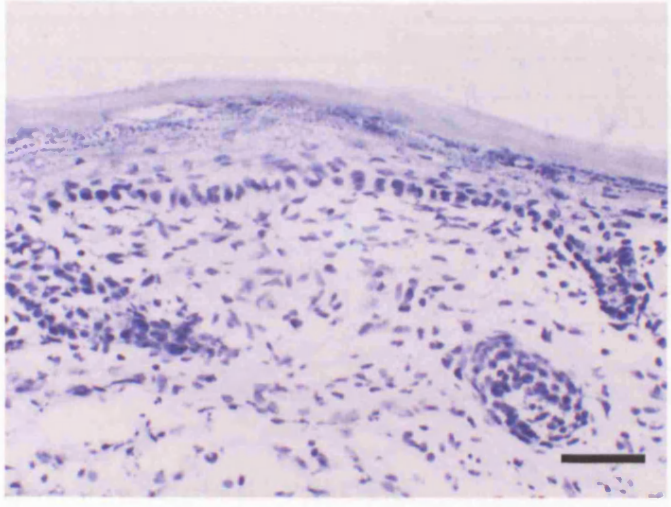

Appendix 1: figure 1.2 : Integrin β1 positive control. (A) Skin of mouse paw - immunostained for integrin β1. (B) Pre-immune rabbit IgG isotype control. Scale bar 50 μm

Data from fibronectin, integrin α5 and β1 Western Blots

Appendix 1: Table 1.1: Fibronectin WB data

	Time-point				
	E14	E16	E18	D1	6wks
Fibronectin Densitometry relative to β-actin	1.15	1.00	0.62	1.93	0.20
	0.88	1.77	0.78	2.31	0.44
	1.93	1.58	1.21	2.26	0.46
	1.81	2.14	1.05	2.43	1.08
	1.73	1.89	1.02	2.54	0.48
	.	1.52	1.60	2.02	0.44

In order to allow comparison between relative trends during development, the data was converted into a relative percentage of the maximum mean data point, as described by (Smeulders et al 2002, 2003).

Appendix 1: Table 1.2: Integrin α5 WB data

	Time-point				
	E14	E16	E18	D1	6wks
Integrin α5 Densitometry relative to β-actin, expressed as a % of maximum (6wk mean)	36.6	60.2	79.8	103.3	109.9
	43.0	55.8	55.5	112.1	110.9
	23.2	58.8	91.4	116.9	140.7
	39.8	63.2	60.6	127.5	73.8
	.	63.4	60.2	53.3	76.6
	.	73.3	70.1	68.2	88.2

Appendix 1: Table 1.3: Integrin β1 WB data

	Time-point				
	E14	E16	E18	D1	6wks
Integrin β1 Densitometry relative to β-actin	0.07	0.35	1.05	1.74	1.00
	0.48	1.15	0.89	0.97	0.72
	0.64	1.14	1.09	0.99	0.87
	.	0.58	1.20	1.82	1.78
	.	0.75	1.19	1.96	1.78
	.	.	1.85	2.05	1.84

Appendix 1: Table 1.4: β-actin expression was unchanged throughout murine bladder development

	Time-point				
	E14	E16	E18	D1	6wks
β-actin densitometry	6242	6590	9486	5124	7816
	5443	9006	9443	11879	7217
	5709	6654	5932	7736	6792
	6484	6754	7748	6329	6373
	8766	7301	9274	6031	6012
	7655	7506	5409	5814	5120
	9150	9971	8809	9226	12112
	16064	8406	5818	8814	14251
	11265	8630	4131	10686	15377
	10950	13464	14680	13432	17852
	7565	15528	14776	12156	22082
	.	15594	11169	18287	19299
	.	10621	12519	7421	5830
	.	11500	12074	8931	6643
	.	11368	10303	6719	6854
	.	8522	8108	7373	6747
	.	9813	7633	7033	7628
	.	9085	7024	6136	7544

There was no change in β-actin densitometry (measured in arbitrary units – AU) during murine bladder development, so this was useful as a loading control for WB data interpretation.

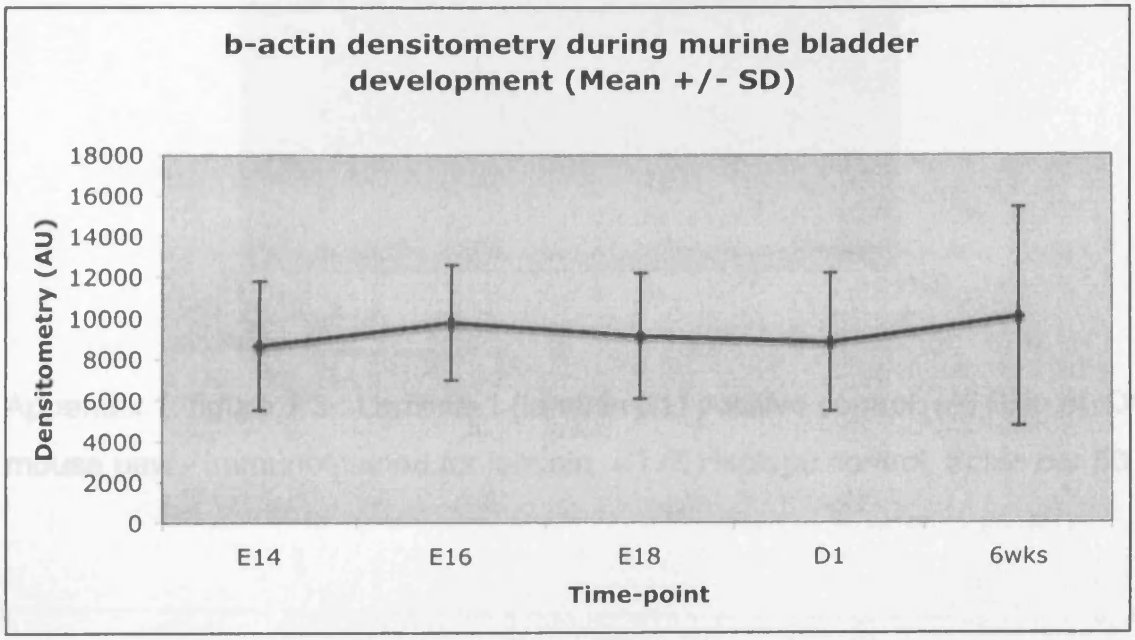

Appendix 1: figure 1.3: Laminin α1 (laminin-1) positive control

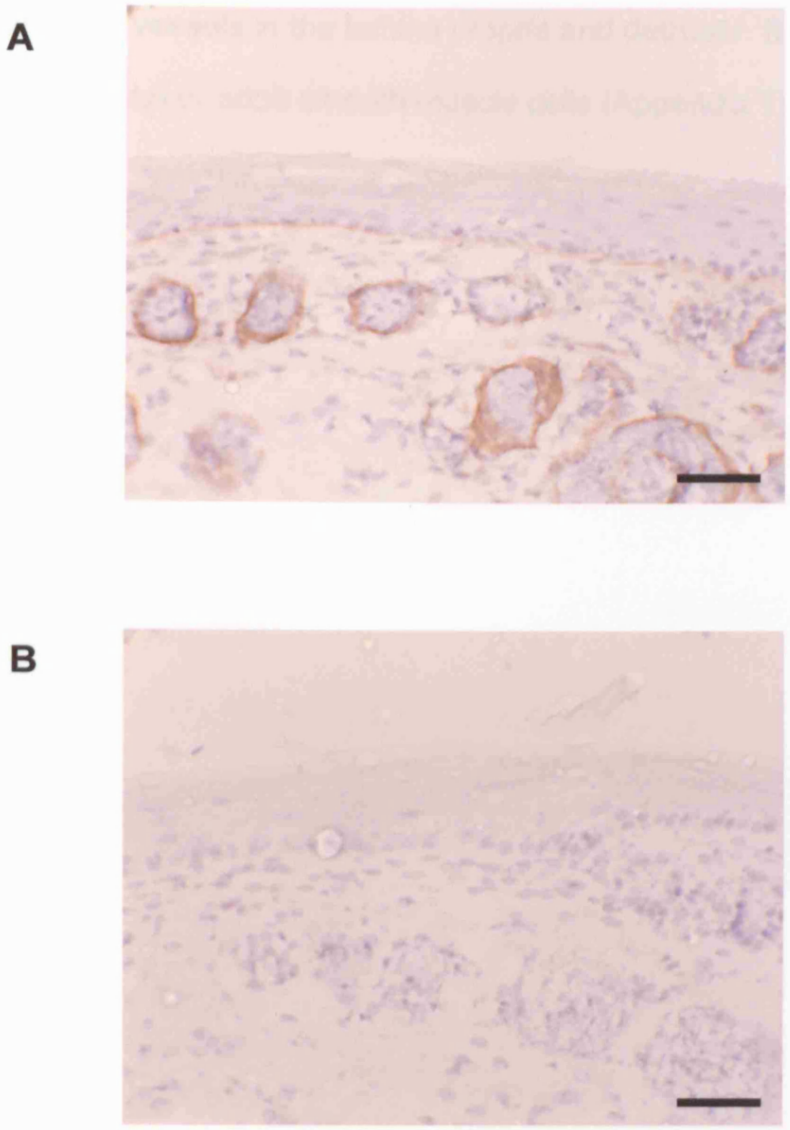

Appendix 1: figure 1.3 : Laminin-1 (laminin α1) positive control. (A) Skin of D1 mouse paw - immunostained for laminin α1 (B) Isotype control. Scale bar 50 μm

Integrin α6 subunit immunohistochemistry

Integrin α6 expression was present in the urothelium, but also in the basal lamina of blood vessels in the lamina propria and detrusor. It was not expressed by fetal or adult smooth muscle cells (Appendix 1: figure 1.5).

A

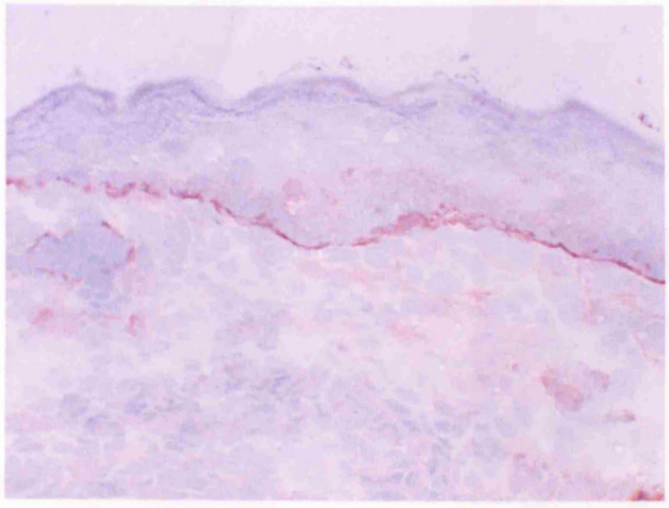

B

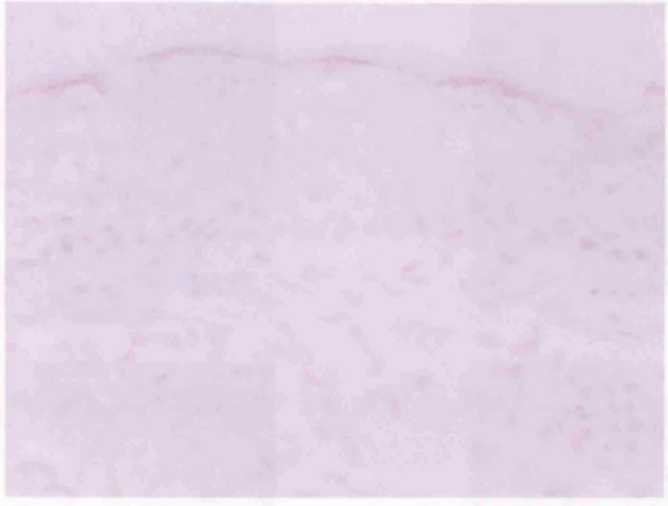

Appendix 1: figure 1.4 : Integrin α6 positive control skin of E18 fetal mouse paw. (A) Skin of paw immunostained for integrin α6. (B) Isotype control

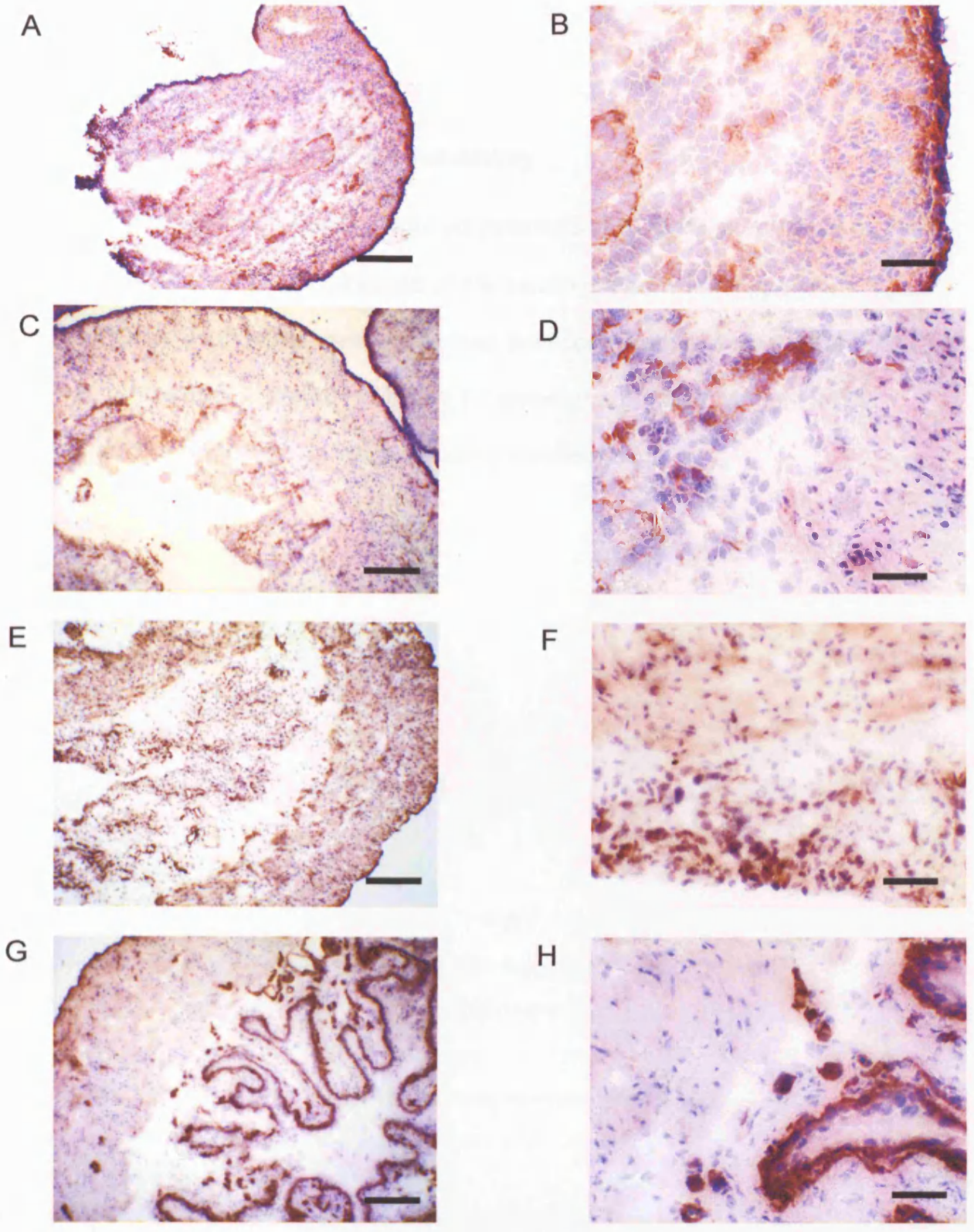

Appendix 1: Figure 1.5: Integrin α6 immunostaining. (A,B) E14; (C,D) E18, (E,F) Day1; (G,H) 6 wks. Scale bars (A,C,E,G) 400μm, (B,D,F,H) 50μm.

Integrin α7 subunit immunohistochemistry

Integrin α7 immunostaining required optimisation of fixation technique by the use of acetone at -20°C, instead of 4% paraformaldehyde) (Appendix 1: figure 1.6). Once fixation had been optimised then optimisation of the DAKO ARK kit was performed. Appendix 1: figure 1.7 shows the positive control for this antibody – myoblasts in the developing mouse paw.

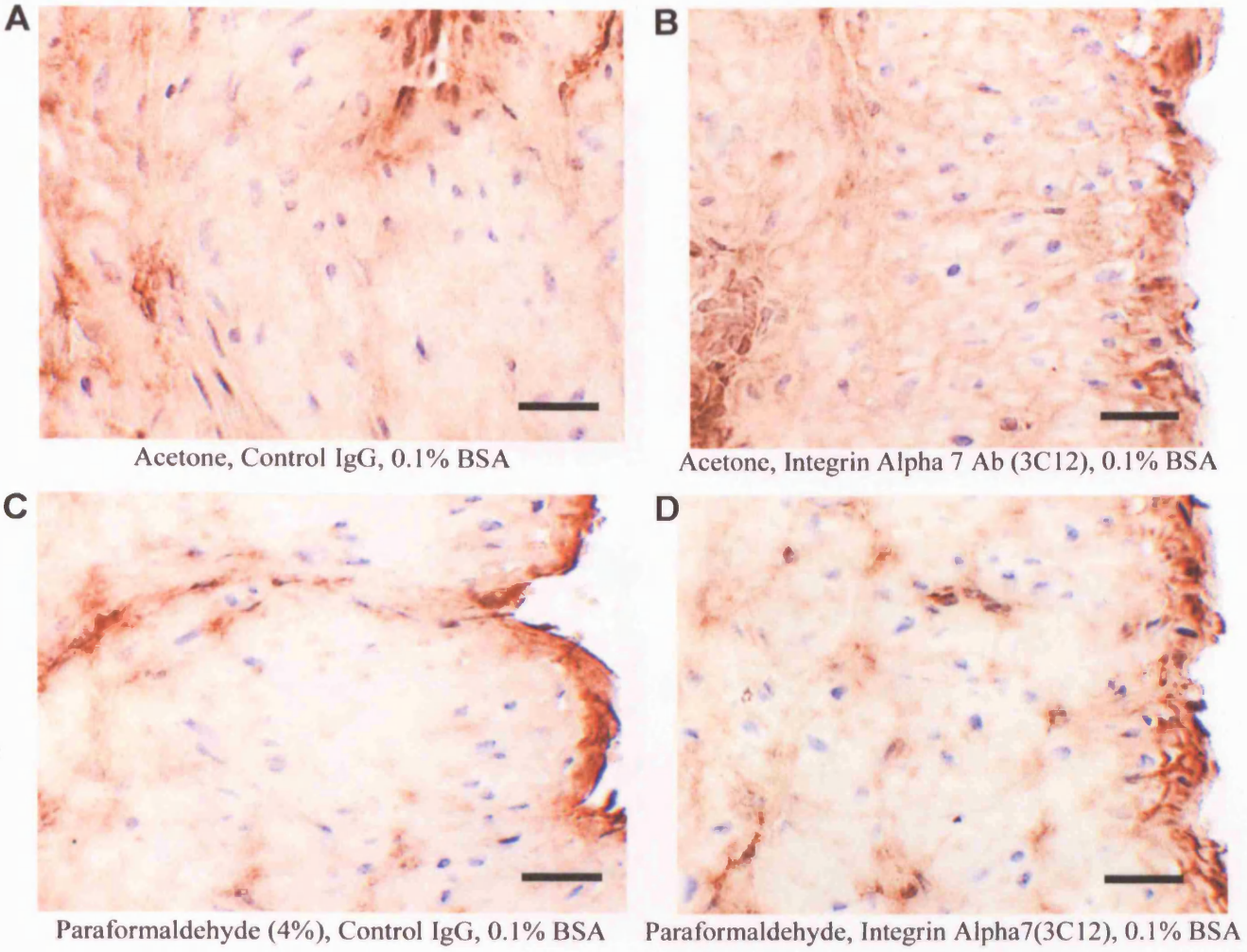

Appendix 1: figure 1.6: Optimisation of integrin α7 immunohistochemistry – fixation technique. (A) and (C) isotype control mouse IgG substituted for primary antibody. (B) and (D) Integrin α7 antibody (3C12) detected using Dako ARK. (A) and (B) are sections where acetone (-20'C) was used, compared to 4% paraformaldehyde in (C) and (D). Acetone fixation was associated with a much greater availability of the antigen (B) than the use of paraformaldehyde (D). Scale bars 50 μm.

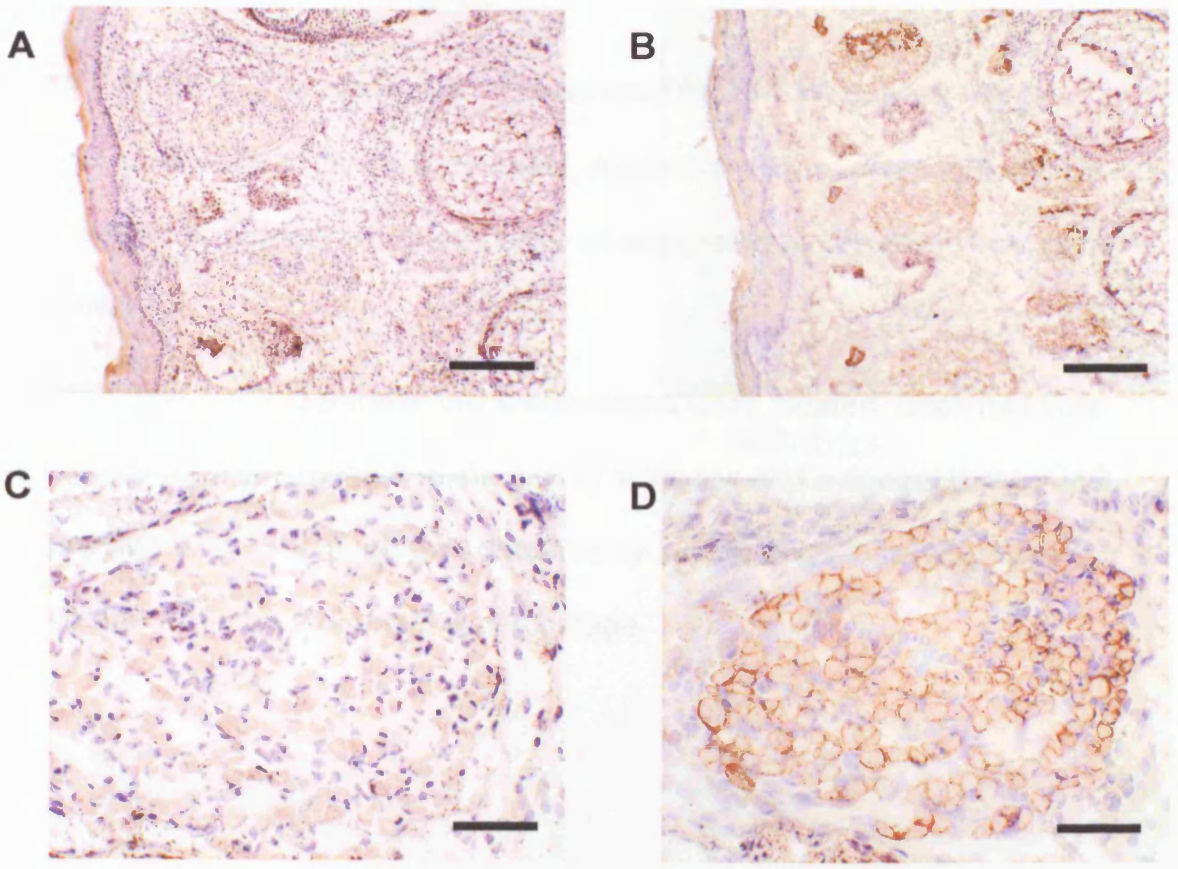

Appendix 1: Figure 1.7: Integrin $\alpha 7$ positive control - skeletal muscle from D1 neonatal mouse paw. (A) and (C) isotype mouse IgG. (B) and (D) integrin $\alpha 7$ immunostaining using Dako ARK technique, with AB blocking kit. Scale bars (A and B) 400μm, (C and D) 50μm.

Integrin α7 subunit FACS analysis

The anti-integrin α7 antibody (3C12) was used for FACS analysis, using protocol as described on the data sheet. A positive control of smooth muscle (from the genito-urinary tract) was used as suggested by the data sheet (data not shown).

For each time-point, 3 parallel cell suspensions were created. Each had flow cytometry performed using anti-integrin a7 antibody and a control isotype IgG. The positive cell percentage was obtained by subtracting the isotype control percentage from the anti-integrin percentage.

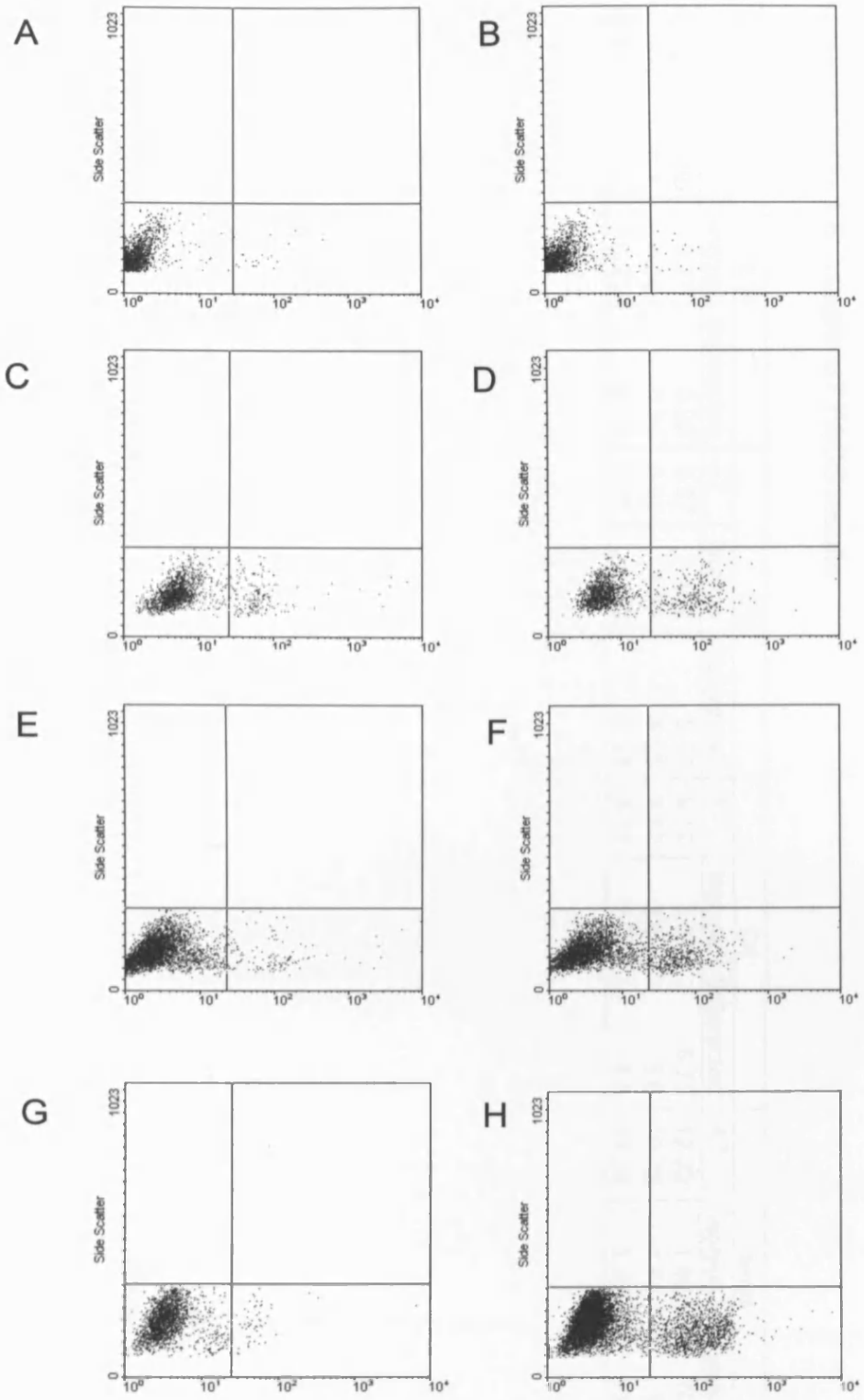

Appendix 1: figure 1.8: flow cytometry dot-plots for integrin $\alpha 7$ in whole bladder suspensions from E14 (A,B); E18(C,D); D1(E,F); 6wks (G,H). (A,C,E,G) are control runs using isotype control pre-immune IgG. (B,D,F,H) are runs using integrin $\alpha 7$ antibody (3C12).

Appendix table 1.6: Integrin α7 FACS results

	E14			E18			D1			6wks		
	A7	Isotype	Subtracted	A7	Isotype	Subtracted	A7	Isotype	Subtracted	A7	Isotype	Subtracted
% Cells	0.29	0.27	0.02	5.37	0.2	5.17	9.12	3.39	5.73	12.22	1.65	10.57
detected	0.1	0.34	-0.24	6.93	1.38	5.55	9.52	3.92	5.6	10.78	1.54	9.24
by FACS	0.1	0.23	-0.13	4.31	1.38	2.93	8.18	3.38	4.8	14.36	2.03	12.33

Appendix 2: Data for Cell adhesion experiments

Background data for cell adhesion experiments

1) Fibronectin plating concentration.

Each suspension was created from 1 litter, using approximately 10 fetal E18 bladders. Three parallel cell suspensions were created, to produce n=3 fro this preliminary experiment.

Appendix 2: Table 2.1: Initial phase contrast adhesion experiment.

Suspension	Fibronectin conc	Morphology	Count1	Count2	Count3	Count4	Average
1	0	R	23	16	20	8	16.75
2	0	R	22	3	12	11	12
3	0	R	17	4	22	48	22.75
1	10	R	15	13	34	24	21.5
2	10	R	20	19	15	25	19.75
3	10	R	12	13	11	11	11.75
1	20	R	21	26	17	28	23
2	20	R	27	25	29	16	24.25
3	20	R	10	13	9	9	10.25
1	40	R	33	20	20	33	26.5
2	40	R	14	25	16	22	19.25
3	40	R	20	11	8	13	13
1	0	S	18	21	7	7	13.25
2	0	S	5	14	1	0	5
3	0	S	12	0	8	13	8.25
1	10	S	35	29	52	35	37.75
2	10	S	103	122	36	79	85
3	10	S	64	66	33	32	48.75
1	20	S	61	46	32	58	49.25
2	20	S	65	81	95	100	85.25
3	20	S	47	71	47	48	53.25
1	40	S	58	58	53	70	59.75
2	40	S	70	63	63	76	68
3	40	S	63	86	39	29	54.25

This data shows an increase in adhesion of cells (increase is in cells with a spread morphology), up to 10 mcg/ml of plating concentration of fibronectin. There was no significant increase in adhesion after this (ANOVA $p<0.05$, with Bonferroni post-hoc significance of $p<0.05$ for comparisons between 0 and 20μg/ml and 0 and 40μg/ml).

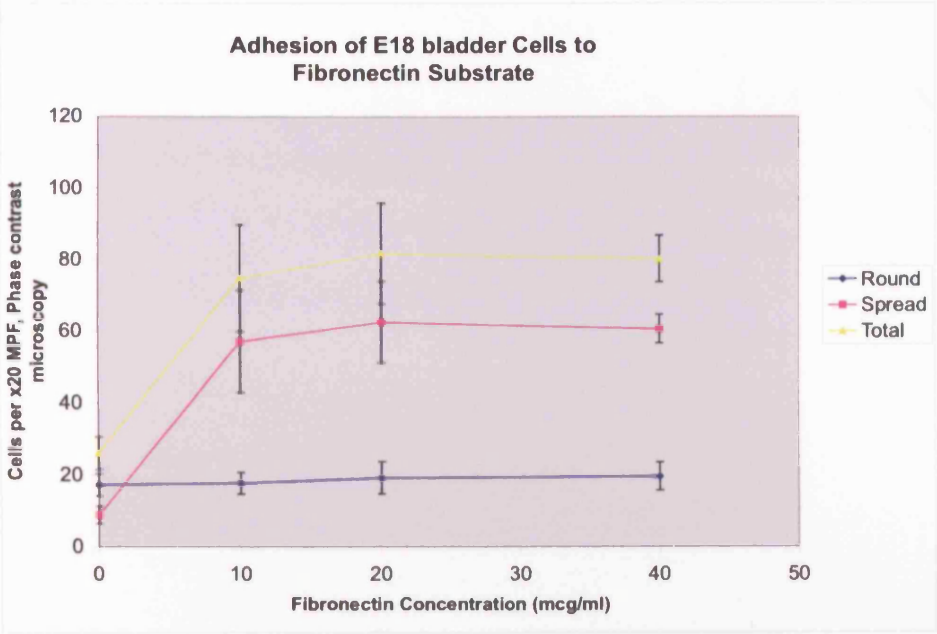

Appendix 2: Figure 2.1: Preliminary fibronectin adhesion experiment, using 3 different E18 cell suspensions. Adhesion was allowed to proceed for 1 hour, and after rinsing, adherent cells were visualized by phase contrast microscopy.

2) Immunocytochemistry

CD31

CD31, platelet endothelial cell adhesion marker was used as a marker of endothelial cells. It is expressed in the developing murine bladder (Appendix 2: figure 2.3).

A

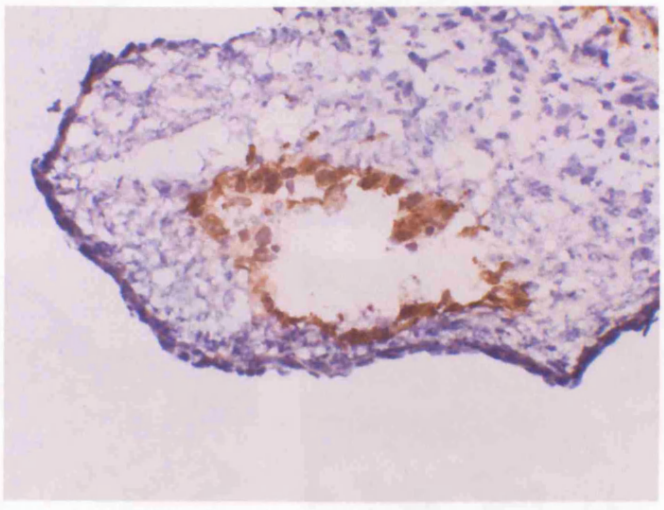

B

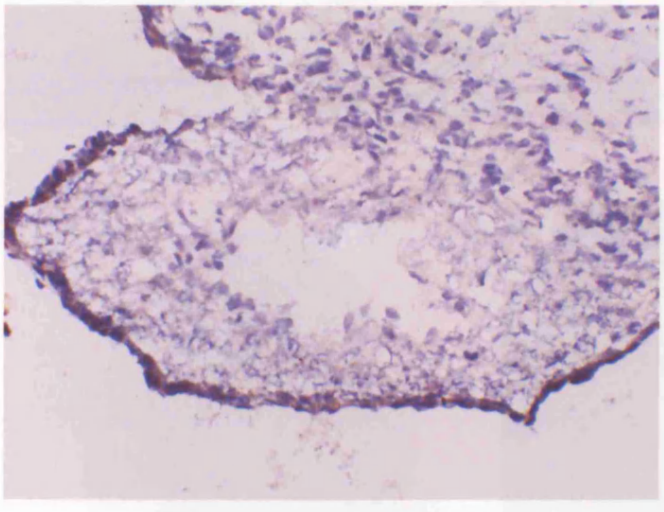

Appendix 2: figure 2.2 : CD31 positive control E14 umbilical artery. (A) Umbilical artery - immunostained for CD31 (B) Isotype control

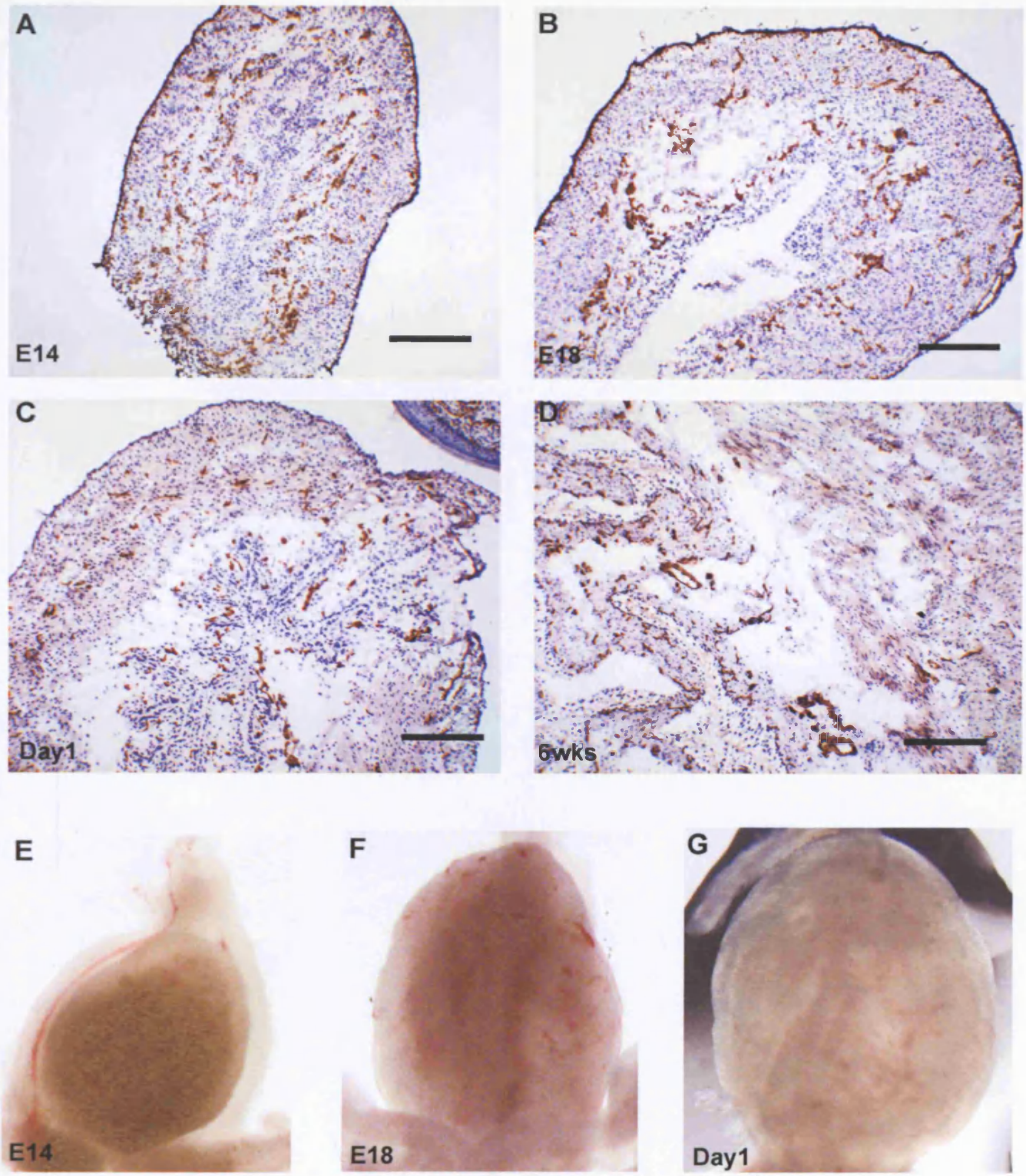

Appendix 2: figure 2.3: Blood vessel development during bladder development. (A-D) IHC from E14 to 6wks showing immunostaining for CD31, Platelet endothelial cell adhesion molecule (PECAM), as a marker of endothelium. Dissection microscope photographs of bladders at E14–day1. The pattern of blood vessels is very similar in both. Scale bars 400μm.

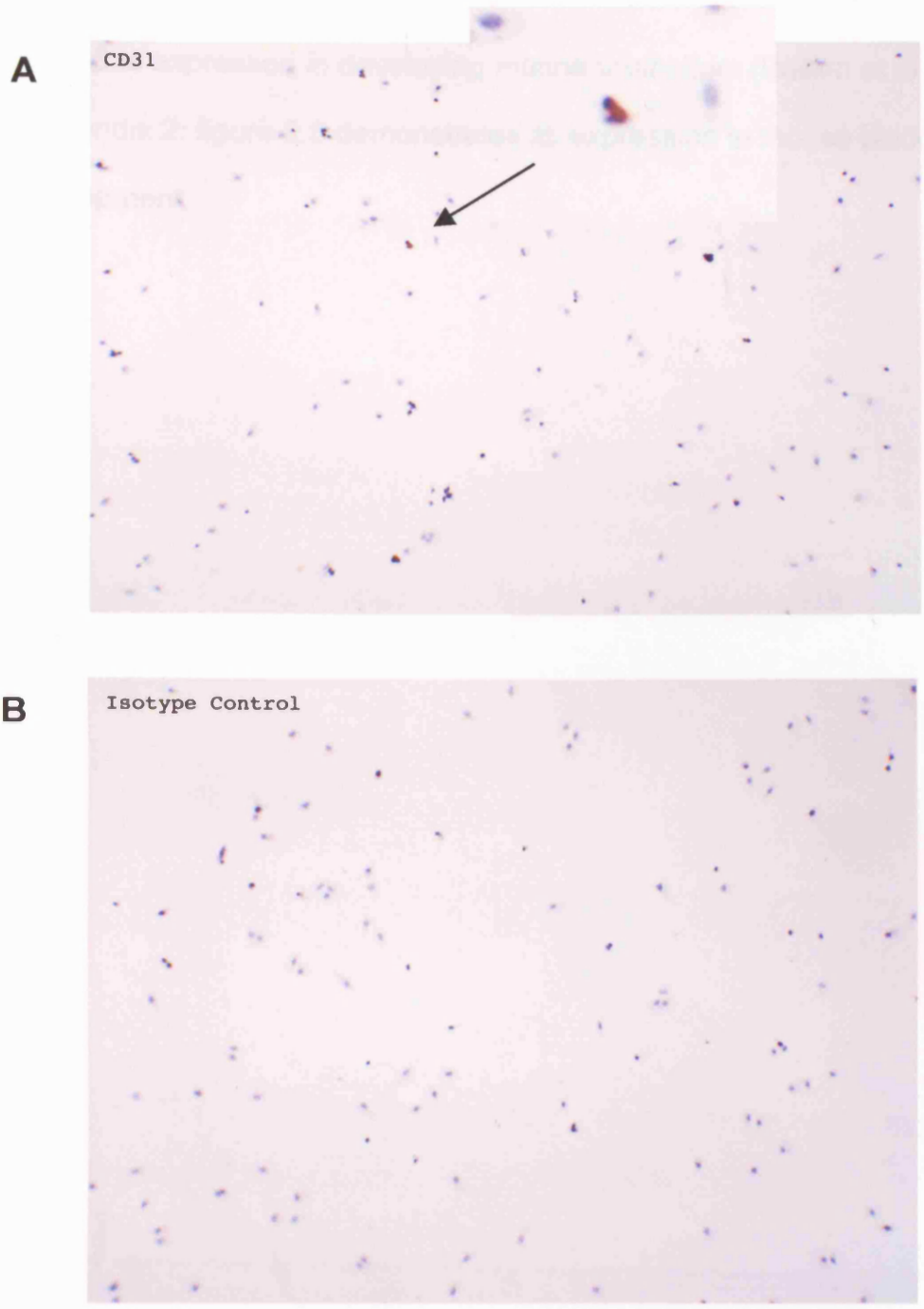

Appendix 2: figure 2.4: Immunocytochemistry of CD31 cells. (A) CD31, positively staining cell shown in close-up. (B) Isotype control IgG instead of CD31 antibody, no staining seen.

Cytokeratin 18

Cytokeratin 18 is expressed in developing murine urothelium (Baskin et al 1996c). Appendix 2: figure 2.5 demonstrates its expression in mouse bladders during development.

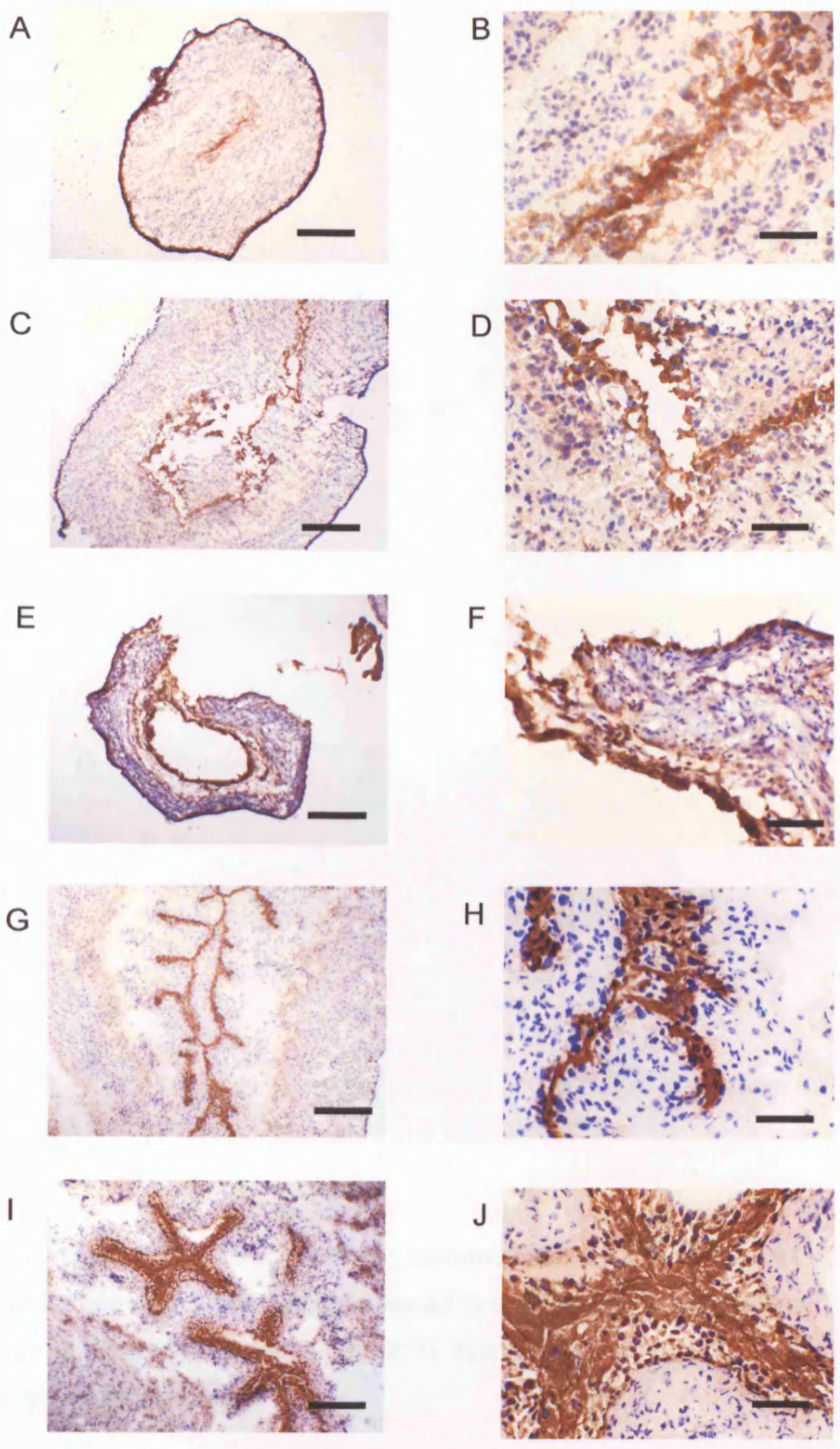

Appendix 2: figure 2.5: Cytokeratin-18 immunostaining throughout bladder development, only present in urothelium. (A,B) E14; (C,D) E16; (E,F) E18; (G,H) D1; (I,J) 6wks. (A,C,E,G,I) Scale bars 400 μm. (B,D,F,H,J) Scale bars 50μm.

A

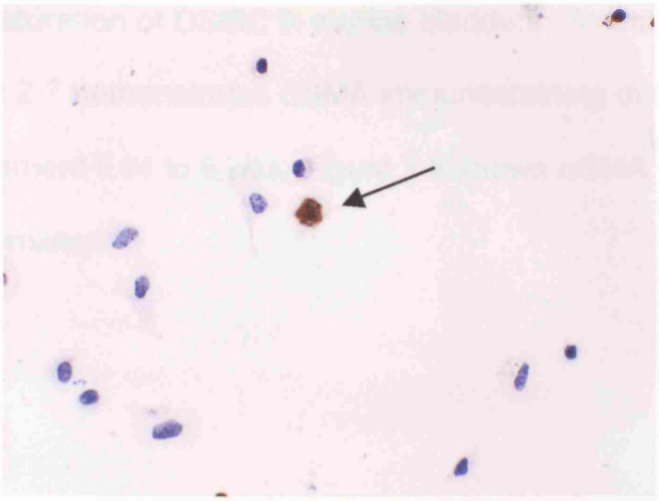

B

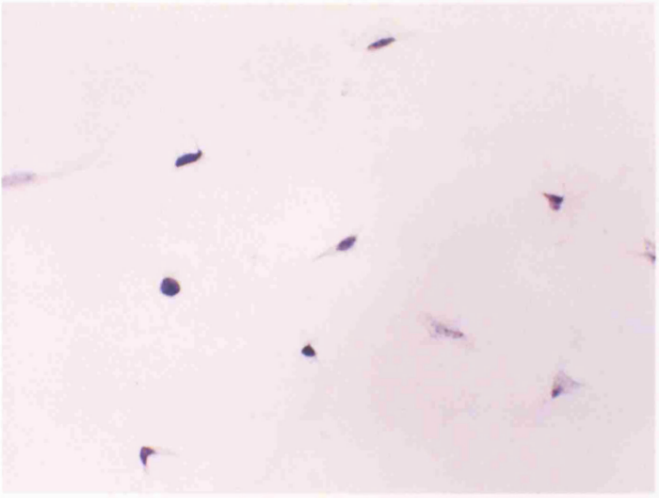

Appendix 2: figure 2.6: Cytokeratin 18 immunocytochemistry. (A) E18 bladder cell suspension immunostained cytokeratin 18, arrow pointing to positively immunostained cell. (B) Isotype control IgG used in place of cytokeratin antibody.

αSMA

αSMA is a marker of smooth muscle cell differentiation, and has been used to demonstrate maturation of DSMC in murine bladders (Smeulders et al 2002). Appendix figure 2.7 demonstrates αSMA immunostaining during mouse bladder development E14 to 6 wks. Figure 2.8 shows αSMA immunocytochemistry.

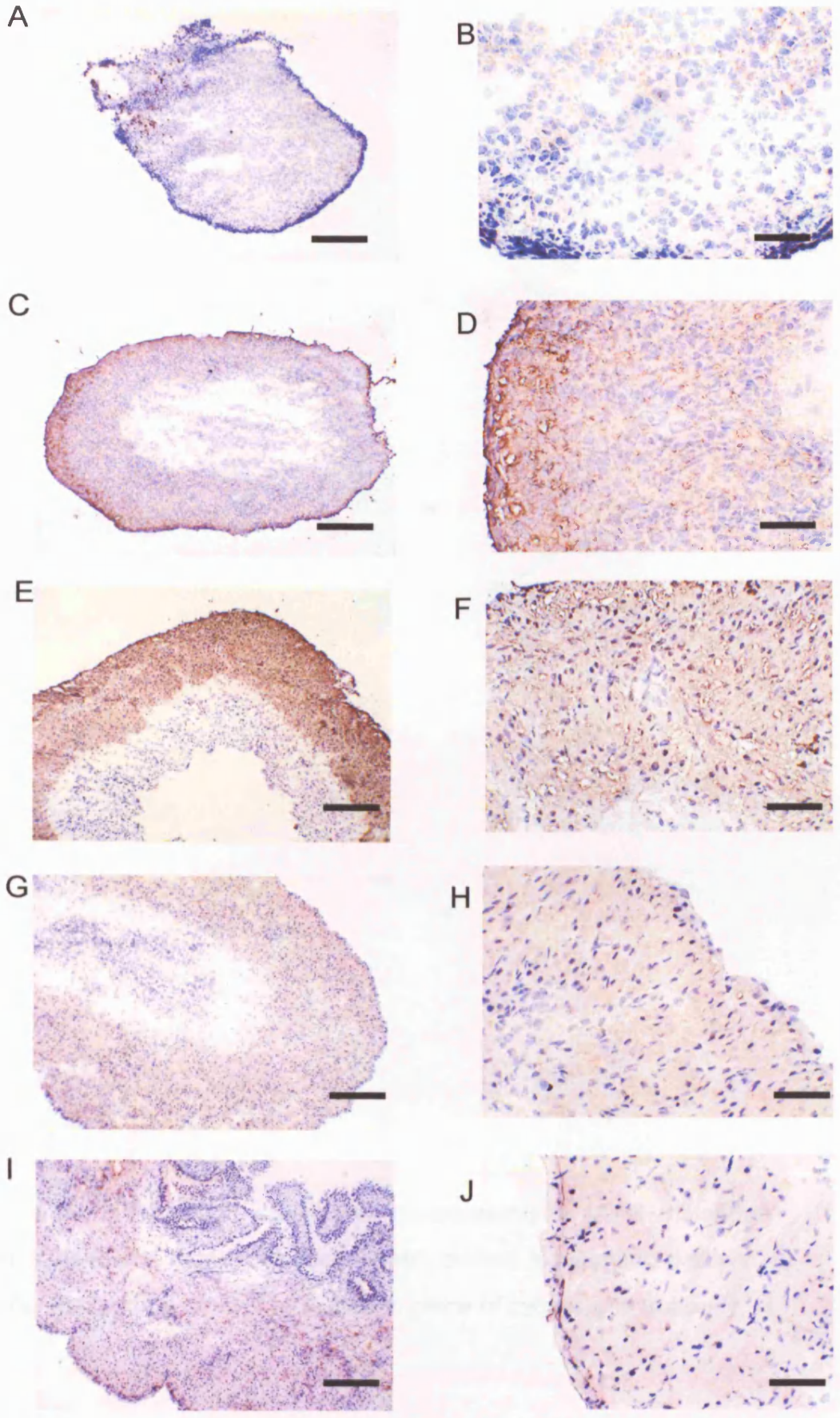

Appendix 2: figure 2.7: αSMA immunostaining throughout bladder development. (A,B) E14; (C,D) E16; (E,F) E18; (G,H) D1; (I,J) 6wks. (A,C,E,G,I) Scale bars 400 μm. (B,D,F,H,J) Scale bars 50μm.

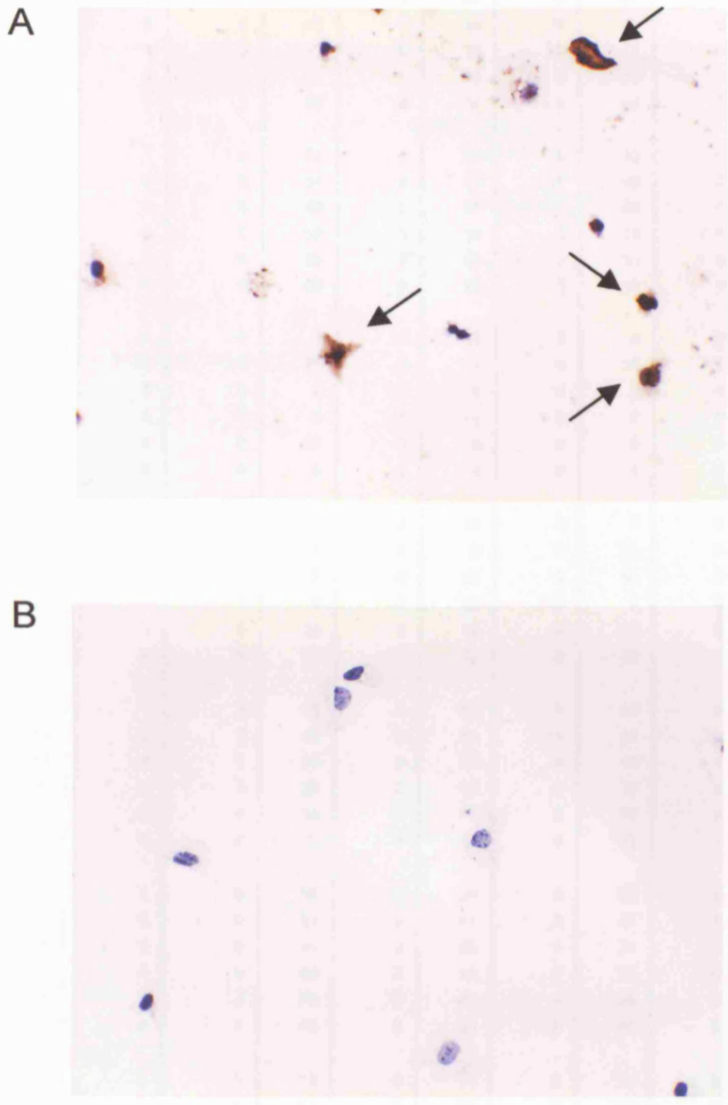

Appendix 2: figure 2.8: αSMA immunocytocemistry. (A) E18 bladder cell suspension immunostained αSMA, arrows highlighting positive cells. (B) Isotype control IgG used in place of cytokeratin antibody.

3) Fibronectin proliferation experiment

Appendix 2: Table 2.2: Fibronectin adhesion proliferation data

Time	Fn	FCS added	Sus-pension	BrdU+1	Total1	BrdU+2	Total2	BrdU+3	Total3	BrdU+4	Total4	AvBrdU+	AvTotal	%BrdU+
1	10	10	1	0	12	0	13	0	26	0	13	0	16	0%
1	10	10	2	0	70	0	61	0	62	0	83	0	69	0%
1	10	10	3	0	45	0	34	0	18	0	28	0	31.25	0%
1	10	10	4	0	13	0	10	0	17	0	8	0	12	0%
1	10	10	5	0	33	0	10	0	29	0	19	0	22.75	0%
1	10	10	6	1	49	0	38	0	45	0	25	0.25	39.25	1%
1	10	0	1	0	37	1	26	0	23	0	33	0.25	29.75	1%
1	10	0	2	0	51	0	49	0	40	0	43	0	45.75	0%
1	10	0	3	0	40	2	51	0	58	0	26	0.5	43.75	1%
1	10	0	4	0	18	0	16	0	13	0	8	0	13.75	0%
1	10	0	5	0	24	0	29	0	31	0	33	0	29.25	0%
1	10	0	6	0	39	0	28	0	41	0	29	0	34.25	0%
1	0	10	1	0	4	0	3	0	4	0	3	0	3.5	0%
1	0	10	2	0	20	0	3	0	15	0	5	0	10.75	0%
1	0	10	3	0	2	0	3	0	3	0	2	0	2.5	0%
1	0	10	4	0	3	0	4	0	2	0	1	0	2.5	0%
1	0	10	5	0	10	0	5	0	5	0	2	0	5.5	0%
1	0	10	6	0	5	0	4	0	1	0	2	0	3	0%
1	0	0	1	0	3	0	10	0	9	0	8	0	7.5	0%
1	0	0	2	0	13	0	9	0	10	0	19	0	12.75	0%
1	0	0	3	0	23	0	31	0	10	0	24	0	22	0%
1	0	0	4	1	8	0	12	0	7	0	14	0.25	10.25	2%
1	0	0	5	0	28	0	18	0	10	0	18	0	18.5	0%
1	0	0	6	0	32	0	32	0	38	0	19	0	30.25	0%
12	10	10	1	3	25	5	63	1	54	6	43	3.75	46.25	8%
12	10	10	2	6	42	3	61	11	64	9	75	7.25	60.5	12%
12	10	10	3	5	50	3	36	4	46	1	61	3.25	48.25	7%
12	10	10	4	1	25	2	36	1	17	3	39	1.75	29.25	6%
12	10	10	5	6	86	3	60	5	31	5	25	4.75	50.5	9%
12	10	10	6	6	50	5	34	4	28	1	33	4	36.25	11%
12	10	0	1	0	36	1	24	0	39	0	48	0.25	36.75	1%
12	10	0	2	0	34	0	41	0	27	0	40	0	35.5	0%
12	10	0	3	0	41	0	45	1	21	0	19	0.25	31.5	1%
12	10	0	4	0	28	0	14	0	24	0	23	0	22.25	0%
12	10	0	5	4	76	3	45	4	25	2	60	3.25	51.5	6%
12	10	0	6	1	48	2	34	0	41	2	86	1.25	52.25	2%
12	0	10	1	0	12	0	19	0	20	0	22	0	18.25	0%
12	0	10	2	0	54	0	52	2	50	0	59	0.5	53.75	1%
12	0	10	3	0	51	0	64	2	46	0	76	0.5	59.25	1%
12	0	10	4	0	15	0	4	0	14	0	5	0	9.5	0%
12	0	10	5	0	26	0	37	0	20	2	64	0.5	36.75	1%
12	0	10	6	0	16	0	25	0	23	0	15	0	19.75	0%
12	0	0	1	0	5	0	5	0	5	0	10	0	6.25	0%
12	0	0	2	0	16	0	12	0	12	0	17	0	14.25	0%
12	0	0	3	0	15	0	7	0	16	0	16	0	13.5	0%
12	0	0	4	0	11	0	10	0	12	0	3	0	9	0%
12	0	0	5	0	9	0	17	0	10	0	7	0	10.75	0%
12	0	0	6	0	19	0	13	0	8	0	16	0	14	0%

4) RGD oligopeptides concentration

Appendix 2: Table 2.3: Preliminary RGD/RAD oligopeptides concentrations vs Fibronectin concentration. Percentage blockade is calculated from total cell numbers adherent for a cell suspension in presence of RAD (control peptide) minus total cell numbers adherent in presence of RGD (active blocking peptide), divided by RAD total and expressed as a percentage.

Suspension	Blocker conc.	Fibronectin conc.	%Blockade
1	10	0	-11.0
2	10	0	-12.5
3	10	0	13.3
1	10	5	30.6
2	10	5	29.5
3	10	5	26.4
1	10	10	22.5
2	10	10	26.6
3	10	10	-22.1
1	10	20	-6.8
2	10	20	-6.7
3	10	20	-20.5
1	20	0	-24.4
2	20	0	16.0
3	20	0	-3.1
1	20	5	46.6
2	20	5	25.0
3	20	5	-15.6
1	20	10	20.1
2	20	10	7.1
3	20	10	23.4
1	20	20	36.0
2	20	20	18.3
3	20	20	23.8
1	40	0	37.0
2	40	0	-2.2
3	40	0	-17.3
1	40	5	-5.1
2	40	5	12.0
3	40	5	20.1
1	40	10	29.1
2	40	10	30.0
3	40	10	20.2
1	40	20	15.2
2	40	20	58.7
3	40	20	-11.5

From appendix 2: figure 2.9 it can be seen that with low concentration of oligopeptide blockers, the blockade of adhesion to the fibronectin substrate is reduced as the fibronectin coating concentration increases. With 20 mcg/ml of oligopeptides, the blockade increases with increasing fibronectin coating concentration. With 40 μg/ml of oligopeptide, the blockade is not as marked as it is with 20 μg/ml of oligopeptide, raising the possibility of increasing non-specific effects. In comparing the percentage blockade of oligopeptides at 20 μg/ml vs 10 μg/ml on 40 μg/ml of fibronectin, there was a significant increased blockade (-11% vs 26%) (students t-test $p<0.05$), whereas there was a reduced effect for 40 μg/ml oligopeptide, and no significant difference. The oligopeptide concentration chosen for subsequent blocking experiments was therefore 20 μg/ml.

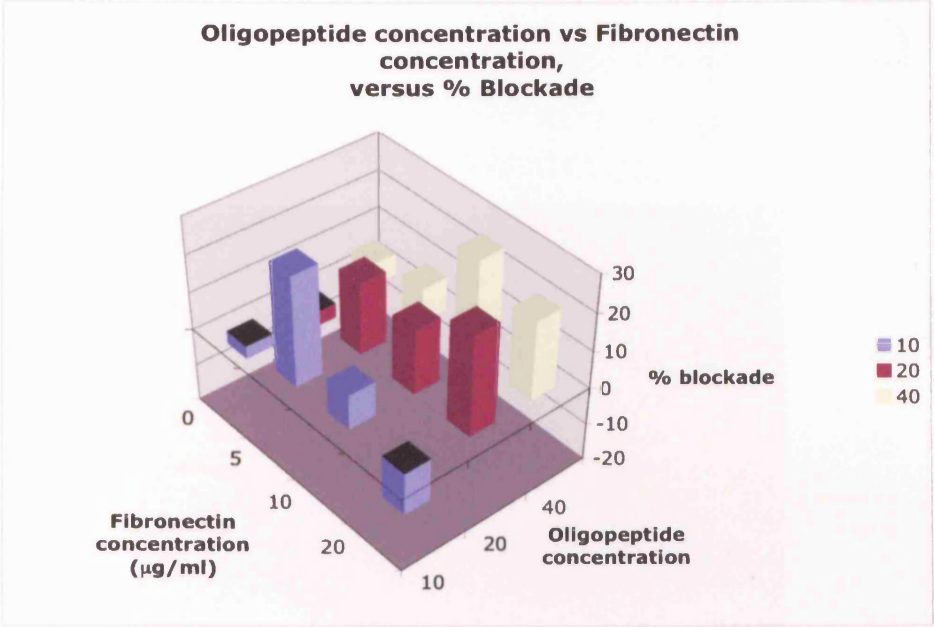

Appendix 2: figure 2.9: Blockade E18 cell adhesion (%) versus. fibronectin (coating concentration (µg/ml)) versus. RGD/RAD oligopeptide concentration (µg/ml). Percentage blockade calculated by subtracting cell counts with RGD from cell counts in presence RAD (control), divided by RAD cell count.

Appendix 2: figure 2.10: TUNEL test control. Negative control rTdT not added

Appendix 3

Generating fetal mouse bladder explant model

Preliminary experiments were performed to optimise the growth conditions: the first comparison was between antibiotics and FCS, vs. FCS, vs. ITS. The protein estimations from bladders harvested after 3 days of explant culture are listed below.

Appendix 3: Table 3.1: Comparison media additives and explant growth after three days

Medium	Protein
Abx+FCS	0.075510204
Abx+FCS	0.025820763
Abx+FCS	0.052144336
Abx+FCS	0.04208814
FCS	0.067957802
FCS	0.061029759
FCS	0.075515667
FCS	0.058510471
FCS	0.047488584
FCS	0.062289403
ITS	0.052842072
ITS	0.172823177
ITS	0.140387341
ITS	0.063234136
ITS	0.105117304
ITS	0.073941112

Anova ($p<0.05$), for growth medium comparing ITS to FCS, to Antibiotics and FCS.

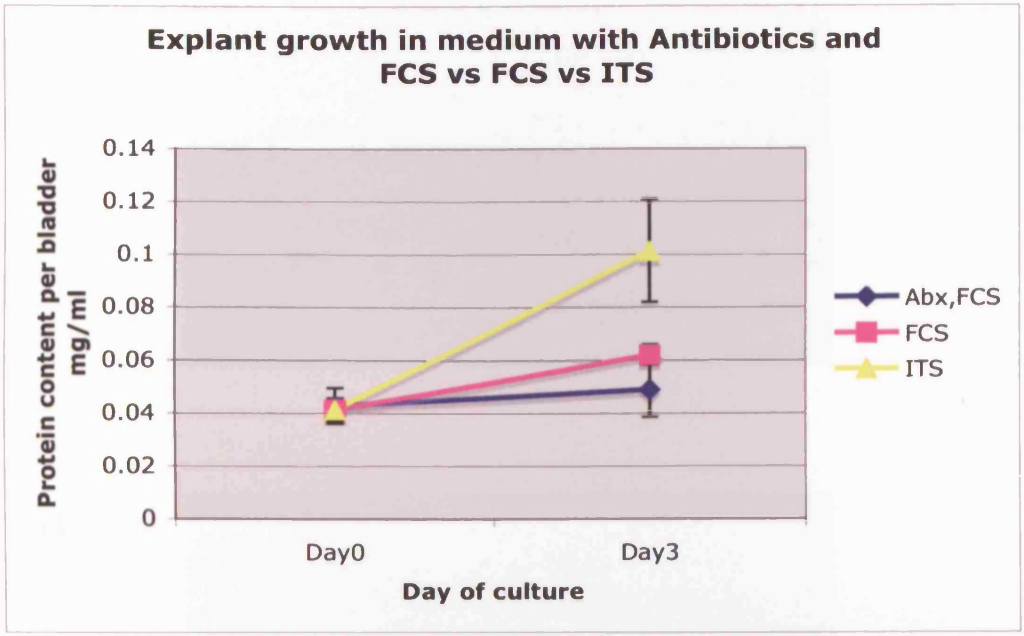

Appendix 3: Figure 3.1: Initial growth of E14 explant bladders in 3 different media: 1) Antibiotics and FCS, 2) FCS, 3) ITS. Data plotted as mean±SEM.

A

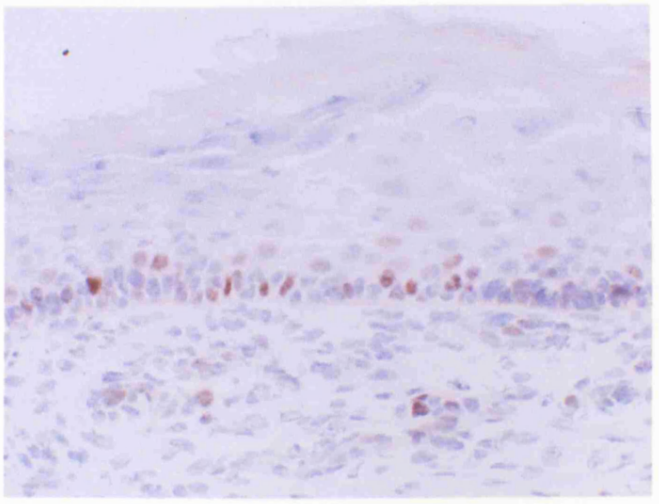

B

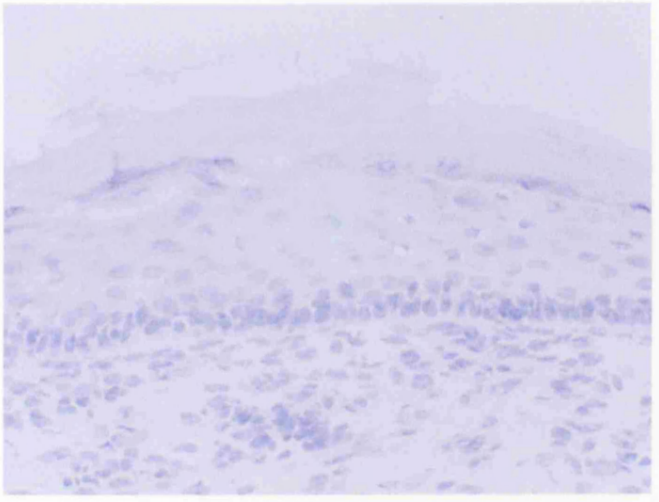

Appendix 3: figure 3.2 : PCNA positive control. - skin from paw of DI mouse (A) skin from paw - immunostained for PCNA (B) Isotype control

Appendix 4

Positive controls for anti-human Fibronectin antibody and anti-human Desmin antibody.

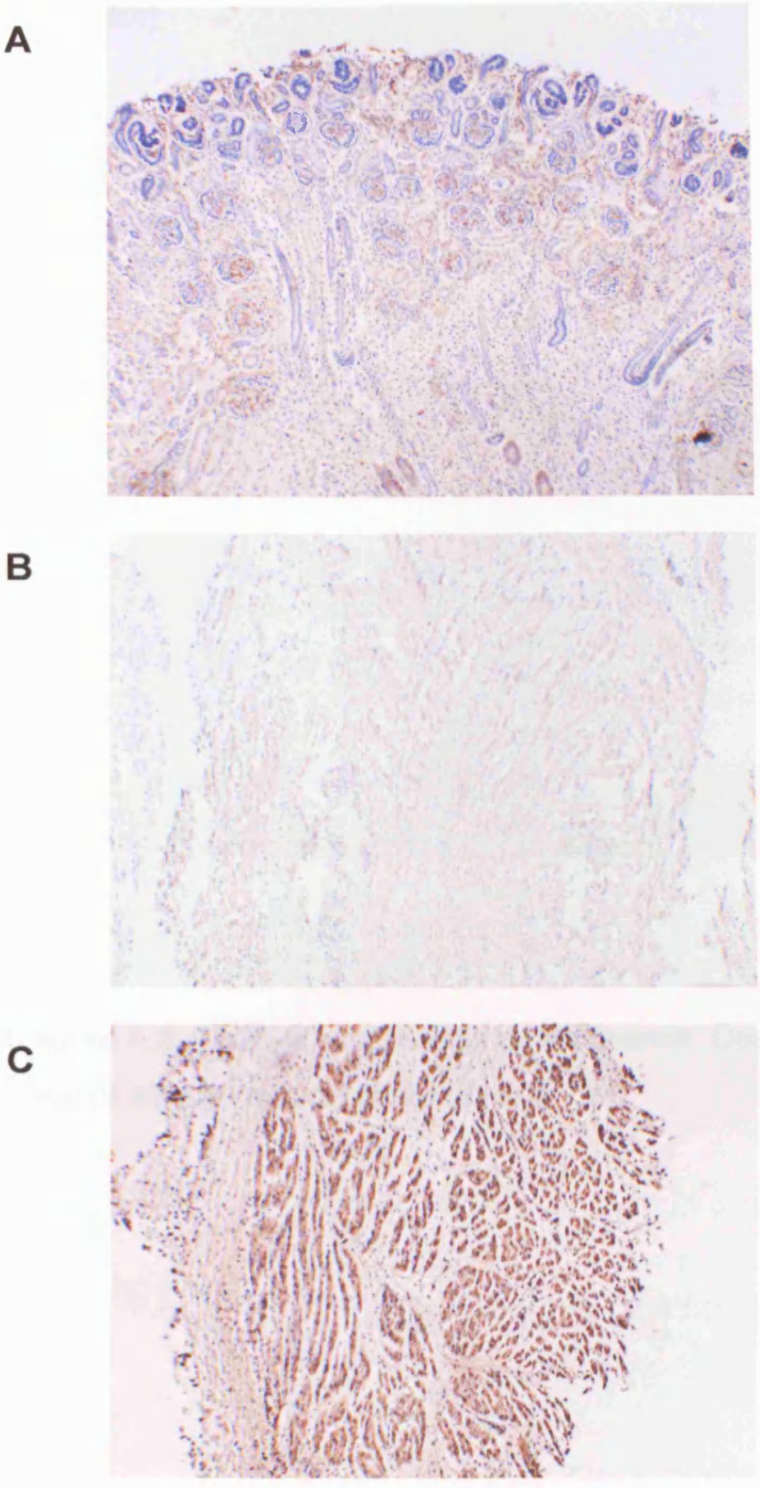

Appendix 4: figure 4.1: Positive control anti-human fibronectin. (A) Fibronectin immunostaining of stroma and undifferentiated mesoderm in human fetal kidney. (B) Rabbit isotype IgG control showing minimal non-specific staining of human fetal bladder. (C) Serial section of same human fetal bladder immunostained with anti-human fibronectin antibody (A0245, DAKO) .

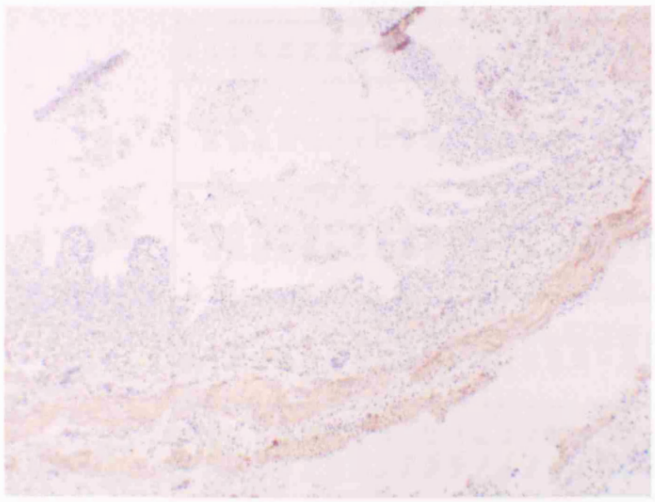

Appendix 4: figure 4.2: Positive control anti-human desmin. Desmin immunostaining of smooth muscle in human fetal GIT

Appendix 4: Table 4.1: Tabulated results for human bladders

Fetus	Bladder outflow obstruction?	Gestational age (weeks)	Sex	Total wall thickness (mm)	Thickness lamina propria (mm)	Detrusor thickness (mm)	Muscle area ratio (%)	Collagen area ratio (%)	Muscle/collagen ratio (%)	Fibronectin area (%) - Detrusor	Fibronectin area (%) - Lamina Propria	Muscle Dysmorphology score (0-6)	Renal dysplasia score (0-15)	Pumonary hypoplasia (Lung/total body wt)	Oligohydramnios
1	n	16	F	0.5	0.16	0.34	30.8%	40.0%	76.9%	8.5%	3.6%	2	4	4.1%	No
2	n	16	M	0.67	0.21	0.47	18.9%	25.6%	73.7%	21.1%	3.0%	1	4	3.8%	No
3	n	18	M	0.78	0.29	0.5	9.3%	35.6%	26.1%	11.8%	3.8%	2	1	3.3%	No
4	n	20	F	1	0.29	0.71	15.7%	36.0%	43.6%	14.5%	2.4%	1	0	3.1%	No
5	n	20	M	1.15	0.46	0.69	10.7%	25.6%	41.6%	14.2%	1.0%	2	1	3.1%	No
6	n	21	M	1.1	0.25	0.85	21.7%	32.2%	67.4%	24.6%	20.1%	0	1	1.6%	No
7	n	24	M	1.42	0.25	1.17	18.3%	26.9%	67.8%	14.0%	8.5%	0	0	1.8%	No
8	n	26	M	1.09	0.25	0.84	18.2%	31.2%	58.4%	13.3%	4.3%	0	0	4.2%	No
9	n	27	F	1.25	0.11	1.14	23.3%	27.9%	83.4%	23.2%	17.5%	0	0	2.4%	No
10	n	28	F	1.08	0.31	0.77	21.9%	26.3%	83.4%	20.6%	3.9%	1	.	2.2%	No
11	n	30	M	1.23	0.46	0.77	20.1%	23.3%	86.3%	32.5%	5.6%	2	0	1.8%	No
12	n	31	F	1.63	0.53	1.09	29.0%	26.0%	111.8%	24.1%	8.5%	0	1	0.0%	No
13	y	18	M	1.26	0.68	0.58	15.6%	56.7%	27.6%	1.4%	1.5%	5	15	2.4%	Yes
14	y	18	M	2.22	0.21	2.01	19.5%	25.3%	77.3%	2.3%	7.1%	5	10	0.9%	Yes
15	y	18	M	1.4	0.44	0.97	18.8%	41.8%	45.0%	15.5%	5.0%	2	7	2.7%	No
16	y	19	M	2.05	0.41	1.65	20.5%	24.4%	84.1%	14.1%	4.3%	2	7	1.5%	No
17	y	20	M	1.98	0.95	1.03	11.4%	47.8%	23.8%	1.6%	2.2%	6	11	3.3%	Yes
18	y	21	M	1.22	0.69	0.53	12.3%	42.2%	29.0%	4.4%	17.7%	6	13	1.4%	Yes
19	y	22	M	1.86	0.79	1.07	19.4%	38.2%	50.8%	.	.	2	.	1.0%	Yes
20	y	24	M	.	.	0.78	11.4%	23.5%	48.4%	19.5%	5.7%	5	8	2.2%	No

Appendix 4: Table 4.2: Tabulated results for human bladders – cell turnover

Fetus	Bladder outflow obstruction?	Gestational age (weeks)	Sex	Ki67 (%) in urothelium	Ki67 (%) in lamina propria	Ki67 (%) in detrusor	Apoptosis (%) in urothelium	Apoptosis (%) in lamina propria	Apoptosis (%) in detrusor
1	n	16	F	5.59%	6.73%	3.89%	0.14%	0.14%	0.03%
2	n	16	M	5.17%	2.08%	0.28%	0.00%	2.57%	0.17%
3	n	18	M	3.59%	12.26%	3.25%	0.00%	0.30%	0.04%
4	n	20	F	4.09%	7.30%	1.83%	0.14%	1.50%	0.41%
5	n	20	M	0.71%	0.39%	0.52%	0.40%	0.40%	0.48%
6	n	21	M	0.09%	0.00%	0.00%	0.00%	0.46%	0.02%
7	n	24	M	0.94%	1.66%	0.53%	0.00%	0.25%	0.13%
8	n	26	M	3.52%	2.71%	0.60%	0.00%	0.07%	0.02%
9	n	27	F	0.00%	0.48%	0.06%	0.00%	0.08%	0.01%
10	n	28	F	.	0.00%	0.00%	0.14%	0.14%	0.02%
11	n	30	M	.	0.78%	0.12%	2.14%	0.42%	0.00%
12	n	31	F	1.36%	1.18%	0.86%	1.05%	0.21%	0.34%
13	y	18	M	4.05%	5.50%	4.43%	0.00%	0.05%	0.04%
14	y	18	M	.	.	2.20%	1.73%	0.00%	0.09%
15	y	18	M	3.22%	7.72%	3.03%	16.84%	0.09%	0.09%
16	y	19	M	7.38%	9.43%	1.36%	0.00%	0.08%	0.04%
17	y	20	M	2.20%	1.59%	0.81%	0.10%	0.12%	0.17%
18	y	21	M	0.40%	2.42%	0.08%	6.87%	0.07%	0.01%
19	y	22	M	.	.	.	0.00%	0.01%	0.20%
20	y	24	M	.	.	0.00%	.	.	0.96%

Appendix 4: Table 4.3: Area of fibronectin immunostaining vs. area of detrusor muscle

Fetus	Bladder outflow obstruction?	Gestational age (weeks)	Sex	Muscle area (AU)	Fibronectin area - Detrusor (AU)
1	n	16	F	0.54	0.09
2	n	16	M	0.42	0.21
3	n	18	M	0.29	0.22
4	n	20	F	0.48	0.26
5	n	20	M	0.38	0.33
6	n	21	M	0.82	0.68
7	n	24	M	0.72	0.32
8	n	26	M	0.58	0.41
9	n	27	F	0.96	0.89
10	n	28	F	0.88	0.56
11	n	30	M	0.63	0.82
12	n	31	F	1.29	0.80

Assessment of cell turn-over in human fetal bladders

Ki67

Ki67 immunostaining was used as the marker of proliferation in the human fetal bladders.

A

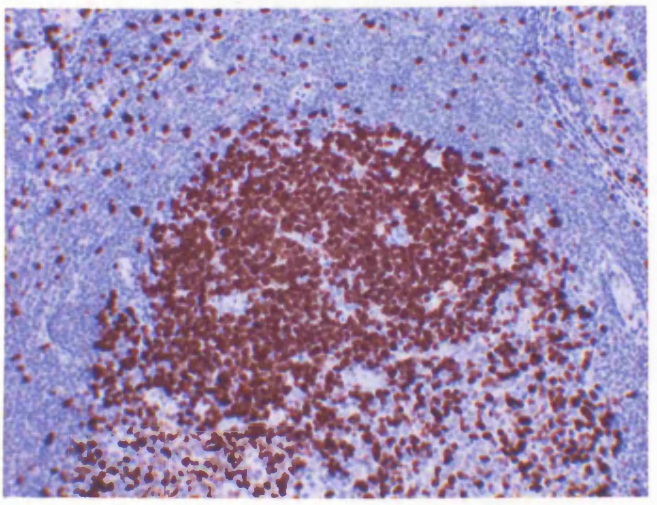

B

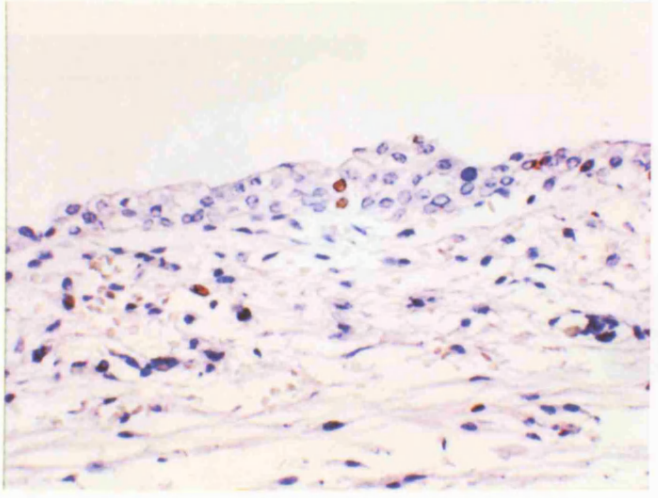

Appendix 4: figure 4.3: Ki67 immunostaining. (A) Human tonsil positive control. (B) Ki67 positive cells in urothelium and lamina propria of human fetal bladder. Scale bars (A) 400 μm, (B) 50 μm.

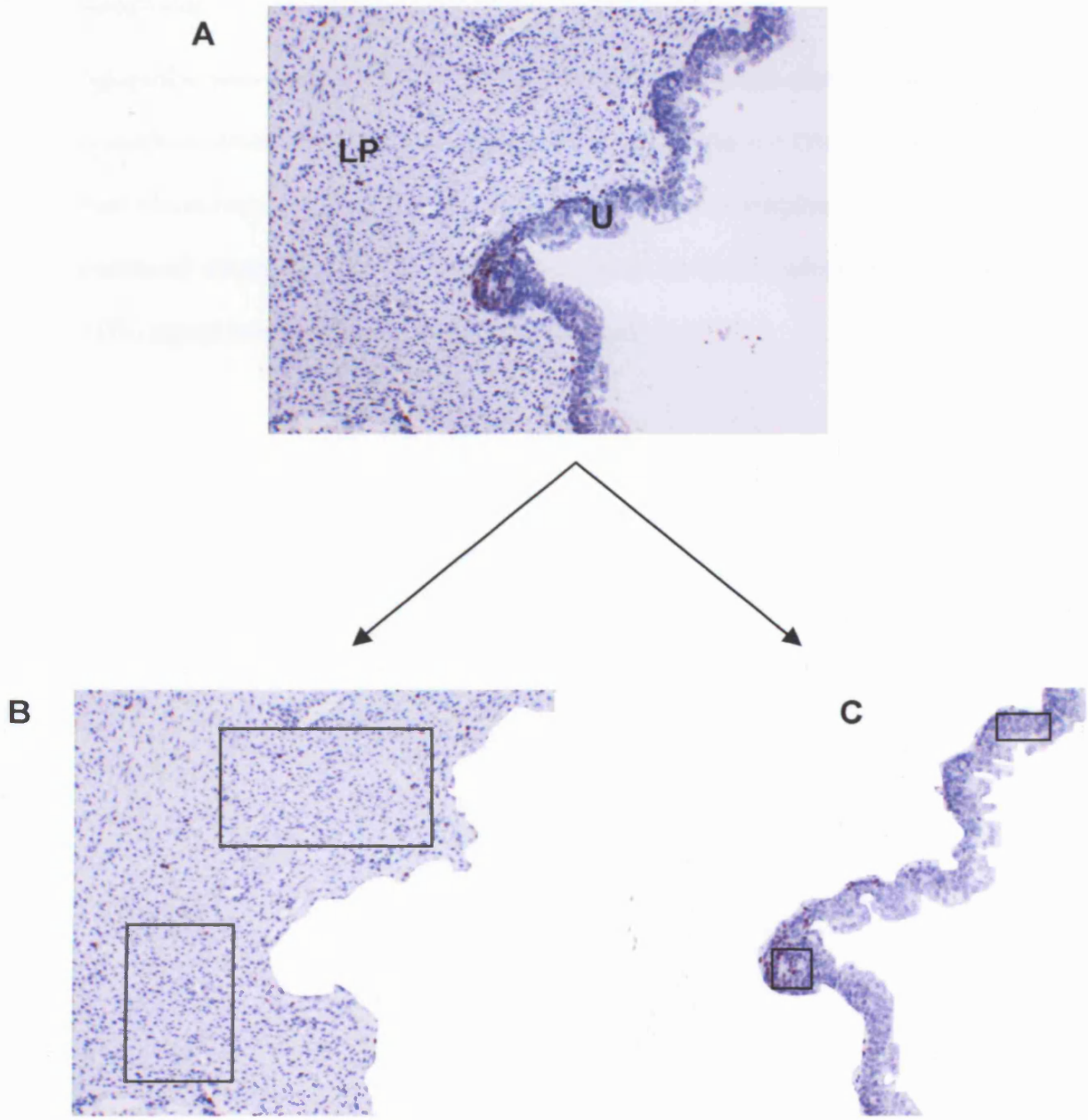

Appendix 4: Figure 4.4: (A) Urothelium and lamina propria from human bladder immunostained with Ki67, counter-stained haematoxylin, (B) Lamina propria area measured, Ki67 positive nuclei counted, to derive Ki67 cells / area. (this was repeated on 3 separate photomicrographs for each specimen. Cell density was calculated by measuring cell density in 4 typical sections of the lamina propria from each slide (Black boxes). Ki67 (%) could thus be derived. (C) Ki67 positive cells were counted, and area measured in a similar way for the urothelium. U, urothelium; LP, lamina propria

Apoptosis

Apoptosis was assessed by the TUNEL test and counter-staining with propidium iodide. FITC was tagged to the ends of the cut DNA (green colour). Red blood cells can autofluoresce at the similar wavelengths to FITC. A positively apoptotic cell was therefore taken to be one in which the TUNEL FITC signal and propidium iodide colocalized.

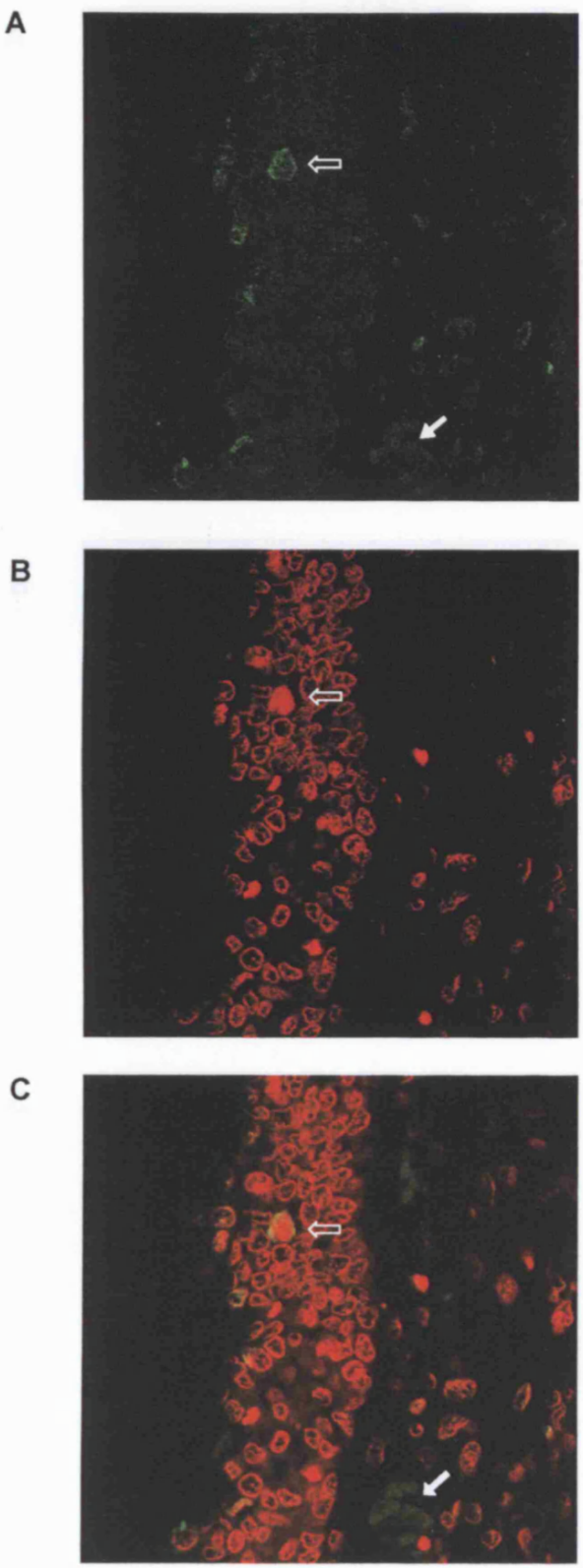

Appendix 4: Figure 4.5: Human bladder urothelium TUNEL test counterstained with propidium iodide. (A) TUNEL test showing apoptotic nucleus (hollow arrow), and autofluorescent RBCs (filled arrow), (B) PI staining of nuclei (closed arrow) apoptotic nucleus. (C) composite overlay of PI and TUNEL, apoptotic nucleus (hollow arrow), and autofluorescent RBCs (filled arrow).

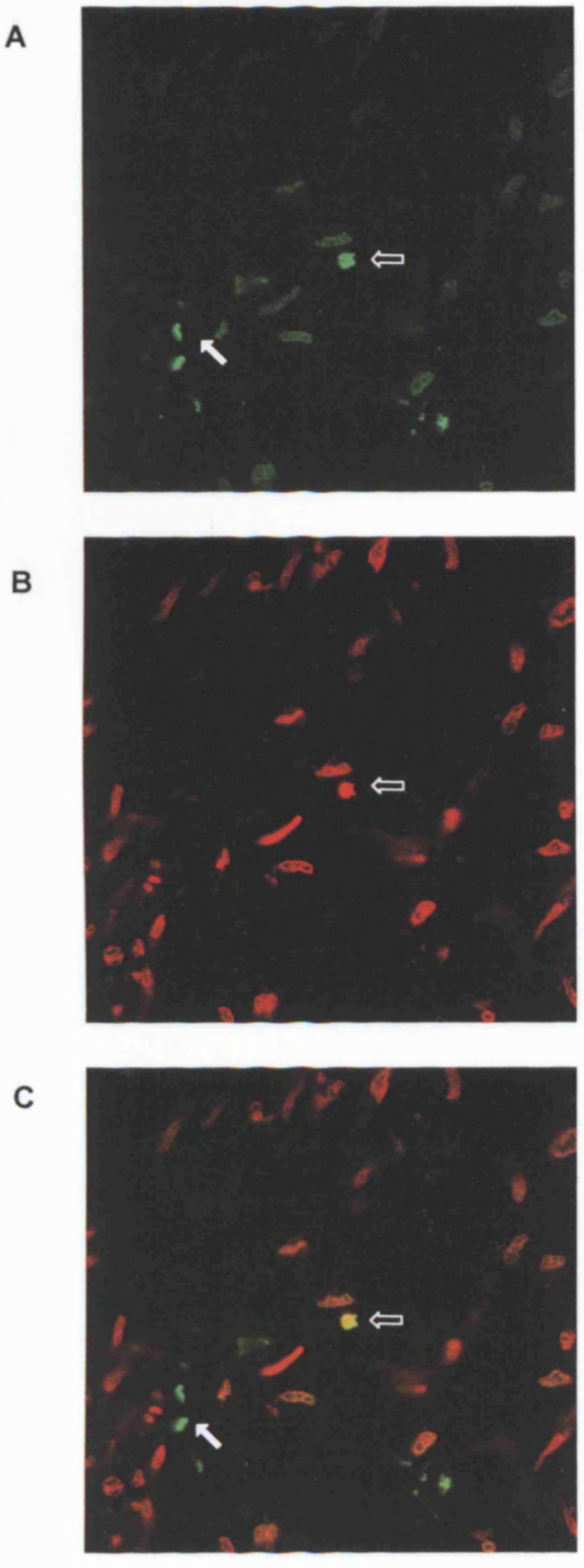

Appendix 4: Figure 4.6: Human bladder lamina propria TUNEL test counterstained with propidium iodide. (A) TUNEL test showing apoptotic nucleus (hollow arrow), and autofluorescent RBCs (filled arrow), (B) PI staining of nuclei (closed arrow) apoptotic nucleus. (C) composite overlay of PI and TUNEL, apoptotic nucleus (hollow arrow), and autofluorescent RBCs (filled arrow).

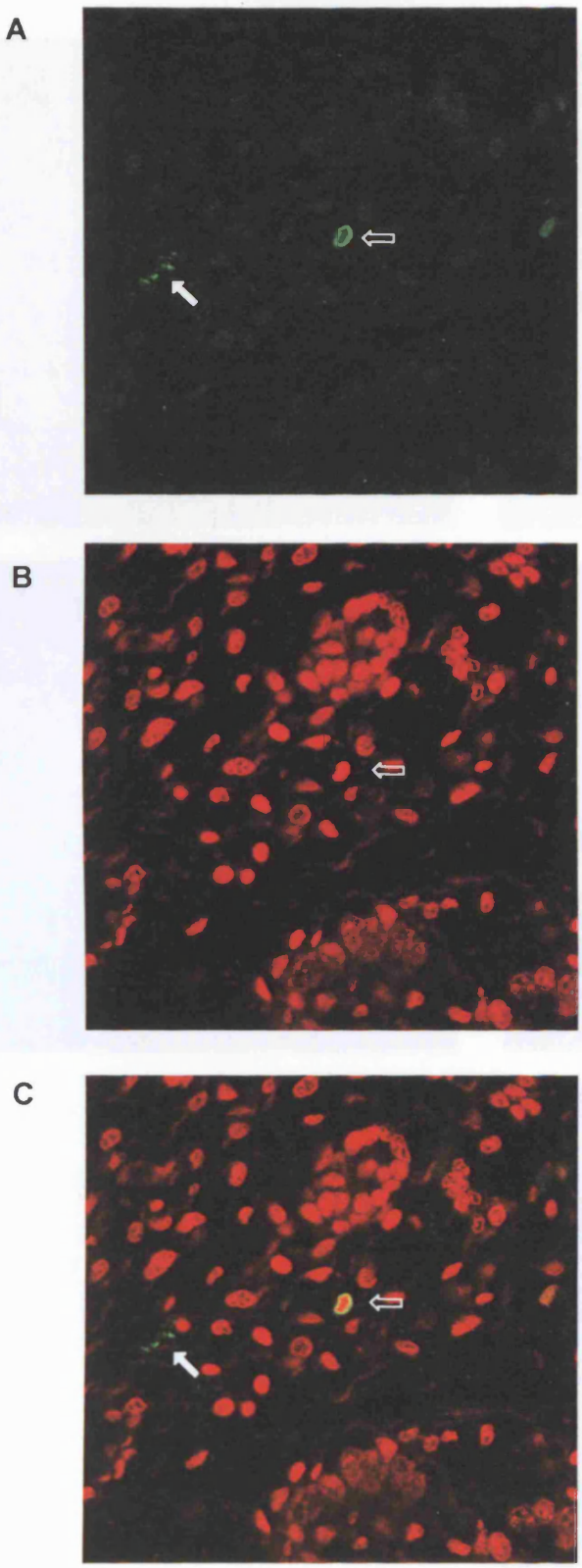

Appendix 4: Figure 4.7: Human bladder detrusor TUNEL test counterstained with propidium iodide (A) TUNEL test showing apoptotic nucleus (hollow arrow), and autofluorescent RBCs (filled arrow), (B) PI staining of nuclei (closed arrow) apoptotic nucleus. (C) composite overlay of PI and TUNEL, apoptotic nucleus (hollow arrow), and autofluorescent RBCs (filled arrow).

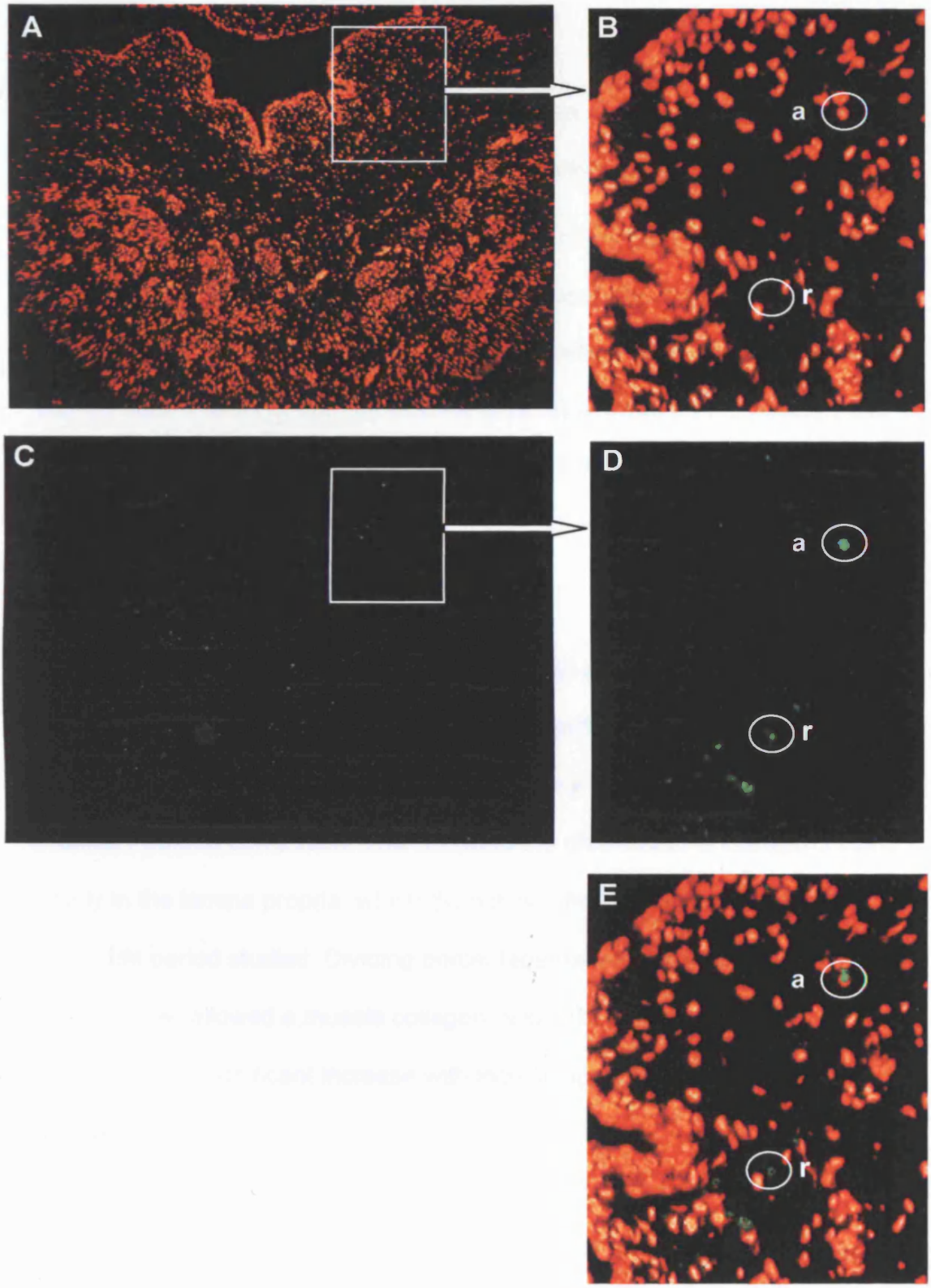

Appendix 4:Figure: 4.8: Low power views of human bladder, (A) PI counter-staining, (B) close-up of (A); (C) TUNEL staining, low power view, (D) close-up of the same region. a, apototic nucleus present on both PI and TUNEL images, whereas r, red blood cell, is only present on TUNEL image. (E) Rapid flicking between images highlights truly apoptotic nuclei, whereas autofluorescence of RBCs does not coincide with a nucleus on PI staining.

Muscle area, muscle percentage of surface area (%), Collagen and collagen percentage of surface area (%) and Muscle Collagen ratio

Measurements of muscle area (mm^2) for each of the bladder sections showed a significant correlation with increasing gestational age, $p<0.01$, 2–tailed Pearson correlation. Muscle percentage of surface area (ie percentage of total cross-sectional area of section which is muscle) showed an increasing trend over the period samples were available, but this did not reach significance. (Muscle increased, but so did the wall thickness – density remained approximately static therefore.)

The area of collagen in normal bladders showed a tendency to increase with gestational age, but this correlation was not significant. The proportion of collagen in the bladder walls did however show a significant decrease, $p<0.05$ 2–tailed Pearson correlation. This reflected the distribution of collagens being mainly in the lamina propria, which did not significantly increase in width during the period studied. Dividing percentage muscle area by percentage collagen area allowed a muscle collagen ratio to be derived for each bladder. This showed a significant increase with increasing gestational age ($p<0.05$ Pearson 2–tailed test).